Backman, J., Duncan, R. A., et al., 1988
Proceedings of the Ocean Drilling Program, Initial Reports, Vol. 115

10. SITE 712 AND 713[1]

Shipboard Scientific Party[2]

SITE 712

Hole 712A

Date occupied: 0705 L, 16 June 1987

Date departed: 2045 L, 16 June 1987

Time on hole: 13 hr, 40 min

Position: 04°12.99′S, 73°24.38′E

Water depth (sea level; corrected m, echo-sounding): 2904.3

Water depth (rig floor; corrected m, echo-sounding): 2914.8

Bottom felt (m, drill pipe): 2902.9

Penetration (m): 115.3

Number of cores: 12

Total length of cored section (m): 115.3

Total core recovered (m): 41.6

Core recovery (%): 36.1

Oldest sediment cored:
Depth (mbsf): 115.3
Nature: nannofossil chalk and volcanic ash
Age: middle Eocene
Measured velocity (km/s): 1.6

SITE 713

Hole 713A

Date occupied: 2330 L, 16 June 1987

Date departed: 1300 L, 20 June 1987

Time on hole: 4 days, 13 hr, 30 min

Position: 04°11.58′S, 73°23.65′E

Water depth (sea level; corrected m, echo-sounding): 2915.3

Water depth (rig floor; corrected m, echo-sounding): 2925.8

Bottom felt (m, drill pipe): 2920.3

Penetration (m): 191.7

Number of cores: 22

Total length of cored section (m): 191.7

Total core recovered (m): 115.0

Core recovery (%): 60

Oldest sediment cored:
Depth (mbsf): 155.1
Nature: nannofossil chalk and volcanic ash
Age: middle Eocene
Measured velocity (km/s): 2.6

Basement rocks:
Depth (mbsf): 107.0 to 191.7
Nature: basalt
Age: middle Eocene
Measured velocity (km/s): 5.7

Principal results: In transit from Site 711 to Sites 712 and 713, the *JOIDES Resolution* crossed the Central Indian Ridge, which forms the boundary between the African and Indian plates (Fig. 1). This spreading ridge has been active since Chron 13 time (35 Ma), when the Chagos Bank was rifted from the Nazareth Bank and the Ninetyeast Ridge was separated from the Kerguelen hotspot. Before this time, the plate boundary spreading system was located further to the south (McKenzie and Sclater, 1971; Schlich, 1982). Our rationale for drilling at the Chagos Bank was to sample hotspot volcanism midway between the Deccan flood basalts and ocean island basalts at Réunion and Mauritius (see "Background and Objectives" section, this chapter).

Sites 712 and 713 are located on the northern margin of the Chagos Bank. Site 712 is at 4°12.99′S, 73°24.38′E, in 2892.4-m water depth. Because of hole instability problems, basement could not be reached at this site, so drilling was relocated 1.6 nmi to the north. Site 713 is at 4°11.58′S, 73°23.65′E, in 2909.8-m water depth. Shallow-water carbonate reefs and banks lie 70 nmi to the south and southwest. An abrupt scarp, probably related to transform faulting before 35 Ma, drops 3000 m just 30 nmi to the east. In the immediate region of these sites is a gently dipping volcanic apron which deepens to the north to the 4500-m channel that separates the Chagos Bank from the Maldive Islands.

Site 712

The basement rocks in this region form a series of offset steps, probably resulting from extension and normal faulting. At this site, the sediment cover is about 190 m thick, whereas only 1.6 nmi away at Site 713 the basement is 106 mbsf. Hole 712A was terminated in middle Eocene nannofossil oozes and volcanic ashes at 115.3 mbsf. Rotary coring averaged 60% recovery through the first 58 m of nannofossil oozes, then fell abruptly to nearly nothing for the next 40 m. This zone was probably an unconsolidated coarse carbonate sand as it continually caved in on the drill pipe and eventually ended drilling at this site. Fair recovery was achieved again in the last two cores of nannofossil ooze mixed with volcanic ashes.

The major lithologies we recognized in Hole 712A are as follows:

Unit I (0–58 mbsf) contains foraminifer-bearing nannofossil ooze and foraminifer-nannofossil ooze with thin turbidites and minor bioturbation. With depth, these sediments become more consolidated as foraminifer-nannofossil chalks. Unit I sediments range in age from Pleistocene to middle Miocene.

Unit II (58–106 mbsf) provided essentially no recovery except for drilling rubble, including coarse fragments of recrystallized limestone. Sediments are of late Oligocene age.

Unit III (106–115 mbsf) is composed of foraminifer-bearing and foraminifer-nannofossil chalk with numerous, thin interbedded volcanic ashes. It is middle Eocene in age.

Site 713

Total penetration at this site was 192 m by rotary coring. The 22 cores yielded an average recovery rate of 60%. During the cutting of Core 115-713A-20R, the drilling rate dropped to less than 2 m/hr, and we assumed that the four-cone bit might be worn out. A reentry cone was deployed, seated in the hole using the video camera system, and the pipe tripped to replace the bit. Surprisingly, the old bit was not badly

---

[1] Backman, J., Duncan, R. A., et al., 1988. *Proc. ODP, Init. Repts.*, 115: College Station, TX (Ocean Drilling Program).

[2] Shipboard Scientific Party is as given in the list of Participants preceding the contents, with the addition of Isabella Premoli Silva and Silvia Spezzaferria, Dipartimento di Scienze della Terra, Universitá di Milano, Via Mangiagalli 34, I-20129, Milano, Italy.

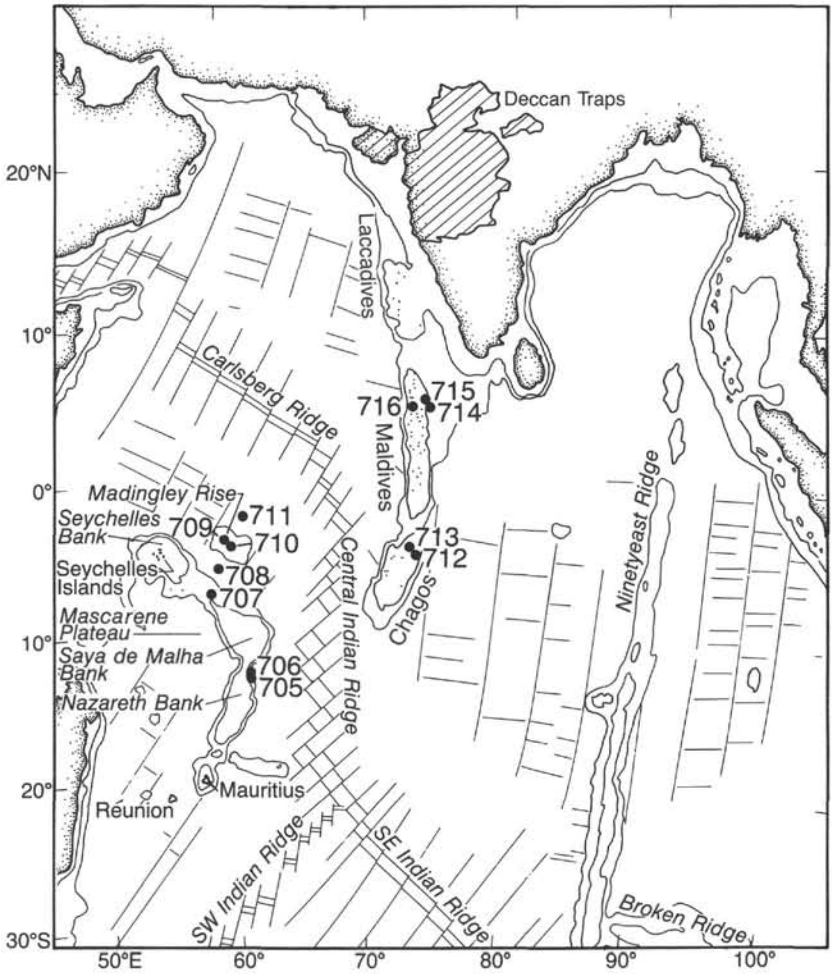

Figure 1. Regional setting and location of Sites 712 and 713, Chagos Bank, central Indian Ocean. Drilling on this elevated ridge was intended to sample a midway point on the hotspot track connecting active volcanism in the region of the island of Réunion with the Deccan flood basalts, western India.

worn. We installed a diamond bit and reassembled the drill string for reentry, which was accomplished in fairly rough weather, again using the camera. The new bit cut only 8.4 m at a very slow pace, and we felt that bit failure was imminent. Drilling stopped, and the drill string was recovered. The new bit had indeed nearly fallen apart (see "Operations" section, this chapter).

Hole 713A bottomed in basalt flows of olivine tholeiitic composition, intercalated with nannofossil chalks of early middle Eocene age (47–48 Ma). The basalts vary from thicker (10 m), more vesicular flows at the top, to thinner (1 m), more compact flows with depth. Some 35 separate flow units were distinguished on the basis of sediment interbeds and glassy, chilled margins. The basalts were erupted well below sea level, but the degree of vesicularity in some of the flows indicates conditions a good deal shallower than the present depth (3000 m). Thermal subsidence considerations (Sclater et al., 1977) predict a depth for this site of about 1000 m during volcanic activity. The benthic foraminiferal assemblage observed between the lava flows indicates a deeper-water environment (see "Biostratigraphy" section, this chapter).

A significant finding was the large amount of magnificently preserved black volcanic ash increasing toward the base of the sediment column and intercalated with the basalt flows. Preliminary examination indicates that these may represent much more evolved magmas than those identified from the basaltic rocks. The ashes are undoubtedly of local origin, but the variability of the compositions among the fresh glasses will allow a much more complete assessment of the range of volcanic products at this location on the hotspot track.

We measured stable and consistent paleomagnetic field directions from the basaltic rocks at Site 713. These yield an estimated paleolatitude for the site of 12.2° ± 3.1° S. From the hotspot model we expected a paleolatitude between 21° and 30° S, so this result is, for the present, puzzling and anomalous with respect to other site paleolatitudes (see "Principal results" section, "Site 715" chapter, this volume). The evidence for faulting of the basaltic rocks (see "Seismic Stratigraphy" section, this chapter) may provide a possible mechanism for rotation of basement blocks (10°–20° about an east-west horizontal axis). Since the laminae in sediments interbedded with the basalts do not show any consistent tilt, however, this may not be a satisfactory solution.

The major lithologies recovered in Hole 713A can be summarized as follows:

Unit I (0–31 mbsf) contains foraminifer-nannofossil ooze to foraminifer-bearing nannofossil ooze and chalk. Sediments range in age from Pleistocene to late Miocene.

Unit III (31–107 mbsf) is dominated by foraminifer-bearing nannofossil chalk, clay-bearing in parts, with volcanic ashes increasing in occurrence and thickness with depth. Spectacular bioturbation and small-scale faulting are preserved and clearly seen because of the color contrast. Sediments are middle Eocene in age.

Unit IV (107–192 mbsf) is composed of vesicular to compact submarine basalts of olivine basalt composition. Flows vary from 1 to 10 m in thickness and are interbedded with middle Eocene nannofossil chalks and volcanic-ash layers.

The geologic columns for the two sites (Fig. 2) show that there is a major hiatus between late Miocene and middle Eocene sediments at Site 713, with Unit II sediments missing. Oligocene sediments of Unit II were found at Site 712, only 1.6 nmi to the south, indicating highly variable patterns of erosion and subsidence.

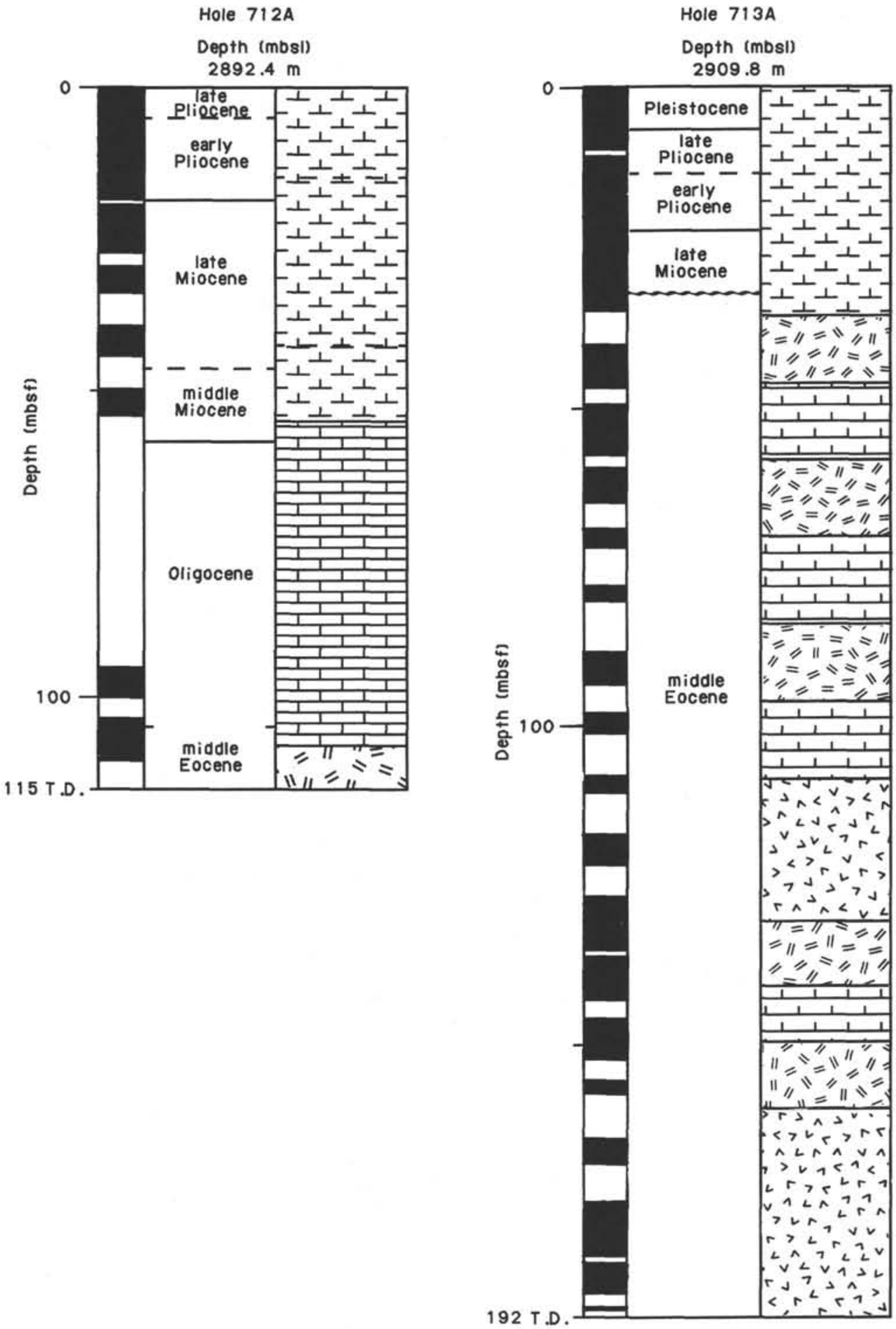

Figure 2. Stratigraphic summary of Sites 712 and 713. Black column represents recovered section.

BACKGROUND AND OBJECTIVES

The Mascarene-Chagos-Maldive-Laccadive volcanic lineament is a major aseismic ridge system in the central Indian Ocean basin. It connects young volcanic activity in the vicinity of Réunion Island with the massive volumes of continental flood basalt erupted along India's western margin near the time of the Cretaceous/Tertiary boundary. This lineament parallels the remarkable Ninetyeast Ridge, and the two together record the northward motion of the Indian subcontinent away from stationary hotspots near Réunion and Kerguelen Islands, respectively (Fig. 3).

Our overall strategy for sampling this volcanic trend is presented in the Site 705/706 chapter. Age-progressive volcanism along the Ninetyeast Ridge has already been documented (Duncan, 1978), and comparable age determinations along the western trend will allow precise calculation of rotation poles for Indian plate motion during Tertiary time. This will have applications in plate reconstructions for the Indian Ocean, the timing of India's collision with Asia, and the rise of the Himalaya

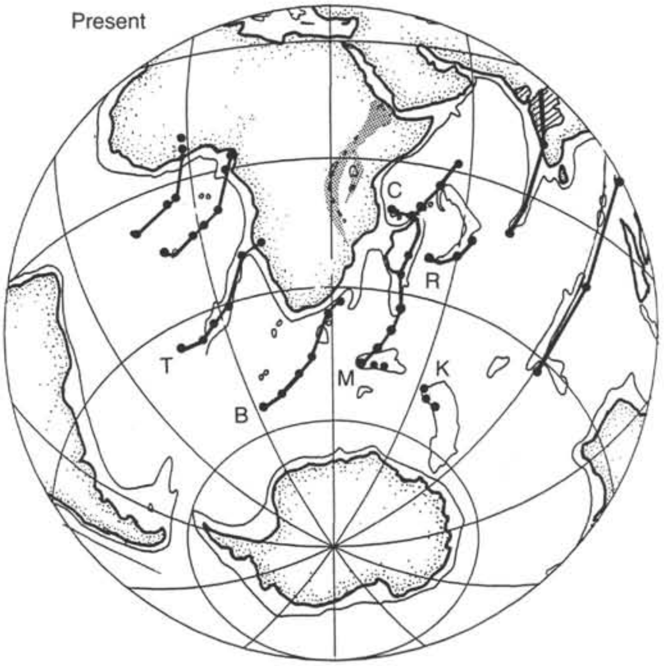

Figure 3. Predicted hotspot tracks and present-day distribution of aseismic ridges in the Indian and South Atlantic Oceans. Letters refer to Réunion (R), Comores (C), Kerguelen (K), Bouvet (B), Marion (M), and Tristan (T) hotspots. The present outcrop of flood basalts of the Deccan Traps is shown in western India (from Emerick, 1985).

Mountains. Another necessary result will be a direct test of the proposition that the Indian and Atlantic basin hotspots have maintained a fixed geometry throughout the period of volcanic activity (Morgan, 1981; Duncan, 1981).

From the known relative plate motions across the Central Indian Ridge and ages along the Ninetyeast Ridge, the predicted age of Site 713 on the Chagos Bank is 45-50 Ma (Emerick, 1985). This age would provide an important intermediate point between Site 706 (36 Ma) and the Deccan flood basalts (66-68 Ma).

Of further interest is the geochemical composition of basalts erupted along this lineament. Potential mantle source regions for melting include the hotspot itself, the uppermost suboceanic mantle (the source of Mid-Ocean Ridge basalts), and the subcontinental mantle. At the southern extreme the basalts of Réunion and Mauritius probably best represent hotspot compositions, and at the north the Deccan basalts have had melt contributions from the mantle beneath India. In between, we may expect to see evidence of magma mixed from these sources and the Central Indian Ridge, depending on the position of the hotspot with respect to continental India and the spreading ridge through time. The Chagos Bank formed well south of India and before rifting on the Central Indian Ridge (Fig. 4), so we expect to see a strong hotspot signature in the basalt compositions (trace element and isotopic compositions).

We also hoped to investigate the phenomenon of true polar wander at Site 713. If the position of the earth's spin axis changes relative to its figure (due, say, to mass redistribution), then the hotspot reference frame will appear to move with respect to the geomagnetic pole (aligned with the spin axis). Thus, a straightforward test is to determine the paleomagnetic latitude of sites along the hotspot track. If the hotspot has not moved with respect to the spin axis, then all sites should exhibit the same paleolatitude. Systematic departures indicate true polar wander. The Deccan flood basalts yield a paleolatitude of about 29°S (Courtillot et al., 1986), or 8°S of Réunion. Thus, there has been 8° of true polar wander since about 67 Ma. Paleolatitudes from additional sites along this lineament will allow us to determine when the true polar wander occurred.

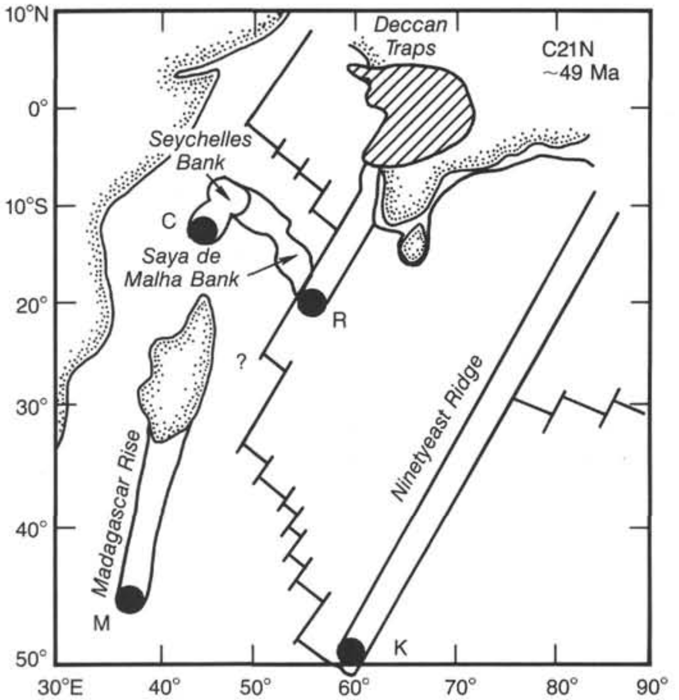

Figure 4. Reconstruction of the western Indian Ocean for the predicted age of Site 713, northern Chagos Bank, in the hotspot reference frame. The hotspot lies under the Indian plate and to the north of a spreading ridge segment. Letters refer to Comores (C), Réunion (R), Marion (M), and Kerguelen (K) hotspots.

OPERATIONS

Site 712 was an alternate site added to the leg when permission to drill in Mauritian territorial waters was rescinded. The survey gear was streamed 2 hr prior to arriving at Site CB-1 to ensure that a complete survey was made. At 2400 hr, 15 June 1987, the beacon was dropped to establish Site 712.

Hole 712A

The objective of Hole 712A was to penetrate and recover basement rocks of presumed basaltic composition. The bottom hole assembly (BHA) was lowered to the seafloor, and the mud line was established at 2892.4 m. Recovery started out well until a chert stringer was encountered at 2930.7 m (38.3 mbsf). We penetrated the chert stringer, but recovery still dropped off considerably. Virtually no core was recovered from 2949.9 to 2978.8 m, at which time the deplugger was dropped. When coring continued, recovery was low and the hole was getting tight. Each time the drill string was picked up, the hole was lost and had to be washed back down. Gel/water mud was used to sweep the hole with little effect.

With hole conditions becoming worse, we decided to abandon Hole 712A. Total penetration was 115.3 mbsf to 3007.7 m, with 41.6 m of core recovered for a recovery rate of 36% (Table 1). An alternate site was then chosen by the Co-Chiefs from seismic survey data in hopes of finding better drilling conditions. We pulled the drill string 100 m above the seafloor and moved the ship 1.6 nmi north-northwest in the dynamic positioning (DP) mode. We dropped a beacon at 2200 hr on 16 June 1987 to establish Site 713.

Table 1. Coring summary, Sites 712 and 713.

Core no.	Date (June 1987)	Time (local)	Depth (mbsf)	Cored (m)	Recovered (m)	Recovery (%)
115-712A-						
1R	16	0730	0–9.4	9.4	9.40	100.0
2R	16	0815	9.4–19.0	9.6	8.13	84.7
3R	16	0900	19.0–28.6	9.6	6.44	67.1
4R	16	0930	28.6–38.3	9.7	3.67	37.8
5R	16	1015	38.3–47.9	9.6	3.30	34.4
6R	16	1045	47.9–57.5	9.6	3.60	37.5
7R	16	1115	57.5–67.2	9.7	0	0
8R	16	1200	67.2–76.8	9.6	0.05	0.5
9R	16	1330	76.8–86.4	9.6	0	0
10R	16	1415	86.4–96.1	9.7	0.13	1.3
11R	16	1645	96.1–105.7	9.6	2.32	24.1
12R	16	2045	105.7–115.3	9.6	4.52	47.1
115-713A-						
1R	17	0015	0–1.6	1.6	1.63	102.0
2R	17	0100	1.6–11.2	9.6	8.48	88.3
3R	17	0145	11.2–20.8	9.6	9.87	103.0
4R	17	0230	20.8–30.5	9.7	9.67	99.7
5R	17	0315	30.5–40.1	9.6	4.53	47.2
6R	17	0400	40.1–49.7	9.6	6.95	72.4
7R	17	0445	49.7–59.4	9.7	8.50	87.6
8R	17	0530	59.4–69.1	9.7	5.21	53.7
9R	17	0600	69.1–78.7	9.6	3.13	32.6
10R	17	0645	78.7–88.4	9.7	2.32	23.9
11R	17	0730	88.4–98.1	9.7	5.05	52.0
12R	17	0830	98.1–107.7	9.6	3.23	33.6
13R	17	1230	107.7–117.2	9.5	2.78	29.2
14R	17	1545	117.2–126.7	9.5	4.35	45.8
15R	17	2000	126.7–136.2	9.5	7.76	81.7
16R	17	2130	136.2–145.7	9.5	6.61	69.6
17R	17	2245	145.7–155.2	9.5	6.34	66.7
18R	18	0145	155.2–164.4	9.2	1.85	20.1
19R	18	0815	164.4–173.9	9.5	3.27	34.4
20R	18	1500	173.9–183.3	9.4	8.25	87.7
21R	20	0045	183.3–190.2	6.9	4.72	68.4
22R	20	0330	190.2–191.7	1.5	0.48	32.0

Hole 713A

The rotary core barrel (RCB) BHA was lowered back to the seafloor, and coring commenced at 2345 hr, 16 June, establishing the mud line at 2909.8 m. We encountered basalt at 3016.8 m (107 mbsf). After Core 115-713A-19R, the hole became tight. The drill string was worked, the hole was swept with gel/water mud, and coring resumed. While cutting Core 115-713A-20R, penetration dropped off to 1 m/hr. Because of the possibility of junking the hole due to a broken bit, we decided to drop a minicone, pull out of the hole, and reenter with a diamond bit.

The top of the BHA was pulled to the mud line, and a minicone was deployed at 1900 hr, 18 June. At 1930 hr, the camera was lowered. After finding that the minicone was positioned properly in the hole, the BHA was pulled through with no problem. We then tripped out the camera and drill string.

The roller cone bit was replaced by the diamond bit, and the BHA was lowered back to the seafloor. The camera was lowered to begin reentry. After 2 hr of searching and 1 hr of positioning over the cone, reentry was made. We retrieved the camera, washed the hole down to bottom at 3093.1 m (183.3 mbsf), with no fill found, and resumed coring.

After 6.9 m of penetration on Core 115-713A-21R, we had to retrieve the core barrel due to jamming. While cutting Core 115-713A-22R, penetration had slowed to nothing and the pump pressure had climbed to 1800 psi. Whenever the bit was picked up off bottom, pump pressure would drop to 250 psi. Everything indicated that the bit was worn out and further penetration was impossible. Therefore, we tripped out the drill string and abandoned Hole 713A. The diamond bit had only penetrated 8.4 m of basalt and recovered 5.2 m of core. Total penetration was 191.7 mbsf to 3101.5 m, with 115 m of core recovered for a recovery rate of 60% (Table 1).

Site 713 to the Maldive Islands

With everything secured at 1300 hr, 20 June, the ship was under way to the Maldive Islands. We encountered a storm with 35–40-kt winds, gusting to 65 kt, and heavy rains in the early morning hours on 21 June, which continued throughout the transit to the Maldives. The storm slowed the ship to 9 kt, and arrival at Male in the Maldives was at 1100 hr, 22 June, 2 hr behind schedule. Because of high winds and associated seas, we did not anchor the ship but remained positioned approximately 1 nmi south of Male in the DP mode. Dr. Philip Rabinowitz had made the trip from Ocean Drilling Program headquarters to Male to secure drilling clearance for two of the Maldive sites. Dr. Rabinowitz, two observers, and customs, immigration, and security officials from the Maldives came on board at Male.

LITHOSTRATIGRAPHY

Introduction

Sites 712 and 713 are located within 1.6 nmi of each other on the northern margin of the Chagos Bank at water depths of 2892.4 and 2909.8 m, respectively. Because our principal objective at this location was to penetrate and sample basement rocks, we selected these sites because of their relatively thin sediment cover, paying little attention to the completeness of the stratigraphic sequence. Site 712 was rotary cored to a depth of 115.3 mbsf, where hole instability problems forced the termination of drilling short of basement. Site 713 was offset slightly to the north and drilled to a total depth of 191.7 mbsf, with basalt reached at 106 mbsf.

The sedimentary sequence at Sites 712 and 713 is punctuated by hiatuses, but we can divide it nonetheless into three major units (Fig. 5). Unit I is composed of foraminifer-nannofossil ooze, foraminifer-bearing nannofossil ooze, and foraminifer-nannofossil chalk; it ranges in age from Pleistocene to middle Miocene in the two sites. Unit II consists of an unconsolidated sequence of coarse carbonate sands and limestone rubble, known only from spotty recovery at Site 712 and missing completely at Site 713. Limited biostratigraphic data suggests a late Oligocene age for at least part of this unit. Unit III is composed of a rather spectacular interbedded sequence of nannofossil and micritic chalks and volcanic ash of middle Eocene age which directly overlies basement in Site 713, and which was also found intercalated within the olivine tholeiitic basalt flows.

Each of the three major sedimentary units is described in more detail in the following sections.

Unit I: Cores 115-712A-1R through -6R (0–57.5 mbsf) and Cores 115-713A-1R through -4R (0–30.5 mbsf); Age: Pleistocene to middle Miocene.

Unit I in Holes 712A and 713A consists of foraminifer-nannofossil ooze, foraminifer-bearing nannofossil ooze, and foraminifer-nannofossil chalk. This purely pelagic sequence is further divided into two subunits on the basis of the induration differences between the ooze and chalk.

Subunit IA: Cores 115-712A-1R through -4R (0–38.3 mbsf) and Cores 115-713A-1R through -4R (0–30.5 mbsf); Age: Pleistocene to late Miocene.

Subunit IA is composed of a foraminifer-nannofossil ooze at the top which grades downhole into a foraminifer-bearing nannofossil ooze. Foraminifers typically make up 35%–45% of the

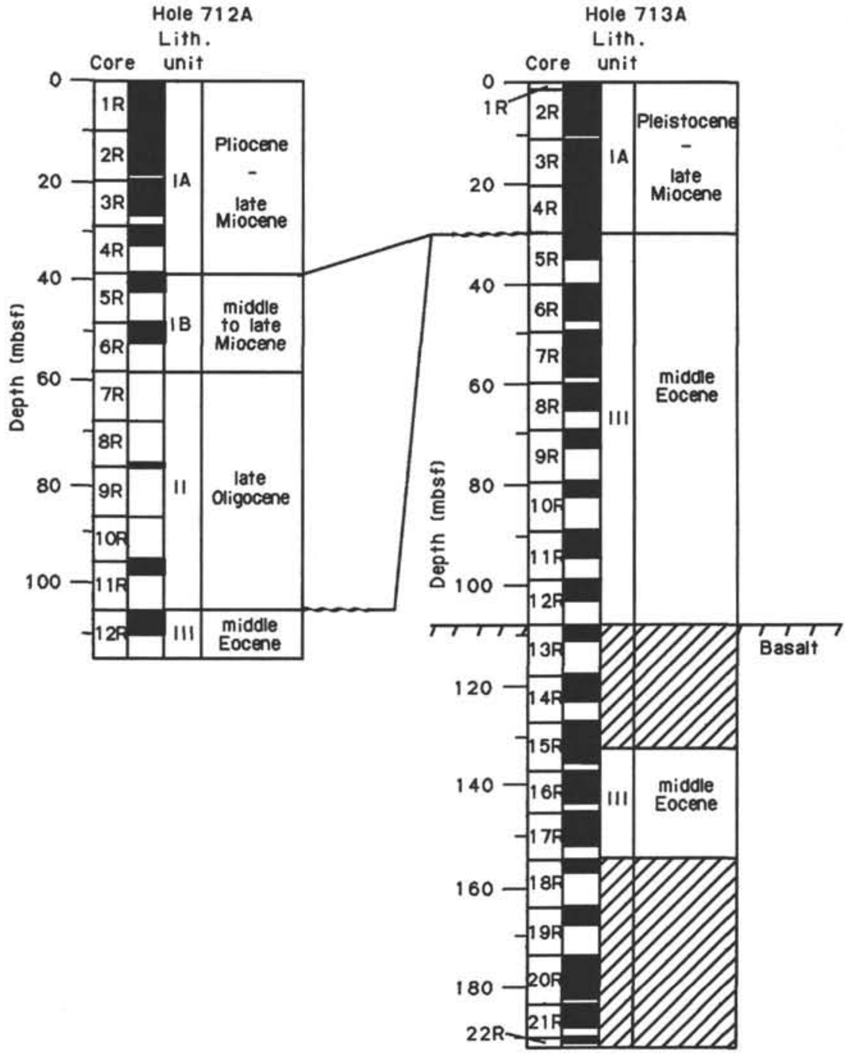

Figure 5. Summary of lithostratigraphic units recognized at Sites 712 and 713. Major hiatuses are shown based on biostratigraphic data presented in "Biostratigraphy" section, this chapter.

sediment near the mud line and 15%-20% of the sediment near the base of the subunit. Well-preserved calcareous nannofossils are the dominant component throughout and generally comprise 45%-70% of the total. Other biogenic components present in minor (<10%) and trace amounts include radiolarians, sponge spicules, diatoms, and occasional fish debris. Clay, quartz, feldspar, volcanic ash, dolomite rhombs, and pyrite are nonbiogenic components present in similarly small amounts. The carbonate content of these sediments appears to be very uniform and averages about 94%, based on the few measurements from samples taken for the study of physical properties (see "Geochemistry" section, this chapter).

The sediments of Subunit IA are predominantly white (10YR 8/1-8/2, N9), very pale brown (10YR 8/2-8/3), and light gray to very light greenish gray (N8, 10YR 7/2, 5G 8/1). In Hole 712A, a number of very thin light gray (10YR 7/1) to very light yellowish gray (2.5Y 7/2), and very light green (5G 8/2) horizons are faintly visible throughout the subunit. Core disturbance from rotary drilling has deformed many of these, and no such distinct layers were observed in Hole 713A, which recovered a considerably more disturbed sequence. Mottling due to bioturbation, visible in sediment from Hole 712A, was difficult to detect in Hole 713A because of the much poorer core quality.

A small number of thin turbidites interrupt the sequence in Holes 712A and 713A. These are most numerous in the upper 5 m of the subunit. The turbidites range in thickness from 10 to 60 cm, are normally graded, and generally consist of pelagic material only slightly coarser than the surrounding sediments. No shallow-water platform debris was identified in any of these allogenic layers, indicating that they must not have originated too far upslope.

The stratigraphic distribution of Subunit IA sediments is shown in Figure 5. Biostratigraphic data ("Biostratigraphy" section, this chapter) indicate an age range of Pleistocene to late Miocene for the subunit, although Pleistocene sediments are present in only a thin veneer (<70 cm) at the top of the sequence at Site 712.

Subunit IB: Cores 115-712A-5R and -6R (38.3-57.5 mbsf); Age: late to middle Miocene.

Subunit IB consists of semi-indurated, foraminifer-nannofossil chalk with interbedded foraminifer-nannofossil ooze. Sediment color is white (N9) to very light greenish gray (5G 8/1), and the subunit is generally indistinguishable from the overlying Subunit IA except for the incipient lithification. Foraminifers and calcareous nannoplankton dominate the sediment and are present in roughly equal numbers. Sediment texture reflects this largely two-component system, being typically 35%–50% sand, 10% silt, and 40%–55% clay. The carbonate content of these sediments ranges from 93% to 97%.

The chalky material in Subunit IB is moderately to heavily disturbed by the rotary coring, particularly in Core 115-712A-6R where much of the ooze may actually be a drilling paste. Numerous pebble-sized, subangular fragments of shallow-water limestone were found in Section 115-712A-6R-1, but these were scattered throughout the interval and not concentrated in one obvious horizon.

The stratigraphic distribution of Subunit IB chalks and oozes is shown in Figure 5. Sediments of Subunit IB are completely missing from Hole 713A and are known only from their recovery in Hole 712A. Biostratigraphic data suggest that sediment deposition in the latter hole was continuous across the Subunit IA/IB transition. Subunit IB sediments range in age from late to middle Miocene.

Unit II: Cores 115-712A-7R through -11R (57.5–105.7 mbsf); Age: late Oligocene.

The lithology and extent of Unit II is poorly known because of the rather dismal rate of recovery achieved in Cores 115-712A-7R through -11R. Of the approximately 48 m that was continuously cored in this interval, only 2.5 m of material was recovered (5% recovery), and this was mostly drilling rubble. Therefore, we assigned the unit boundaries to encompass the entire interval of low recovery and assumed that the small amount of material obtained was representative of the lithology of the entire sequence.

Unit II is thought to consist of an unconsolidated sequence of coarse carbonate sands and limestone rubble. Core 115-712A-8R recovered a total of three wackestone and packstone pebbles, with preserved bryozoans and moldic porosity suggesting shallow-water origins. Core 115-712A-10R contained several small pieces of foraminifer-bearing nannofossil chalk and a single fragment of well-lithified foraminifer grainstone in the core catcher. The chalk fragments resemble the chalks of Subunit IA, but we have no data to evaluate if they originated uphole. Finally, Core 115-712A-11R recovered a veritable bonanza of material, nearly a section and a half of unconsolidated coarse carbonate sand and angular to subrounded recrystallized limestone rubble. Most of this material was too abraded and recrystallized to identify.

A single age determination from nannofossils in Core 115-712A-11R indicates a late Oligocene age for at least the lower part of Unit II (see "Biostratigraphy" section, this chapter). This age fits relatively well with the sedimentation-rate data on this site, suggesting that the coarse sand and gravel was deposited in place and is not part of a larger slump feature. In addition, the apparent collapse of this material around the drill pipe, which eventually terminated operations at Site 712, seems to indicate that the material was unconsolidated at the time of its drilling. We suspect that Unit II represents a coarse submarine lag deposit, the material probably having originated from the shallow reefs and carbonate banks to the south and southwest. Unit II sediments are not found in the stratigraphic sequence of Site 713, just 1.6 nmi away.

Unit III: Core 115-712A-12R (105.7–115.3 mbsf), Cores 115-713A-5R to Section 115-713A-12R, CC (30.5–107.7 mbsf), and Section 115-713A-15R-5, 112 cm, through Core 115-713A-17R (133.8–155.2 mbsf); Age: middle Eocene.

Unit III is composed of a complexly interbedded sequence of fine-grained chalks and volcanic ash that is moderately to heavily bioturbated. This unit records considerable evidence of microfaulting and local tectonic activity. The result is a colorful and rather spectacular sequence which extends from the base of Subunit IA to the first basalt encountered in Hole 713A, and occurs again intercalated in a roughly 20-m-thick layer within the massive olivine tholeiitic basalt flows. We also reached Unit III sediments in the last core of Hole 712A before we abandoned drilling at Site 712 (Fig. 5). Biostratigraphic data indicate that the entire Unit III sequence is of middle Eocene age.

The chalks of Unit III consist of foraminifer-bearing nannofossil chalks at the top which grade quickly downhole into the more common nannofossil chalks that characterize the unit. In the more complete sequence in Hole 713A, calcareous nannofossils dominate the carbonate fraction down through the base of Core 115-713A-8R, typically making up 60%–90% of the sediment. Foraminifers reach a maximum abundance of 10%–12% near the top of Unit III and rarely reach more than a few percent further downhole. In Core 115-713A-9R and deeper cores, most of the fine carbonate in the chalk is unidentifiable and could be of either nannofossil or shallow-water origin. Because of this uncertainty, we use the term "micritic chalk" to describe this particular lithology. Chalks preserved within the basalt, however, in Cores 115-713A-15R, -16R, and -17R, are clearly of nannofossil origin.

Volcanic-ash layers increase in frequency toward the base of the unit, generally averaging a few centimeters in thickness, and are interspersed at intervals ranging from 3 to 5 cm to a few tens of centimeters. The ash layers appear to vary widely in composition, based on color differences and our observations of widely different alteration states of the volcanic glass in smear slides. Many of the ash layers have sharp bases and preserve sedimentary structures, including graded bedding ranging from coarse sand to silt-sized, parallel laminae, and cross-stratification (Fig. 6). These features seem to indicate that at least some of the ash layers were deposited as turbidites, in addition to those which settled out of suspension in a more typical fashion.

The purest chalk layers are white (10YR 8/2, 8/3, 7/3), light gray (2.5Y 7/2, 10YR 7/2), and very pale brown (10YR 8/3). The most concentrated ash layers range from black (N2) to grayish brown (2.5Y 5/2), very dark gray (N3), and very dark grayish brown (2.5Y 3/2). Most chalk layers between the ash layers contain variable proportions of dispersed and altered volcanic ash, which causes colors to vary typically between gray (5Y 5/1), light olive brown (2.5Y 5/4), and light brownish gray (2.5Y 6/2).

A relatively thick and unconsolidated trachytic volcanic ash, very fresh in appearance, was observed in Sample 115-713A-10R-2, 13–41 cm. Below this major ash horizon, both sediments and ash have an olive green tint to them, suggesting a possible redox transition in the sediment column. Chalks throughout the rest of the unit are light olive gray to pale olive (5Y 7/2, 6/2, 6/3), and light greenish gray to greenish gray (5GY 7/1–6/1). When not black (N2), ash layers tend to be dark green (5G 4/1) to dark greenish gray (5GY 4/1). This greenish hue to both chalks and ash is also found in those sediments recovered from within the basement in Cores 115-713A-15R, -16R, and -17R.

Minor lithologies that occur in Unit III include clay-bearing nannofossil chalk, nannofossil clay, and nannofossil-bearing clay. These clay-rich intervals are typically very pale brown (10YR 7/3) to light yellowish brown (10YR 6/4), or greenish gray (5GY 7/1) to grayish olive green (5GY 3/2), and occur as thin lenses within the predominantly chalk/ash sequence. In general, the average clay content of sediments intercalated within the basalt flows is higher than in those sediments overlying the basement.

Sediments of Unit III also preserve evidence of considerable local tectonic activity in the form of microfaulting, shearing, fracture filling, and numerous types of soft-sediment deforma-

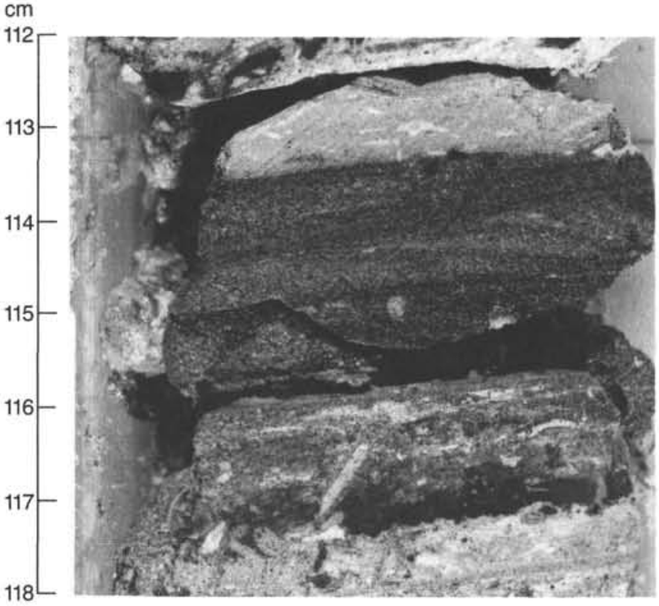

Figure 6. Cross-stratification observed in a volcanic-ash bed (115-713A-7R-1, 112–118 cm).

tion. Microfaults are both normal and reversed, recording both extensional and compressional stress fields, and several generations of faulting may be visible in a single core. We can see some of the more spectacular examples of these microfaults in Figures 7 and 8.

Summary

Sediments at these two adjacent sites record a history of interrupted deposition and considerable local volcanic and tectonic activity. The absence of Subunit IB and Unit II sediments in Hole 713A can be explained by a major hiatus at about 30 mbsf which represents a gap in time of approximately 36 m.y. At Site 713, the late Miocene nannofossil oozes of Unit IA directly overlie the middle Eocene chalks and ashes of Unit III. A similar hiatus, although representing a much shorter interval of time, has been inferred from paleontologic data at Site 712, where the late Oligocene carbonate sands and rubble of Unit II also overlie the sediments of Unit III. Site 712, therefore, represents a somewhat more complete sequence.

BIOSTRATIGRAPHY

Introduction

The sedimentary sequences recovered by rotary drilling at both Sites 712 and 713, located only 1.6 nmi apart, show similar lithologies and microfossil contents. These sequences can be described from top to bottom as follows:

1. At Sites 712 and 713, the upper 57.5 m and 30.5 m of the sediment column, respectively, consist of a foraminifer-nannofossil ooze of Pleistocene through middle Miocene age, which grades downhole into a semi-indurated chalk.
2. At Site 712, a 48-m thick sequence (57.5–105.5 mbsf), largely unrecovered, is tentatively identified as an unconsolidated section of coarse carbonate sands and limestone rubble of presumably late Oligocene age.
3. A 9.8-m thick sequence (105.5–115.3 mbsf) at Site 712 and a 76.5-m thick sequence (30.5–107.0 mbsf) at Site 713 consist of a complexly interbedded section of fine-grained chalk and volcanic ashes of middle Eocene age.

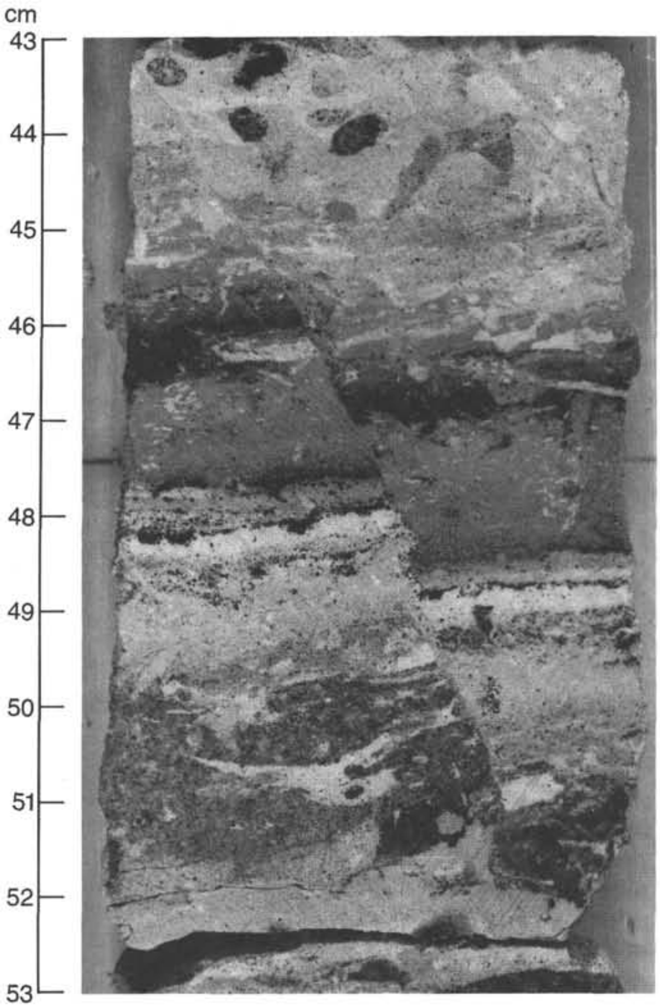

Figure 7. A typical example of microfaulting observed in the interbedded nannofossil chalk and volcanic-ash sequence of Unit III (115-713A-11R-2, 43–53 cm).

Calcareous nannofossils are abundant throughout the sediments recovered. Preservation is generally moderately good, with various degrees of recrystallization coupled with slight dissolution. In a few intervals, poor preservation is recorded by extensive overgrowth of discoasters.

Planktonic foraminifers are abundant throughout the Neogene; they are well preserved in the Pliocene-Pleistocene and moderately well preserved in the Miocene. In Oligocene sediments, planktonic foraminiferal faunas show mixed assemblages, including reworked Eocene faunas and contamination by Pliocene forms displaced by drilling disturbance. Middle Eocene planktonic foraminiferal faunas are poorly preserved.

Moderately well-preserved benthic foraminifers are present throughout the sedimentary sequence. These assemblages are typical of deep-water faunas.

Siliceous microfossils are present in upper Neogene sediments. Radiolarians are well to moderately well preserved, being common in the Pliocene and decreasing in abundance in the upper Miocene. Diatoms are common to few in that interval and are generally moderately to poorly preserved. The remainder of the sequence is almost barren of siliceous fossils except for an interval in the middle Eocene of Site 713 which yielded rare and poorly preserved radiolarians.

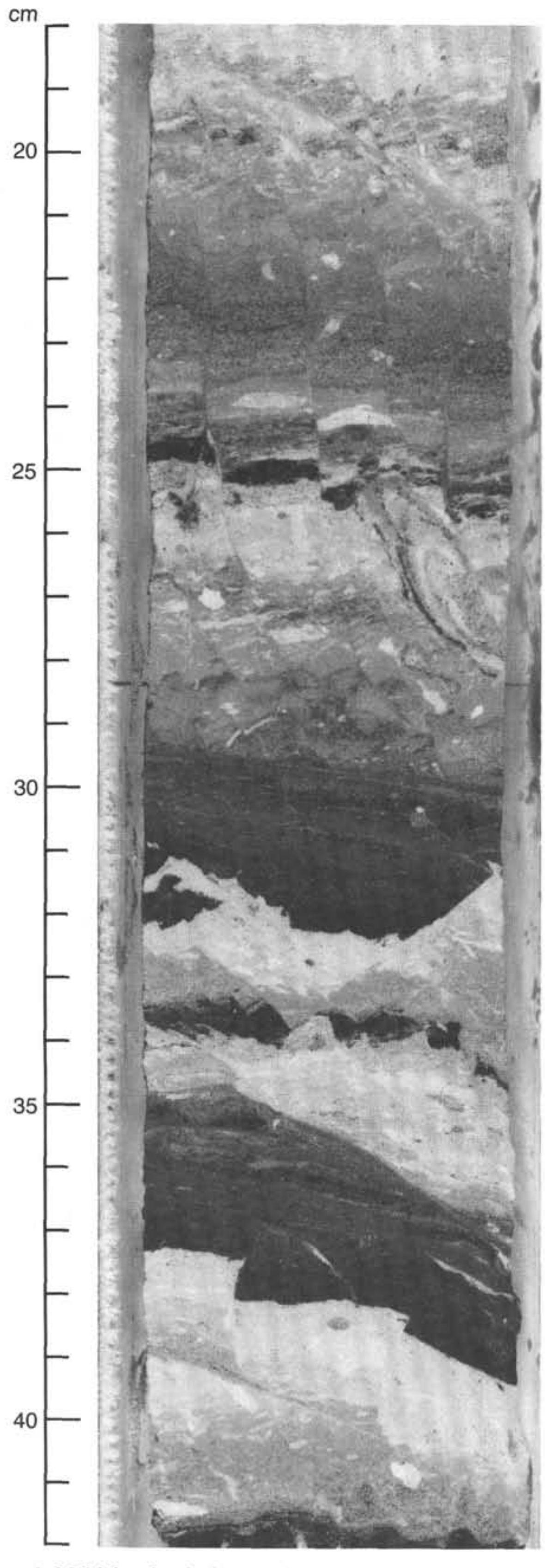

Figure 8. Multiple microfaults record several phases of deformation in Unit III sediments in this example (115-713A-11R-2, 18–42 cm).

A biostratigraphic summary for Sites 712 and 713 is presented in Figures 9 and 10.

Calcareous Nannofossils

Hole 712A

Although we recovered Pleistocene to middle Eocene assemblages, major hiatuses were observed at Hole 712A. The intervals represented by these hiatuses include a major portion of the Pleistocene (CN14) as well as intervals within the upper Miocene (CN7), the upper middle Miocene (CN5), the lower Miocene to uppermost Oligocene (CN3–CP19b), and the lower Oligocene to upper middle Eocene (CP18–CP14b). Nannofossils are generally moderately well preserved, with varying degrees of recrystallization coupled with slight dissolution. Due to the heavy recrystallization, however, identification is difficult in occasional intervals within the Neogene sequence.

Pleistocene

We did not recognize Pleistocene calcareous nannofossils in this sequence except at the very top of Core 115-712A-1R, where *Gephyrocapsa oceanica* occurs together with abundant late Pliocene calcareous nannofossils. Because the underlying sample (115-712A-1R-1, 70 cm) contains a noncontaminated upper Pliocene assemblage, the Pleistocene sequence was estimated to be less than 70 cm thick at Hole 712A.

Pliocene

Cores 115-712A-1R and -2R are Pliocene in age. The upper two sections of Core 115-712A-1R contain a poorly preserved assemblage assignable to upper Pliocene Zone CN12. In Sample 115-712A-1R-2, 70 cm, we observed the last occurrence (LO) of *Sphenolithus abies* (3.45 Ma).

The LO of *Reticulofenestra pseudoumbilica* (3.56 Ma) occurs in the underlying Sample 115-712A-1R-3, 50 cm. The first occurrences (FO) of *Ceratolithus rugosus* (base of Subzone CN10c) and *Ceratolithus acutus* (base of Subzone CN10b) were observed in Sample 115-712A-2R-5, 75 cm, and Section 115-712A-2R, CC, respectively. We located the Miocene/Pliocene boundary between this section and Sample 115-712A-3R-1, 75 cm, where we observed the LO of *Discoaster quinqueramus*.

Miocene

Cores 115-712A-3R to -6R yielded Miocene assemblages. Nannofossils are moderately well preserved in this sequence, except for the occasional interval in which extensive overgrowth of discoasters was observed.

The assemblage observed in the interval between Samples 115-712A-3R-1, 75 cm, and 115-712A-4R-2, 80 cm, is assigned to upper Miocene Subzone CN9b. Three ceratolith species, *Amaurolithus delicatus, A. primus*, and *A. tricorniculatus*, associated with abundant *Discoaster berggrenii* and *D. quinqueramus*, were observed in this assemblage. Calcareous nannofossils are well preserved in this interval, and the assemblage is quite diversified.

Sample 115-712A-4R-2, 93 cm, and two samples taken from Section 115-712A-5R-1 (at intervals of 40–41 cm and 130–131 cm) yielded common *Discoaster neohamatus*, but no *D. quinqueramus*. This assemblage is assigned to Zone CN8 (NN10), and a hiatus spanning the lower part of Zone CN9b to the upper part of CN8 is possible in Section 115-712A-4R-2.

Sample 115-712A-5R-2, 40–41 cm, and Section 115-712A-5R, CC, are assignable to Zones CN7 and CN6, respectively. We assigned Core 115-712A-6R to the early-middle Miocene Zone CN4 (NN5). Since the entire interval representing Zone CN5 (10.8–13.2 Ma) is missing, another hiatus is inferred between Cores 115-712A-5R and -6R.

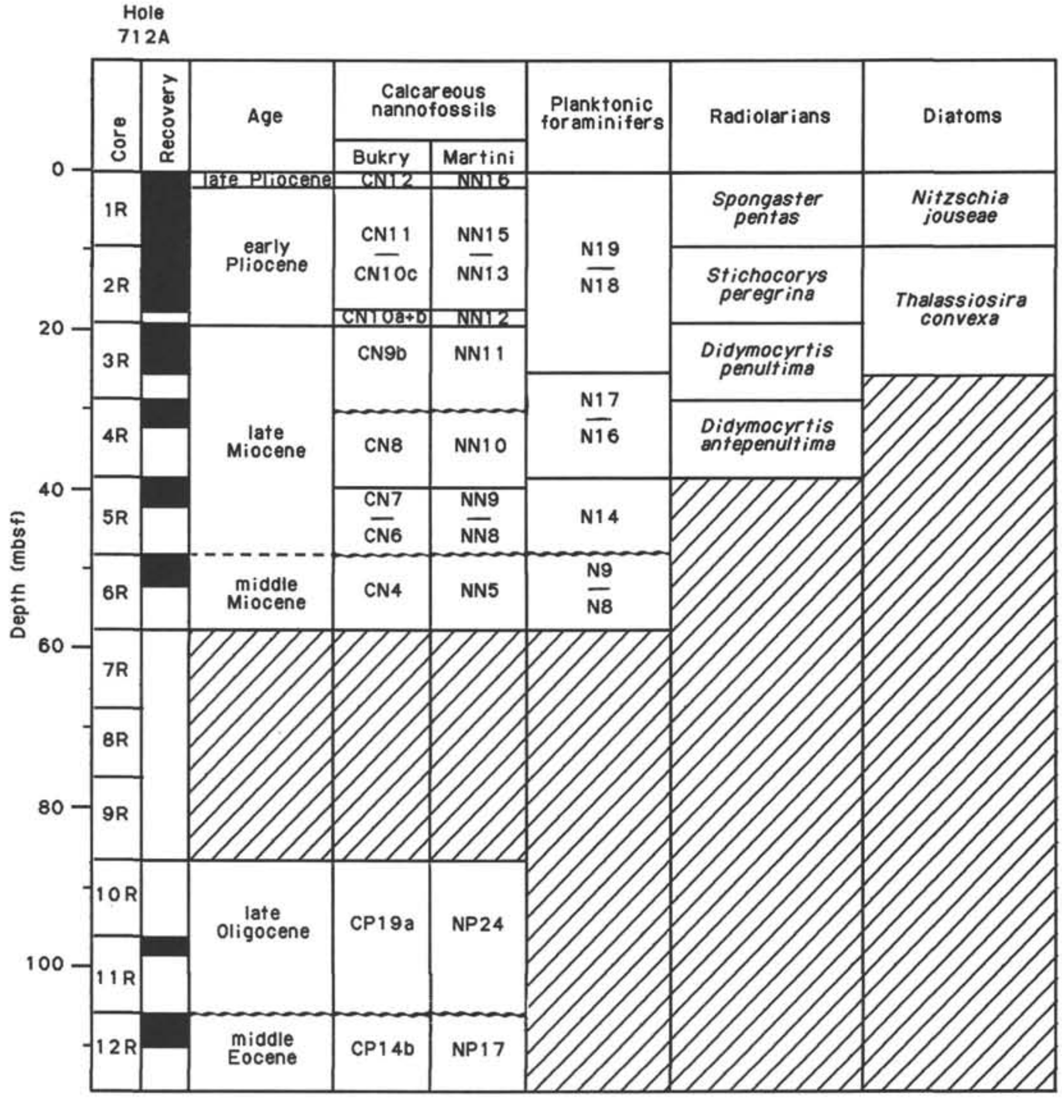

Figure 9. Biostratigraphic summary for Site 712. Black bars represent recovery in Hole 712A.

Cores 115-712A-7R and -9R were empty, while Core 115-712A-8R recovered only three limestone pebbles in the core catcher. They were all barren of nannofossils.

Oligocene

Core 115-712A-10R recovered only a small amount of sediment in the core catcher, and Core 115-712A-11R recovered 2.3 m of sediment. These materials can be assigned to the upper Oligocene Subzone CP19a. *Sphenolithus ciperoensis* was not abundant but was consistently present in these cores.

Eocene

We assigned the entire portion of sediment recovered in Core 115-712A-12R to the upper middle Eocene Subzone CP14b. Thus, another hiatus encompassing the late Eocene to early Oligocene is inferred at Site 712. The nannoflora contains abundant *Coccolithus pelagicus* and *Discoaster floridanus*. Other major components of the assemblage include *Bramletteius serraculoides, Discoaster barbadiensis, Sphenolithus spiniger, S. furcatulithoides*, and *Reticulofenestra samodurovii*. The oldest sediment recovered in Hole 712A is of middle Eocene age (42.3–46.0 Ma).

Hole 713A

Pleistocene through late Miocene and middle Eocene assemblages were recovered at Site 713A. Except in the Pleistocene, where the preservation is good, nannofossils are moderately well preserved throughout the sequence. Moderate recrystallization is ubiquitous, and dissolution is negligible.

The LO of *Chiasmolithus gigas* (47.0 Ma) was observed in a thin sediment layer intercalated within basalt flows which underlie the sediment column. Future radiometric dating of the two basalt flows which enclose this layer will provide essential data for the dating of this event.

Pleistocene

Because of the heavy disturbance caused by rotary drilling, we did not examine any samples from Section 115-713A-1R-1. The interval between Section 115-713A-1R, CC, and Sample 115-713A-2R-2, 40–41 cm, yielded abundant *Gephyrocapsa oceanica* and *Pseudoemiliania lacunosa*, and was assigned to Subzone CN14a. Sample 115-713A-2R-3, 40–41 cm, contained no *G. oceanica*, but *Discoaster brouweri* occurred in abundance. The Pliocene/Pleistocene boundary, therefore, is likely to be located within the lower part of Section 115-713A-2R-2. Reworked

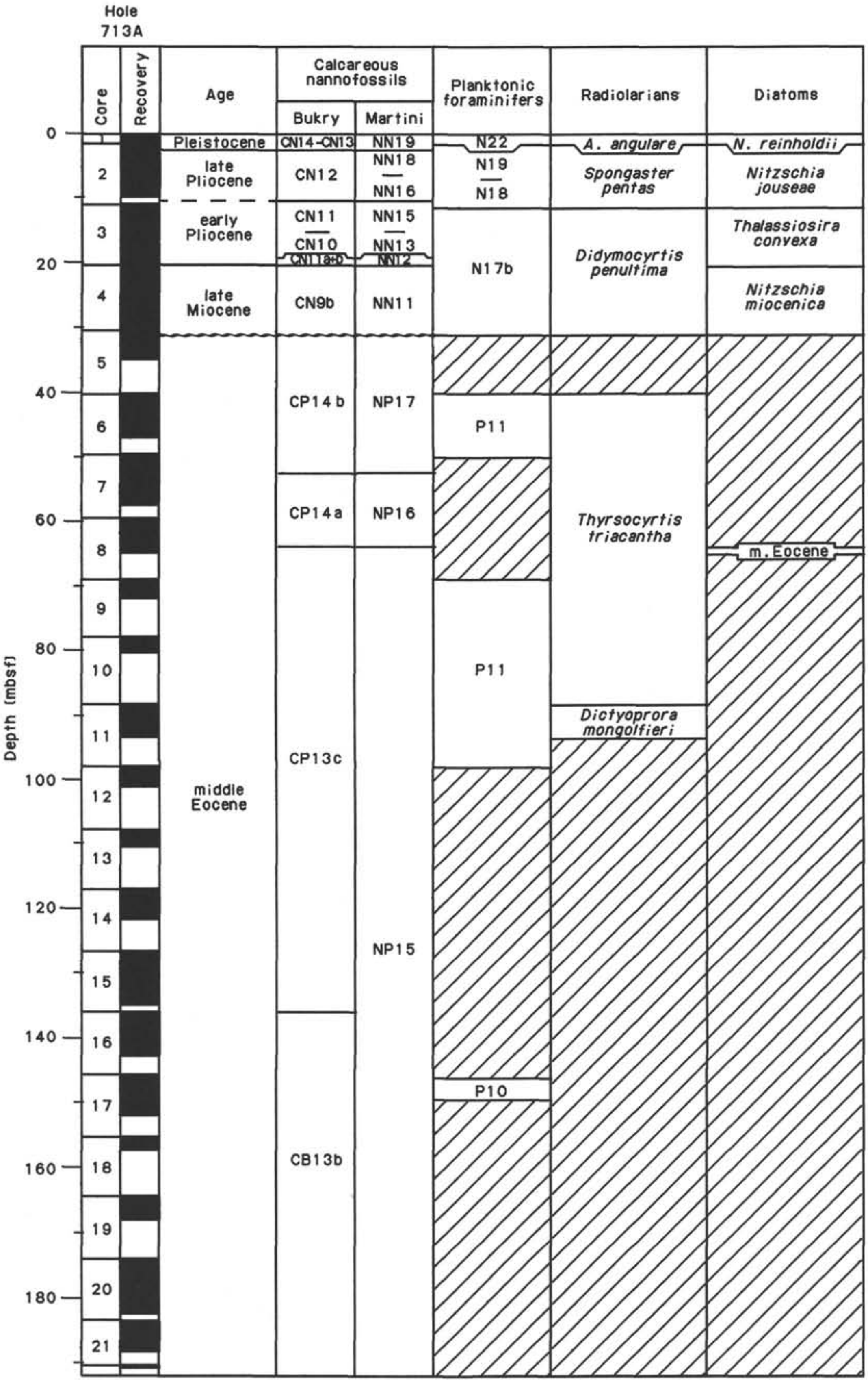

Figure 10. Biostratigraphic summary for Site 713. Black bars represent recovery in Hole 713A.

Pliocene forms are abundant in the few investigated samples of the Pleistocene sequence.

Pliocene

The LO of *Reticulofenestra pseudoumbilica*, which approximates the lower/upper Pliocene boundary, was detected in Section 115-713A-2R, CC. The interval between Samples 115-713A-2R-3, 50 cm, and 115-713A-2R-6, 50 cm, was assigned to the upper Pliocene Zone CN12.

We located the Miocene/Pliocene boundary between Sample 115-713A-3R-6, 75 cm (the FO of *Ceratolithus acutus*) and Section 115-713A-3R, CC (the LO of *Discoaster quinqueramus*). The interval between the latter sample and Section 115-713A-2R, CC, is assigned, therefore, to Zones CN10 and CN11. We observed the FO of *Ceratolithus rugosus* (base of Subzone CN10b) in Sample 115-713A-3R-6, 75 cm.

Thus, the upper Pliocene is represented by approximately 6 m of sediments, whereas the lower Pliocene is represented by approximately 9 m of sediments.

Miocene

Core 115-713A-4R yielded an assemblage indicative of late Miocene Subzone CN9b. Calcareous nannofossils are well preserved in this interval, and solution-susceptible forms such as *Scyphosphaera* spp. and *Helicosphaera* spp. were frequently observed with no visible sign of dissolution.

Eocene

Eocene assemblages were recovered from Cores 115-713A-5R through -21R. Nannofossils are moderately well preserved in this sequence with slight to moderate recrystallization.

We assigned the interval between Sections 115-713A-5R-1 and 115-713A-8R-3 to the upper middle Eocene Zone CP14, and the LO of *Chiasmolithus solitus* in Sample 115-713A-7R-3, 55-56 cm, marks the top of Subzone CP14a. As was observed in previous sites of Leg 115, the relative abundance of *Reticulofenestra umbilica* varies greatly between samples, and the thickness of Subzone CP14a is unproportionally thin compared with that of Subzone CP14b.

The sequence between Sections 115-713A-8R-4 and 115-713A-12R-2 can be referred to Subzone CP13c. The assemblage in this interval is dominated by *Cyclicargolithus floridanus*, and the major components of the flora are similar to those observed at Sites 707, 709, and 711.

We recovered the first samples of basalt between Sections 115-713A-12R, CC, and 115-713A-15R-5. Below this layer of basalt, a sequence of fossiliferous pyroclastic sediment was recovered between Sections 115-713A-15R-5 and 115-713A-17R, CC. The assemblage observed in the interval between Sample 115-713A-15R-5, 130 cm, and Section 115-713A-15R, CC, can be assigned to Subzone CP13c, the same subzone assigned to the sediment directly overlying the basalt.

The LO of *Chiasmolithus gigas* (47.0 Ma) was observed in Sample 115-713A-16R-1, 17-18 cm, and the sedimentary sequence between this sample and the bottom of Core 115-713A-17R is assignable to the middle Eocene Subzone CP13b (47.0-48.8 Ma). Heavily overgrown *Nannotetrina* spp. were a common member of the flora, and we also noticed rare occurrences of *Nannotetrina alata*.

From Core 115-713A-18R to the deepest core of this hole (115-713A-22R), basalt was again drilled and partially recovered. As we observed at Sites 706 and 707, small pieces of fossiliferous sediment, baked into the basalt, were again recovered. Samples 115-713A-20R-4, 112-113 cm, and 115-713A-21R-2, 143-144 cm, yielded heavily overgrown *C. gigas*, enabling assignment of the assemblage to Subzone CP13b. Sphenoliths and large species of placoliths such as *Coccolithus eopelagicus* and *Chiasmolithus grandis* were heavily overgrown, but smaller species such as *Campylosphaera dela, Helicosphaera seminulum*, and *Pontosphaera plana* were relatively free from recrystallization.

The age of the igneous activity at this site is well established by nannofossil biostratigraphy: the main activity occurred between 47 and 48.8 Ma, and the last episode of activity occurred between 46 and 47 Ma.

Planktonic Foraminifers

Neogene

Site 712

Planktonic foraminifers are abundant throughout the Neogene, being well preserved in the Pliocene interval and moderately well preserved in the Miocene.

Sections 115-712A-1R, CC, through 115-712A-3R, CC, are assigned to the lower Pliocene zonal interval N19-N18. Sections 115-712A-1R, CC, and 115-712A-2R, CC, contain common *Globorotalia tumida* and *G. limbata* and rare *G. plesiotumida*. The common occurrence of *Dentoglobigerina altispira* and *Sphaeroidinellopsis* spp. in these samples indicates an age older than 3 Ma for the uppermost Section 115-712A-1R, CC. The assemblage in Section 115-712A-3R, CC, is similar to those in Sections 115-712A-1R, CC, and 115-712A-2R, CC. The species *G. tumida*, however, is rare and shows primitive forms, which places this sample in the lower part of the zonal interval in the basal Pliocene.

Section 115-712A-4R, CC, is assigned to the upper Miocene interval N16-N17. The assemblage in this sample is dominated by the two solution-resistant forms *Globoquadrina venezuelana* and *Sphaeroidinellopsis* spp. and contains rare specimens of the menardiform complex *Globorotalia limbata-plesiotumida-merotumida*. We did not find species of *Pulleniatina*, which may have been eliminated by dissolution. Section 115-712A-5R, CC, is assigned to Zone N14 based on the co-occurrence of *Paragloborotalia siakensis, P. mayeri*, and *Globigerina nepenthes*. Section 115-712A-6R, CC, is assigned to the zonal interval N8-N9 based on the presence of *Globigerinoides sicanus*.

Site 713

Planktonic foraminifers are abundant throughout the Neogene sequence, being, as at Site 712, well preserved in the Pliocene-Pleistocene and moderately well preserved in the Miocene (Sections 115-712A-3R, CC, and 115-712A-4R, CC).

Section 115-713A-1R, CC, belongs to Zone N22 based on the presence of rare *Globorotalia truncatulinoides*. The co-occurrence of the latter species with *Globigerinoides fistulosus* (also rare) places this sample in the lower part of the zone between 1.6 and 1.9 Ma. Section 115-713A-2R, CC, belongs to the lower Pliocene interval N19-N18. It contains common *Globoratalia limbata* and *Dentoglobigerina altispira* and rare *Sphaeroidinellopsis* spp. The presence of the latter two species indicates an age older than 3 Ma for this sample. Sections 115-713A-3R, CC, and 115-713A-4R, CC, belong to the upper Miocene Zone N17b based on the presence of rare *Globorotalia plesiotumida* and rare *Pulleniatina primalis*.

Paleogene

Paleogene planktonic foraminifers were recovered in middle Eocene-Oligocene levels of both Sites 712 and 713. Because Oligocene sediments contain a melange of Pliocene through middle Eocene planktonic foraminifers in a matrix of drill-damaged carbonate fragments, the samples were not studied in detail.

Middle Eocene samples (Sections 115-712A-11R-1 to 115-712A-12R, CC, and Section 115-713A-5R, CC, to Sample 115-

713A-17R-2, 118 cm) contained poorly preserved planktonic foraminiferal faunas in more or less indurated volcanic sediments. The characteristic green minerals in this sediment indicate submarine volcanism. In the few samples where whole planktonic specimens could be retrieved, a solution-resistant fauna dominated by the *Globigerinatheka conglobata* group also included *Acarinina densa, Morozovella aragonensis, M. acuta, Subbotina eocaena*, and *S. gortanii*. This fauna belongs to middle Eocene Zone P11, probably the top of the zone. The only well-preserved fauna from Site 713 (Sample 115-713A-17R-2, 118 cm) was assignable, instead, to Zone P10 because of the lack of *Globigerinatheka semiinvoluta* in a fauna dominated by morozovellids and the *G. subconglobata* group, but lacking the large subbotinids typical in Zone P11 above.

Benthic Foraminifers

Moderately well-preserved, deep-water benthic foraminifers were present in the majority of Pliocene- through Eocene-age cores recovered at Sites 712 and 713. In the middle Eocene just above basement (Cores 115-713A-9R through -15R), foraminifers were difficult to separate from the volcanic ash and glass, and few were recovered intact. In one level (Sample 115-713A-17R-2, 118 cm), a good benthic fauna was recovered and could be used to estimate that the site lay at deep water depths (> ~ 1800 m) in the early middle Eocene.

Miocene-Pliocene

The early Pliocene through late Miocene (Zone CN12–CN9b) portion of the record at Site 713 was found in Cores 115-713A-1R through -3R). Although the sediments were coarse grained and occasionally formed a slurry, *in-situ* faunas were delimitable and at least one emigration episode of abyssal benthic foraminifers was recognized. The early Pliocene deep-water fauna at Sites 712 and 713, an association of *Melonis pompilioides* and *Uvigerina proboscidea–Globocassidulina subglobosa*, also included *Uvigerina auberiana*, the poreless morph of *Cibicides wuellerstorfi, Cibicidoides kullenbergi, Bulimina rostrata, Melonis affinis, Stilostomella subspinosa*, and *Ehrenbergina spinosissima*.

Miliolids, represented by the quinqueloculinids, were infrequent and cibicidids were rare. Brizalinids entered the faunas for most of the late Miocene; species included *Brizalina subaenariensis* and *B. pusilla*. The ehrenberginids were more common in the Pliocene; the globocassidulinids, in the late Miocene. Occasional large nodosariid fragments were present but not consistently. The most common agglutinant is *Martinottiella petrosa*. The austral species, *Hopkinsina mioindex*, is present throughout the sequence.

This fauna is in sharp contrast to the late Miocene–early Pliocene deep-water fauna at Site 709, a *Favocassidulina favus-Gyroidinoides soldanii* assemblage accompanied by a large component of the tropical, intermediate-water Car Nicobar fauna (Srinivasan and Sharma, 1980), including *Chrysalogonium equisetiformis, Nodosaria skobrina, Orthomorphina setosa, Triloculina lucernula*, and *Cibicidoides cicatricosus*. At Site 709, faunas were composed of much larger individuals of each species and were much higher in diversity and benthic number.

Contrasts between the two deep-water faunas and their geographic locations suggest that bottom conditions were significantly different at Sites 709 and 712/713. The faunal composition at Sites 712/713 is typical of deep-water faunas, in general. The presence of the hispid uvigerinids in low numbers suggests low rates of sediment accumulation and oxidizing conditions (Boersma, 1984). The influx of brizalinids in the late Miocene suggests slightly lower oxygen conditions (Douglas and Heitman, 1979) than at Site 709.

Early-Middle Miocene

Benthic foraminifers were rare in the poorly preserved middle Miocene sediments at Site 712 (Cores 115-712A-5R and -6R). Deep-water faunas were dominated by generalists and rotaloid forms including *Oridorsalis umbonatus, Globocassidulina subglobosa, Gyroidinoides girardana, Cibicidoides kullenbergi*, and *C. havanensis*. The most common buliminid was *Bulimina consanguinea* and the stilostomellid, *Stilostomella subspinosa*. No uvigerinids were found in these faunas. Chunks of micritized carbonate and a few shallower-water benthic foraminifers in these samples suggest moderate sediment redeposition.

Paleogene

Oligocene sediments are badly preserved, and at Site 712 whole specimens exist in a finer-grained matrix of angular carbonate particles produced during drilling. Some samples (e.g., Sample 115-712A-11R-1, 0 cm) contain a mixture of Pliocene through Eocene planktonic foraminifers apparently emplaced both through reworking and by the drilling process.

We recovered Eocene-age samples at Site 713 where sediments were composed largely of ash, glass, and other volcanic debris. In most samples above basement, the benthic foraminifers were dissolved. The poorly preserved faunas just above basement (Section 115-713A-11R-2) contained a small, probably deep- or deep-intermediate-water fauna, including pullenids and lenticulinids similar to the deep-water form, *Lenticulina vortex*. The presence of one very large upper bathyal, flat lenticulinid suggests downdepth sediment redeposition.

At one level within basement, a well-preserved foraminiferal ooze was recovered (Sample 115-713A-17R-2, 118 cm). The fauna includes *Globocassidulina subglobosa, Anomalinoides acuta, A. aragonensis, Cibicidoides subspiratus, Heterolepa grimsdalei, Nutallides truempyi, Bulimina semicostata*, and *Hanzawaia ammophila*, the *H. cushmani* morph. This fauna is similar to that at Site 709C in the middle Eocene and is indicative of moderately deep water (Tjalsma and Lohmann, 1983).

Radiolarians

Site 712

Identifiable radiolarians at Site 712 are present only within the upper Neogene cores. We made the following zonal assignments on the basis of shipboard sample analysis.

Section 115-712A-1R, CC, may be assigned to the *Spongaster pentas* Zone of early Pliocene age. Radiolarians are common and well preserved. Diagnostic taxa include *Phormostichoartus doliolum, P. fistula, Lychnodyctium audax, Stichocorys peregrina*, and *Didymocyrtis avita*.

We assigned Section 115-712A-2R, CC, to the *Stichocorys peregrina* Zone of early Pliocene age. Radiolarians are common and moderately preserved. Diagnostic taxa include *Solenosphaera omnitubus, Didymocyrtis penultima*, and *Stichocorys peregrina*.

The *Didymocyrtis penultima* Zone of late Miocene age occurs in Section 115-712A-3R, CC. Radiolarians are few and moderately preserved. Diagnostic taxa include *Stichocorys delmontensis, Solenosphaera omnitubus, Didymocyrtis penultima, Dendrospyris bursa*, and *Siphostichartus corona*.

Section 115-712A-4R, CC, may be assigned to the *Didymocyrtis antepenultima* Zone of late Miocene age. Radiolarians are rare and only moderately preserved, with sponge spicules dominating the coarse fraction. Diagnostic radiolarian taxa include *Didymocyrtis antepenultima, Diartus hughesi, Stichocorys johnsoni*, and *S. delmontensis*.

Sections 115-712A-5R, CC, and 115-712A-6R, CC, are barren of radiolarians. Sections 115-712A-7R, CC, through 115-

712A-10R, CC, were empty. Sections 115-712A-11R, CC, and 115-712A-12R, CC, are also barren of radiolarians.

Site 713

Identifiable radiolarians are present within two stratigraphic intervals at Site 713: the late Neogene and the middle Eocene. We made the following zonal assignments:

Section 115-713A-1R, CC, may be assigned to the *Anthocyrtidium angulare* Zone of Quaternary age. Radiolarians are few and moderately preserved. Diagnostic taxa include *Anthocyrtidium angulare, A. ophirense, A. zanguebaricum, Theocorythium trachelium*, and *Didymocyrtis tetrathalamus*.

Section 115-713A-2R, CC, may be assigned to the *Spongaster pentas* Zone of early Pliocene age. Radiolarians are common and well preserved. Diagnostic taxa include *Phormostichoartus doliolum, P. fistula, Anthocyrtidium michelinae, Stichocorys peregrina*, and *Lychnodyctium audax*.

We assigned Samples 115-713A-3R-4, 70–75 cm, through Section 115-713A-4R, CC, to the *Didymocyrtis penultima* Zone of late Miocene age. Radiolarians are common and well preserved. Diagnostic taxa include *Didymocyrtis penultima, Stichocorys delmontensis, S. johnsoni, Phormostichoartus doliolum, Anthocyrtidium michelinae, A. jenghisi, A. pliocenica*, and *Dendrospyris bursa*.

Samples 115-713A-5R-2, 70–75 cm, through Section 115-713A-5R, CC, are barren of radiolarians.

The *Thyrsocyrtis triacantha* Zone of middle Eocene age occurs in Samples 115-713A-6R-2, 70–75 cm, through Section 115-713A-10R, CC. Radiolarians are rare and poorly preserved in the upper part of this interval and improve significantly in both abundance and preservation downward. Diagnostic taxa include *Podocyrtis papalis, P. phyxis, Thyrsocyrtis triacantha, T. rhizodon, Eusyringium fistuligerum, E. lagena, Sethochytris babylonis, Dictyoprora amphora, D. mongolfieri, Calocyclas hispida*, and *Phormocyrtis striata striata*.

Samples 115-713A-11R-3, 70–75 cm, may be assigned to the *Dictyoprora mongolfieri* Zone of middle Eocene age. Radiolarians are common and well preserved. Diagnostic taxa include *Dictyoprora mongolfieri, Eusyringium lagena, Thyrsocyrtis tensa, Lithocyclia ocellus*, and *Podocyrtis sinuosa*.

Diatoms

Site 712

Of the 12 cores recovered at Site 712, diatoms are present in the three uppermost core-catcher samples of early Pliocene–late Miocene ages.

Section 115-712A-1R, CC, contains a well-preserved and diversified assemblage, which includes such age-diagnostic species as *Nitzschia jouseae, N. reinholdii, Thalassiosira convexa* var. *aspinosa*, and *T. oestrupii*, referring the sample to the early Pliocene *N. jouseae* Zone.

The diatom assemblage of Section 115-712A-2R, CC, is less diversified and more poorly preserved. It contains *T. convexa* var. *aspinosa* but lacks *N. jouseae, Nitszchia miocenica*, and *Thalassiosira miocenica*, placing the sample in the upper part of the early Pliocene–late Miocene *T. convexa* Zone.

Diatoms are fairly common but moderately to poorly preserved in Section 115-712A-3R, CC. The flora includes *T. convexa* var. *aspinosa* and *N. miocenica*, which places the sample in the lower part of the *T. convexa* Zone. No diatoms are present in core-catcher samples below Section 115-712A-3R-3, CC.

Site 713

Of the 11 cores recovered above the first basalt flow in Hole 713A, diatoms are present only in the four uppermost core-catcher samples of early Pleistocene to late Miocene ages. Furthermore, a few valve fragments are present in two core-catcher samples of middle Eocene age.

Section 115-713A-1R, CC, contains a very poorly preserved assemblage, which is referred to the *Nitzschia reinholdii* Zone based on the silicoflagellate *Mesocena quadrangula*.

The diatom flora of Section 115-713A-2R, CC, is poorly preserved, with only a few specimens of the age-diagnostic *N. jouseae* present. We did not observe *Rhizosolenia praebergonii* and therefore referred the sample to the *N. jouseae* Zone.

Sections 115-713A-3R, CC, and 115-713A-4R, CC, yielded diatom floras which are diversified and moderately preserved. Section 115-713A-3R, CC, is placed in the *Thalassiosira convexa* Zone based on the presence of *T. miocenica*. Section 114-713A-4R, CC, contains *Nitzschia cylindrica, N. miocenica, N. marina*, and *Rhizosolenia praepaleacea*, placing the sample in the lower part of the *N. miocenica* Zone. A few fragments of mainly neritic, and presumably middle Eocene, diatoms of the genera *Triceratium* sp. and *Melosira* sp. are present in Sections 115-713A-7R, CC, and 115-713A-8R, CC. The remainder of the Eocene core-catcher samples are barren of diatoms.

PALEOMAGNETICS

Introduction

Because the sediments recovered at Sites 712 and 713 were rotary cored, they are likely to be highly disturbed. Consequently, our study of their paleomagnetic signature consisted of an analysis of several discrete sediment samples taken from the least disturbed intervals. The basement sections recovered at Site 713 do not appear to be unduly disturbed; unfortunately, these rocks were too highly magnetized to be measured with the pass-through magnetometer system.

Results

Sediments

Three sediment samples taken from the Eocene chalk in Core 115-712A-12R yielded poor results when subjected to progressive alternating-field (AF) demagnetization. The Zijderveld orthogonal projection diagram shown in Figure 11 (top) represents the best result obtained from this core. In this sample, there appears to be one or two relatively stable magnetization components, although these are not well isolated. For the most part, the demagnetization sequence is dominated by inconsistent magnetization directions, especially near the origin. Although the more stable initial portion of the demagnetization curve is not defined very well, these data (and data for the two samples not shown) suggest the presence of a component which points upward at a shallow angle.

The three chalk samples taken at Site 713 also give unstable results, as shown in Figure 11 (bottom). This sample, taken from the lowermost sediments overlying the basalts (Core 115-713A-11R), shows perhaps two components: the lower coercivity component is quite shallow (near 0°), while the higher coercivity component points upward at about 40°. A shallow component is also isolated in the progressive demagnetization of two sediment samples from Section 115-713A-12R-1 (at 76–78 cm and at 40–42 cm); however, the moderately steep component of Sample 115-713A-11R-2, 76–78 cm, does not appear clearly defined in Core 115-713A-12R.

We sampled 4 ash layers in sediments just above basement as well as 8 ash layers in those sediments found between the 2 basalt sequences. Of the 12 ash samples, we measured 7, and all showed relatively stable directions with positive inclinations. Typical results from one of these ash layers (Sample 115-713A-17R-4, 26–28 cm) shows a moderately shallow downward (presumably reversed polarity) component of magnetization (Fig. 12).

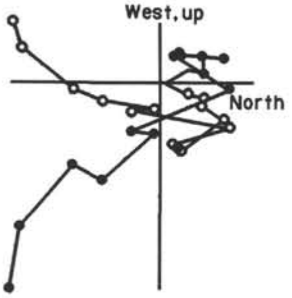

Sample 115-712A-12R-1, 114-116 cm

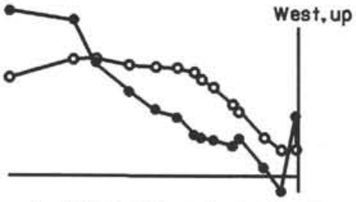

Sample 115-713A-11R-2, 76-78 cm

Figure 11. Zijderveld orthogonal projection diagram for chalk sediment samples. Open circles represent projection onto the vertical plane, closed circles represent projection onto the horizontal plane. Progressive demagnetization is by alternating-field (AF) treatment. No consistency in the declination of these rotary-drilled samples is expected.

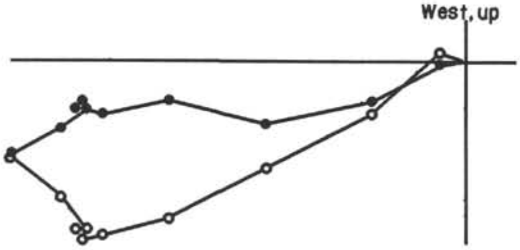

Sample 115-713A-17R-4, 26-28 cm

Figure 12. Zijderveld diagram for a sample from volcanic ash found in sediments between two basaltic sequences at Site 713. Demagnetization was achieved by AF treatment. Plotting conventions as in Figure 11.

Basalts

In contrast to the relatively weak and unstable magnetized sediments, the basalt samples show uniformly good magnetic behavior. The Zijderveld demagnetization diagrams for 6 typical basalt samples are shown in Figure 13. These 6, as well as 29 others measured, display stable and consistent directions. Most show shallow downward directions (presumably indicating reversed polarity), but 3 give moderately shallow upward (i.e., normal polarity) directions. The apparent normal polarity of these 3 samples may, however, be caused by errors in sample orientation. Sample 115-713-18R-2, 9–11 cm, for instance, shows a negative inclination (-28.4°), while Sample 115-713-18R-1, 136–138 cm, from the same unit shows a positive inclination (10.5°). Orientation problems are suspected also for the 2 other negative inclinations measured, since the natural remanent magnetization (NRM) of all other samples from the same units shows consistently positive inclinations (reverse polarity).

The paleomagnetic analysis of the basalt samples shows that AF treatment of 5–15 mT typically removes a low-coercivity component, and that subsequent demagnetization displays a univectorial decay to the origin. The results of principal component analysis for this higher-coercivity component are given in Table 2. Inclinations from the 27 basalt units combined with the 7 ash layer results give an average inclination of 24.0° (SD = 10.2°).

Discussion

Since the basement rocks produce far more convincing paleomagnetic directions, we will consider these first. The strong and stable remanence displayed in the high-coercivity component found in the basalt samples suggests that this is, in fact, a primary thermoremanent magnetization. The lower-coercivity component may be caused by viscous acquisition in the present-day field or, alternatively, may well be some form of drilling remanence. The large variation of the inclinations determined from the basalt and ash layers makes it difficult to assume that the directions are primary and that the scatter represents the normal secular variation of the field. If so, the maximum likelihood estimate of inclination ($I = 24.4°$, $N = 34$, kappa (κ) = 29.2, alpha 95 = 4.6°) might not be a good representation of the time-averaged field. This inclination corresponds to a paleolatitude of 12.8° ± 2.6°.

As the few chalk-sediment results appear to be of poor quality, these do not offer a reliable addition to the basalt and ash layer data. The shallow upward component found in the chalk samples could be a normal polarity primary field. In that case, the sediments would tend to support the basalt/ash results. It is more likely, however, that this shallow upward direction is simply a result of the present-day field.

Magnetic Susceptibility

Site 712

We measured magnetic susceptibility at intervals of 10 cm on all sections of cores recovered from Hole 712A. The rotary-drilled sequence obtained from this hole was both highly fragmented and also contaminated by drilling artifacts (probably pipe rust, although particles of rust were not observed during the course of susceptibility measurements). Contamination was suspected in the uppermost 10–20 cm of at least 3 out of the 10 cores in which sediment was recovered from this hole (Cores 115-712A-2R, -3R, and -4R). Susceptibility values, other than those attributable to contamination, were very low ($<5 \times 10^{-6}$ cgs) throughout the sequence of upper Oligocene to lower Pliocene foraminifer-nannofossil oozes and chalks, and clay-bearing foraminifer-nannofossil oozes. However, in the underlying volcanic-ash-rich limestones and foraminifer-bearing nannofossil chalks of middle Eocene to late Oligocene age, susceptibility values were generally much higher (between 1.5 and 9×10^{-5} cgs) and more variable. The results of susceptibility measurements made at Site 712 are not reproduced here.

Site 713

Magnetic susceptibility measurements were made at intervals of 10 cm on all sections of cores recovered from Hole 713A, to a depth of 101 mbsf (Cores 115-713A-1R through -12R). Susceptibility measurements were also made on the basaltic lava flow and basement rocks cored below 101 mbsf, but the results of these measurements are reported elsewhere (see "Basement Rocks," this chapter). Measurements were made with a Bartington Instruments' susceptibility meter (Model MS1) and a pass-through sensor-coil of 80-mm inner diameter (Model MS2C). The results of susceptibility measurements made on the sedimentary sequence overlying the basaltic lava flow at approximately 101 mbsf are shown in Figure 14.

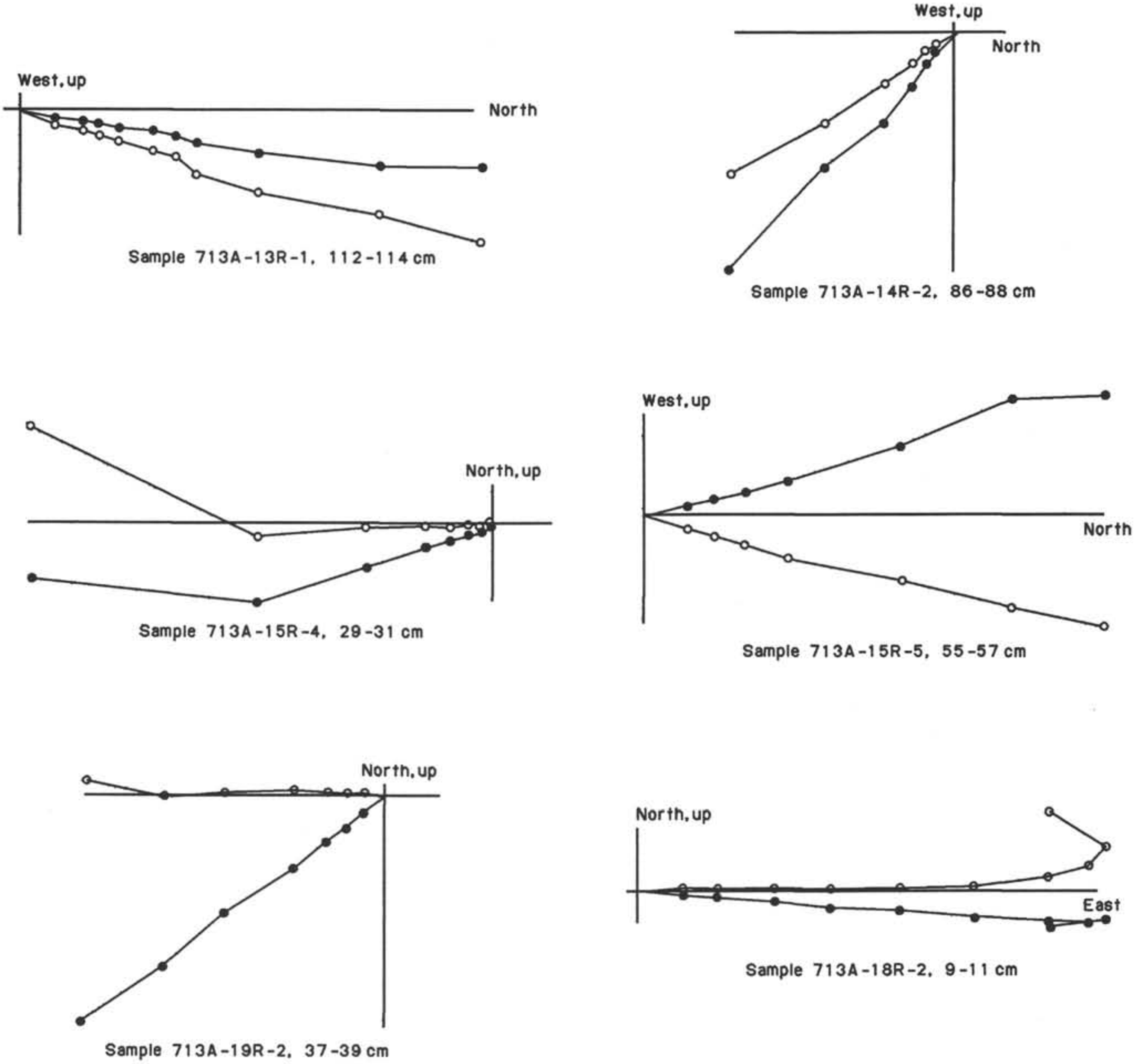

Sample 713A-13R-1, 112-114 cm

Sample 713A-14R-2, 86-88 cm

Sample 713A-15R-4, 29-31 cm

Sample 713A-15R-5, 55-57 cm

Sample 713A-19R-2, 37-39 cm

Sample 713A-18R-2, 9-11 cm

Figure 13. Zijderveld diagrams for six basalt samples showing typical behavior. All demagnetization is by AF treatment. Plotting conventions as in Figure 11.

Pipe-rust contamination of the cores did not occur at Site 713. The rotary-drilled sedimentary sequence obtained from Hole 713A was, like that of Hole 712A, fragmented due to lack of recovery in the volcanic-ash-rich nannofossil oozes and chalks, and clay-bearing oozes and chalks of Eocene age (30–101 mbsf), but was complete in the foraminifer-nannofossil oozes and nannofossil-bearing foraminifer oozes of late Miocene (11–30 mbsf), early Pliocene (1.6–11.2 mbsf), and Pleistocene (0–1.6 mbsf) age. Susceptibility values in the late Miocene to Pleistocene sequence of extremely pure, carbonate-rich foraminifer-nannofossil oozes are uniformly low (generally $<5 \times 10^{-6}$ cgs), unlike those of the Eocene sequence of volcanic-ash-rich chalks, which are much higher and more variable (between 2 and 25 $\times$ 10^{-5} cgs).

The disparity between the susceptibility values of the two main sedimentary lithologic units of Hole 713A is most probably due to the high proportion of primary titanomagnetite normally present in volcanic ashes (e.g., Kennett, 1981). Although the Eocene volcanic-ash-rich chalks exhibit susceptibility values which are an order of magnitude higher than those of the overlying upper Miocene to Pleistocene oozes, they are themselves an order of magnitude less than the susceptibility values of the underlying basaltic lava flow and basement rocks.

SEDIMENTATION RATES

Although Sites 712 and 713 are located only 1.6 nmi apart, the geologic setting, as shown by seismic profiles at both sites, is quite different. The basement between the two sites is offset, presumably by faulting. Site 712 is located in a grabenlike structure where a strong reflector marks the Oligocene rubble interval; this interval is not present at Site 713. The sedimentation-rate history at the two sites reflects this difference in geologic setting. We constructed sedimentation-rate curves for both sites

Table 2. Directions of primary component of magnetization in basalt samples from Site 713 as determined from principal component analysis.

Sample interval (cm)	Number of samples	MAD	Inclination (degrees)	Intensity (mA/m)	Hard rock unit
115-713A-					
12R-2, 27–29	7	3.6	34.7	0.024	A
13R-1, 112–114 (Piece 10D)	6	2.5	24.9	13.721	1
13R-2, 91–93 (Piece 13A)	9	1.0	21.1	11.935	1
14R-2, 86–88 (Piece 4)	4	1.0	28.0	5.674	3
15R-2, 16–18 (Piece 1B)	4	9.1	12.2	2.210	3
15R-4, 29–31 (Piece 1)	8	1.9	4.8	2.220	3
15R-4, 121–123 (Piece 6)	6	0.7	43.1	11.742	4
15R-4, 140–142 (Piece 6)	5	0.8	22.7	17.762	4
15R-5, 18–20 (Piece 2)	9	0.6	23.1	31.576	5
15R-6, 55–57 (Piece 4)	4	0.5	26.2	58.219	5
16R-2, 117–119	11	3.8	25.4	0.013	A
16R-4, 134–136	6	4.4	18.1	0.020	A
16R-5, 31–33	6	2.2	56.3	0.060	A
17R-1, 11–13	6	5.6	33.8	0.022	A
17R-2, 38–40	3	5.8	27.2	0.097	A
17R-4, 26–28	3	5.5	37.0	0.063	A
18R-1, 80–82 (Piece 7)	7	1.2	42.5	2.254	6
18R-1, 136–138 (Piece 13)	6	1.0	10.5	5.075	7
18R-2, 9–11 (Piece 2)	4	10.2	−28.4	1.085	7
19R-1, 29–31 (Piece 4C)	10	0.6	16.8	3.957	8
19R-1, 62–64 (Piece 6)	7	0.6	36.1	6.139	8
19R-1, 123–125 (Piece 12)	6	0.6	29.4	4.806	10
19R-2, 37–39 (Piece 3B)	4	1.3	2.2	6.947	10
19R-3, 52–54 (Piece 3)	4	1.2	18.9	7.430	11
20R-2, 24–26 (Piece 2B)	4	1.3	−29.6	6.641	12
20R-2, 122–124 (Piece 6C)	2	0	28.5	3.651	13
20R-3, 36–38 (Piece 6A)	7	0.6	31.5	10.901	14
20R-3, 86–88 (Piece 4B3)	5	1.2	18.5	4.423	15
20R-3, 108–110 (Piece 7A1)	4	1.1	20.1	7.142	16
20R-4, 46–48 (Piece 3B3)	5	1.7	5.7	8.180	18
20R-5, 77–79 (Piece 5C)	5	1.2	35.5	4.924	20
20R-5, 113–115 (Piece 6B)	9	1.1	23.0	6.286	21
20R-6, 12–14 (Piece 1C)	7	0.7	21.4	4.802	22
20R-6, 48–50 (Piece 11)	3	1.7	−12.4	10.558	23
21R-1, 6–8 (Piece 1A)	10	1.0	25.4	5.535	25
21R-1, 44–46 (Piece 3B)	8	0.4	23.1	9.353	26
21R-1, 82–84 (Piece 4C)	6	0.8	5.0	6.665	27
21R-2, 4–6 (Piece 1)	6	0.9	19.3	6.090	28
21R-2, 107–109 (Piece 5E)	5	0.9	11.0	5.062	31
21R-3, 79–81 (Piece 4A)	5	0.9	18.3	3.092	33
21R-4, 104–106 (Piece 15)	5	0.8	30.5	2.605	34
22R-1, 26–28 (Piece 4)	3	2.8	9.2	2.885	35

Note: MAD = mean angular deviation of fit, A = volcanic ash.

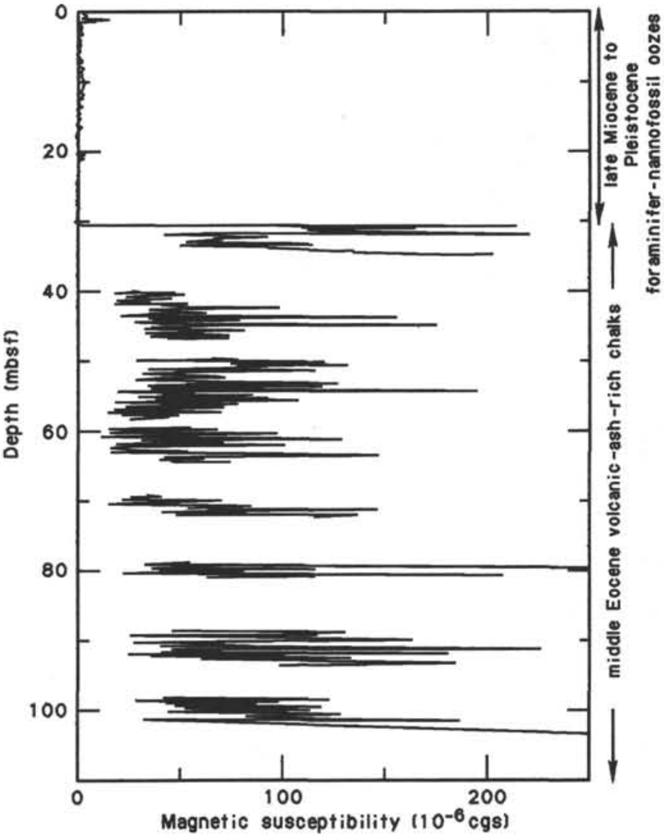

Figure 14. Whole-core magnetic susceptibility profile of the sedimentary sequence overlying the uppermost basaltic lava flow in Hole 713A.

(Figs. 15 and 16) based on the biostratigraphic datums given in Table 3.

At Sites 712 and 713, sediments younger than about 3.0 and 1.6 Ma, respectively, are missing. After 6.5 Ma, calcareous oozes accumulated at an average rate of 9.2 m/m.y. at Site 712, and at a rate of 5.5 m/m.y. at Site 713.

A major hiatus spanning almost 36 m.y. (6.5–42.3 Ma) occurred at Site 713; during that time interval, however, sediments accumulated at least intermittently at Site 712. At the latter site, two hiatuses of shorter duration were documented between 6.5 and 8.2 Ma and between 10.8 and 13.2 Ma, and one longer hiatus between 30.2 and 42.3 Ma. Lack of data between 48.1 and 105.7 mbsf (where sediments apparently consist of coarse sand and limestone rubble, but where recovery was poor) precludes the estimation of sedimentation rate changes and the identification of possible additional hiatuses. Assuming a constant sedimentation rate within this time interval allows us to place the Oligocene/Miocene boundary at 80 mbsf.

The 10-m thick sequence of chalk and ash layers recovered in the bottom of Hole 712A accumulated between 42.3 and 46 Ma—that is, during the time span of nannofossil Subzone CP14a. A minimum sedimentation rate of 3.6 m/m.y. is obtained if we assume that sediments at 105.7 mbsf lie in uppermost Subzone CP14a and that the bottom of the hole at 115.3 mbsf is in lowermost Subzone CP14a. However, the rate for that interval could be higher, as is the case at Site 713. During that time interval (42.3–46 Ma) at Site 713, chalk and ash layers accumulated at a rate of 7.4 m/m.y.

GEOCHEMISTRY

Interstitial Water Studies

Interstitial water samples were collected from five depths in Hole 712A through Core 115-712-6R and from eight depths in Hole 713A. In Hole 713A the deepest sample was taken from sediment intercalated with the two basaltic units at a depth of 150.2 mbsf. These data are presented in Table 4 and Figures 17 and 18.

Calcium and Magnesium

Although similar sediments were encountered at both Sites 712 and 713, substantially different patterns of Ca^{2+} and Mg^{2+} concentrations were encountered. In Hole 712A, little change in the Ca^{2+} and Mg^{2+} gradients was observed over the upper 50 mbsf (Fig. 19). The nonconservative behavior of these elements suggests either contamination by normal seawater or the occurrence of significant reactions within the sediments.

In contrast, at Hole 713A a conservative relationship was observed between magnesium and calcium over the same depth interval, with a Ca^{2+}/Mg^{2+} gradient typical of sites overlying basaltic basement. The Ca^{2+} gradient of 0.073 mmol/L/m was the highest observed during Leg 115 (Fig. 20); the gradient over the upper 100 m was 0.032 mmol/L/m. An interesting feature of the downhole gradient in Hole 713A is the change in Ca^{2+} and Mg^{2+} gradients between 100 and 157 mbsf (Fig. 18). This change in gradient coincides with samples taken on either side of a basalt unit and, hence, reflects either alteration within the

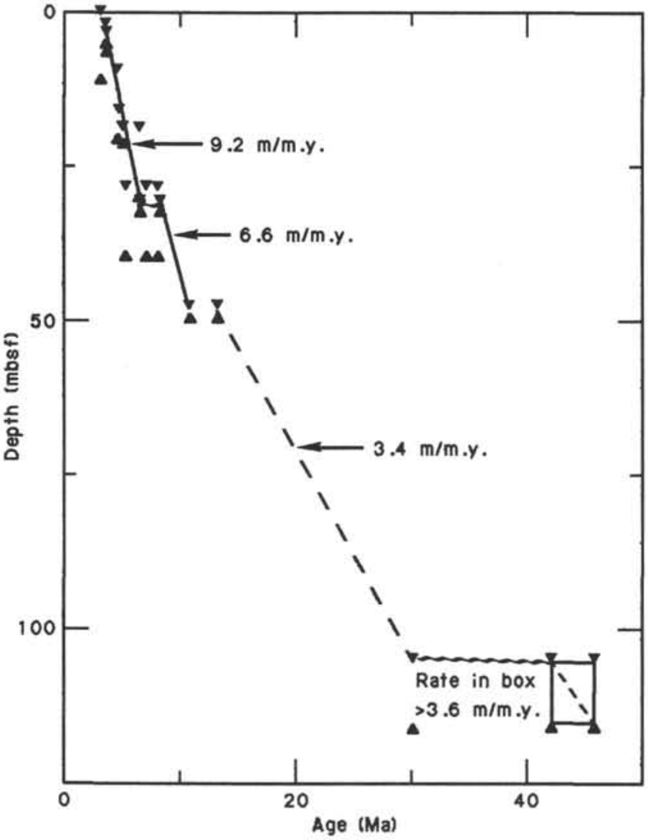

Figure 15. Sedimentation rates at Site 712 based on biostratigraphic datums listed in Table 3.

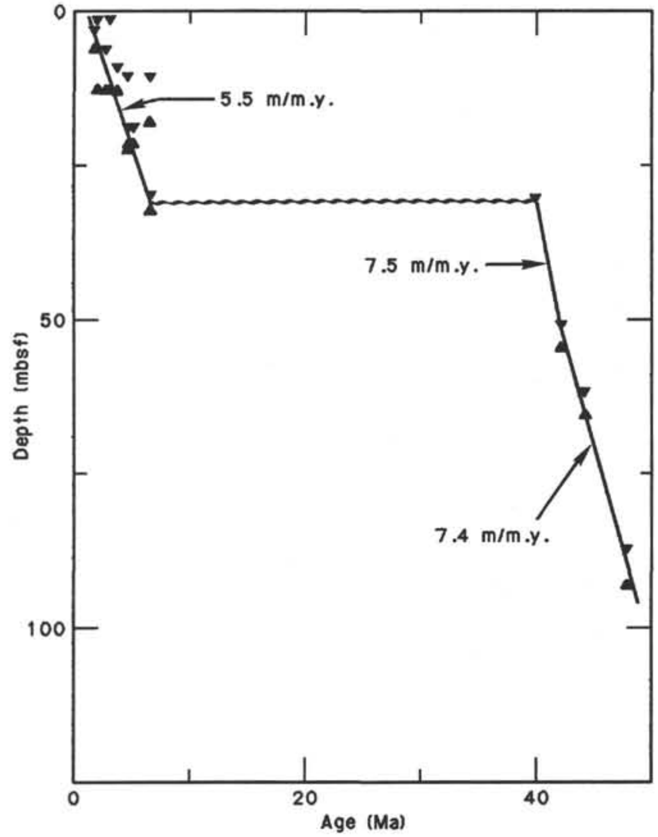

Figure 16. Sedimentation rates at Site 713 based on biostratigraphic datums listed in Table 4.

sediment itself or a change in the diffusion coefficient with increasing depth, as postulated by McDuff (1981). In spite of the conservative nature of the Ca^{2+} and Mg^{2+} gradients, their magnitude strongly suggests that reactions involving the dissolution of feldspars and the formation of clay minerals are occurring within the sediments.

Alkalinity and Sulfate

Although alkalinity exhibits a small increase in the first core of Hole 713A (Fig. 18), there is a gradual decrease with increasing depth, reaching the lowest values measured during Leg 115. The alkalinity low of 1.10 mmol/L was encountered at a depth of 150 mbsf in sediments located between the two basaltic units (see "Lithostratigraphy" and "Basement Rocks" sections, this chapter). The reduction in alkalinity occurs in spite of the fact that the concentration of sulfate, which also decreases over the same depth interval, would normally be expected to increase the alkalinity. In addition, reactions such as those represented below, which can account for the addition of Ca^{2+} to the pore fluids by the alteration of plagioclase, tend to leave alkalinity unaffected:

$$CaAl_2Si_2O_8 + H^+ + HCO_3^- + H_2O = Ca^{2+} + 2HCO_3^- + Al_2Si_2O_5(OH)_4 \quad (1)$$

Therefore, in order to account for the decrease in alkalinity, some precipitation of $CaCO_3$ must be taking place near the basalt-sediment interface. The reaction in eq. (1) utilizes H^+ ions and therefore can account for the increase we observed in pH from 7.5 at 33.45 mbsf to 8.1 at 150.22 mbsf.

Taking into consideration the changes in pH, alkalinity, and calcium concentrations, we calculated that the saturation index (SI) of calcite, as defined by eq. (2),

$$SI = IAP/K_{Sp} \quad (2)$$

where IAP = ion activity product and K_{Sp} = solubility product of calcite, actually increases from 0.261 to 0.607 between 33.45 and 150.22 mbsf. (These calculations have not been corrected for any change in alkalinity and/or pH as a result of the squeezing artifacts identified from the use of the downhole water sampler—see "Geochemistry" section, "Site 709" chapter, this volume—or changes in the solubility constant of calcite as a result of pressure.)

In contrast, Hole 712A exhibits practically no variation in alkalinity and sulfate in the cores examined (Fig. 17). This lack of variation may be caused by contamination, diagenetic reactions within the sediments, or water movement (convection) through the sediment (see "Lithostratigraphy" and "Physical Properties" sections, this chapter).

Silica

The concentration of silica rises rapidly to 605 μmol/L at 31.50 mbsf at Site 712 (Fig. 17). Although the concentration of silica in the bottom waters is not known, the gradient observed in the upper three cores indicates that the samples from this hole are not contaminated by seawater, particularly in light of the absence of any variation in alkalinity, calcium, and magnesium.

At Site 713, concentrations of silica rise to values as high as 775 μmol/L, but toward the basaltic interface they fall rapidly

Table 3. Biostratigraphic datum levels, Holes 712A and 713A.

	Species events	Depth (mbsf)	Age (Ma)
Hole 712A:			
LO	*D. altispira* (F)	0–9.4	2.9
LO	*Sphaeroidinellopsis* (F)	0–9.4	3.0
LO	*S. abies* (N)	2.2–3.5	3.45
LO	*R. pseudoumbilica* (N)	3.5–4.7	3.56
LO	*S. omnitubus* (R)	9.4–19.4	4.3
FO	*N. jouseae* (D)	9.4–19.0	4.5
FO	*C. rugosus* (N)	16.1–19.00	4.6
LO	*D. quinqueramus* (N)	19.0–19.75	5.0
FO	*G. tumida* (F)	28.6–38.3	5.2
	S. delmontensis/peregrina (R)	19.0–28.6	6.4
FO	*A. primus* (N)	30.9–31.03	6.5
LO	*D. hughesi* (R)	28.6–38.3	7.0
FO	*G. plesiotumida* (F)	28.6–38.3	8.0
FO	*D. berggrenii* (N)	30.9–31.03	8.2
FO	*C. coalitus* (N)	47.9–48.3	10.8
LO	*S. heteromorphus* (N)	47.9–48.3	13.2
FO	*S. ciperoensis* (N)	105.7–115.3	30.2
	below top CP14a (N)	115.3	42.3
	above base CP14a (N)	115.3	46.0
Hole 713A:			
FO	*G. oceanica* (N)	3.6–4.4	1.6
FO	*G. truncatulinoides* (F)	1.6–11.2	1.9
FO	*P. doliolus* (D)	1.6–11.2	1.8
LO	*S. peregrina* (R)	6.8–11.2	2.6
LO	*D. altispira* (F)	1.6–11.2	2.9
LO	*Sphaeroidinellopsis* (F)	1.6–11.2	3.0
LO	*R. pseudoumbilica* (N)	9.6–11.2	3.56
FO	*N. jouseae* (D)	11.2–20.8	4.5
FO	*C. rugosus* (N)	19.4–20.0	4.6
LO	*D. quinqueramus* (N)	19.4–20.0	5.0
	S. delmontensis/S. peregrina (R)	11.2–16.4	6.4
FO	*A. delicatus* (N)	30.5–30.9	6.5
	within Zone CP14a	30.9	40.0
LO	*C. solitus* (N)	51.7–53.2	42.3
FO	*R. umbilica* (N)	62.8–64.3	44.4
LO	*C. gigas* (N)	136.2–136.4	47.0
FO	*T. triacantha* (R)	88.4–92.1	48.0

Note: FO = first occurrence, LO = last occurrence, N = nannofossil, F = foraminifer, D = diatom, and R = radiolarian.

to 279 μmol/L. Such values are likely to be below bottom-water concentrations. The decrease in silica suggests that reactions involving the precipitation of silica are taking place near the basalt unit.

X-ray Mineralogy, Carbonate, and Organic Carbon Content

The carbonate content of samples taken from Sites 712 and 713 is shown in Table 5. The sediments of middle Miocene age and younger contain in excess of 90% low-magnesium calcite. At Site 712, this interval extends to Core 115-712A-11R in sediments of Oligocene age. Below this interval, in Eocene sediments, the carbonate content decreases, ranging between <1.0% and 75%.

The same change occurs at much shallower sub-bottom depths at Site 713, where middle Eocene sediments were intersected at the bottom of Core 115-713A-5R. The main noncarbonate materials present in these intervals are volcanic ash, clays, plagioclase, and quartz, all of which appear to have been extensively bioturbated and worked into the carbonate sediments (see "Lithostratigraphy" section, this chapter).

Organic carbon analyses are shown in Table 6. Although concentrations reach values as high as 1.11%, they are generally below detection limits.

BASEMENT ROCKS

Introduction

Rotary coring (in which each "core" represents ~9.5 m of drill penetration) at Site 713 encountered basaltic rocks in the intervals from 107 to 133.8 mbsf and from 155.3 to 191.7 mbsf (bottom of the hole). Cores 115-713A-16R and 115-713A-17R (136.2–155.2 mbsf) contained tuffaceous sedimentary rocks. The average recovery rate for cores composed mostly of basalt was 49.9% (Fig. 21). This section summarizes the description of basalts recovered based on lithostratigraphy, vesicularity, grain size, alteration, and phenocryst type and abundance as compiled on visual core and thin-section description forms.

The subdivision into 35 units was made during the course of the visual core description and was based primarily on the rec-

Table 4. Interstitial water analyses, Holes 712A and 713A.

Sample interval (cm)	Depth (mbsf)	Ca (mmol/L)	Mg (mmol/L)	Cl (mmol/L)	Al (mmol/L)	pH	Salinity (‰)	Si (μmol/L)	SO_4 (mmol/L)
Seawater	0	11.07	55.35	565.4	2.47	8.5	35.0	0	29.15
115-712A-									
1R-5, 145–150	7.45	11.10	54.10	552.0	2.90	7.8	35.2	449	28.55
2R-4, 145–150	15.48	11.18	53.78	554.9	3.03	7.7	35.2	594	28.12
3R-3, 140–150	23.40	11.10	54.02	571.1	3.05	7.7	35.2	655	28.11
4R-2, 140–150	31.50	11.37	55.24	575.8	2.98	7.8	35.8	605	28.60
6R-2, 140–150	50.80	12.25	53.76	560.6	3.01	7.8	35.2	615	28.31
Seawater	0	11.07	55.35	565.4	2.47	8.5	35.2	0	29.15
115-713A-									
2R-4, 145–150	7.55	11.74	54.56	574.9	3.07	7.8	35.0	497	28.51
3R-4, 145–150	17.15	12.13	54.11	569.2	3.00	7.7	35.5	577	28.17
4R-4, 145–150	26.75	12.12	53.06	560.6	2.91	7.7	35.0	756	27.44
5R-2, 145–150	33.45	12.49	52.06	564.4	2.77	7.5	35.0	775	27.72
6R-2, 145–150	43.05	12.82	52.15	573.9	2.63	7.5	35.0	743	28.24
9R-1, 145–150	70.55	14.23	51.74	569.2	2.54	7.7	35.2	554	27.80
12R-1, 147–150	99.57	14.84	50.09	561.5	1.78	8.0	35.0	630	27.22
17R-3, 150–155	150.22	21.56	40.25	574.9	1.10	8.1	34.8	279	26.19

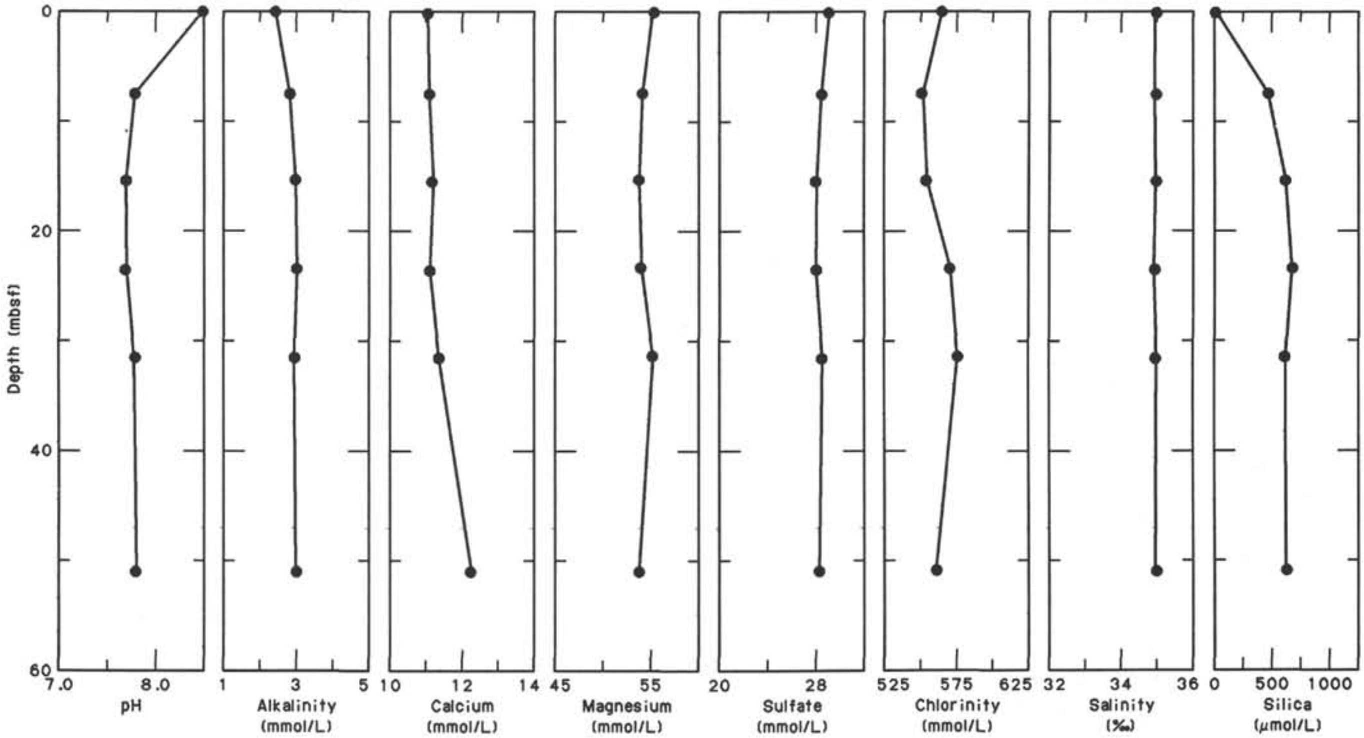

Figure 17. Summary of interstitial water analyses, Hole 712A, as a function of sub-bottom depth. Surface seawater is plotted at 0 mbsf.

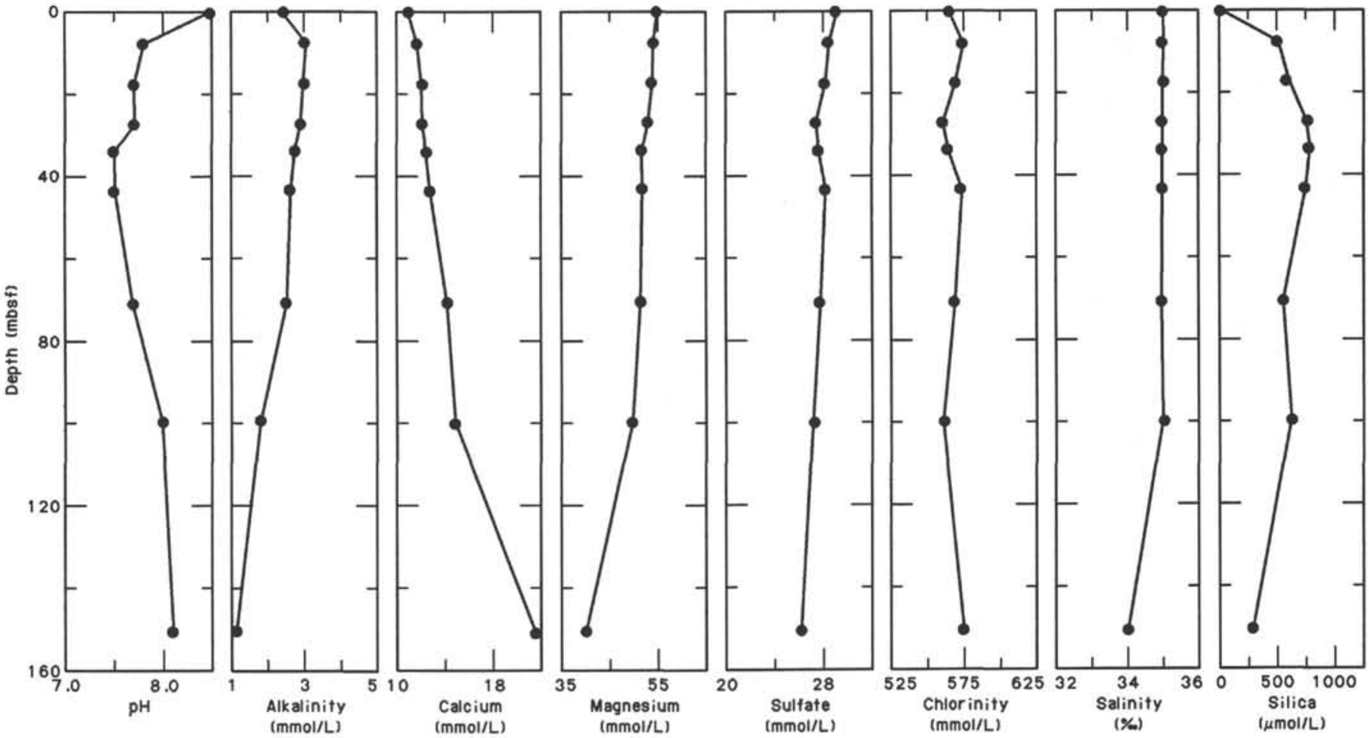

Figure 18. Summary of interstitial water analyses, Hole 713A, as a function of sub-bottom depth. Surface seawater is plotted at 0 mbsf.

ognition of lithologic contrasts between core segments and on the presence of sedimentary intercalations or tachylytic margins in the basalt core (Fig. 22). Chilled margins may, however, represent within-flow boundaries or the chilled margins to pillows in a single flow unit. On the other hand, the incomplete core recovery means that evidence of some flow boundaries may have been lost and that portions of distinct flow units which are similar to the eye may be lumped erroneously into one unit. Such errors may be revealed by subsequent petrographic, petrochemical, or physical property measurements. We have noted such

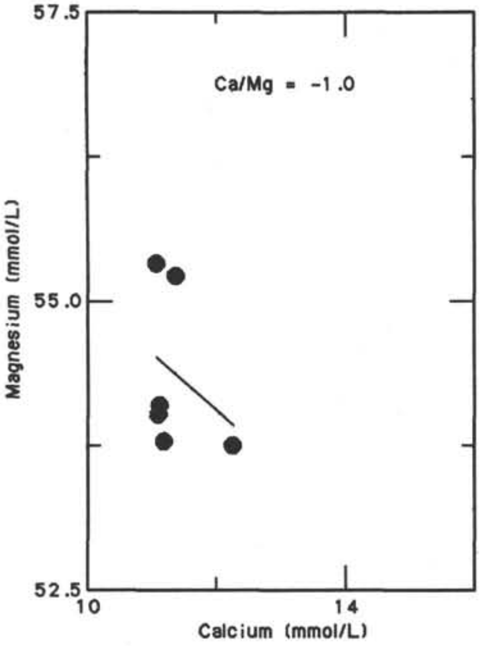

Figure 19. Calcium and magnesium concentrations, Site 712.

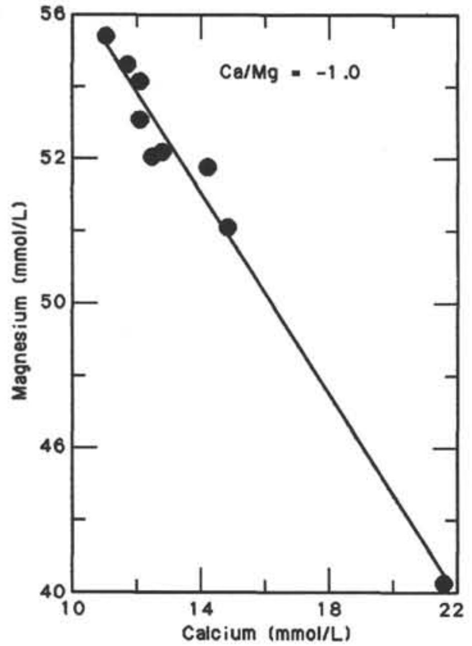

Figure 20. Calcium and magnesium concentrations, Site 713.

anomalies in the original subdivision, when we recognized them, in the text.

Macroscopic Characteristics

Unit 1

This unit, represented by 18 cm in Section 115-713A-12R, CC, and by 3.05 m of recovered core in Core 115-713A-13R, is composed of highly vesicular plagioclase-phyric basalt. Vesicles are evenly distributed and less than 3 mm in diameter. The term "hawaiitic" basalt was used for the rock on the visual description forms because of the low color index.

Table 5. Carbonate content of samples from Holes 712A and 713A.

Sample interval (cm)	Depth (mbsf)	Carbonate (wt%)
115-712A-		
1R-2, 60-64	2.10	93.71
1R-4, 62-64	5.12	94.95
1R-6, 62-64	8.12	94.1
2R-3, 60-62	13.00	93.49
2R-5, 59-61	16.12	95.3
3R-1, 60-62	19.60	92.85
3R-3, 60-62	22.60	93.61
3R-5, 24-27	25.24	93.2
4R-1, 60-62	29.20	93.86
4R-3, 23-25	31.83	93.34
5R-1, 60-62	38.90	92.79
5R-2, 60-62	40.40	93.64
6R-2, 60-62	50.00	97.02
11R-1, 10-13	96.20	99.05
11R-1, 60-62	96.70	99.65
11R-3, 24-26	98.08	98.72
12R-2, 101-103	108.08	71.59
12R-2, 103-105	108.10	81.99
12R-2, 105-107	108.12	75.71
12R-2, 107-109	108.14	76.84
12R-2, 110-112	108.17	95.27
115-713A-		
2R-5, 99-101	8.59	96.78
3R-2, 60-62	13.30	95.17
3R-4, 15-17	15.85	93.59
3R-6, 96-98	19.66	93.32
4R-2, 138-140	23.68	93.8
4R-5, 51-53	27.31	94.5
4R-7, 32-34	30.12	93.73
5R-3, 105-107	34.55	60.12
6R-1, 67-69	40.77	76.67
6R-1, 140-142	41.50	89.74
6R-5, 27-30	46.37	76.48
7R-3, 60-62	53.30	70.75
7R-5, 60-62	56.30	67.59
8R-2, 103-106	61.93	84.48
8R-4, 23-25	64.13	58.42
9R-2, 120-122	71.80	15.52
10R-1, 71-73	79.41	77.98
10R-2, 15-17	80.35	0.05
11R-1, 10-13	88.50	0.2
11R-1, 113-116	89.53	57.41

Unit 2

A single piece of "trachybasalt" (7 cm long) at the bottom of Core 115-713A-13R contained fewer vesicles than Unit 1 and was assigned to Unit 2. It could represent the chilled contact of Unit 1 or Unit 3.

Unit 3

Unit 3 is represented by all of Core 115-713A-14R (4.35 m recovered) and by 5.3 m of the 6.92 m in Core 115-713A-15R. It shows lower vesicularity than Unit 1. Most parts of the core are slightly altered, medium-grained clinopyroxene-plagioclase-phyric basalt with clots of plagioclase ± clinopyroxene crystals. We identified olivine only in the lowermost part of the unit in Core 115-713A-15R. The segment of the unit represented in Core 115-713A-15R is distinctly coarser grained than that in Core 115-713A-14R and may constitute a separate unit.

Units 4 and 5

These units, represented by 0.51 and 1.11 m (respectively) of basalt at the base of Core 115-713A-15R, resemble the above units in having phenocrysts of plagioclase, clinopyroxene, and olivine. A glassy piece of core containing a thin sediment layer

Table 6. Percent organic carbon, Sites 712 and 713.

Sample interval (cm)	Depth (mbsf)	Organic carbon (%)
115-712A-		
1R-2, 60-64	2.1	0.03
1R-4, 62-64	5.12	0
2R-3, 60-62	13.0	0
2R-5, 59-61	16.12	0
3R-1, 60-62	19.60	0
3R-3, 60-62	22.60	0
4R-1, 60-62	29.20	0
4R-3, 23-25	31.83	0.02
5R-2, 60-62	40.40	0
6R-2, 60-62	50.00	0.04
11R-3, 24-26	98.08	0
12R-2, 110-112	108.17	0
12R-2, 101-103	108.08	1.11
115-713A-		
2R-5, 99-101	8.59	0
3R-2, 60-62	13.30	0.08
3R-4, 15-17	15.85	0
4R-2, 138-140	23.68	0
4R-7, 32-34	30.12	0
5R-3, 105-107	34.55	0.21
6R-5, 27-30	46.37	0
7R-3, 60-62	53.30	0
8R-2, 103-106	61.93	0
9R-2, 120-122	71.80	0
10R-2, 15-17	80.35	0.01
11R-1, 113-116	89.53	0.07

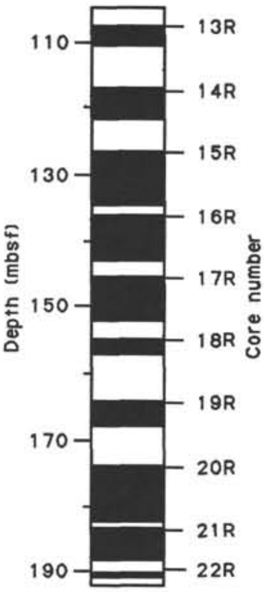

Figure 21. Summary of the amount of basement recovered in Site 713 cores. Note that each numbered "core" represents about 9.5–10.0 m of drill penetration, but that actual core recovery is variable. Overall average recovery at Site 713 was 49.9%.

separates the two units. Both show higher vesicularity in their upper portions. A section of tuffaceous sedimentary rock (13.0 m recovered) composed of all material recovered in Cores 115-713A-16R and -17R and the top 10 cm of Core 115-713A-18R underlies Unit 5.

Units 6 through 10

Units 6 through 10 are represented by 1.80 m of basalt recovered in Core 115-713A-18R and by 3.07 m out of 3.57 m recovered in Core 115-713A-19R. The olivine-bearing, clinopyroxene plagioclase basalts (hawaiites?) are separated by glassy chilled margins and appear slightly altered and only slightly vesicular. Macroscopically, they resemble the upper basalt Units 4 and 5.

Unit 11

The lower 50 cm of basalt recovered from Core 115-713A-19R and the upper 28 cm recovered from Core 115-713A-20R were assigned to Unit 11. The unit resembles Units 5 through 10 but is distinguished by an absence of olivine phenocrysts.

Units 12 through 29

The total recovered length of these units is 10.27 m recovered in Cores 115-713A-20R and -21R. Each unit consists of moderately altered olivine, clinopyroxene, and plagioclase phyric basalt separated by glassy contacts which may represent boundaries between pillows in a single subaqueous lava flow.

Unit 30

We assigned a 0.33-m (recovered length) portion of Core 115-713A-21R which has a higher percentage of clinopyroxene than overlying units to Unit 30.

Units 31 through 35

These units are represented by 3.52 m of basalt recovered in Cores 115-713A-21R and -22R. They resemble Units 12 through 29, but Unit 35 appears to have a slightly higher plagioclase percentage.

Microscopic Characteristics

Modal phenocryst compositions of Site 713 basalts are illustrated in Figure 22. Some of the Hole 713A basement rocks were thought to be "hawaiites" or "trachytes" based on visual core examination; on the other hand, microscopically they contain large percentages of mafic phases (clinopyroxene and opaque minerals) in the ground mass and should be termed "basalts."

Fresh olivine only occurs in the clear brown glass at the chilled margins of units. Olivine is apparently always altered in the interiors. Variolitic pyroxene grains occur in some quenched glassy samples.

All basalts from the site contain plagioclase phenocrysts (< 5 mm in length). These sometimes show a bimodal size distribution, with most of the larger grains containing dusty inclusions of undetermined composition and displaying reverse and oscillatory zoning. Smaller phenocrysts are characterized by normal zoning and an absence of dusty inclusions.

Clinopyroxene phenocrysts from this site, like those from Site 706, often display strong sector and normal zoning. Sector zoning is rare in Site 707 pyroxenes. However, some Site 706 pyroxenes tend to be slightly brownish in color whereas Site 707 and 713 pyroxenes are relatively colorless.

Discussion

In general, two points suggest the submarine eruption of all the lavas cored in Hole 713A: (1) lava flows are interbedded with marine sediments, and (2) designated units show obvious chilled contacts, especially in the lower half of the hole. However, basalts recovered in the upper portions of the hole (Cores 115-713A-13R through -15R) are distinct from those below the sedimentary section (i.e., Cores 115-713A-18R through -22R). The upper lava units (Units 1 and 3 especially) appear much thicker than units below, suggesting eruption subaerially or in

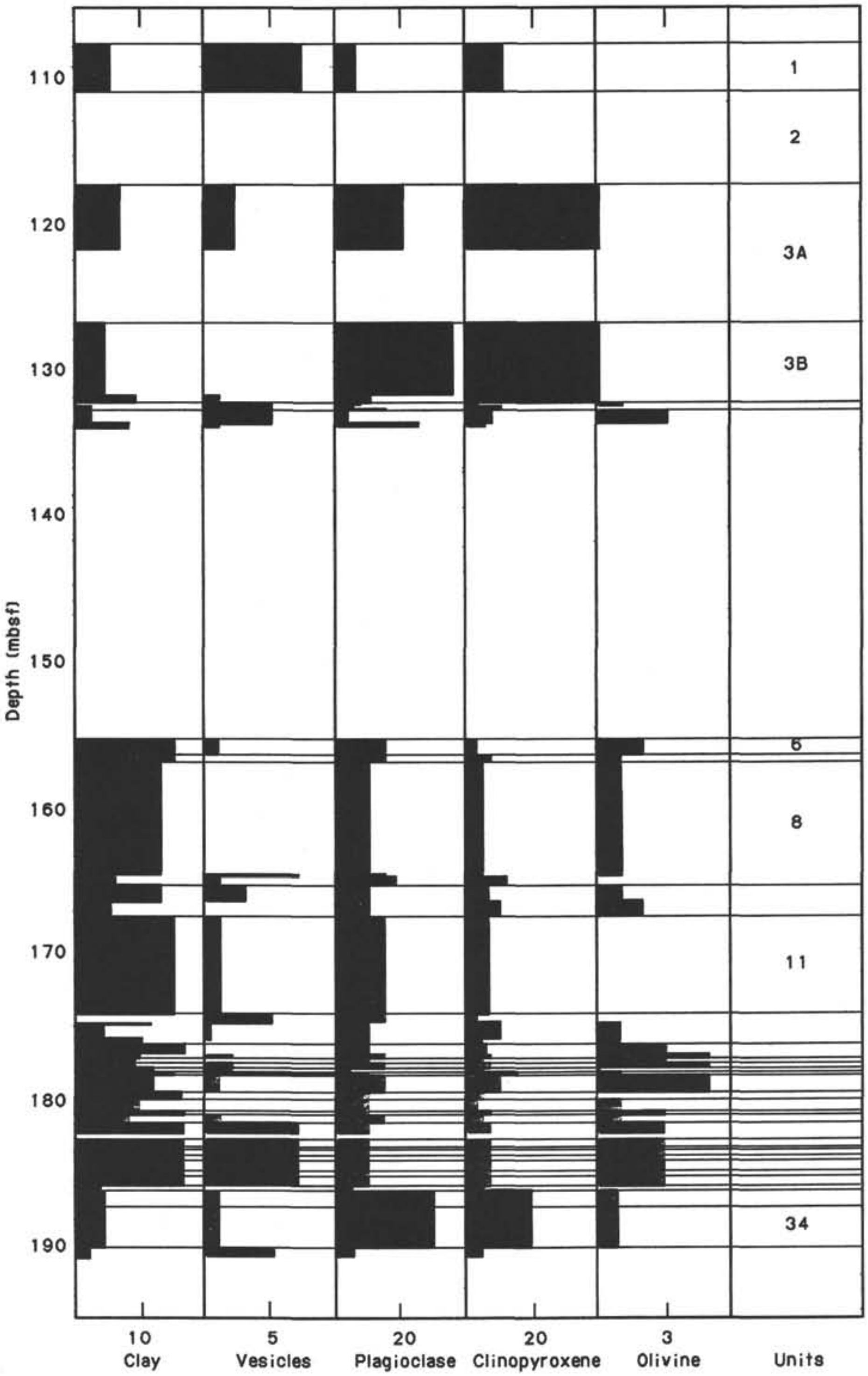

Figure 22. Graphic summary of the petrographic characteristics of basalts from Hole 713A. Alteration percentages appear in first column as percent clay minerals. Vesicle percentages are given in second column. The columns for plagioclase, clinopyroxene, and olivine refer to the modal percentages of those particular phenocrysts. In most cases, olivine has been altered to clay minerals.

very shallow water. Alternatively, it may merely reflect a larger volume (or rate) of submarine lava production. The highly vesicular nature of basalts from Unit 1 is consistent with a shallower eruption depth for these rocks. However, sedimentary rocks between flow units contain benthic foraminifers of interpreted deep-water origin (1000–2000 m; see "Biostratigraphy" section, this chapter). This conclusion appears at odds with the abundance of vesicles in the flows.

Magnetic susceptibility data (Fig. 23) indicate that two distinct units are represented by the core segments recovered in Cores 115-713A-14R and -15R, though no major lithologic differences were observed and the bulk of both cores were assigned

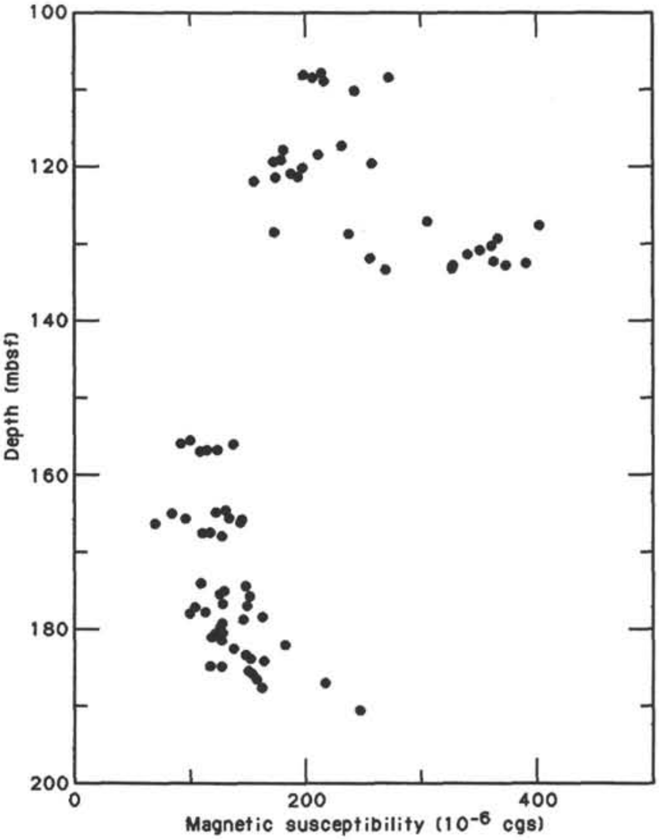

Figure 23. Plot of the magnetic susceptibility of 713A basalts. Note the contrast in average susceptibility of basalt in Cores 115-713A-14R (117.2–126.7 mbsf) and -15R (126.7–136.2 mbsf), which indicates that they represent distinct petrologic "units." No difference was noted in the visual core description, however, and both were assigned to Unit III.

to Unit 3. However, microscopic examination indicates a greater modal abundance of iron-titanium oxides in Core 115-713A-15R. The rather constant (and relatively low) magnetic susceptibility of basalts from the lower half of the hole supports the hypothesis that glassy boundaries between units are not flow boundaries but pillow margins in a single lava flow.

Sedimentary rocks overlying and intercalated with the basaltic lavas contain a number of ash layers with fresh glass. The number of ash layers increases toward the contact with the upper basalt units in both the overlying and underlying sedimentary layers, suggesting that the same volcanic activity produced both the lavas and the ashes. However, the presence of green pyroxene phenocrysts, probably of aegirine augite composition, suggests that some of the ashes have a much more evolved chemical composition than the associated basalts and that they probably have strong alkaline affinities.

Shipboard major element and trace element analyses (Table 7) show that basalts from above the sedimentary break (Units 1-5) can be distinguished from the lower basalts (Units 6–35) by, for example, higher titanium dioxide, barium, zirconium, chromium, and nickel concentrations. This implies that the upper basalts are slightly more alkaline than the lower basalts.

Although the phenocryst and groundmass phases are similar for Sites 706, 707, and 713 basalts, clinopyroxenes from Sites 707 and 713 do not show the brownish color characteristic of titaniferous pyroxenes from sialic magmas seen in Site 706 basalts. This suggests that Site 707 and 713 magmas are less alkaline than those from Site 706. These indications are confirmed by shipboard geochemical data (Table 7) showing that Site 707 and 713 basalts are similar to one another and much more similar in terms of their titanium dioxide contents, for example, to ocean floor basalts than are the Site 706 basalts.

PHYSICAL PROPERTIES

Site 712

We drilled a total of 115.3 m at Site 712 using rotary techniques, but only 41.6 m of sediments were recovered. These consisted mainly of homogeneous foraminifer-bearing nannofossil oozes showing increasing lithification downhole. The upper 57.5 m of the sequence is composed of a foraminifer-nannofossil ooze and foraminifer-nannofossil chalk. The chalk became increasingly fractured and biscuited with increasing depth and finally reverted into soft ooze (drilling paste?). The lack of recovery from 57.5 to 96 mbsf was followed by recovery of drilling rubble, consisting of carbonate sands and limestone rubble. A highly bioturbated series of sediments were recovered below 105 mbsf, which included foraminifer-bearing nannofossil chalk with interbedded volcanic-ash layers, partly clay-rich chalks, and clay-bearing nannofossil chalk. Signs of significant drilling disturbance were present in most of the recovered sediments. No basement rocks were recovered at this site.

The following physical properties measurements were determined: index properties, compressional- (V_p) and shear-wave velocities (V_s), shear strength, and thermal conductivity. The number of discrete measurements taken was limited by the poor recovery and drilling disturbance. Furthermore, the low rigidity of the soupy ooze and the brittleness of the chalk meant that it was difficult to obtain representative V_p, V_s, and shear strength measurements even on less disturbed samples. No whole-core logging was possible at Sites 712 and 713 because the *P*-wave logger and GRAPE were being transferred at the time to a vertical logging arrangement.

Index Properties

The results of index property measurements are given in Table 8 and Figure 24. The variation in the index properties reflects the different amounts of consolidation and disturbance in the recovered sediments at Site 712. The uppermost part of Hole 712A is dominated by highly porous, "soupy" nannofossil ooze. The porosity gradually decreases from 69.82% to 60.41% from the seafloor to 25.24 mbsf. This decrease is accompanied by an increase of wet-bulk density from 1.56 to 1.73 g/cm^3. Between 20 and 40 mbsf, within the more cohesive nannofossil ooze, the index properties are approximately constant but are scattered due to differing degrees of drilling disturbance. The data at 40.40 mbsf were taken on "undisturbed chalk," and the measurement at 50.00 mbsf was made in the remolded nannofossil ooze. The index property measurements of samples from the drilling rubble at about 100 mbsf are also included in Figure 24 and Table 8. The carbonate contents of samples on which index properties were determined are plotted in Figure 25.

Compressional-Wave Velocity and Acoustic Impedance

The "soupy" ooze and brittle chalk recovered at Site 712 were unsuitable for use in the Hamilton Frame. Therefore, only a few measurements of the compressional-wave velocity (V_p) were made. The results are shown in Figure 26 and Table 9. From about 1500 to 1636 m/s, V_p increases steadily with depth. The acoustic impedances calculated from wet-bulk density and V_p data are also shown in Figure 26. The low impedances of 2300–2400 g/cm^2 × s × 10^2 in the uppermost 10 m are followed by a slight increase to 2600 g/cm^2 × s × 10^2. The impedance then appears to increase linearly with depth, although the sample spacing is too wide to resolve lithologic changes.

Shear-Wave Velocity and Shear Strength

The shear-wave velocities (V_s) shown in Figure 27 and Table 10 are scattered over the range of 65–110 m/s. Nannofossil chalk and underlying drilling rubble prohibited any further measurements. There is no obvious correlation of the V_s with shear strength.

The shear strength measurements at Site 712 (Fig. 27 and Table 11) clearly show the gradual consolidation of the nannofossil ooze to chalk. The strength of the ooze gradually increases from the cohesionless "soup" within the top few meters, to an average of approximately 50 kPa for the semicompacted ooze between 25 and 40 mbsf. The shear strength then drops dramatically to 4.7 kPa for the brittle chalk at 50.37 mbsf. This low experimental measurement was due to cracking and failure of the chalk on insertion of the blade. The lithification of the sediments caused breakage as soon as torsional stress was applied to the vane.

Thermal Conductivity

The results for thermal conductivity at Site 712 are shown in Table 12 and Figure 28. The thermal conductivity shows a large and steady increase from the surface to 20.10 mbsf. The interval from 20 to 28 mbsf was selected for a very detailed survey of thermal conductivity to study the variability at very short depth intervals. A fair amount of small-scale variability was present, with isolated "extreme" values also observed. Below this depth, core conditions and recovery led to fewer measurements with no significant trend. The lowermost measurements show the high degree of variability which we found characteristic of these partially consolidated sediments.

Summary

The sediments recovered at Site 712 are characterized by varying states of cohesion, compaction, and drilling disturbance in what is primarily nannofossil ooze. The excessive disturbance was due to coring with the rotary technique. There was a gradual increase of consolidation of the nannofossil ooze with depth. This increase affected all physical property measurements at Site 712. We detected the transition from soupy to more cohesive ooze by variations in the wet-bulk density and porosity and, in particular, by the shear strength. The compressional-wave velocity and acoustic impedance rose linearly with increasing compaction within the ooze. The shear-wave velocity measurements were too scattered to make any comparisons with other physical properties.

Site 713

Site 713 was drilled to a depth of 192 mbsf using the RCB system. A total of 115 m of cored material was recovered: 68 m of sediments and 47 m of underlying basement rocks. Soft sediments were highly disturbed and consisted of foraminifer-nannofossil ooze grading into foraminifer-bearing nannofossil (sometimes clay-bearing) ooze at around 38 mbsf. Harder foraminifer-bearing chalks in a disturbed oozelike drilling paste were recovered from 38 mbsf to about 50 mbsf. A complex, highly bioturbated series of interbedded ashes and impure foraminifer-bearing nannofossil chalk was intersected at this depth. This series was well consolidated and generally undisturbed; it extended downward to 107 mbsf, where the first basalts were recovered. We distinguished 35 different flow units (see "Basement Rocks" section, this chapter). Over 10 m of alternating nannofossil and micrite chalks with interbedded ashes were recovered between flow units 6 and 7.

Sediments

Index Properties

The index properties results for the sediments from Site 713 are shown in Figure 29 and Table 8. Changes in wet-bulk density, water content, and porosity are due mainly to variations in the lithology and degree of drilling disturbance, while the grain density is generally insensitive to local disturbance and degree of consolidation.

The wet-bulk density data are highly scattered between the seafloor and 38 mbsf. The data between 10 and 38 mbsf were obtained on highly disturbed foraminifer-nannofossil ooze. The scatter for the data between 38 and 50 mbsf is due to variations in clay content and disturbance of the semiconsolidated nannofossil chalk. The carbonate content varies significantly in the sedimentary section (Fig. 30 and Table 8), and in sections of low carbonate content the sediment becomes rich in clay. The remainder of the index properties data were collected on the consolidated, ash-bearing, impure nannofossil chalk. All the index properties show a fair amount of scatter in this interval, but a trend of decreasing porosity, water content, and grain density and increasing wet-bulk density is apparent.

Compressional-Wave Velocity and Acoustic Impedance

The compressional-wave velocity (V_p) and wet-bulk density measurements taken on the same discrete sediment samples from Site 713 are shown in Figure 31 and Table 9. The density is approximately constant with an average of 1.6 g/cm^3. However, V_p and acoustic impedance show a strong increase with depth. There is an increase in V_p at depths greater than 40 mbsf, from 1550 m/s in the soft foraminifer-nannofossil ooze, to 1600 and 1700 m/s in the harder foraminifer-bearing chalks. Within the impure chalk, V_p remains constant to a depth of 65 mbsf. At greater depths micritic chalk is present, causing a steady increase in V_p due to a combination of increased ash content and lithification. The impedance and V_p profiles (Fig. 31) are similar as the density is relatively constant.

Shear Strength

A few shear strength measurements were taken in the highly disturbed soft foraminifer-nannofossil ooze at Site 713. These data are presented in Table 11 and Figure 32.

Thermal Conductivity

The thermal conductivity results for Site 713 are shown in Table 12 and in Figure 33. The surficial sediments at this site have a surprisingly high conductivity, greater than 1.6 $W \cdot m^{-1} \cdot K^{-1}$, but this rapidly decreases over the next 10 m. (We have seen this pattern in several of the sites.) Thermal conductivity in the depth range of 10–38 mbsf is high (about 1.3 $W \cdot m^{-1} \cdot K^{-1}$) and variable. This is the combined result of real lithologic variation and drilling disturbances. Below 38 mbsf, in the chalks and ash layers, the conductivity is 1.1–1.2 $W \cdot m^{-1} \cdot K^{-1}$ and is much less variable. The measurements just above the basalt, from 100 to 107 mbsf, show an increase from 1.1 to 1.3 $W \cdot m^{-1} \cdot K^{-1}$. Surprisingly, this trend continues within the uppermost basalt layer, reaching 1.6 $W \cdot m^{-1} \cdot K^{-1}$ at 132 mbsf. The trend within the basalt is probably related to a decrease in porosity with depth. It may be only a coincidence that it happens to agree roughly with the trend in the chalks above the basalt, but, as the basalt was approached, the proportion of ash in the sediment increased steadily.

We encountered interbedded chalks from 135 to 150 mbsf; their conductivity was slightly higher than the chalks above the basalt layer, but still only about 1.2 $W \cdot m^{-1} \cdot K^{-1}$. The lower ba-

Table 7. Basalt major and trace element chemistry, Site 713.

Core, Section	13R-1	13R-3	14R-2	15R-4	15R-4	15R-5	18R-1	18R-1	19R-1	19R-1	19R-1	19R-3
Interval (cm)	63–69	16–20	68–71	7–13	143–146	90–94	73–75	145–148	27–29	91–93	116–118	13–15
wt%:												
SiO_2	49.57	49.32	49.71	49.36	49.07	49.60	49.45	49.49	49.90	50.47	49.29	49.49
TiO_2	1.40	1.31	1.38	1.31	1.52	1.58	0.98	1.03	1.02	1.19	0.99	0.98
Al_2O_3	15.35	14.51	15.90	14.13	13.58	13.76	15.29	15.93	16.14	17.75	15.37	15.12
Fe_2O_3	12.07	12.85	11.64	13.27	14.71	14.43	11.86	10.16	9.95	8.99	11.25	11.74
MnO	0.19	0.18	0.17	0.19	0.25	0.23	0.18	0.16	0.16	0.12	0.18	0.19
MgO	6.46	7.11	6.91	8.58	5.64	6.38	7.13	7.61	7.78	8.36	6.97	7.27
CaO	13.10	12.01	12.14	11.32	12.11	12.03	13.05	13.21	12.92	9.91	13.41	13.17
Na_2O	2.24	2.08	2.41	2.18	2.29	2.23	2.05	2.14	2.05	2.83	1.97	2.04
K_2O	0.26	0.34	0.18	0.15	0.77	0.32	0.41	0.10	0.06	0.44	0.30	0.32
P_2O_5	0.11	0.10	0.11	0.08	0.13	0.14	0.06	0.06	0.06	0.08	0.06	0.07
Total	100.75	99.81	100.55	100.57	100.07	100.70	100.46	99.89	100.04	100.14	99.79	100.39
Ignition loss	0.55	0	0.98	0.22	1.12	0.50	0.47	1.25	0.43	0	0.80	0.15
ppm:												
Nb	6.0	6.5	7.1	4.6	7.5	6.9	3.7	3.2	3.3	4.0	3.7	4.2
Zr	90.7	85.5	95.6	73.1	102.8	104.2	51.1	52.7	54.3	61.3	51.9	51.7
Y	35.9	33.2	36.1	32.5	41.4	41.4	25.2	24.3	23.6	21.9	27.7	27.6
Sr	105.0	98.8	118.4	91.8	96.4	98.1	99.9	106.6	110.7	115.3	99.3	99.7
Rb	4.3	9.2	3.4	2.7	23.6	11.4	9.4	0	0.5	1.8	5.9	5.9
Zn	100.6	89.4	104.7	84.1	110.9	111.2	80.2	81.2	84.4	84.2	79.7	82.3
Cu	193.4	147.6	194.9	187.1	63.4	248.0	92.8	153.7	159.0	176.7	162.8	111.1
Ni	92.3	61.0	77.0	85.8	52.6	92.1	60.9	76.8	78.1	82.5	72.1	63.4
Cr	202.3	217.0	183.8	221.7	134.8	145.6	130.5	126.3	119.7	145.2	124.6	129.4
V	391.4	359.3	355.7	372.6	418.3	441.9	311.9	335.8	337.2	397.2	324.3	310.5
Ce	9.8	7.8	9.0	7.4	9.8	11.8	1.1	6.7	6.6	3.2	4.7	1.0
Ba	40.2	47.6	52.1	47.5	50.3	59.5	33.8	19.9	21.1	34.5	27.3	33.0

salts were more altered than the upper ones (i.e., more vein filling). The conductivity of the basalts from 155 to 170 mbsf was very high, ranging from 1.7 to 2.4 $W \cdot m^{-1} \cdot K^{-1}$. The lowermost samples, below 175 mbsf, had values ranging from 1.4 to 1.7 $W \cdot m^{-1} \cdot K^{-1}$. The lower values here were in the more fractured samples.

Basement

Basaltic lavas and hard nannofossil chalks were recovered from the basement. Only V_p, wet-bulk density, and thermal conductivity measurements were taken on these rocks. These data are shown in Figures 33 and 34 and in Tables 12 and 13. There are obvious "steps" in these data due to the lithology change from basalt to chalk at 134 mbsf, then to basalt again at 155 mbsf.

The wet-bulk density of the basalts is constant, rarely deviating from an average of about 2.85 g/cm³. The density of the chalk is about 1.7 g/cm³. The V_p measurements show a fair amount of scatter within the basalts. However, the experimental error in V_p measurements was determined at less than 2% (approximately 100 m/s). There is a sharp increase in V_p from 3000 to 5000 m/s at the top of the two series of basalt flow units: at 110 mbsf and at 167 mbsf. The velocity and impedance are constant throughout the remainder of the basalt series.

Summary

The recovered rotary-drilled cores from Site 713 can be divided into four categories based upon physical properties measurements:

1. Highly disturbed soft oozes and clay-bearing oozes with shear strengths of less than 30 kPa, scattered porosities between 60% and 80%, scattered thermal conductivities of around 1.3 $W \cdot m^{-1} \cdot K^{-1}$, and constant V_p of 1550 m/s.
2. Stiff, cemented, impure ash-chalk, similar to the overlying oozes in porosity and thermal conductivity, but too cohesive for shear strength measurements, and with a V_p increasing with depth from 1550 to 2600 m/s.
3. Chalks from between flow units 6 and 7, with constant density of about 1.7 g/cm³, thermal conductivity of 1.2 $W \cdot m^{-1} \cdot K^{-1}$, and V_p between 2100 and 2600 m/s.
4. Basalt Units 1 to 35, showing sharp increases in V_p from below 3500 to above 5500 m/s between Units 1 and 3, and also between Units 7 and 9, V_p ranging from 5000 to 6000 m/s for other units, with high thermal conductivities of 1.4–2.4 $W \cdot m^{-1} \cdot K^{-1}$, and constant densities of 2.85 g/cm³.

The strong differences in density and V_p between rocks from categories 2, 3, and 4 give a steplike impedance profile. The magnitude of the impedance contrasts allows good definition of seismic reflectors.

SEISMIC STRATIGRAPHY

Sites 712 and 713 are located on the northern margin of the Chagos Bank, in water depths of 2892.4 m and 2909.8 m, respectively. The Chagos Bank forms the southern terminus of a continuous line of shallow carbonate banks and islands which stretch northward and intersect the western margin of India near Bombay. This ridge is believed to have been formed by volcanic activity over the Réunion hotspot as the Indian plate moved northward in early Tertiary time (see "Background and Objectives" section, this chapter).

The Chagos Bank was connected earlier in time with the Mascarene Plateau at the northern margin of the Nazareth Bank (in the region of Site 706). These two elevated blocks were separated from 35 Ma to the present by seafloor spreading on the Central Indian Ridge (McKenzie and Sclater, 1971). There is also a distinct break in topography between the Chagos Bank and the Maldive Islands, next in line to the north. This may represent a temporary lull in hotspot activity, a period of rapid northward plate motion, or a brief failed attempt at rifting.

Table 7 (continued).

20R-1 77–82	20R-2 142–147	20R-3 51–54	20R-3 73–77	20R-3 112–115	20R-3 137–139	20R-4 35–37	20R-4 140–145	20R-5 24–28	20R-5 127–130	21R-3 55–57	22R-1 20–23
49.99	49.59	49.14	49.03	49.76	49.59	49.89	49.38	49.41	49.59	49.61	49.76
1.06	0.99	1.00	0.97	1.12	1.06	0.98	0.98	0.99	1.01	0.98	0.98
16.54	15.87	15.87	15.31	14.65	14.25	15.81	15.26	15.54	15.43	15.04	15.27
9.52	10.55	10.43	11.20	12.58	12.17	10.84	11.52	10.88	10.83	11.55	11.43
0.16	0.19	0.19	0.20	0.19	0.19	0.18	0.20	0.19	0.19	0.20	0.20
8.19	7.77	7.38	7.37	8.01	7.70	7.70	7.20	7.68	7.79	7.51	7.54
12.39	13.20	13.38	13.92	11.47	12.56	13.23	13.66	13.21	13.01	13.29	13.29
2.19	1.95	2.16	2.09	2.37	2.03	2.01	1.90	1.94	1.94	1.93	1.86
0.10	0.06	0.10	0.18	0.34	0.37	0.06	0.21	0.06	0.06	0.05	0.05
0.06	0.05	0.06	0.06	0.07	0.06	0.05	0.06	0.06	0.05	0.05	0.05
100.20	100.20	99.71	100.33	100.56	99.95	100.75	100.37	99.96	99.90	100.21	100.43
1.40	1.45	0.81	0.83	0.52	0.79	0.33	0.30	0.71	0.71	0.33	0.28
3.8	4.6	3.6	4.0	4.3	4.4	3.9	3.9	3.9	4.0	3.5	4.1
54.5	51.6	52.3	51.0	56.6	56.0	50.2	51.7	52.1	52.5	51.3	50.9
22.4	25.1	25.9	25.9	29.0	26.6	24.5	26.4	25.3	25.2	25.4	25.9
108.7	105.6	105.0	101.4	97.8	95.5	103.1	101.0	102.6	102.9	99.0	99.4
0.3	1.0	0.9	3.3	7.4	11.3	0.5	4.5	1.0	0.5	1.1	0.8
82.6	81.7	82.2	79.3	91.8	85.7	79.8	80.3	79.1	82.8	76.8	77.6
61.6	153.2	151.5	181.8	248.1	45.6	151.7	139.0	152.1	155.3	154.2	151.2
77.2	76.1	89.0	89.4	62.9	64.4	72.6	87.0	71.9	73.2	70.7	68.9
122.5	110.2	121.6	121.8	84.9	98.2	111.6	129.1	108.6	118.4	106.1	104.5
353.7	331.7	326.9	327.2	359.8	341.2	324.4	314.2	327.4	326.2	320.7	315.6
2.4	2.3	4.5	4.4	4.5	8.3	4.2	4.1	2.5	5.0	1.4	0.2
29.6	22.7	24.6	30.0	25.7	23.7	28.5	20.1	21.9	30.3	22.4	26.5

The region around these sites slopes gently to the north and west and is bounded 25 nmi to the east by a steep 3000-m scarp, presumably related to an ancient interval of transform faulting (Fig. 35). We used seismic reflection profiles Wilkes 1731 and Vema 29-02 to determine the most suitable position for detailed surveying by the *JOIDES Resolution*. Our surveys included 3.5- and 12-kHz depth recorders and magnetometer profiles, as well as the usual 80 in.^{3} water-gun seismic reflection profile. Along a north-south line, the basement reflector appears as a series of discrete steps beneath 100–200 m of sediments (Fig. 36). This morphology is probably due to small-scale (100-m offset) normal faulting.

We observed in detail two or three distinct reflectors at Site 712 (Fig. 37). The first occurs at about 0.05 s (two-way traveltime) below the sediment-water interface. This corresponds to thin chert layers encountered within otherwise uniform nannofossil oozes at 40 mbsf. A somewhat stronger reflector occurs at about 0.08 s and is probably the top of a zone of silicified chalks in which core recovery was particularly poor. The basement reflector occurs at 0.18 s. We had to abandon drilling at this site because of hole instability. Loose calcareous sands below the chalks caved into the hole, threatening loss of the BHA.

At Site 713, 1.6 nmi to the north of Site 712, no distinct reflectors are seen above the basement, which occurs at 0.11 s. The total sedimentary section here is 106 m of carbonate ooze and chalks containing numerous volcanic-ash beds toward the base.

REFERENCES

Boersma, A., 1984. *Handbook of Common Tertiary* Uvigerina: New York (Microclimates Press).

Courtillot, V., Besse, J., Vandamme, D., Montigny, R., Jaeger, J.-J., and Cappetta, H., 1986. Deccan flood basalts at the Cretaceous-Tertiary boundary? *Earth Planet. Sci. Lett.*, 80:361–374.

Douglas, R. G., and Heitman, H., 1979. Slope and basin benthic foraminifera of the California borderland. *In* Doyle, L., and Pilkey, O. (Eds.), *Geology of Continental Slopes*, Spec. Publ. Econ. Paleontol. Mineral., 27:231–246.

Duncan, R. A., 1978. Geochronology of basalts from the Ninetyeast Ridge and continental dispersion in the eastern Indian Ocean. *J. Volcanol. Geotherm. Res.*, 4:283–305.

________, 1981. Hotspots in the southern oceans—an absolute frame of reference for motion of the Gondwana continents. *Tectonophysics*, 74:29–42.

Emerick, C. M., 1985. Age-progressive volcanism in the Comores Archipelago and northern Madagascar [Ph.D. dissert.]. Oregon State University, Corvallis.

Kennett, J. P., 1981. Marine tephrochronology. *In* Emiliani, C. (Ed.), *The Sea* (Vol. 7): New York (Wiley), 1373–1436.

McDuff, R. E., 1981. Major cation gradients in DSDP interstitial waters: the role of diffusive exchange between seawater and upper oceanic crust. *Geochim. Cosmochim. Acta*, 45:1705–1713.

McKenzie, D. P., and Sclater, J. G., 1971. The evolution of the Indian Ocean since the Late Cretaceous. *Geophys. J. R. Astron. Soc.*, 25: 437–528.

Morgan, W. J., 1981. Hotspot tracks and the opening of the Atlantic and Indian Oceans. *In* Emiliani, C. (Ed.), *The Sea* (Vol. 7): New York (Wiley), 443–487.

Schlich, R., 1982. The Indian Ocean: aseismic ridges, spreading centers, and oceanic ridges. *In* Nairn, A.E.M., and Stehli, F. G. (Eds.), *The Ocean Basins and Margins* (Vol. 6): New York (Plenum), 51–147.

Sclater, J. G., Abbott, D., and Thiede, J., 1977. Paleobathymetry and sediments of the Indian Ocean. *In* Heirtzler, J., et al. (Eds.), *Indian Ocean Geology and Biostratigraphy*: Washington (American Geophysical Union), 25–59.

Srinivasan, M. S., and Sharma, V., 1980. *Schwager's Car Nicobar Foraminifera in the Reports of the Novara Expedition—A Revision*. New Delhi (Today and Tomorrow Publ.).

Tjalsma, R. C., and Lohmann, G. P., 1983. *Paleocene-Eocene bathyal and abyssal benthic foraminifera from the Atlantic Ocean*, Spec. Publ. 4: New York (Micropaleontology Press).

Ms 115A-111

Table 8. Index-properties data, Sites 712 and 713.

Section interval (cm)	Depth (mbsf)	Water content (%)	Porosity (%)	Wet-bulk density (g/cm^3)	Dry-bulk density (g/cm^3)	Grain density (g/cm^3)	Carbonate content (wt%)
115-712A-							
1R-2, 62	2.12	46.15	69.82	1.56	0.84	2.73	93.71
1R-4, 62	5.12	46.10	70.85	1.57	0.85	2.87	94.95
1R-6, 62	8.12	44.25	68.21	1.57	0.88	2.73	94.10
2R-3, 60	13.00	40.14	65.90	1.68	1.00	2.92	93.49
2R-5, 59	16.12	37.04	61.78	1.71	1.08	2.78	95.30
3R-1, 60	19.60	39.77	64.77	1.69	1.02	2.82	92.85
3R-3, 60	22.60	39.98	65.27	1.67	1.00	2.86	93.61
3R-5, 24	25.24	36.18	60.41	1.73	1.10	2.73	93.20
4R-1, 60	29.20	39.15	63.11	1.70	1.03	2.69	93.34
4R-3, 23	31.83	46.16	69.85	1.58	0.85	2.73	93.34
5R-1, 60	38.90	44.66	69.65	1.63	0.90	2.88	92.79
5R-2, 60	40.40	44.82	70.49	1.58	0.87	2.98	93.64
6R-2, 60	50.00	29.76	52.53	1.75	1.23	2.65	97.02
11R-1, 10	96.20	30.01	54.68	1.86	1.30	2.85	99.05
11R-1, 60	96.70	40.03	64.80	1.93	1.16	2.79	99.65
11R-3, 24	98.08	30.32	53.66	1.89	1.32	2.70	98.72
12R-2, 101	108.21	39.70	65.00	1.70	1.03	2.86	71.59
12R-2, 103	108.23	38.70	63.40	1.71	1.05	2.78	81.99
12R-2, 105	108.25	38.90	62.90	1.80	1.10	2.70	75.71
12R-2, 107	108.27	37.00	61.90	1.75	1.10	2.80	76.84
12R-2, 110	108.30	37.00	61.90	1.75	1.10	2.80	95.27
115-713A-							
2R-2, 77	3.87	47.13	71.38	1.57	0.83	2.83	—
2R-5, 99	8.59	46.33	69.41	1.55	0.83	2.66	96.78
3R-2, 60	13.30	35.49	59.09	1.84	1.19	2.66	95.17
3R-4, 15	15.85	37.14	62.67	1.75	1.10	2.88	93.59
3R-6, 96	19.66	40.53	64.76	1.63	0.97	2.73	93.32
4R-2, 138	23.68	37.53	62.25	1.71	1.07	2.78	93.80
4R-5, 51	27.31	36.03	60.48	1.75	1.12	2.75	94.50
4R-7, 32	30.12	37.11	68.54	1.76	1.10	3.75	93.73
5R-3, 105	34.55	45.42	69.60	1.56	0.85	2.78	60.12
6R-1, 67	40.77	51.67	74.69	1.51	0.73	2.79	76.67
6R-1, 140	41.50	39.60	65.08	1.70	1.02	2.88	89.74
6R-5, 27	46.37	44.63	69.44	1.62	0.90	2.85	76.48
7R-3, 60	53.30	44.19	67.84	1.61	0.90	2.69	70.75
7R-5, 62	56.32	35.63	61.64	1.40	0.90	2.94	62.90
8R-2, 103	61.93	40.28	65.22	1.68	1.01	2.81	84.48
8R-4, 23	64.13	48.22	70.55	1.60	0.83	2.60	58.42
9R-2, 120	71.80	46.27	70.14	1.62	0.87	2.76	15.52
10R-1, 71	79.41	34.90	59.22	1.77	1.15	2.74	77.98
10R-2, 15	80.35	40.72	62.46	1.64	0.97	2.45	0.05
11R-4, 20	93.10	—	—	1.84	—	—	—

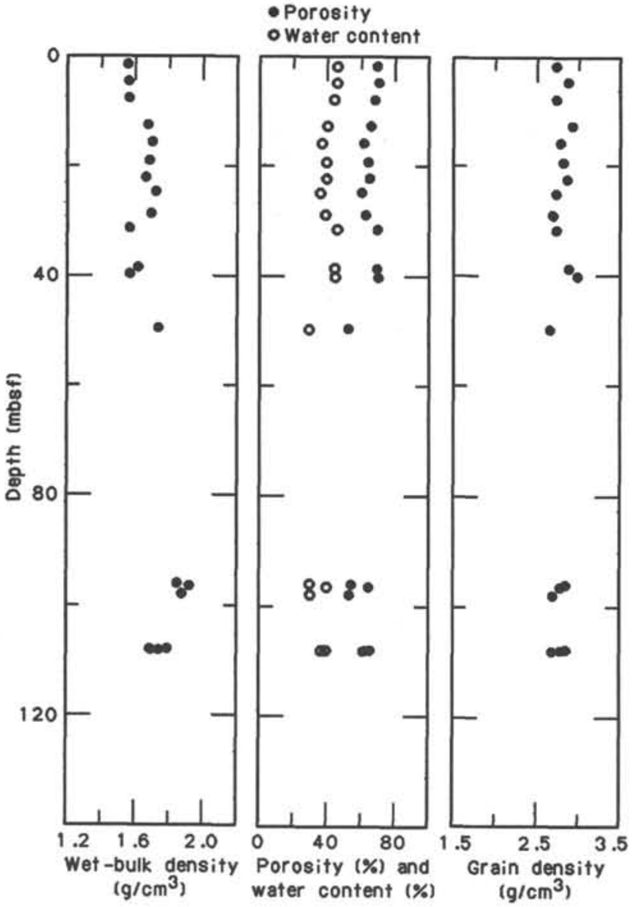

Figure 24. Index properties (wet-bulk density, water content, porosity, and grain density) at Site 712.

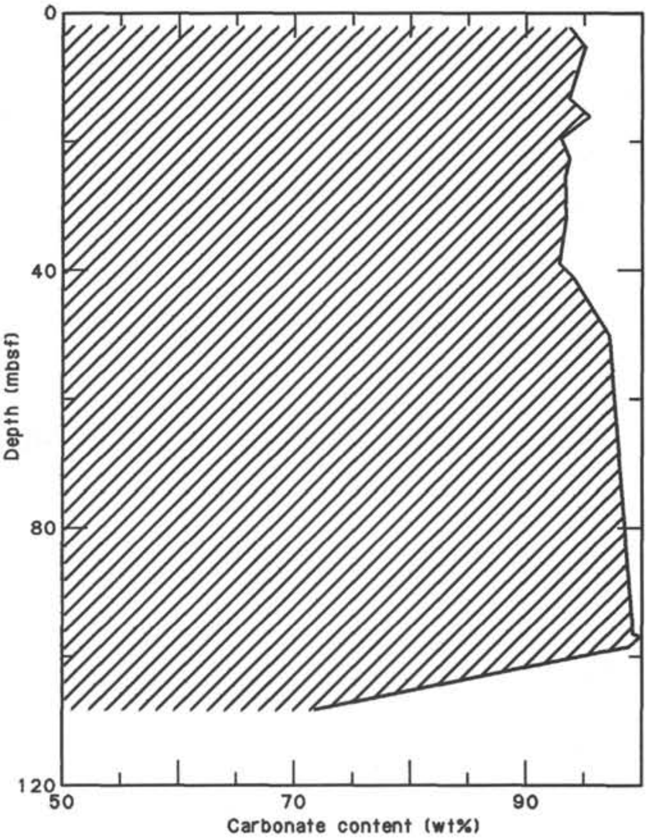

Figure 25. Carbonate content of samples for which the index properties were measured at Site 712.

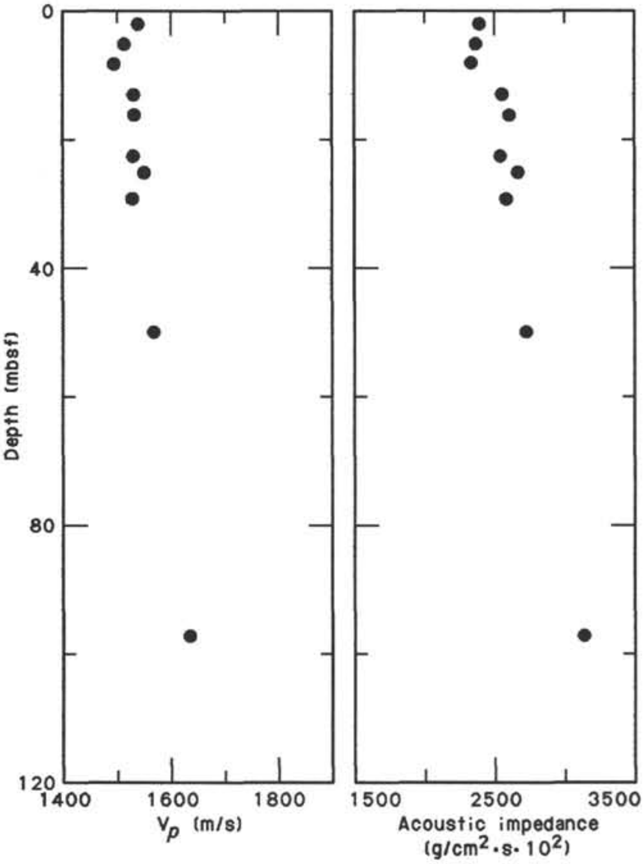

Figure 26. Compressional-wave velocity (V_p) and acoustic impedance at Site 712.

Table 10. Shear-wave velocity data, Site 712.

Section interval (cm)	Depth (mbsf)	V_s (m/s)
115-712A-		
1R-2, 48	1.98	65
1R-4, 37	4.87	99
1R-6, 50	8.00	87
2R-3, 54	12.94	106
2R-5, 67	16.20	69
3R-2, 53	21.03	66
3R-4, 54	24.04	110
4R-2, 78	30.88	110
5R-2, 93	40.73	63

Table 11. Motorized shear strength data, Sites 712 and 713.

Section interval (cm)	Depth (mbsf)	Peak (kPa)
115-712A-		
1R-2, 60	2.10	2.4
1R-4, 60	5.10	2.3
1R-6, 78	8.28	19.0
2R-3, 82	13.22	17.8
2R-5, 103	16.56	28.4
3R-2, 58	21.08	21.3
3R-4, 66	24.16	54.5
4R-2, 61	30.71	51.0
5R-2, 98	40.78	52.2
6R-2, 97	50.37	4.7
115-713A-		
2R-5, 81	8.41	2.6
3R-2, 86	13.56	16.4
3R-6, 86	19.56	8.8
4R-5, 63	27.43	16.1
4R-7, 30	30.10	27.0
6R-1, 138	41.48	11.1

Table 9. Compressional-wave velocity and acoustic impedance data, Holes 712A and 713A.

Section interval (cm)	Depth (mbsf)	V_p (m/s)	Acoustic impedance (g/cm^2·s·10^4)
115-712A-			
1R-2, 62	2.12	1540	24.02
1R-4, 62	5.12	1514	23.76
1R-6, 62	8.12	1495	23.47
2R-3, 60	13.00	1532	25.73
2R-5, 59	16.12	1534	26.23
3R-3, 60	22.60	1532	25.58
3R-5, 24	25.24	1552	26.84
4R-1, 60	29.20	1530	26.01
6R-2, 60	50.00	1569	27.45
11R-1, 98	97.08	1636	31.57
115-713A-			
3R-6, 88	19.58	1546	25.19
4R-5, 51	27.31	1556	27.23
5R-3, 104	34.54	1687	26.31
6R-1, 67	40.77	1619	24.44
6R-1, 141	41.51	1532	26.04
6R-5, 27	46.37	1688	27.34
7R-3, 60	53.30	1672	26.92
7R-5, 60	56.30	1671	23.39
8R-2, 103	61.93	1648	27.68
8R-4, 23	64.13	1645	26.32
9R-2, 119	71.79	1818	29.45
10R-1, 71	79.41	1790	31.68
10R-2, 62	80.82	2094	34.34
11R-1, 13	88.53	2219	0
11R-2, 35	90.25	2425	0
12R-1, 39	98.49	1846	0
12R-2, 150	101.10	2592	0

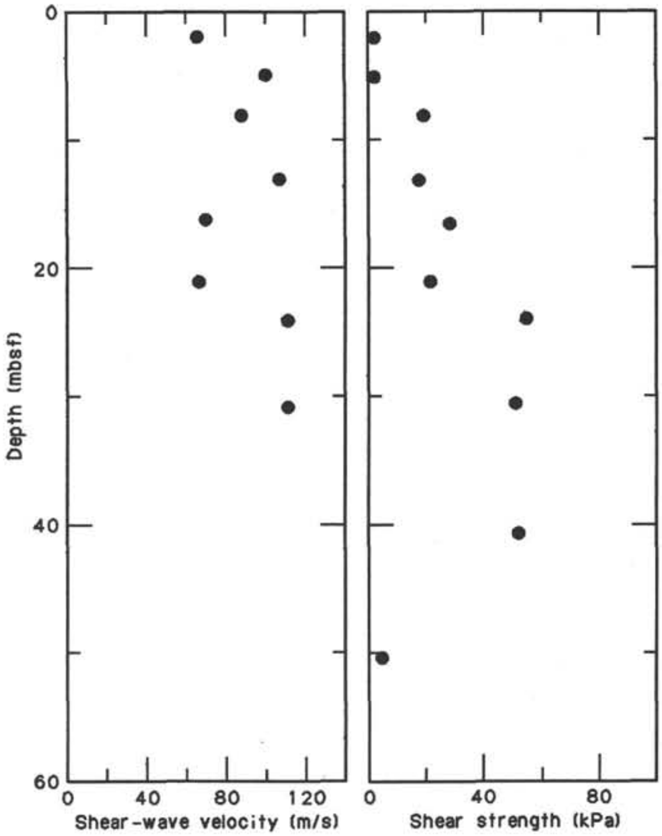

Figure 27. Shear-wave velocity (V_s) and shear strength at Site 712.

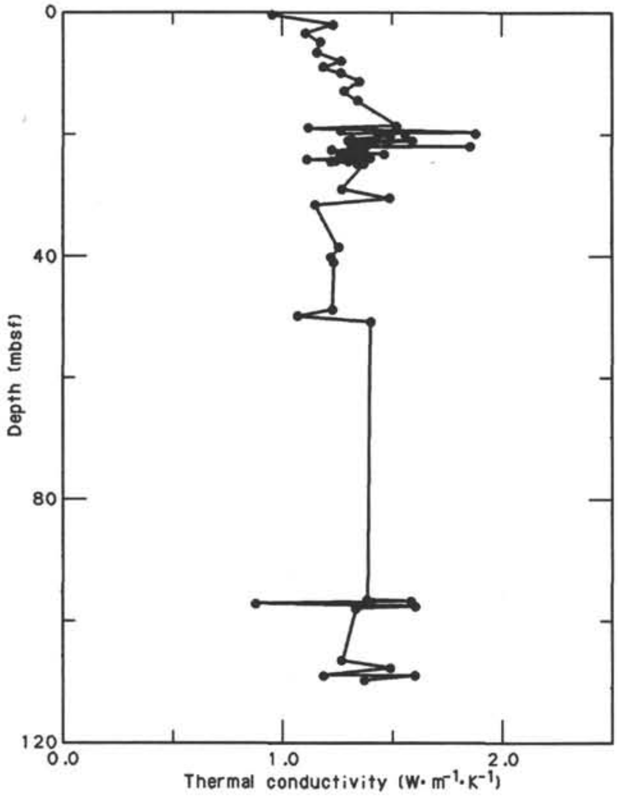

Figure 28. Thermal conductivity at Site 712.

Table 12. Thermal conductivity data, Sites 712 and 713.

Section interval (cm)	Depth (mbsf)	Thermal conductivity $(W \cdot m^{-1} \cdot K^{-1})$
115-712A-		
1R-1, 80	0.80	0.941
1R-2, 80	2.30	1.218
1R-3, 80	3.80	1.095
1R-4, 80	5.30	1.157
1R-5, 80	6.80	1.145
1R-6, 80	8.30	1.250
1R-7, 20	9.20	1.178
2R-1, 80	10.20	1.254
2R-2, 80	11.70	1.337
2R-3, 80	13.20	1.268
2R-4, 80	14.83	1.326
3R-1, 10	19.10	1.504
3R-1, 40	19.40	1.111
3R-1, 50	19.50	1.115
3R-1, 80	19.80	1.255
3R-1, 110	20.10	1.869
3R-1, 120	20.20	1.252
3R-1, 130	20.30	1.546
3R-1, 140	20.40	1.464
3R-2, 10	20.60	1.420
3R-2, 20	20.70	1.476
3R-2, 80	21.30	1.308
3R-2, 90	21.40	1.289
3R-2, 100	21.50	1.576
3R-2, 112	21.62	1.410
3R-2, 120	21.70	1.314
3R-2, 130	21.80	1.466
3R-2, 140	21.90	1.317
3R-3, 10	22.10	1.369
3R-3, 20	22.20	1.371
3R-3, 30	22.30	1.313
3R-3, 40	22.40	1.846
3R-3, 50	22.50	1.301
3R-3, 60	22.60	1.359
3R-3, 70	22.70	1.335
3R-3, 80	22.80	1.336
3R-3, 90	22.90	1.307
3R-3, 110	23.10	1.216
3R-4, 10	23.60	1.286
3R-4, 20	23.70	1.447
3R-4, 30	23.80	1.368
3R-4, 50	24.00	1.330
3R-4, 60	24.10	1.251
3R-4, 70	24.20	1.347
3R-4, 80	24.30	1.387
3R-4, 90	24.40	1.383
3R-4, 100	24.50	1.102
3R-4, 110	24.60	1.331
3R-4, 120	24.70	1.232
3R-4, 130	24.80	1.212
3R-4, 140	24.90	1.292
3R-5, 12	25.12	1.326
3R-5, 25	25.25	1.359
4R-1, 80	29.40	1.261
4R-2, 80	30.90	1.472
4R-3, 40	32.00	1.143
5R-1, 75	39.05	1.243
5R-2, 80	40.60	1.210
5R-3, 10	41.40	1.224
6R-1, 115	49.05	1.216
6R-2, 80	50.20	1.060
6R-3, 25	51.15	1.389
11R-1, 50	96.60	1.377
11R-1, 80	96.90	1.574
11R-1, 120	97.30	0.871
11R-2, 12	97.72	1.598
11R-3, 25	98.09	1.327
12R-1, 75–80	106.45	1.260
12R-2, 69–74	107.76	1.480
12R-3, 40–45	108.97	1.180
12R-3, 46–51	109.03	1.590
12R-3, 115–120	109.72	1.360
115-713A-		
2R-1, 80	2.40	1.653
2R-2, 80	3.90	1.503
2R-3, 80	5.40	1.509
2R-3, 114	5.74	1.365
2R-4, 50	6.60	0.904
2R-4, 100	7.10	0.746
2R-5, 50	8.10	0.662
2R-5, 100	8.60	1.212
2R-6, 50	9.60	1.210
3R-1, 80	12.00	1.189
3R-2, 50	13.20	1.338
115-713A- (Cont.)		
3R-3, 80	15.00	1.310
3R-4, 60	16.30	1.459
3R-5, 50	17.70	1.410
3R-5, 100	18.20	1.098
3R-6, 50	19.20	1.009
3R-6, 100	19.70	1.184
3R-7, 30	20.50	1.009
4R-1, 80	21.60	1.292
4R-2, 50	22.80	1.214
4R-3, 50	24.30	1.107
4R-3, 50	24.30	1.107
4R-3, 100	24.80	1.534
4R-4, 80	26.10	1.344
4R-5, 50	27.30	1.515
4R-5, 100	27.80	0.967
4R-6, 80	29.10	1.362
4R-7, 30	30.10	1.346
5R-2, 50	32.50	1.253
5R-2, 100	33.00	1.464
5R-3, 50	34.00	1.149
5R-3, 100	34.50	1.044
6R-1, 34–40	40.44	1.190
6R-4, 13–20	44.73	1.200
6R-4, 116–122	45.76	1.160
6R-5, 48–58	46.58	1.010
7R-1, 41–50	50.11	1.060
7R-2, 136–142	52.56	1.180
7R-3, 30–37	53.00	1.110
7R-4, 22–29	54.42	1.180
7R-5, 35–44	56.05	1.040
8R-1, 44–50	59.84	1.070
8R-2, 24–32	61.14	1.080
8R-3, 53–60	62.93	1.110
9R-1, 20–30	69.30	1.170
9R-2, 69–75	71.29	1.330
9R, CC, 1–10	72.06	1.140
10R-1, 2–14	78.72	1.220
10R-2, 1–6	80.21	1.200
10R, CC, 1–11	81.71	1.150
11R-1, 14–21	88.54	1.060
11R-2, 4–16	89.94	1.140
11R-3, 114–121	92.54	1.120
11R-4, 38–44	93.28	1.080
12R-1, 92–105	99.02	1.090
12R-2, 89–90	100.49	1.180
12R, CC, 9–20	101.22	1.290
13R-1, 72–80	108.42	1.320
13R-2, 16–25	109.29	1.360
13R-3, 14–20	110.73	1.450
14R-1, 58–70	117.78	1.470
14R-2, 1–10	118.68	1.400
14R-3, 107–115	120.86	1.450
14R-4, 47–59	121.70	1.600
15R-1, 81–89	127.51	1.660
15R-2, 123–133	129.43	1.650
15R-3, 58–75	130.28	1.560
15R-4, 47–64	131.67	1.600
15R-5, 26–37	132.96	1.660
15R-5, 120–140	135.40	1.170
15R-6, 62–71	136.33	1.130
16R-1, 35–44	136.55	1.090
16R-2, 72–80	138.21	1.100
16R-3, 66–79	139.66	1.180
16R-4, 76–83	141.16	1.090
16R-5, 39–48	142.27	1.210
17R-1, 79–88	146.49	1.090
17R-2, 85–98	148.05	1.220
17R-3, 108–119	149.80	1.160
17R-4, 10–19	150.37	1.190
18R-1, 118–130	156.38	1.820
19R-1, 6–14	164.46	1.770
19R-2, 114–124	167.04	1.930
19R-3, 24–30	167.64	2.410
20R-1, 51–60	174.41	2.070
20R-2, 80–87	176.20	1.370
20R-3, 64–70	177.54	1.540
20R-4, 1–16	178.21	1.510
20R-5, 83–97	180.53	1.700
20R-6, 81–88	182.01	1.650
21R-1, 100–110	184.30	1.420
21R-2, 116–123	185.46	1.660
21R-3, 65–73	186.95	1.720
21R-4, 98–108	188.78	1.620
22R-1, 8–15	190.28	1.780

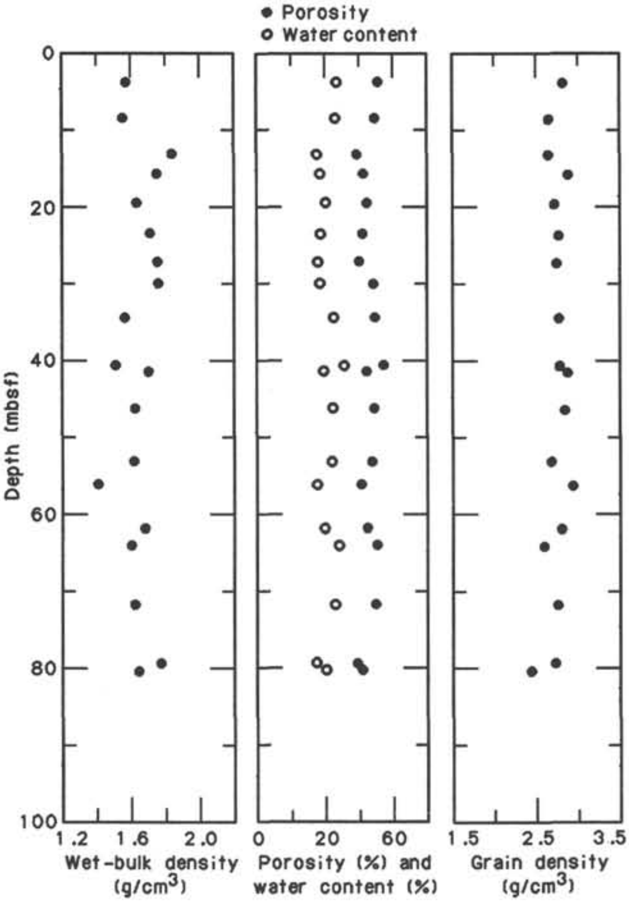

Figure 29. Index properties (wet-bulk density, water content, porosity, and grain density) at Site 713.

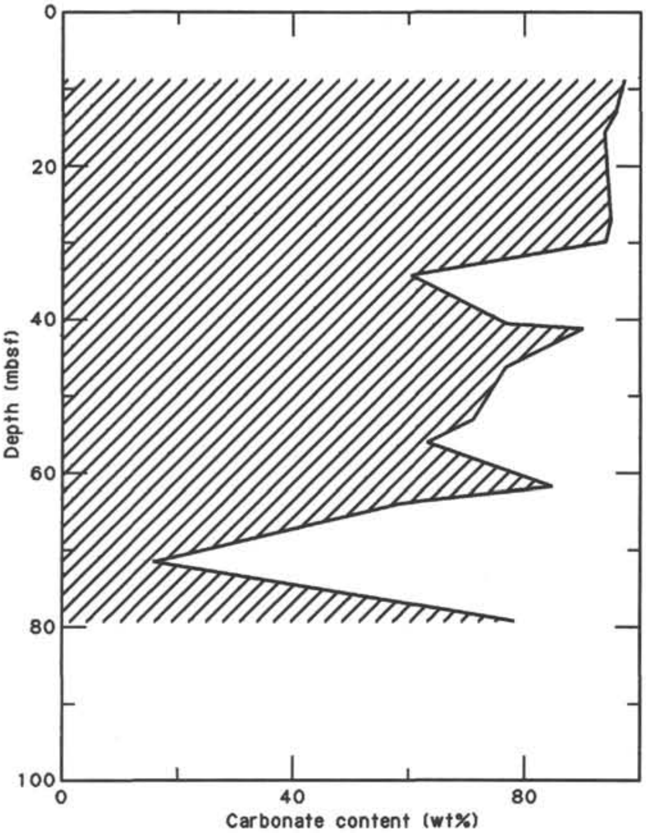

Figure 30. Carbonate content of samples for which the index properties were measured at Site 713.

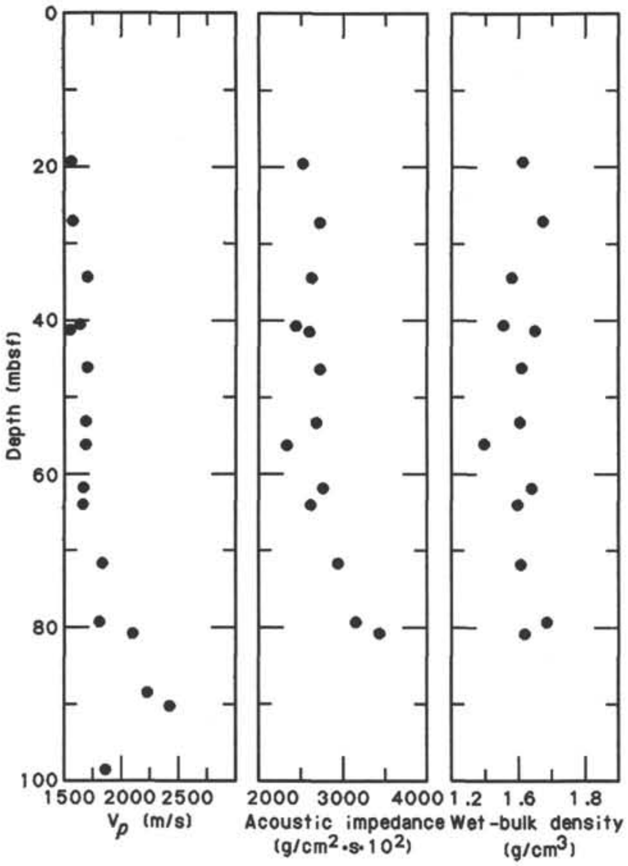

Figure 31. Compressional-wave velocity (V_p), computed acoustic impedance, and wet-bulk density in the sedimentary section at Site 713.

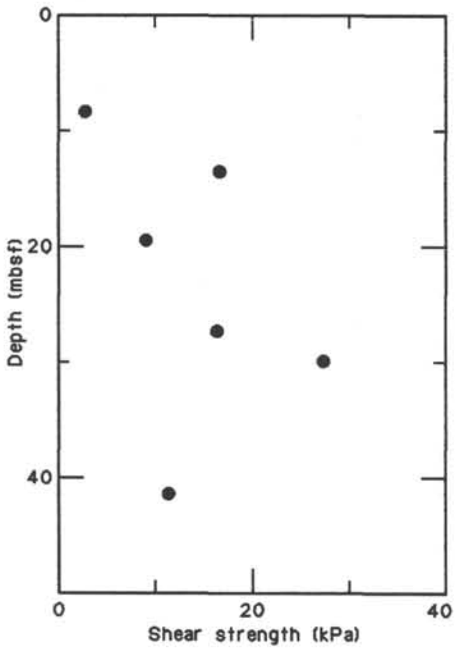

Figure 32. Shear strength at Site 713.

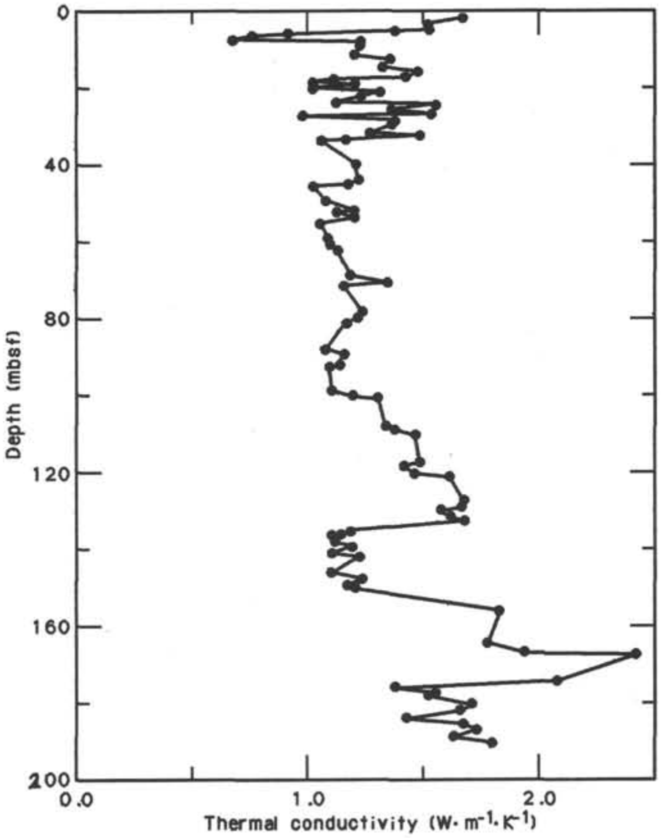

Figure 33. Thermal conductivity at Site 713.

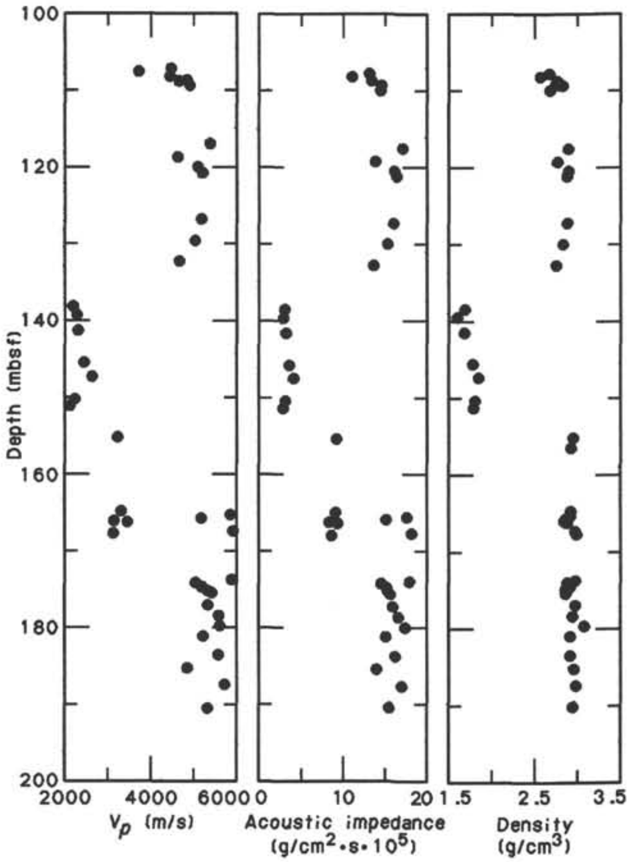

Figure 34. Compressional wave-velocity (V_p), acoustic impedance, and wet-bulk density of basalts and interbedded nannofossil chalks at Site 713.

Table 13. Compressional-wave velocity, wet-bulk density, and acoustic impedance of the basement section at Site 713.

Section interval (cm)	Depth (mbsf)	V_p (m/s)	Wet-bulk density (g/cm^3)	Acoustic impedance (g/cm^2·s·10^5)
115-713A-				
13R-1, 18	107.88	4474	2.67	11.90
13R-1, 59	108.29	3705	2.57	10.18
13R-1, 112	108.82	4446	2.76	12.27
13R-2, 29	109.42	4847	2.74	13.28
13R-2, 34	109.47	4681	2.82	13.20
13R-2, 91	110.04	4918	2.68	13.18
14R-1, 48	117.68	5410	2.90	15.68
14R-2, 69	119.36	4650	2.77	12.88
14R-3, 80	120.59	5121	2.90	14.85
14R-4, 8	121.31	5248	2.88	15.11
15R-1, 73	127.43	5201	2.88	14.97
15R-3, 46	130.16	5062	2.84	14.37
15R-5, 18	132.88	4696	2.76	12.96
16R-2, 117	138.66	2165	1.70	3.68
16R-3, 73	139.73	2248	1.61	3.61
16R-4, 134	141.74	2291	1.69	3.87
17R-1, 11	145.81	2434	1.79	4.35
17R-2, 38	147.58	2625	1.86	4.88
17R-4, 26	150.53	2212	1.82	4.02
17R-4, 122	151.49	2104	1.80	3.78
18R-1, 24	155.44	3224	2.95	9.51
19R-1, 62	165.02	3291	2.93	9.64
19R-1, 123	165.63	5882	2.92	17.17
19R-2, 8	165.98	5222	2.87	14.98
19R-2, 37	166.27	3127	2.86	8.94
19R-2, 54	166.44	3441	2.88	9.91
19R-3, 25	167.65	5942	2.98	17.70
19R-3, 52	167.92	3115	2.99	9.31
20R-1, 15	174.05	5909	2.98	17.60
20R-1, 43	174.33	5061	2.89	14.62
20R-1, 96	174.86	5232	2.92	15.27
20R-1, 139	175.29	5376	2.87	15.42
20R-2, 24	175.64	5464	2.87	15.68
20R-3, 36	177.26	5359	2.98	15.96
20R-4, 46	178.66	5601	2.95	16.52
20R-5, 31	180.01	5627	3.08	17.33
20R-6, 12	181.30	5240	2.92	15.30
21R-1, 45	183.75	5590	2.92	16.32
21R-2, 67	185.47	4855	2.96	14.37
21R-3, 134	187.64	5746	2.98	17.12
22R-1, 26	190.46	5356	2.95	15.80

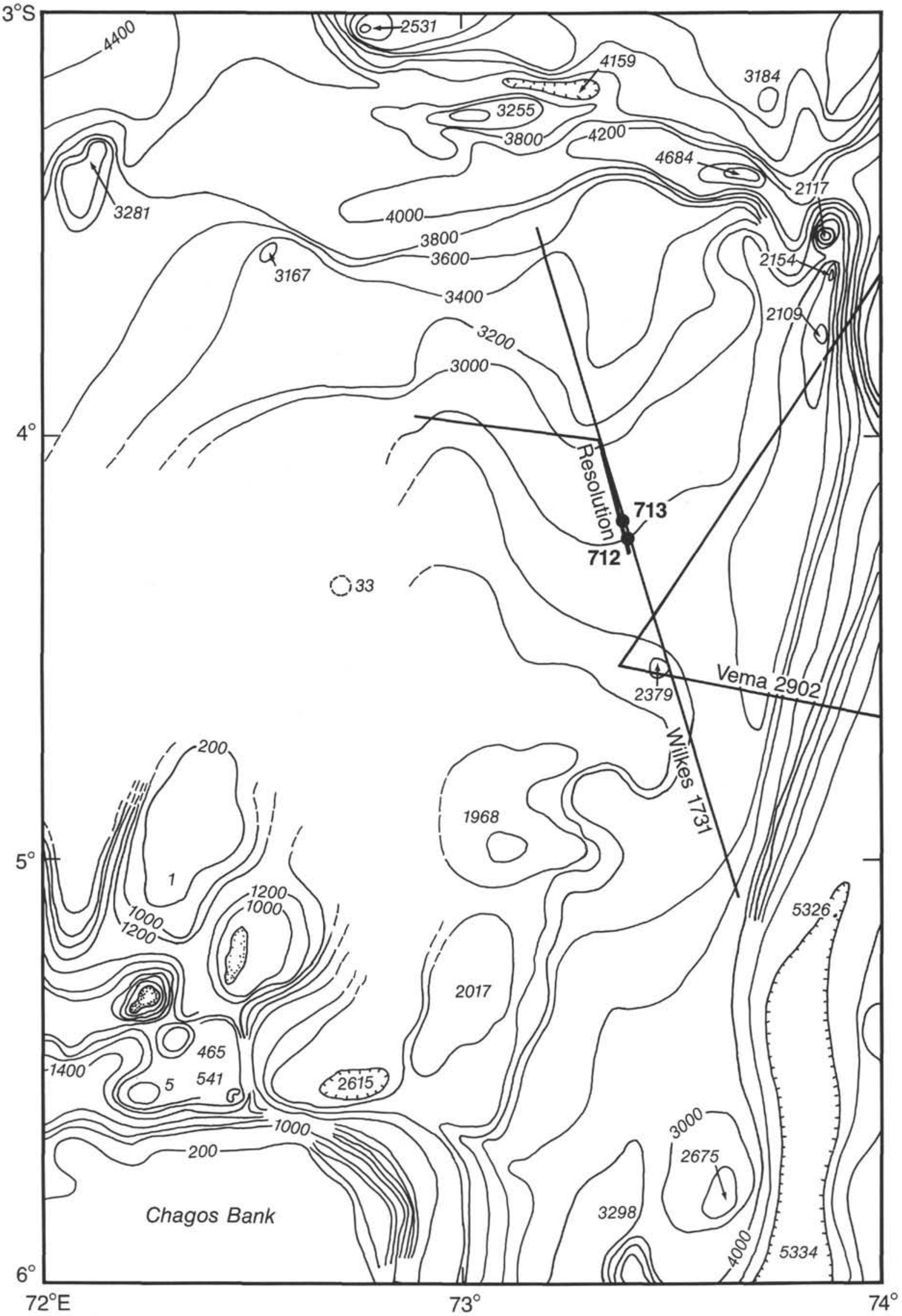

Figure 35. Bathymetry and seismic lines in the region of Sites 712 and 713 at the northern margin of the Chagos Bank.

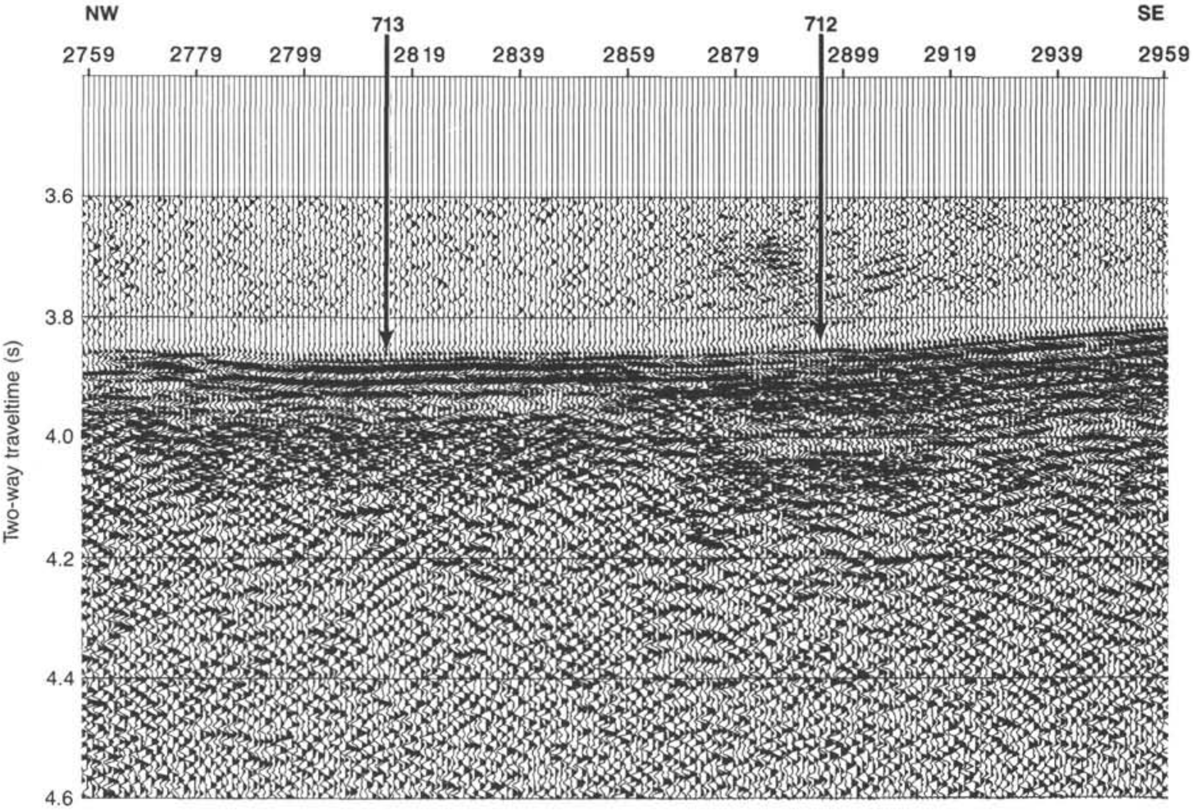

Figure 36. The *JOIDES Resolution* single-channel seismic (SCS), water-gun reflection profile over Sites 712 and 713. The clear basement reflector steps up to the north between the sites, but generally it slopes down in a series of ~100-m offsets. Sediment thickness varies between 100 and 200 m.

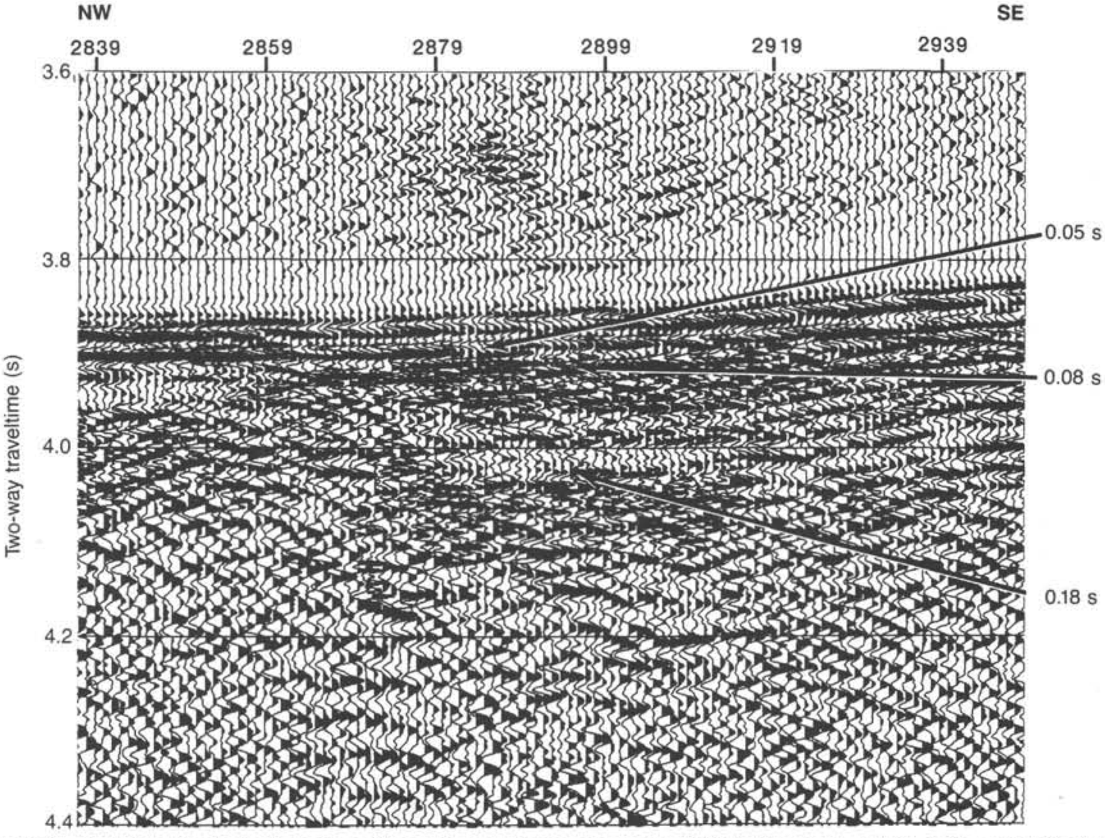

Figure 37. Detailed seismic stratigraphy at Sites 712 and 713 reveals several distinct reflectors; at 0.05, 0.08, and 0.18 s (two-way traveltimes). From the *JOIDES Resolution* single-channel seismic (SCS), water-gun reflection profile.

SITE 712 HOLE A CORE 1R CORED INTERVAL 2892.4-2901.8 mbsl; 0.0-9.4 mbsf

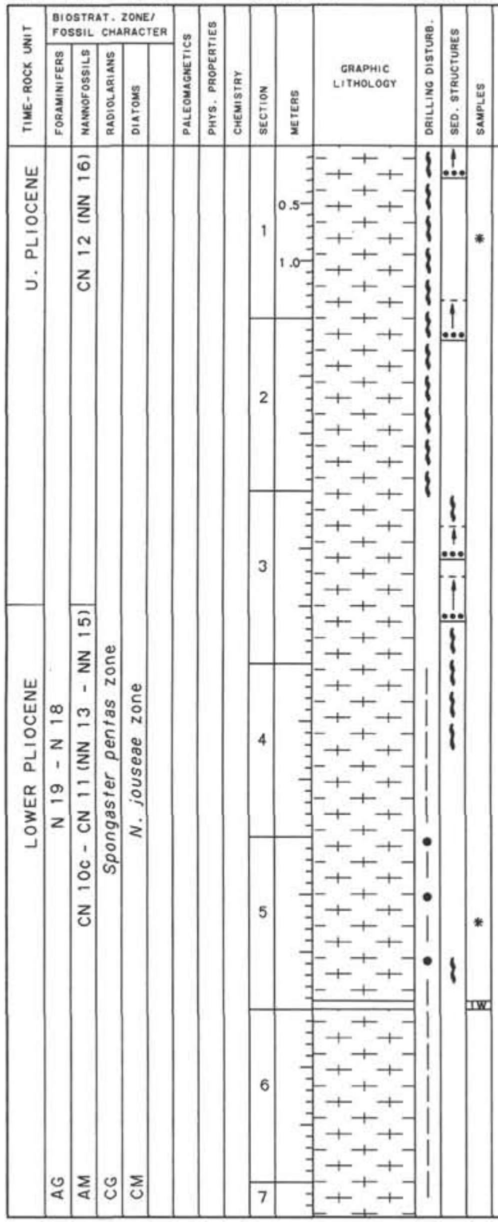

LITHOLOGIC DESCRIPTION

FORAMINIFER-NANNOFOSSIL OOZE

Major lithology: Foraminifer-nannofossil ooze, very pale brown (10YR 7/3, 8/3) to white (10YR 8/1, 8/2), weakly bioturbation mottled. Much of core is slightly to moderately disturbed.

SMEAR SLIDE SUMMARY (%):

	1, 80 D	5, 80 D
TEXTURE:		
Sand	40	30
Silt	10	20
Clay	50	50
COMPOSITION:		
Quartz	Tr	Tr
Mica	Tr	—
Clay	15	5
Foraminifers	40	40
Nannofossils	45	53
Radiolarians	Tr	1
Sponge spicules	—	1

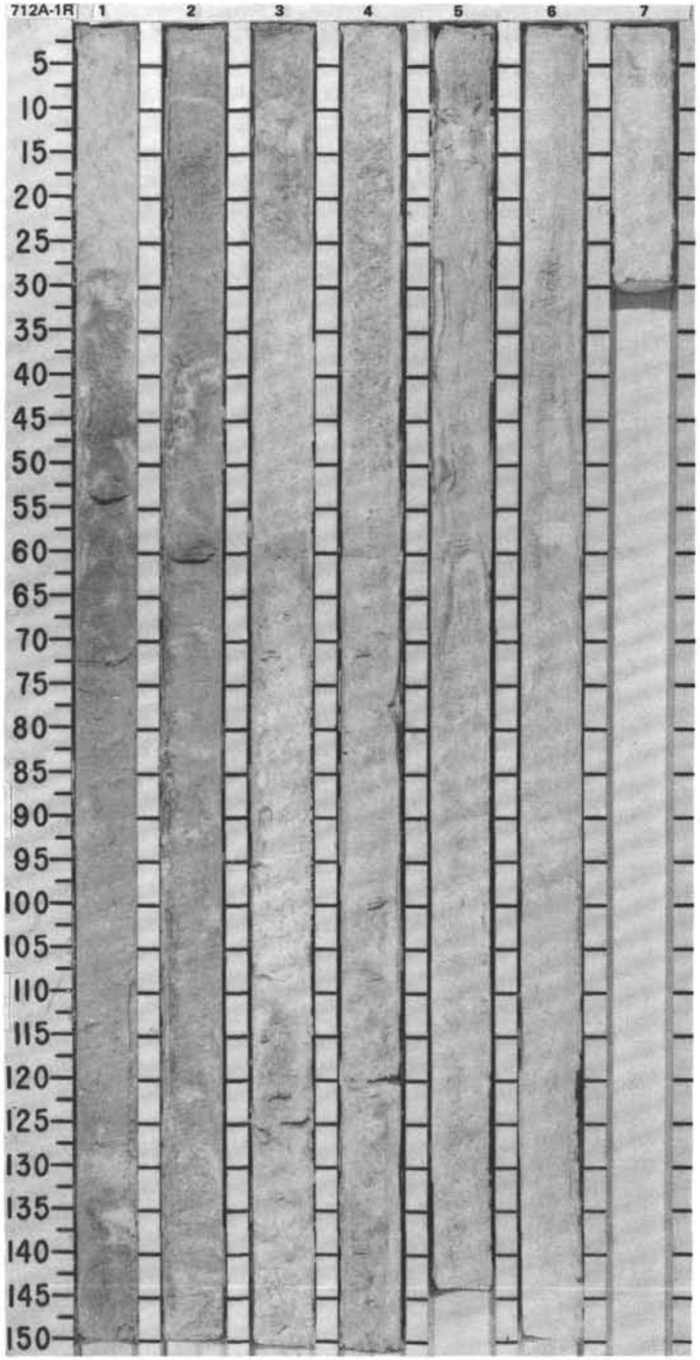

SITE 712 HOLE A CORE 2R CORED INTERVAL 2901.8-2911.4 mbsl; 9.4-19.0 mbsf

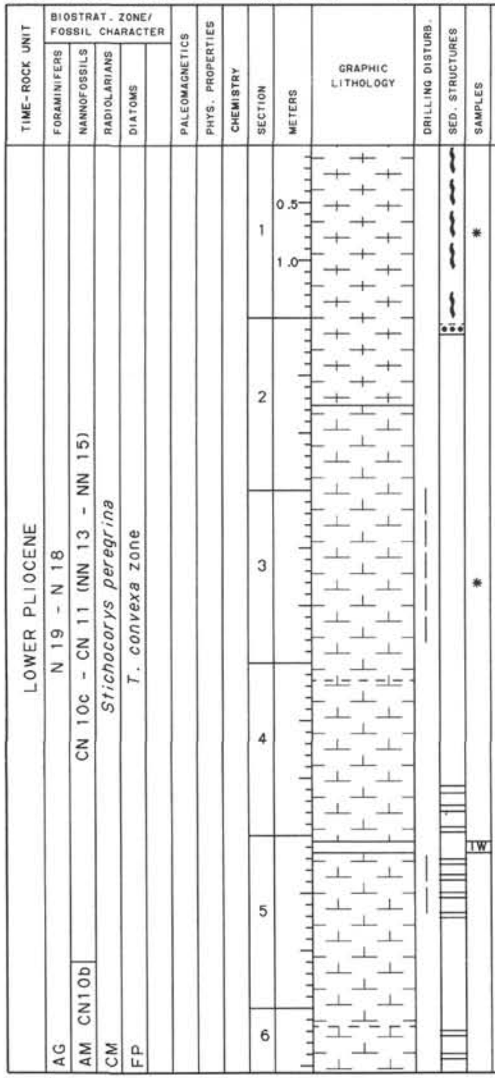

LITHOLOGIC DESCRIPTION

FORAMINIFER-NANNOFOSSIL OOZE and FORAMINIFER-BEARING NANNOFOSSIL OOZE

Major lithology: Foraminifer-nannofossil ooze, white (10YR 8/2) to very pale brown (10YR 7/3), weakly color mottled; grading downcore to foraminifer-bearing nannofossil ooze, white (N9), homogeneous, with scattered pyrite stains and a few thin, faint light gray (5Y 7/1) horizons where indicated in Sections 4, 5, and 6.

Note: Section 3 was cut 13 cm too long, thus confusing true sub-bottom depths in deeper sections. True section breaks are therefore plotted with dashed lines.

SMEAR SLIDE SUMMARY (%):

	1, 80 D	3, 80 D
TEXTURE:		
Sand	30	20
Silt	15	10
Clay	55	70
COMPOSITION:		
Quartz	Tr	Tr
Feldspar	Tr	—
Clay	8	5
Dolomite	—	Tr
Foraminifers	35	20
Nannofossils	55	69
Diatoms	—	1
Radiolarians	2	3
Sponge spicules	Tr	2

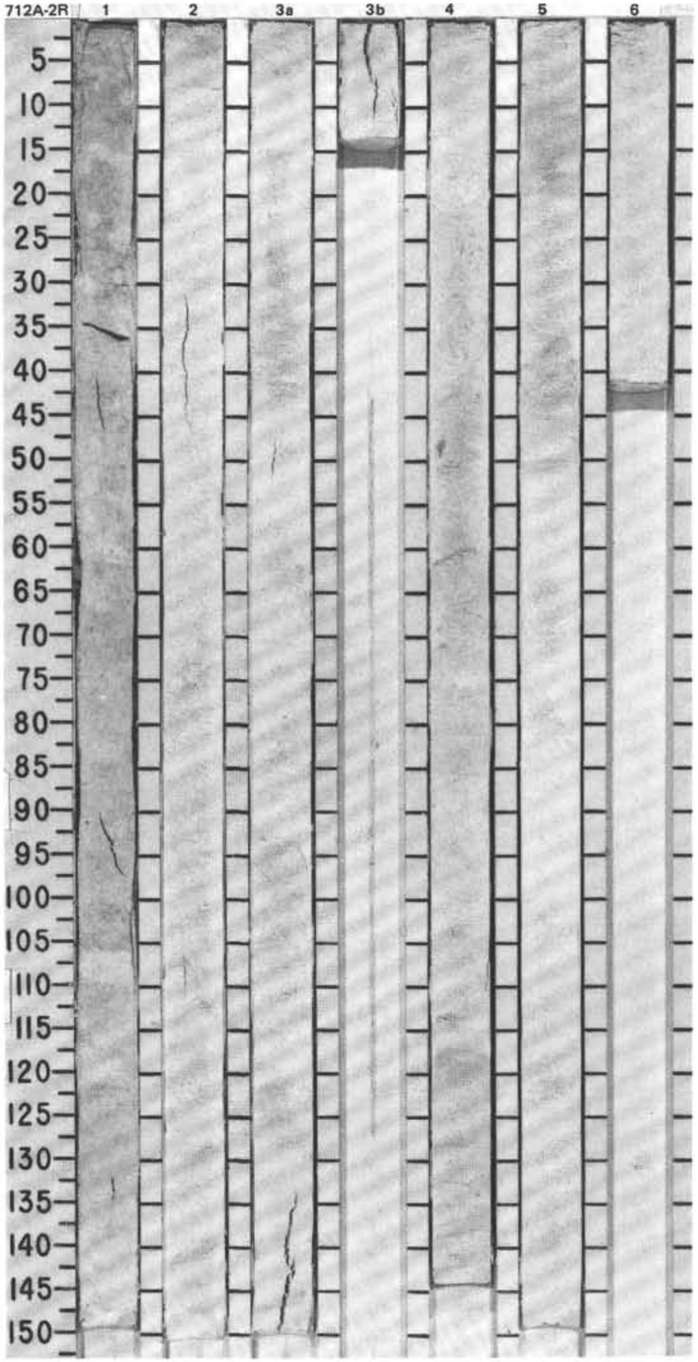

SITE 712 HOLE A CORE 3R CORED INTERVAL 2911.4-2921.0 mbsl; 19.0-28.6 mbsf

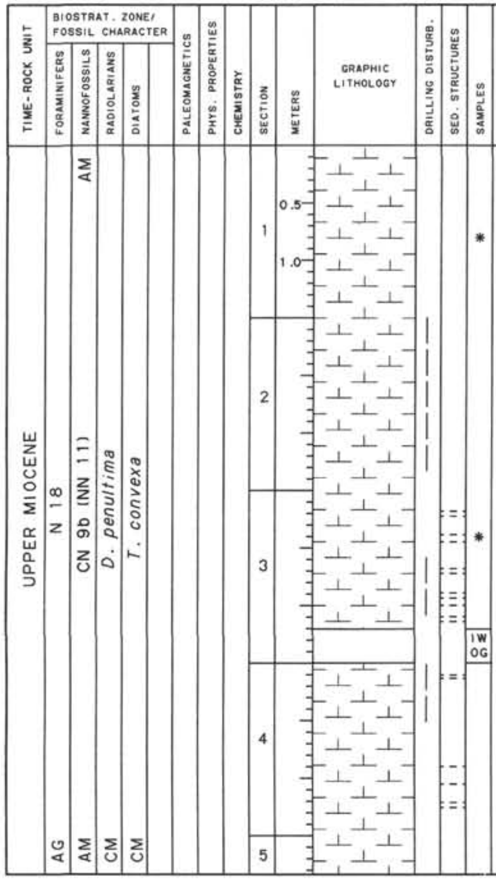

LITHOLOGIC DESCRIPTION

FORAMINIFER-BEARING NANNOFOSSIL OOZE

Major lithology: Foraminifer-bearing nannofossil ooze, white (N9) to very light gray (N8, 5Y 8/1), homogeneous, with numerous faint light yellowish gray (5Y 7/1) to light gray (N7) horizons as indicated in Sections 3 and 4. Pyrite stains were also observed in Section 4, 50-100 cm.

SMEAR SLIDE SUMMARY (%):

	1, 80 D	3, 42 D
TEXTURE:		
Sand	20	15
Silt	10	20
Clay	70	65
COMPOSITION:		
Quartz	—	Tr
Clay	5	8
Volcanic glass	Tr	1
Foraminifers	20	15
Nannofossils	69	65
Diatoms	Tr	6
Radiolarians	3	5
Sponge spicules	3	Tr
Fish remains	Tr	—

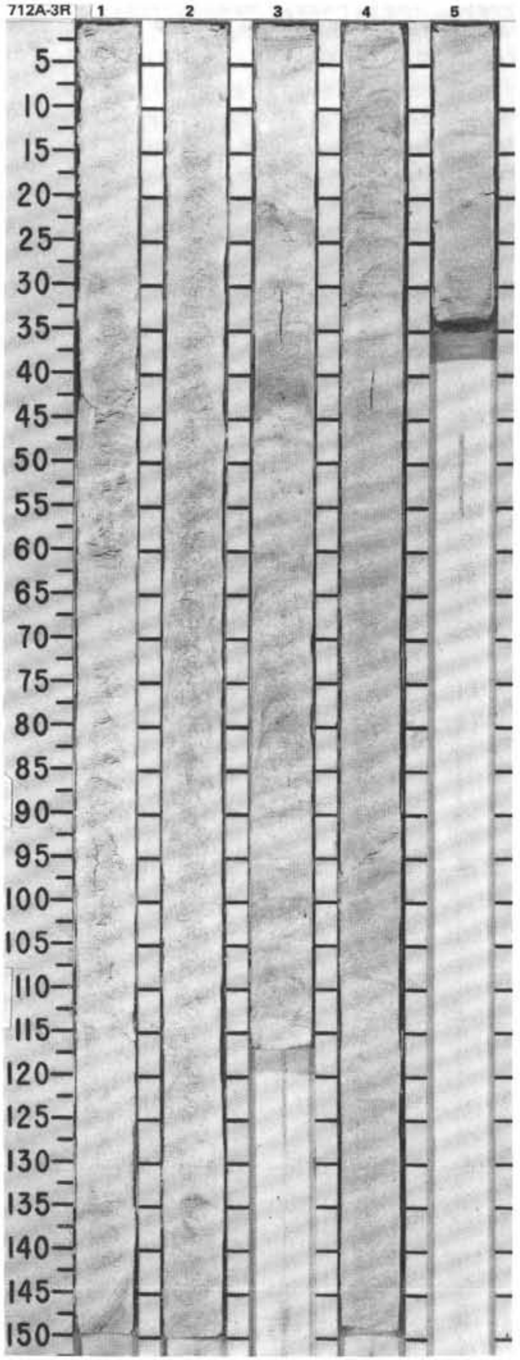

SITE 712 HOLE A CORE 4R CORED INTERVAL 2921.0-2930.7 mbsl; 28.6-38.3 mbsf

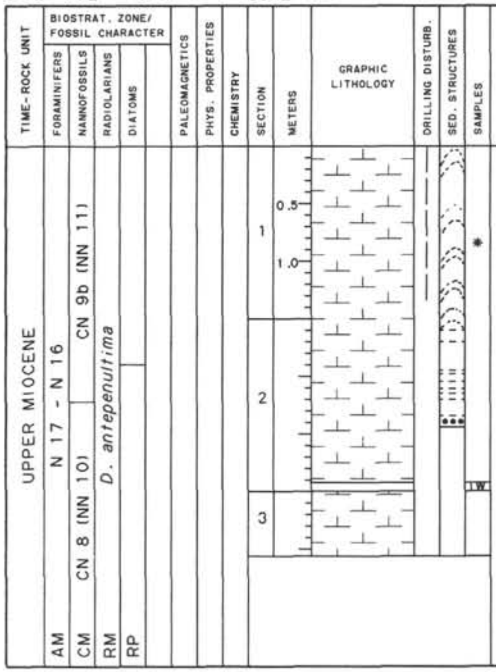

LITHOLOGIC DESCRIPTION

FORAMINIFER-BEARING NANNOFOSSIL OOZE

Major lithology: Foraminifer-bearing nannofossil ooze, grayish white (N8) to very light greenish gray (5G 8/1), homogeneous, with numerous faint light yellowish gray (5Y 7/1) to light gray (N7) horizons as indicated in Sections 1 and 2. Core disturbance in Section 1 has deformed these slightly darker horizons.

Thin turbidite consisting of a slightly coarser, white (10YR 8/2) foraminifer-nannofossil ooze, with sharp base at Section 2, 95 cm.

SMEAR SLIDE SUMMARY (%):

	1, 80 D
TEXTURE:	
Sand	15
Silt	20
Clay	65
COMPOSITION:	
Clay	5
Volcanic glass	Tr
Foraminifers	15
Nannofossils	65
Diatoms	1
Radiolarians	8
Sponge spicules	6

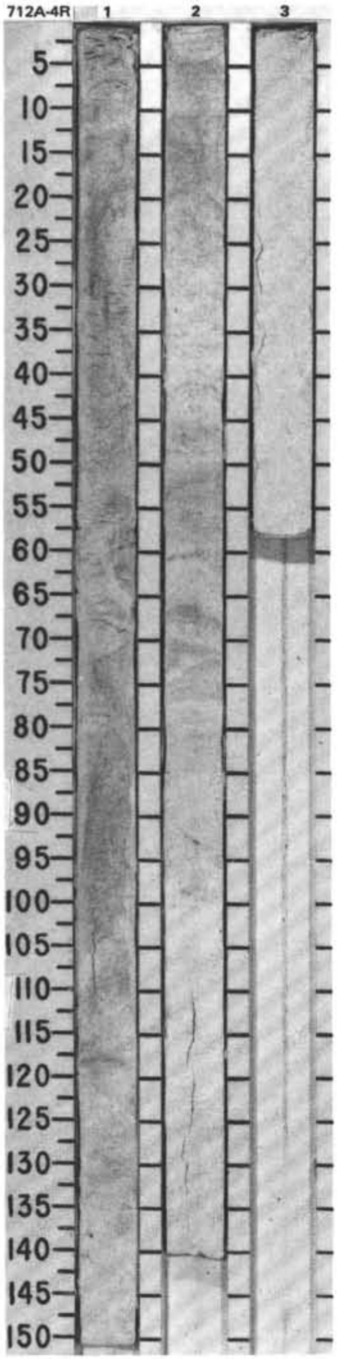

SITE 712 HOLE A CORE 5R CORED INTERVAL 2930.7-2940.3 mbsl; 38.3-47.9 mbsf

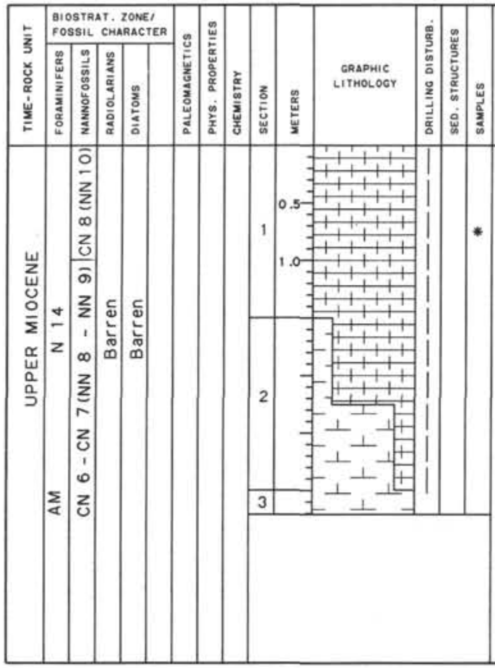

LITHOLOGIC DESCRIPTION

FORAMINIFER-NANNOFOSSIL CHALK and FORAMINIFER-NANNOFOSSIL OOZE

Major lithology: Semi-indurated foraminifer-nannofossil chalk, grading downcore to foraminifer-nannofossil ooze. Very light greenish gray (5G 8/1) and homogeneous throughout, except for the incipient lithification near the top of the core. Chalky material is slightly disturbed.

SMEAR SLIDE SUMMARY (%):

	1, 80 D
TEXTURE:	
Sand	35
Silt	10
Clay	55
COMPOSITION:	
Mica	Tr
Clay	5
Foraminifers	40
Nannofossils	50
Radiolarians	3
Sponge spicules	2
Silicoflagellates	Tr

SITE 712 HOLE A CORE 6R CORED INTERVAL 2940.3-2949.9 mbsl; 47.9-57.5 mbsf

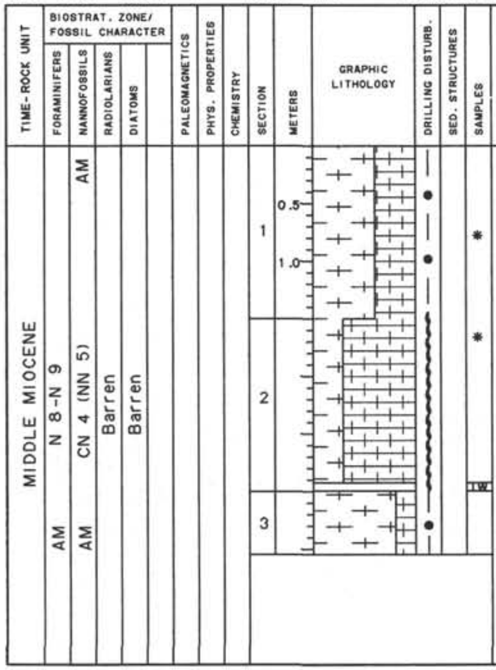

LITHOLOGIC DESCRIPTION

NANNOFOSSIL-FORAMINIFERAL OOZE and NANNOFOSSIL-FORAMINIFERAL CHALK

Major lithology: Interbedded nannofossil-foraminiferal ooze and chalk, white (N9), homogeneous in appearance but moderately to heavily disturbed throughout. Section 1 contains numerous pebble-sized subangular fragments of shallow water limestone and, possibly, dolomite. A small pocket of pale green (5G 6/2) altered volcanic ash was observed at Section 2, 18 cm.

SMEAR SLIDE SUMMARY (%):

	1, 80 D	2, 18 M
TEXTURE:		
Sand	50	20
Silt	10	60
Clay	40	20
COMPOSITION:		
Clay	—	10
Volcanic glass	Tr	80
Dolomite	Tr	—
Foraminifers	55	2
Nannofossils	45	8
Radiolarians	Tr	—

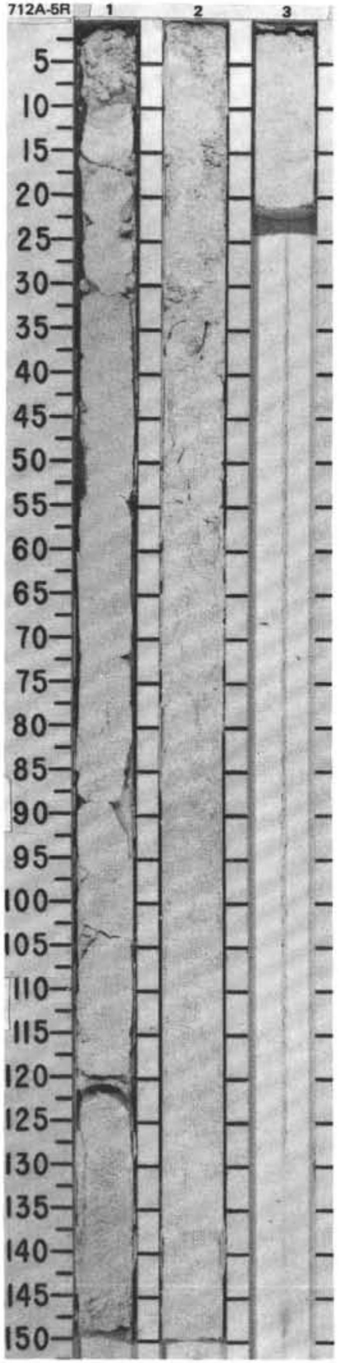

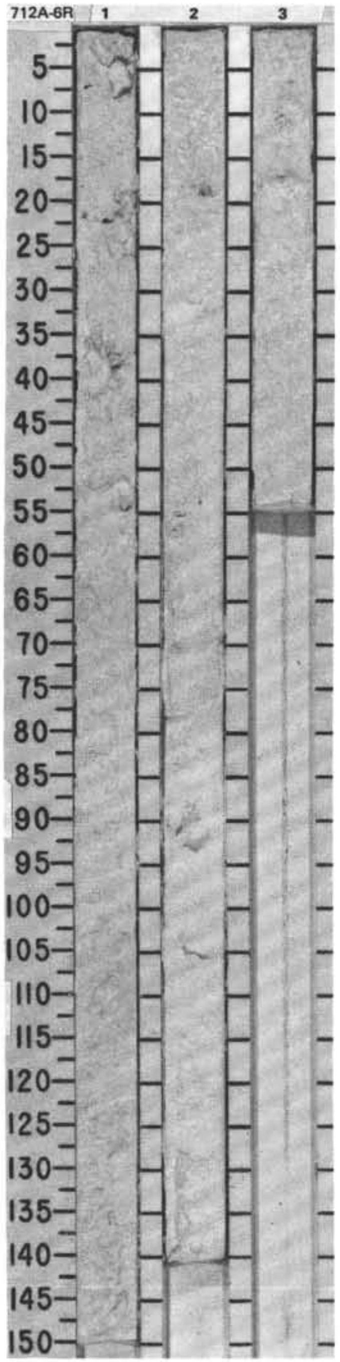

712 A 7R NO RECOVERY

SITE 712 HOLE A CORE 8R CORED INTERVAL 2959.6-2969.2 mbsl; 67.2-76.8 mbsf

TIME-ROCK UNIT	BIOSTRAT. ZONE/ FOSSIL CHARACTER FORAMINIFERS	NANNOFOSSILS	RADIOLARIANS	DIATOMS	PALEOMAGNETICS	PHYS. PROPERTIES	CHEMISTRY	SECTION	METERS	GRAPHIC LITHOLOGY	DRILLING DISTURB.	SED. STRUCTURES	SAMPLES	LITHOLOGIC DESCRIPTION
		Barren		Barren				CC						CALCAREOUS WACKESTONE and PACKSTONE PEBBLES Recovered material consists of three limestone pebbles in the CC: a. Wackestone, one specimen (4 × 2 × 2 cm), white (N9), with preserved bryozoans and moldic porosity. b. Packstone, two specimens (2 × 1 × 1 cm each), white (N9), with unidentifiable grains; both have moldic porosity, but one specimen shows sparry infilling of molds.

712 A 9R NO RECOVERY

SITE 712 HOLE A CORE 10R CORED INTERVAL 2979.8-2988.5 mbsl; 86.4-96.1 mbsf

TIME-ROCK UNIT	BIOSTRAT. ZONE/ FOSSIL CHARACTER FORAMINIFERS	NANNOFOSSILS	RADIOLARIANS	DIATOMS	PALEOMAGNETICS	PHYS. PROPERTIES	CHEMISTRY	SECTION	METERS	GRAPHIC LITHOLOGY	DRILLING DISTURB.	SED. STRUCTURES	SAMPLES	LITHOLOGIC DESCRIPTION
UPPER OLIGOCENE	Barren	CM CP 19a (NP 24)	Barren					CC						FORAMINIFER-BEARING NANNOFOSSIL CHALK CC contains several pebble-sized pieces of white (N9) foraminifer-bearing nannofossil chalk, and a single small fragment of well-lithified foraminifer grainstone.

SITE 712 HOLE A CORE 11R CORED INTERVAL 2988.5-2998.1 mbsl; 96.1-105.7 mbsf

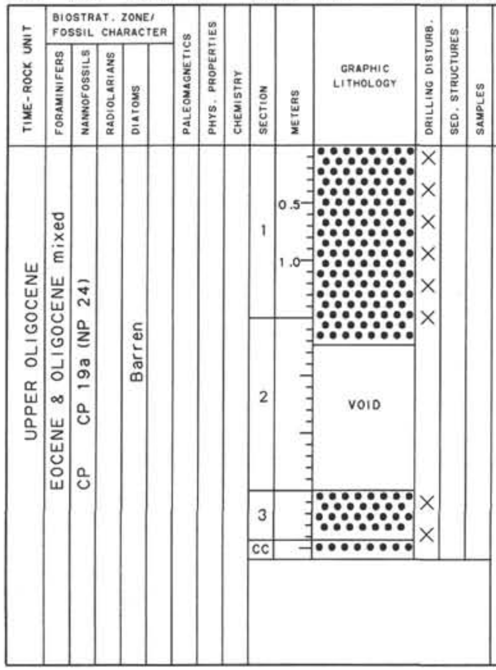

LITHOLOGIC DESCRIPTION

LIMESTONE RUBBLE

Recovered material consists entirely of a drilling rubble made up of small angular to subrounded recrystallized limestone pebbles.

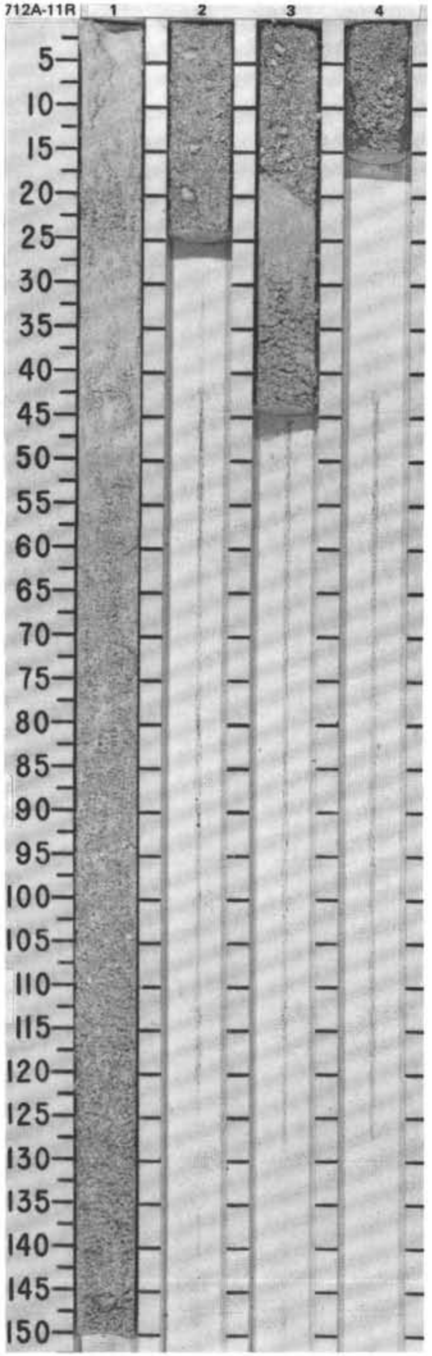

SITE 712 HOLE A CORE 12R CORED INTERVAL 2998.1-3007.7 mbsl; 105.7-115.3 mbsf

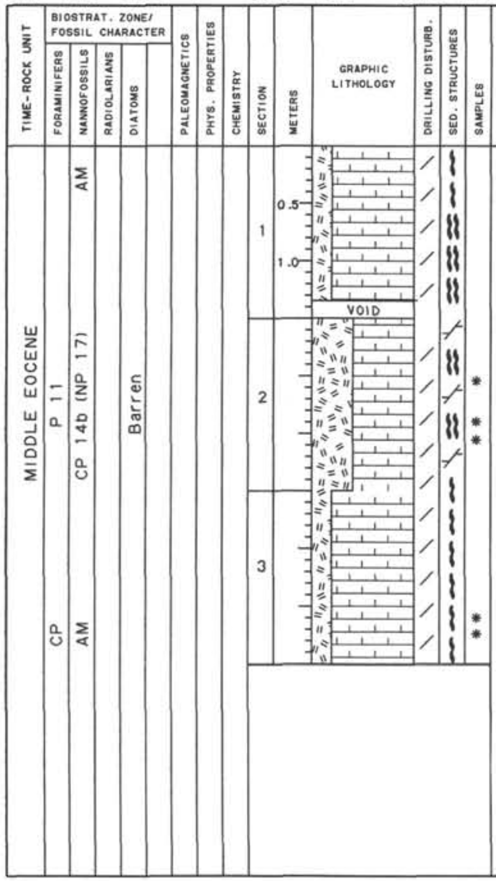

LITHOLOGIC DESCRIPTION

Interbedded FORAMINIFER-BEARING NANNOFOSSIL CHALK and VOLCANIC ASH

Major lithology: Foraminifer-bearing nannofossil chalk and mafic volcanic ash layers, complexly interbedded and heavily bioturbated. Pure chalk layers are white (10YR 8/2), light gray (10YR 7/2), to very pale brown (10YR 8/3), while concentrated ash layers are grayish brown (2.5Y 5/2), very dark gray (N3), to very dark grayish brown (2.5Y 3/2). Chalk layers containing variable proportions of dispersed ash typically range in color from gray (5Y 5/1), light olive brown (2.5Y 5/4), to light brownish gray (2.5Y 6/2). Volcanic ash makes up an estimated 25-30% of the core by volume.

Minor lithology: Clay-bearing nannofossil chalk, distinctive light yellowish brown (10YR 6/4), moderately bioturbated. This lithology occurs rarely as thin lenses in Section 1, 85-90 cm, Section 2, 25-27 and 103-105 cm, and Section 3, 55-58 cm.

Several normal microfaults were observed in Section 2, centered on about 18, 63, and 142 cm.

Note: Section 1 was cut short by mistake and sediments in Sections 1 and 2 are actually continuous.

SMEAR SLIDE SUMMARY (%):

	2, 56 M	2, 93 D	2, 104 D	3, 113 M	3, 118 D
TEXTURE:					
Sand	10	15	5	5	—
Silt	70	5	5	90	15
Clay	20	80	90	5	85
COMPOSITION:					
Quartz	—	—	Tr	Tr	—
Feldspar	Tr	—	—	—	—
Clay	5	5	25	Tr	15
Volcanic glass	91	Tr	3	98	3
Foraminifers	1	20	1	—	—
Nannofossils	3	75	66	2	75
Radiolarians	Tr	—	—	—	4
Sponge spicules	—	—	5	—	2
Calcispheres	—	—	—	—	1

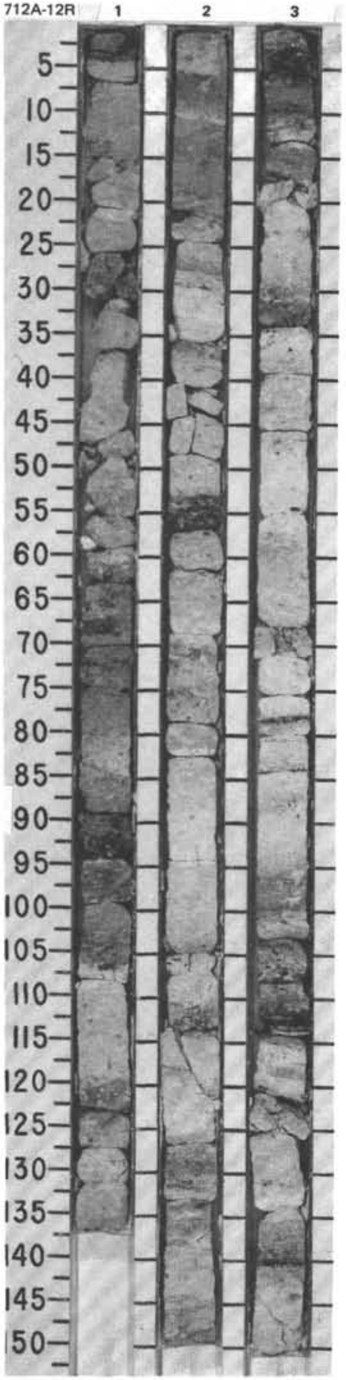

SITE 713 HOLE A CORE 1R CORED INTERVAL 2909.8-2911.4 mbsl; 0.0-1.6 mbsf

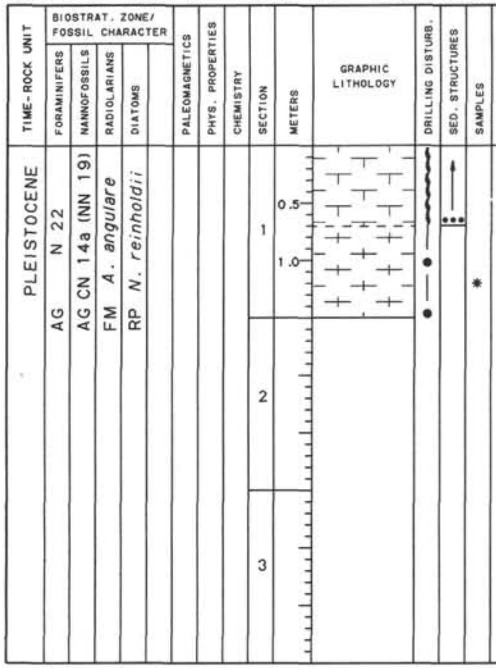

LITHOLOGIC DESCRIPTION

FORAMINIFER-NANNOFOSSIL OOZE

Section 1, 0-70 cm: Badly disturbed by drilling, this interval consists of a coarse, artificially-graded foraminiferal sand (ooze), light gray (10YR 7/2) in color.

Major lithology: Foraminifer-nannofossil ooze, very pale brown (10YR 8/2) to light gray (10YR 7/2), moderately disturbed, with faint distorted mottling. Section 1, 70-152 cm.

SMEAR SLIDE SUMMARY (%):

	1, 120 D
TEXTURE:	
Sand	35
Silt	15
Clay	50
COMPOSITION:	
Volcanic glass	Tr
Accessory minerals:	
Opaques	Tr
Foraminifers	45
Nannofossils	55
Radiolarians	Tr
Sponge spicules	Tr

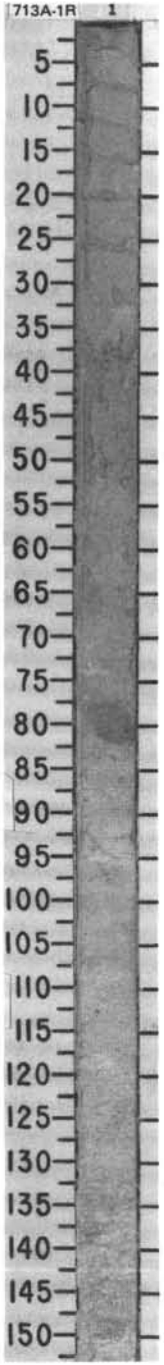

SITE 713 HOLE A CORE 2R CORED INTERVAL 2911.4-2921.0 mbsl; 1.6-11.2 mbsf

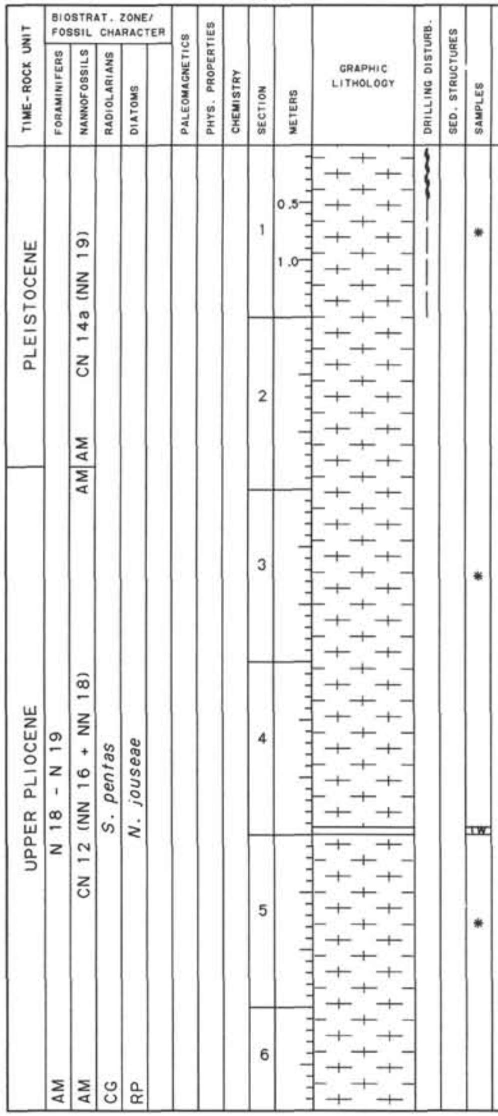

LITHOLOGIC DESCRIPTION

FORAMINIFER-NANNOFOSSIL OOZE

Major lithology: Foraminifer-nannofossil ooze, white (10YR 8/2) to light gray (10YR 7/2), homogeneous but irregularly mottled. Core is badly disturbed in Section 1, 0-60 cm.

SMEAR SLIDE SUMMARY (%):

	1, 71 D	3, 73 D	5, 74 D
TEXTURE:			
Sand	30	30	35
Silt	10	10	10
Clay	60	60	55
COMPOSITION:			
Volcanic glass	—	—	Tr
Dolomite	Tr	—	—
Foraminifers	30	30	35
Nannofossils	70	70	65
Radiolarians	Tr	Tr	Tr
Sponge spicules	Tr	Tr	—

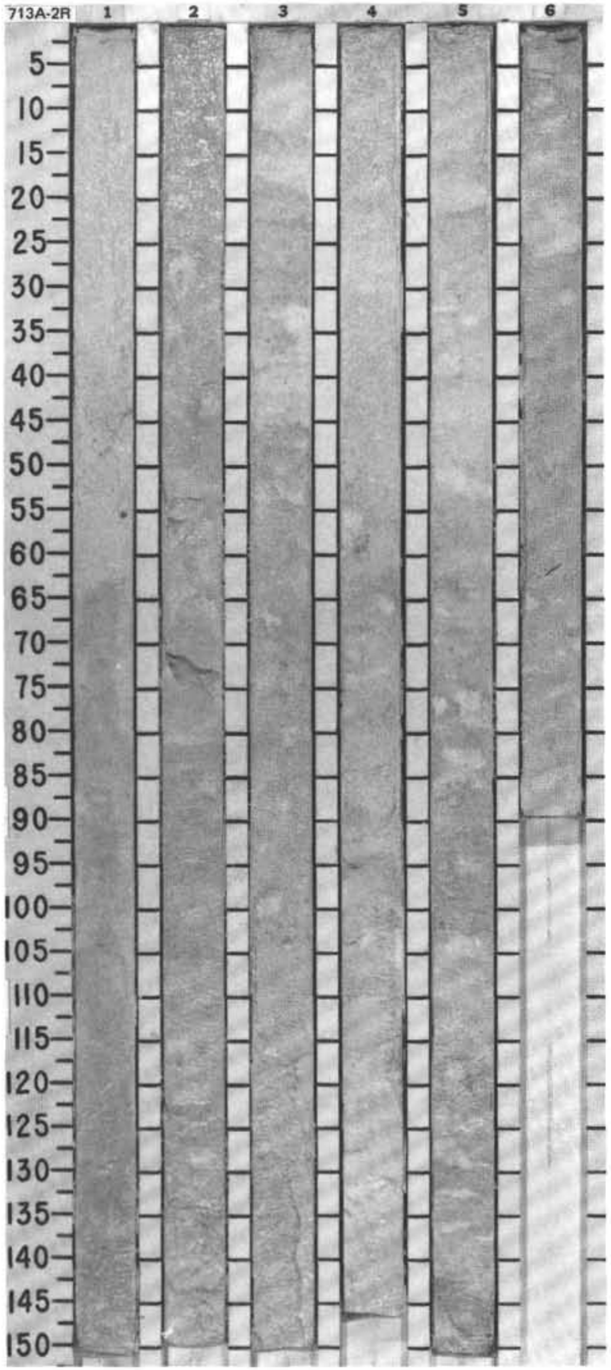

SITE 713 HOLE A CORE 3R CORED INTERVAL 2921.0-2930.6 mbsl; 11.2-20.8 mbsf

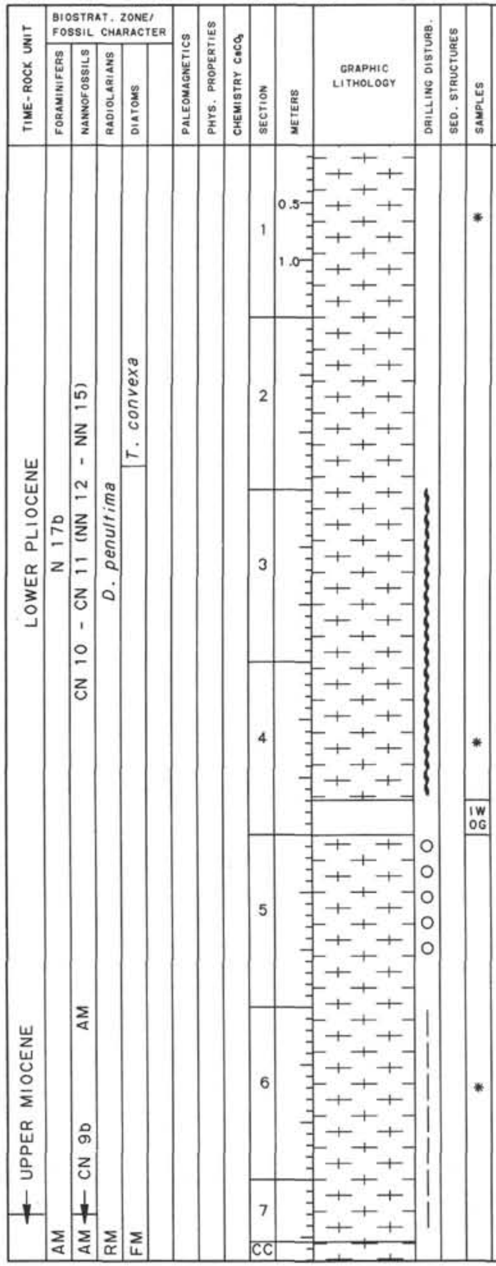

LITHOLOGIC DESCRIPTION

FORAMINIFER-NANNOFOSSIL OOZE

Major lithology: Foraminifer-nannofossil ooze, white (10YR 8/2) to light gray (10YR 7/2), faintly mottled, with much of the core disturbed. Degree of consolidation ranges widely from firmer (undisturbed) ooze in Section 1 to very soft and soupy (disturbed) ooze in Sections 3, 4, and 5.

SMEAR SLIDE SUMMARY (%):

	1, 70 D	4, 70 D	6, 70 D
TEXTURE:			
Sand	30	30	30
Silt	10	10	10
Clay	60	60	60
COMPOSITION:			
Clay	5	5	—
Volcanic glass	—	Tr	—
Foraminifers	30	30	30
Nannofossils	65	65	68
Diatoms	—	—	1
Radiolarians	Tr	—	Tr
Sponge spicules	Tr	Tr	1

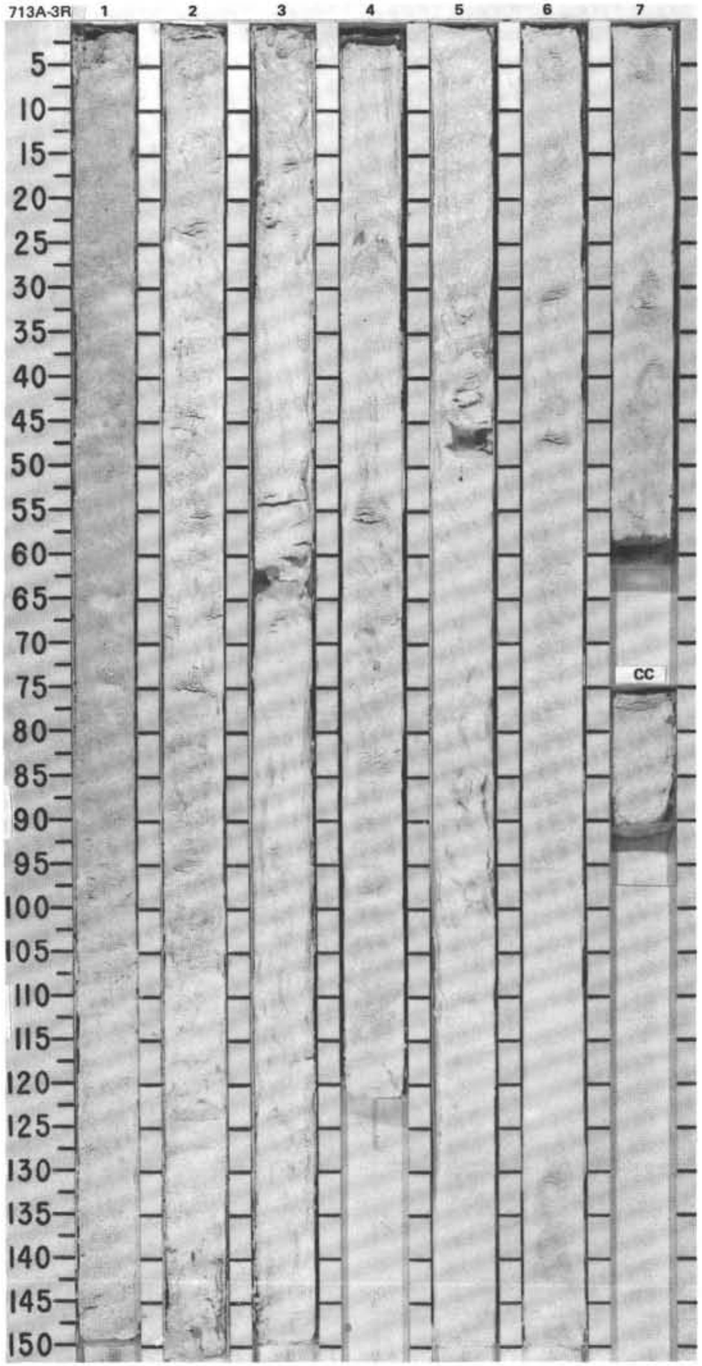

SITE 713 HOLE A CORE 4R CORED INTERVAL 2930.6-2940.3 mbsl; 20.8-30.5 mbsf

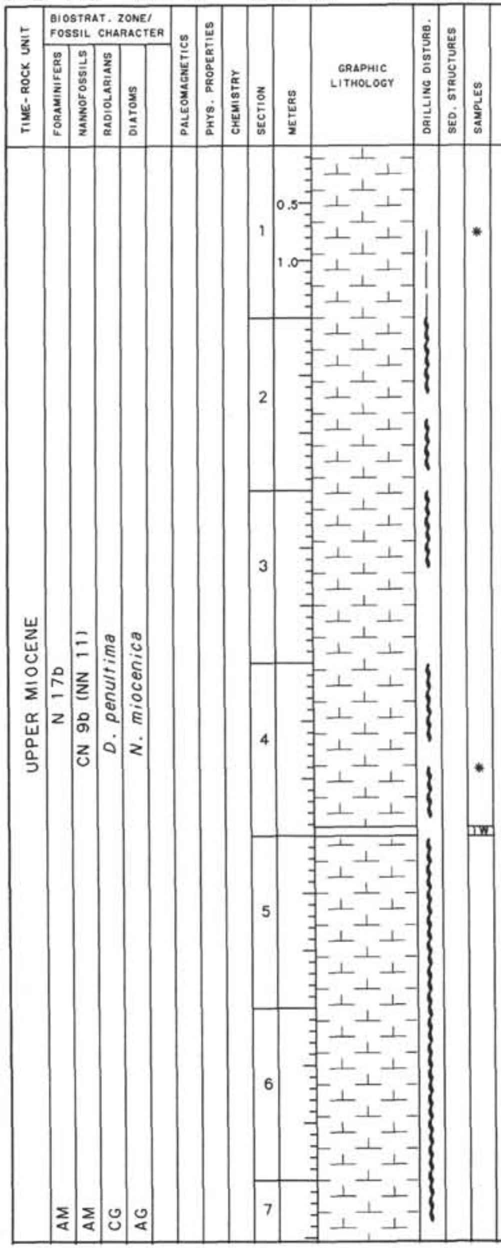

LITHOLOGIC DESCRIPTION

FORAMINIFER-BEARING NANNOFOSSIL OOZE

Major lithology: Foraminifer-bearing nannofossil ooze, homogeneous, white (N9) except for light gray to grayish white (N7, N8) vertical streaks and irregular patches, suggesting flow-in and considerable disturbance throughout much of the core.

SMEAR SLIDE SUMMARY (%):

	1, 78 D	4, 89 D
TEXTURE:		
Sand	20	20
Silt	20	20
Clay	60	60
COMPOSITION:		
Clay	5	5
Volcanic glass	—	Tr
Foraminifers	20	25
Nannofossils	75	70
Diatoms	—	Tr
Radiolarians	Tr	Tr
Sponge spicules	Tr	Tr

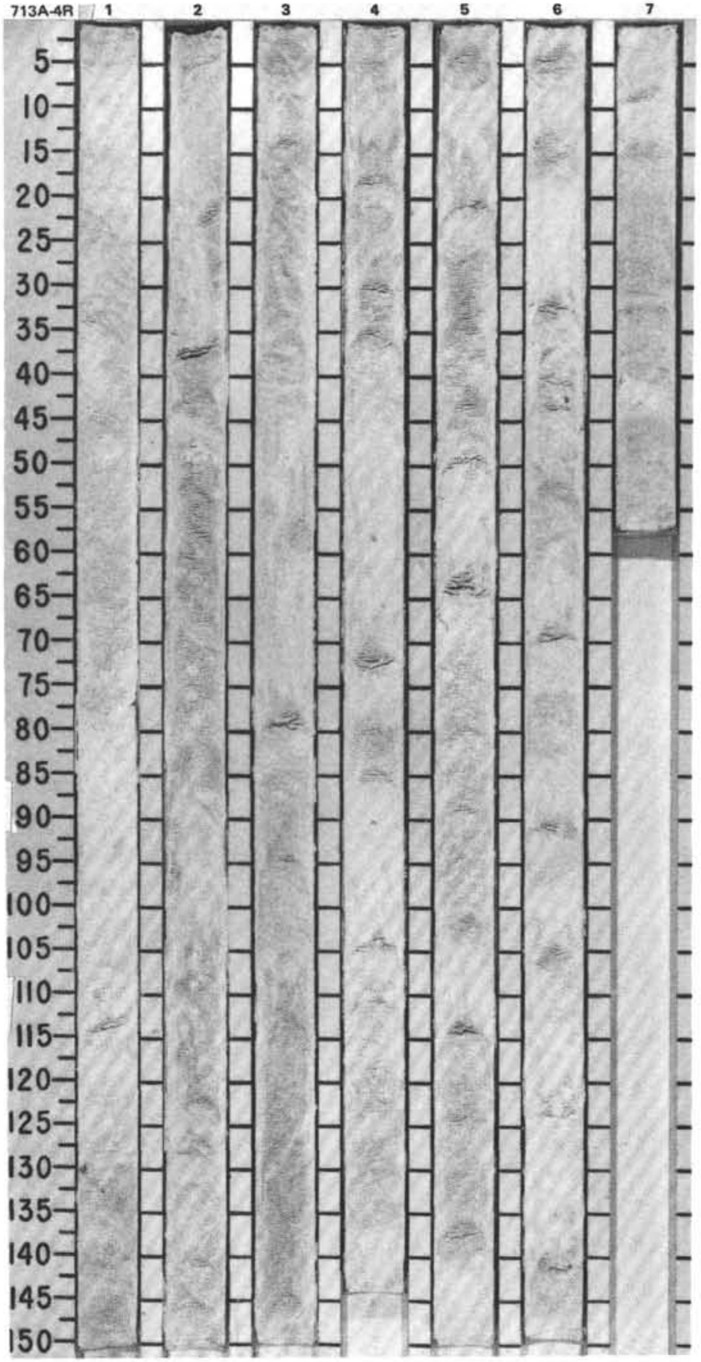

SITE 713 HOLE A CORE 5R CORED INTERVAL 2940.3-2949.9 mbsl; 30.5-40.1 mbsf

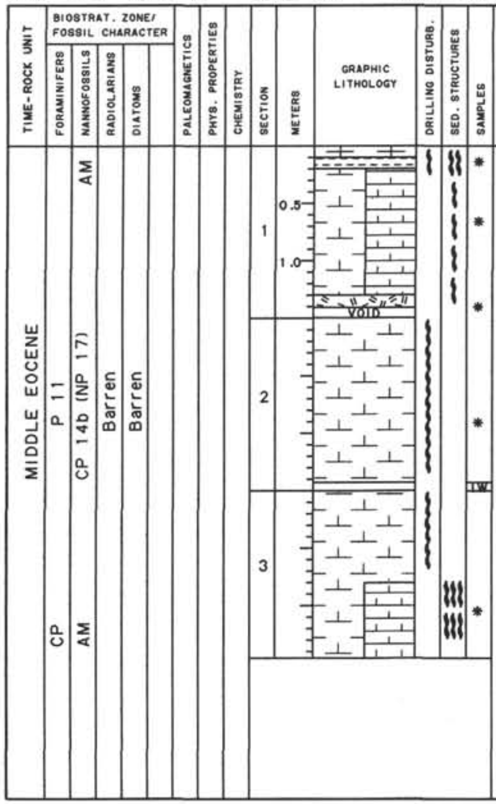

LITHOLOGIC DESCRIPTION

CLAY-BEARING FORAMINIFER-BEARING NANNOFOSSIL OOZE and CLAY-BEARING FORAMINIFER-BEARING NANNOFOSSIL CHALK

Major lithology: Clay-bearing foraminifer-bearing nannofossil ooze alternating over undisturbed intervals with clay-bearing foraminifer-bearing nannofossil chalk. Typically pale yellow (2.5Y 7/4) and very pale brown (10YR 8/3, 7/3) to grayish brown (2.5Y 5/2), and weakly to moderately bioturbated. Section 2 and Section 3, 0-80 cm, contain primarily "soft" nannofossil ooze and appear to be badly disturbed.

Minor lithologies:

a. Foraminifer-nannofossil ooze/chalk, white (N9), with a very abrupt basal contact. Section 1, 0-10 cm.
b. Nannofossil clay, grayish brown to very dark grayish brown (2.5Y 3/2, 5/2), highly bioturbated, with very firm consistency. Section 1, 10-19 cm.
c. Volcanic ash, light olive brown (2.5Y 5/6), altered and disseminated, with indistinct boundaries. Section 1, 130-145 cm.

SMEAR SLIDE SUMMARY (%):

	1, 15 M	1, 68 D	1, 140 M	2, 96 D	3, 107 D
TEXTURE:					
Sand	—	15	20	5	10
Silt	30	10	70	30	30
Clay	70	75	10	65	60
COMPOSITION:					
Quartz	2	—	—	—	—
Feldspar	—	Tr	—	Tr	—
Clay	69	10	8	5	25
Volcanic glass	5	Tr	89	—	2
Foraminifers	Tr	12	1	5	8
Nannofossils	24	75	2	88	63
Sponge spicules	—	—	—	Tr	—
Calcispheres	—	3	—	2	2

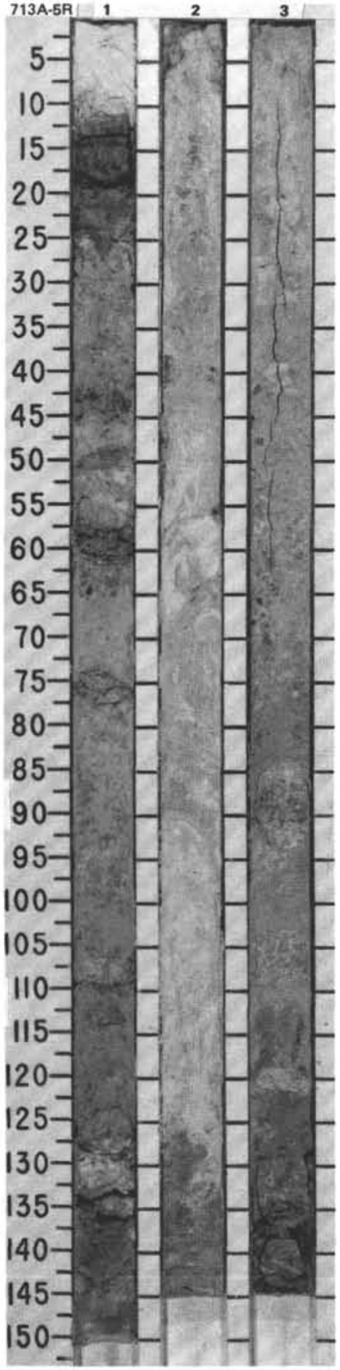

SITE 713 HOLE A CORE 6R CORED INTERVAL 2949.9-2959.5 mbsl; 40.1-49.7 mbsf

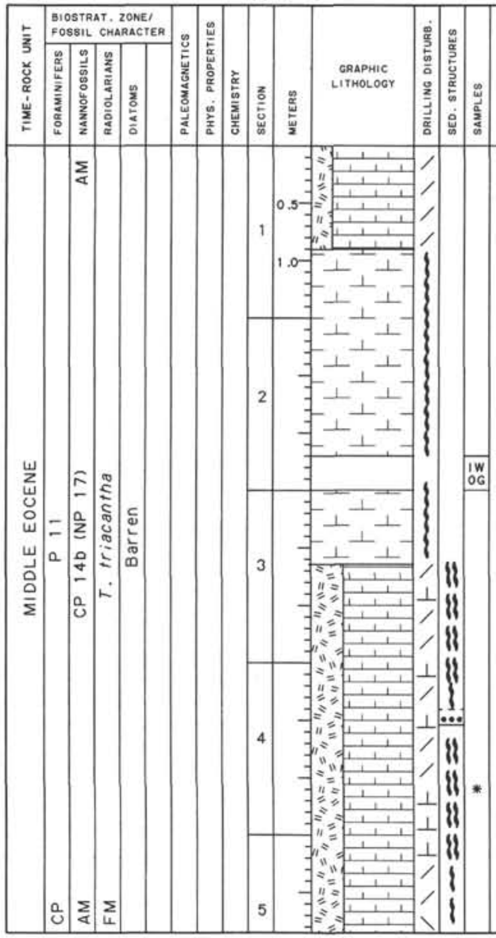

LITHOLOGIC DESCRIPTION

Interbedded FORAMINIFER-BEARING NANNOFOSSIL CHALK and VOLCANIC ASH

Major lithology: Foraminifer-bearing nannofossil chalk and mafic volcanic ash layers, complexly interbedded and heavily bioturbated. Chalk layers range from white and very pale brown (10YR 8/2, 8/3, 7/3) to light gray (2.5Y 7/2) and light brownish gray (2.5Y 6/2), with colors depending on mixture of ash and chalk. Ash layers vary from black (N2) and grayish brown (2.5Y 5/2) to light brownish gray (2.5Y 6/2), depending on degree of alteration and dissemination.

Section 1, 94–150 cm, Section 2, and Section 3, 0–63 cm, contain a highly disturbed drilling paste consisting of a chaotic mixture of nannofossil ooze, ash, and numerous fragments of indurated chalk. No stratigraphic continuity.

Minor lithology: Nannofossil-bearing clay, very pale brown to light yellowish brown (10YR 7/3, 6/4), three thin layers in Section 3 between 68–90 cm.

Thin, graded sequence (turbidite?) in Section 4, 55–59 cm.

SMEAR SLIDE SUMMARY (%):

	4, 110 D
TEXTURE:	
Sand	6
Silt	4
Clay	90
COMPOSITION:	
Quartz	Tr
Clay	5
Volcanic glass	Tr
Foraminifers	Tr
Nannofossils	89
Radiolarians	4
Sponge spicules	2

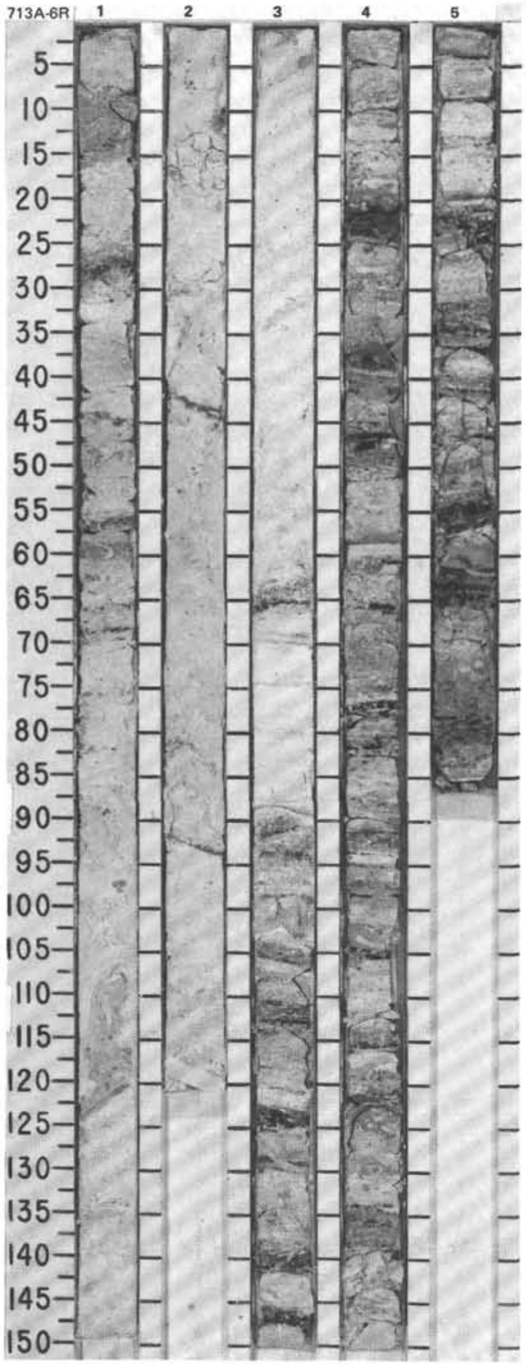

SITE 713 HOLE A CORE 7R CORED INTERVAL 2959.5-2969.2 mbsl; 49.7-59.4 mbsf

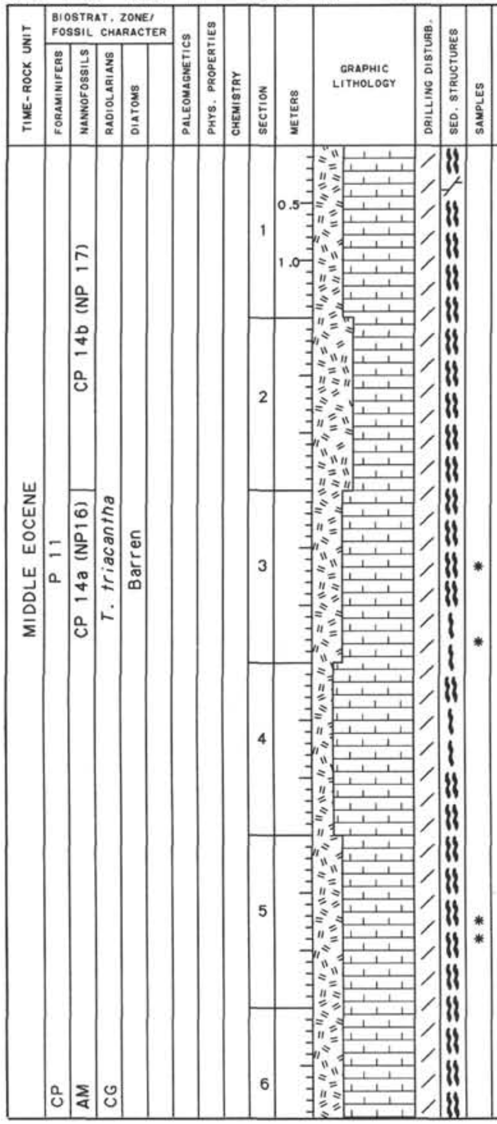

LITHOLOGIC DESCRIPTION

Interbedded NANNOFOSSIL CHALK, FORAMINIFER-BEARING NANNOFOSSIL CHALK, and VOLCANIC ASH

Major lithology: Nannofossil chalk, foraminifer-bearing nannofossil chalk, and mafic volcanic ash layers, complexly interbedded and heavily bioturbated. Chalk layers range from white and very pale brown (10YR 8/2, 8/3, 7/3) to light gray (2.5Y 7/2) and light brownish gray (2.5Y 6/2), depending on mixture of ash and chalk. Concentrated ash layers vary in color from black (N2) and olive (5Y 4/3) to dark brown (7.5YR 4/2). A number of ash layers are either graded, cross-stratified, or show parallel laminations on a mm scale.

Minor lithology: Sponge spicule-bearing clayey nannofossil chalk, very pale brown (10YR 7/4), present as thin layers in Section 3, 64-67, 71-73, 118-121, and 134-139 cm.

A reverse microfault was observed, offsetting lithologies in Section 1, 25-30 cm.

SMEAR SLIDE SUMMARY (%):

	3, 67 M	3, 137 M	5, 71 D	5, 96 M
TEXTURE:				
Sand	50	5	10	5
Silt	30	25	10	80
Clay	20	70	80	15
COMPOSITION:				
Feldspar	5	—	—	5
Clay	2	30	—	—
Volcanic glass	20	—	—	90
Accessory minerals	10	—	—	—
Foraminifers	40	—	5	—
Nannofossils	—	50	85	5
Diatoms	—	Tr	—	—
Radiolarians	10	4	5	—
Sponge spicules	13	15	5	—
Calcispheres	—	1	—	—

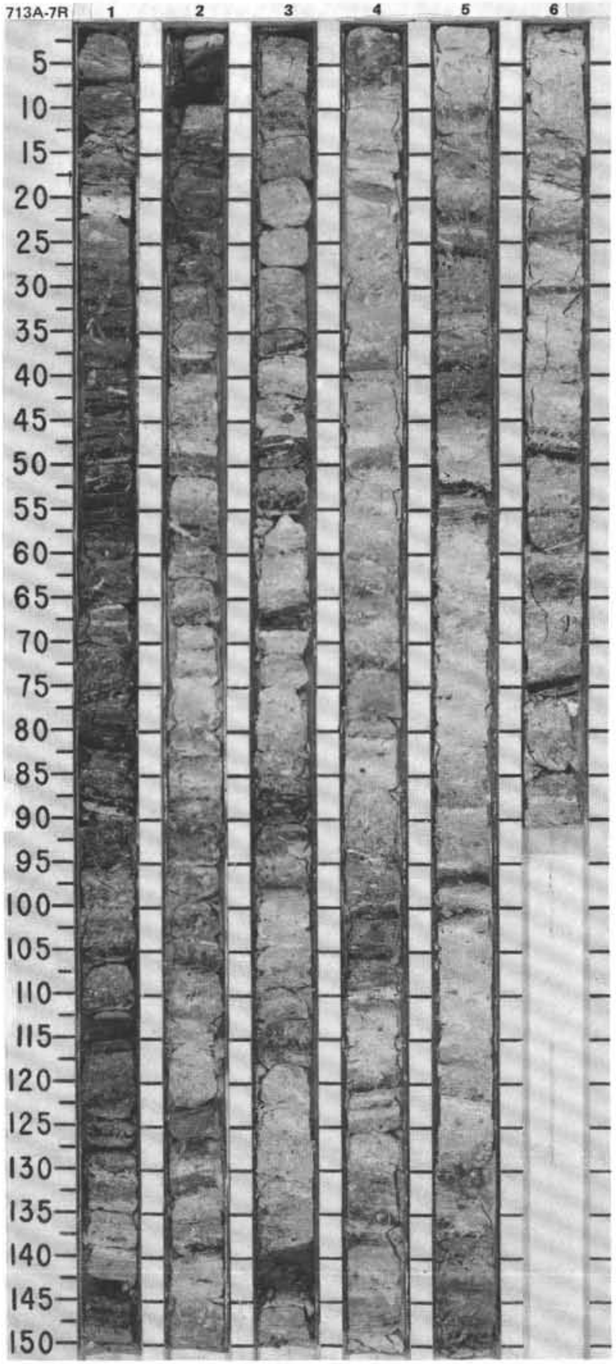

SITE 713 HOLE A CORE 8R CORED INTERVAL 2969.2-2978.9 mbsl; 59.4-69.1 mbsf

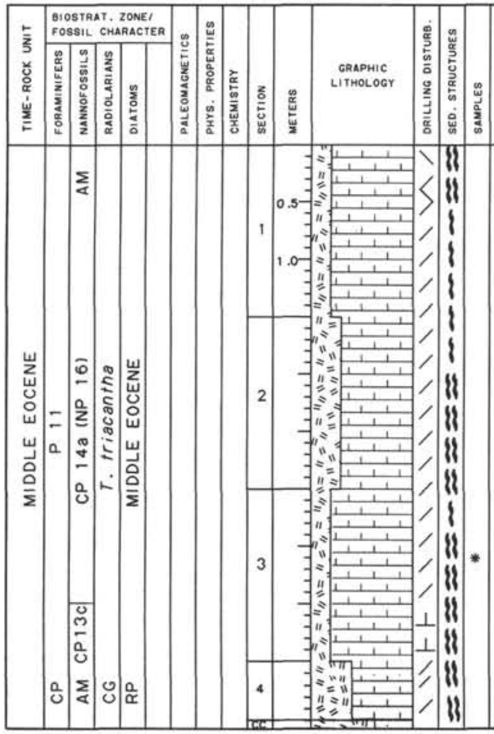

LITHOLOGIC DESCRIPTION

Interbedded NANNOFOSSIL CHALK and VOLCANIC ASH

Major lithology: Nannofossil chalk and mafic volcanic ash, complexly interbedded and heavily bioturbated. Chalk layers range from white and very pale brown (10YR 8/2, 8/3, 7/3) to light gray (2.5Y 7/2) and light brownish gray (2.5Y 6/2), with color depending on the mixture of ash and chalk. Ash layers are typically black (N2) and dark gray or very dark gray (5Y 4/1, 3/1) to dark olive gray (5Y 3/2), and range in grain size from fine to coarse sand.

Section 3, 93-150 cm, is moderately fractured, with large chalk fragments in a matrix of highly disturbed drilling paste.

SMEAR SLIDE SUMMARY (%):

	3, 60 D
TEXTURE:	
Sand	15
Silt	10
Clay	75
COMPOSITION:	
Quartz	Tr
Feldspar	Tr
Clay	5
Volcanic glass	8
Foraminifers	1
Nannofossils	73
Radiolarians	8
Sponge spicules	5

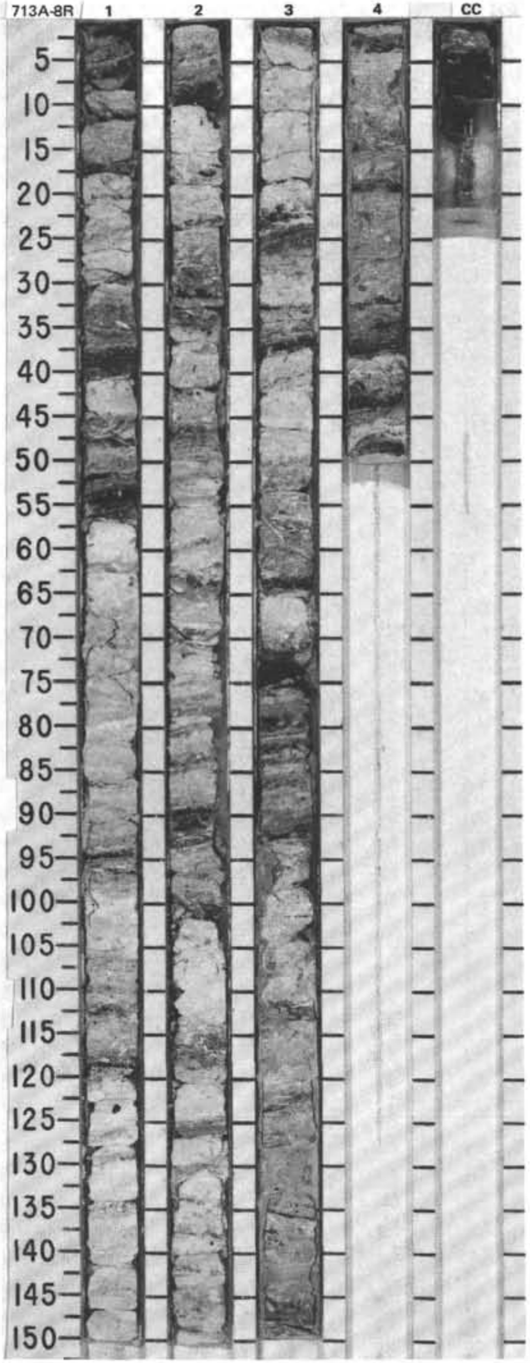

SITE 713 HOLE A CORE 9R CORED INTERVAL 2978.9-2988.5 mbsl; 69.1-78.7 mbsf

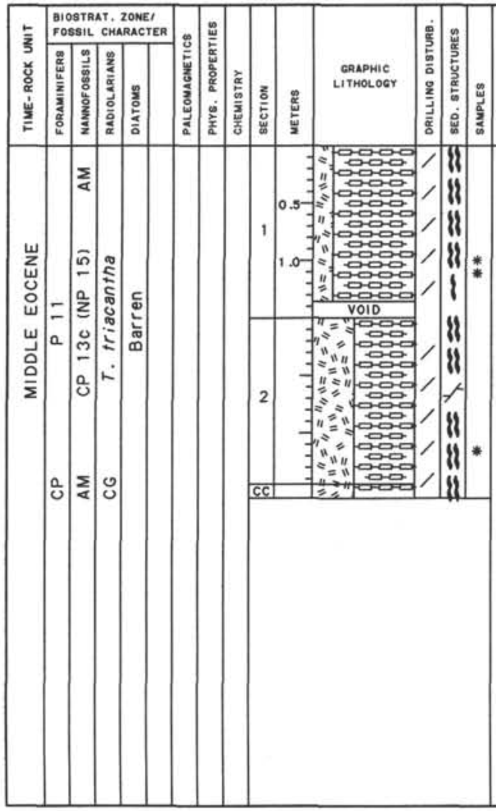

LITHOLOGIC DESCRIPTION

Interbedded MICRITE CHALK and VOLCANIC ASH

Major lithology: Micrite chalk and volcanic ash, complexly interbedded and heavily bioturbated. Fine carbonate making up chalk is mostly unrecognizable beginning with this core. Chalk layers range from white (10YR 8/2) to very pale brown (10YR 8/3), and ash layers are typically black (N2). *Chalk with varying proportions of admixed ash is mostly* gray (5Y 6/1).

Minor lithology: Clayey micrite chalk, very pale brown (10YR 7/4), in thin (1 cm) layers in Section 1, 30, 55, and 58 cm; and Section 2, 74 and 122 cm.

A reverse microfault was observed at Section 2, 80 cm, and a *Zoophycos*-type burrow is preserved in Section 2, 100–101 cm.

SMEAR SLIDE SUMMARY (%):

	1, 100 D	1, 107 D	2, 118 M
TEXTURE:			
Sand	10	5	15
Silt	15	15	70
Clay	75	80	15
COMPOSITION:			
Feldspar	—	—	15
Clay	—	30	—
Volcanic glass	—	3	80
Accessory minerals	—	—	5
Micrite	75	52	—
Foraminifers	5	—	—
Nannofossils	5	5	—
Radiolarians	5	5	—
Sponge spicules	10	5	—
Calcareous spicules	—	Tr	—

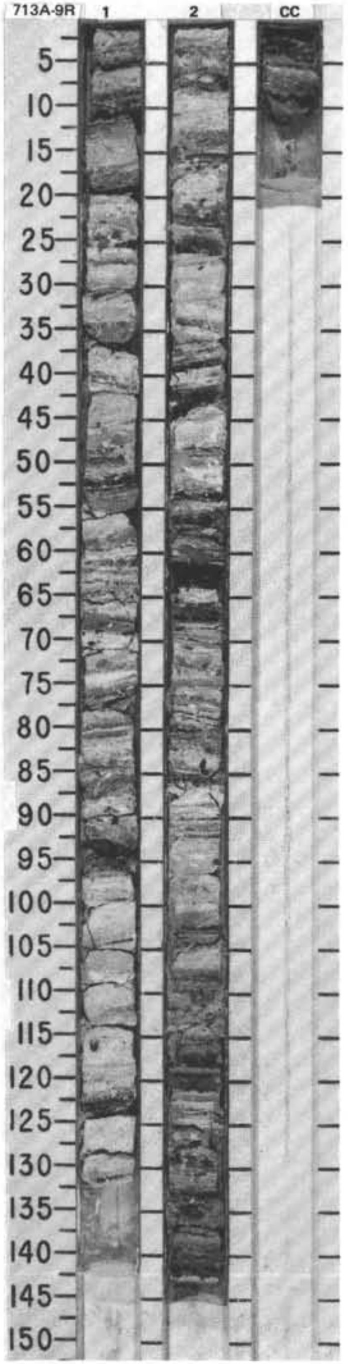

SITE 713 HOLE A CORE 10R CORED INTERVAL 2988.5-2998.2 mbsl; 78.7-88.4 mbsf

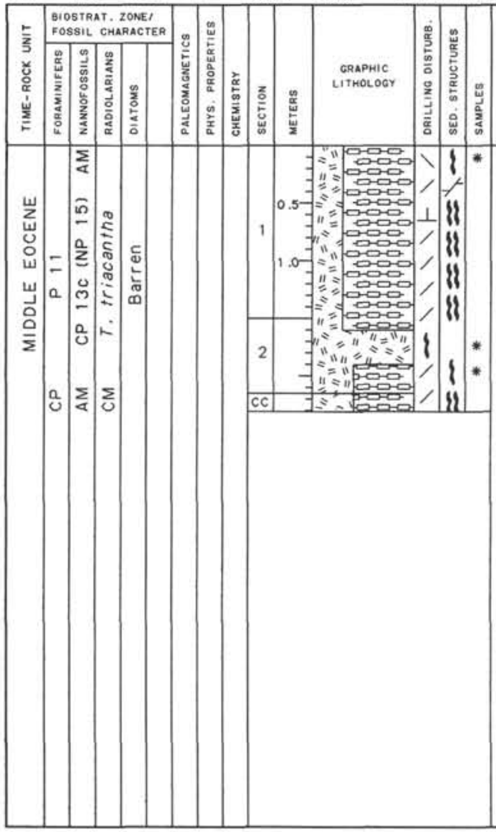

LITHOLOGIC DESCRIPTION

Interbedded MICRITE CHALK and VOLCANIC ASH

Major lithology: Micrite chalk and volcanic ash, complexly interbedded and heavily bioturbated. Chalk layers above Section 2, 40 cm, are white (N9, 10YR 8/1, 8/2), very pale brown (10YR 7/3), and light gray to light brownish gray (2.5Y 7/2, 6/2). Ash layers are black (N9) to dark gray (5Y 4/1), with mixtures of ash and chalk mostly gray (5Y 5/1, 6/1). Below Section 2, 40 cm, both sediments and ash have an olive green tint to them, suggesting a possible redox transition. Chalk is light olive gray to pale olive (5Y 7/2, 6/2, 6/3), and ashes are mostly dark greenish gray (5GY 4/1).

Minor lithology: Trachytic volcanic ash, dark gray (5Y 4/1), silt to very fine sand size grains, unconsolidated and very fresh in appearance, in Section 2, 13-41 cm. Below this major ash horizon, sediments all have a greenish hue as described above.

A normal microfault is observed in Section 1, 32-35 cm.

SMEAR SLIDE SUMMARY (%):

	1, 10 M	2, 25 M	2, 48 M
TEXTURE:			
Sand	10	80	10
Silt	20	10	70
Clay	70	10	20
COMPOSITION:			
Quartz	Tr	Tr	—
Feldspar	Tr	Tr	—
Clay	65	5	10
Volcanic glass	2	92	85
Accessory minerals:			
Micrite	—	—	2
Nannofossils	5	3	1
Radiolarians	8	—	2
Sponge spicules	20	—	—

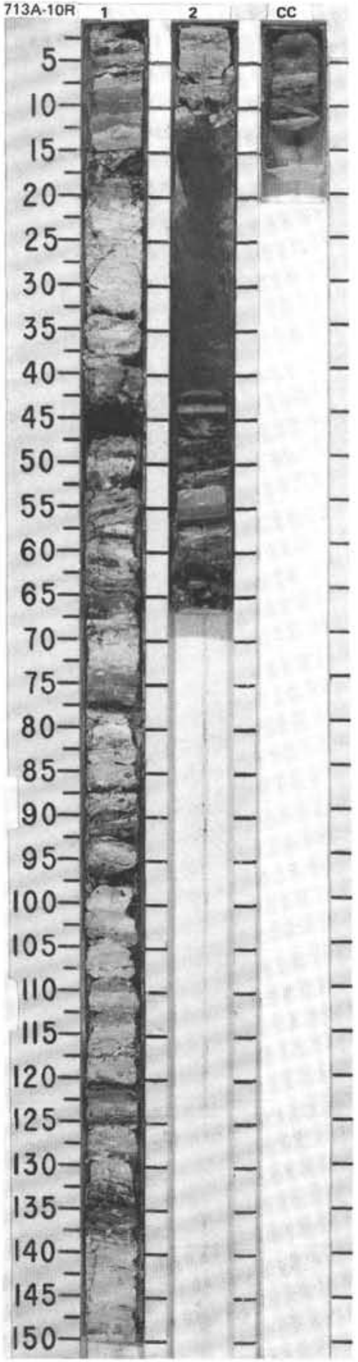

SITE 713 HOLE A CORE 11R CORED INTERVAL 2998.2-3007.9 mbsl; 88.4-98.1 mbsf

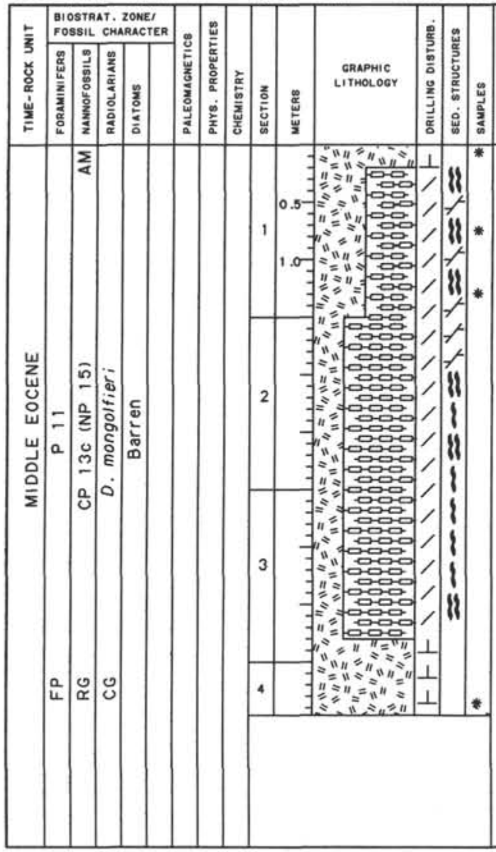

LITHOLOGIC DESCRIPTION

Interbedded MICRITE CHALK and VOLCANIC ASH

Major lithology: Micrite chalk and volcanic ash layers, complexly interbedded and heavily bioturbated. Chalk layers are occasionally clay-bearing, and range in color from light greenish gray (5GY 7/1) to greenish gray (5GY 6/1), with trace amounts of glauconite present. Ash layers are black (N2) and dark gray (5Y 4/1) to dark green (5G 4/1), and in some cases are normally graded or show very fine parallel laminations. Thick, concentrated ash layers are found in Section 1, 0-23 cm, and from Section 3, 132 cm, to Section 4, 44 cm.

Microfaults are commonly preserved in Sections 1 and 2, as is a large *Zoophycos* burrow in Section 2, 72-73 cm.

SMEAR SLIDE SUMMARY (%):

	1, 1 M	1, 80 D	1, 131 M	4, 41 M
TEXTURE:				
Sand	20	5	15	10
Silt	50	5	70	75
Clay	30	90	15	15
COMPOSITION:				
Quartz	—	Tr	—	—
Feldspar	—	—	10	3
Clay	—	10	—	—
Volcanic glass	60	—	82	83
Accessory minerals:				
Opaques	2	—	5	7
Glauconite	Tr	Tr	—	—
Pyroxene	—	—	2	—
Foraminifers	—	1	—	—
Nannofossils	30	5	1	—
Radiolarians	5	5	—	5
Sponge spicules	3	3	—	2
Micrite	—	76	—	—
Calcispheres	—	Tr	—	—

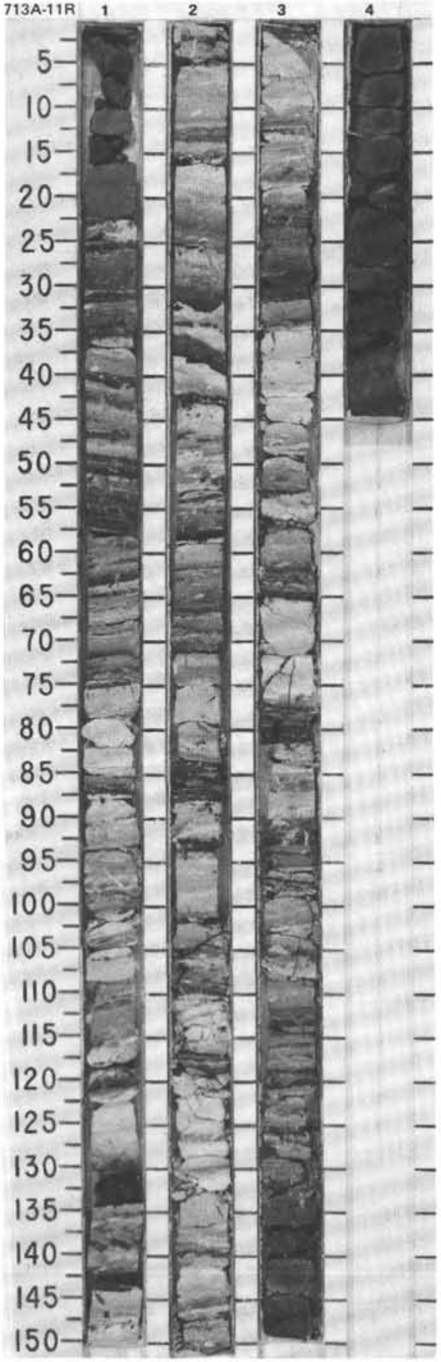

SITE 713 HOLE A CORE 12R CORED INTERVAL 3007.9-3017.5 mbsl; 98.1-107.7 mbsf

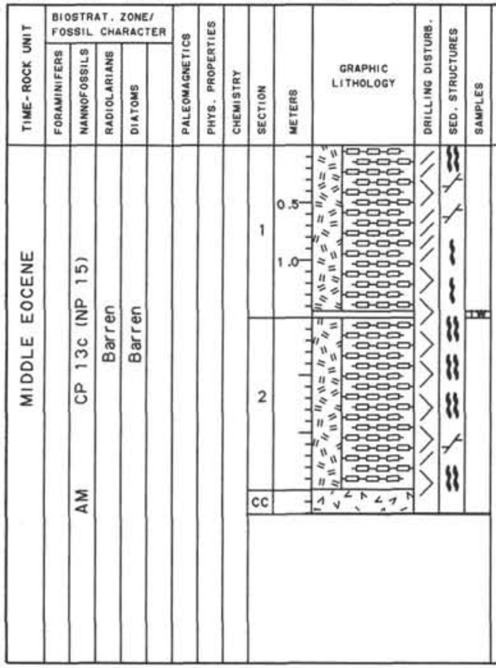

LITHOLOGIC DESCRIPTION

Interbedded MICRITE CHALK and VOLCANIC ASH

Major lithology: Micrite chalk and volcanic ash layers, complexly interbedded and moderately to heavily bioturbated. Chalk layers are typically a mixture of greenish gray (5GY 5/1, 6/1) to light greenish gray (5GY 7/1), while ash layers range from black (N2), when concentrated, to dark greenish gray (5GY 4/1), when more altered and disseminated. Microfaulting is evident in Section 1, 30-60 cm, and in Section 2, 90-100 cm.

CC: only basalt recovered (see visual core description).

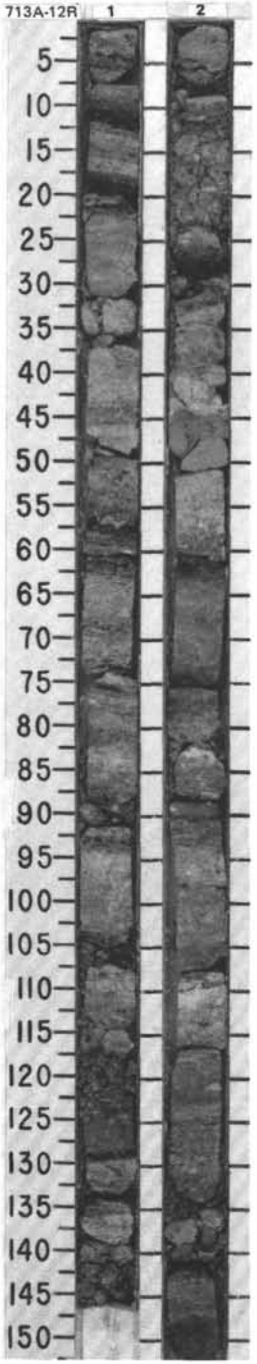

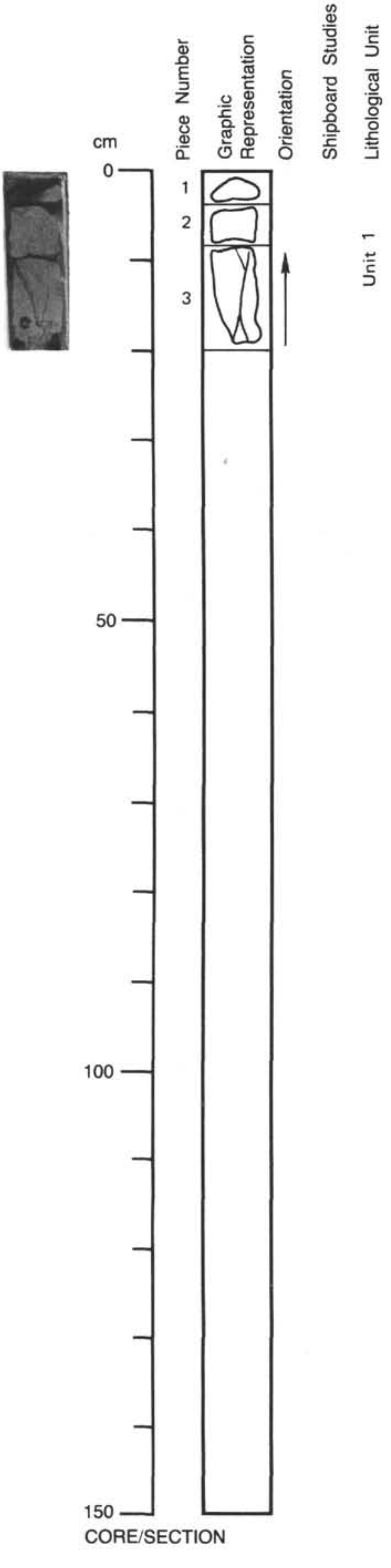

115-713A-12R-CC

UNIT 1: HIGHLY VESICULAR PLAGIOCLASE-PHYRIC BASALT

Pieces 1-3

PHENOCRYSTS: Plagioclase, subhedral, fresh, as long as 1 mm.
GLOMEROCRYSTS: Clots of plagioclase, as large as 2 mm diameter.
GROUNDMASS: Fine grained, hyalo-ophitic, plagioclase-rich.
COLOR: Dark gray (N4).
VESICLES: Highly vesicular (> 10%). Vesicles spherical-ellipsoidal, as large as 3 mm diameter. One large vesicle is 10 mm across. Vesicles partly filled with green clay minerals.
ALTERATION: Slightly altered in matrix to green clay.
VEINS/FRACTURES: Fracture in Piece 3; filled with green clay.

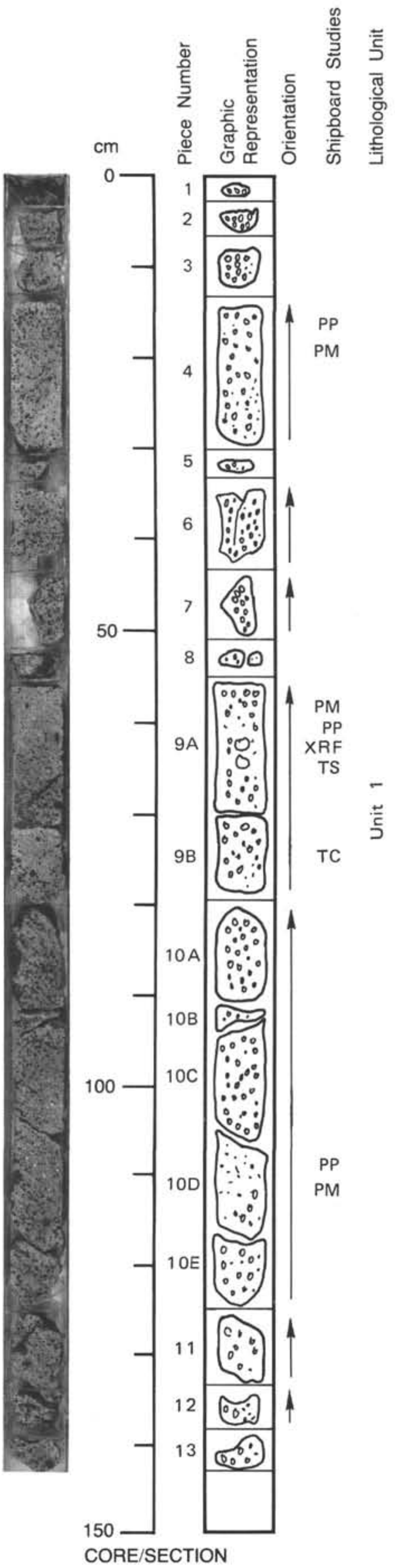

115-713A-13R-1

UNIT 1 (CONTINUED): HIGHLY VESICULAR PLAGIOCLASE-PHYRIC HAWAIITIC BASALT

Pieces 1-13

Continuous with 115-713A-12R-CC, Unit 1

PHENOCRYSTS: Plagioclase, subhedral, <1 mm.
GROUNDMASS: Fine grained, rich in plagioclase. Plagioclase ≫ mafic phases.
COLOR: Gray (N4).
VESICLES: Homogenous distribution, round to ellipsoid, <3 mm. Partly rimmed by gray zeolite-like minerals, especially in Pieces 11C and 11D.
ALTERATION: Slightly altered to fresh.

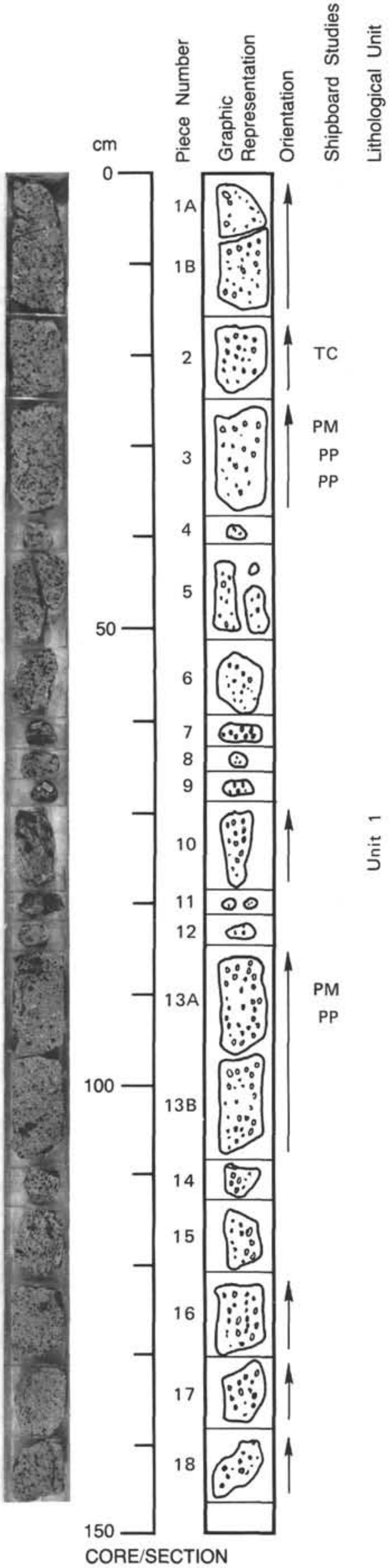

115-713A-13R-2

UNIT 1 (CONTINUED): HIGHLY VESICULAR PLAGIOCLASE-PHYRIC HAWAIITIC BASALT

Pieces 1–18

Continuous with 115-713A-13R-1, Unit 1

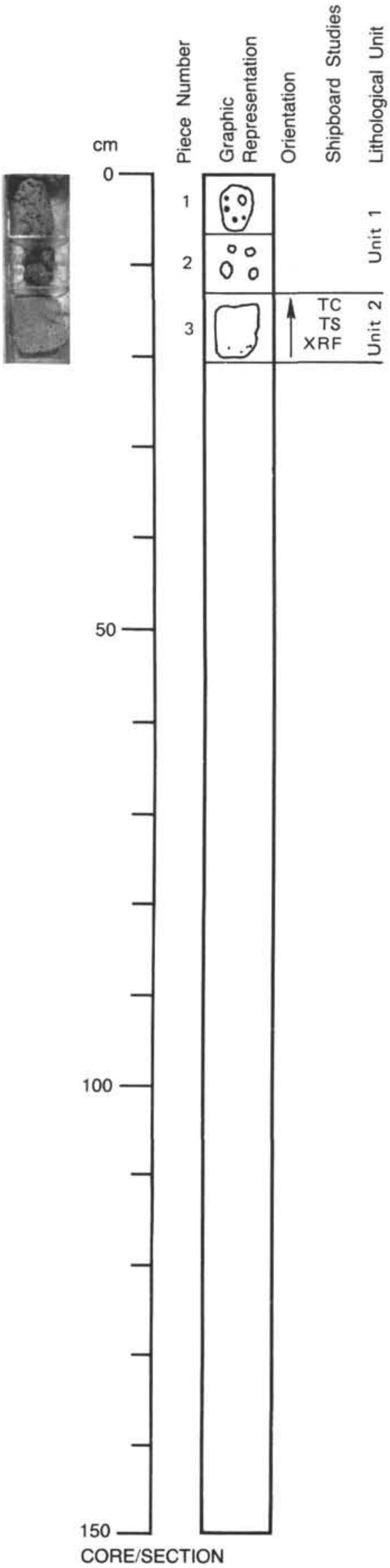

115-713A-13R-3

UNIT 1 (CONTINUED): PLAGIOCLASE-PHYRIC HAWAIITIC BASALT

Pieces 1 and 2

Continuous with 115-713A-13R-2, Unit 1

LITHOLOGY: Mineral assemblage is the same as 115-713A-13R-2, Unit 1.
VESICLES: Piece 2 is much poorer in vesicles than Piece 1. May be the bottom of this unit.

UNIT 2: TRACHYTE

Piece 3

PHENOCRYSTS: Plagioclase, 1-2 mm in size, mafic phase.
GROUNDMASS: Fine-grained matted feldspar, with oxides and pyroxene(?).
COLOR: Gray.
VESICLES: Evenly distributed, round, 1-2 mm in size, rimmed with gray clay.
ALTERATION: Slightly altered to fresh.

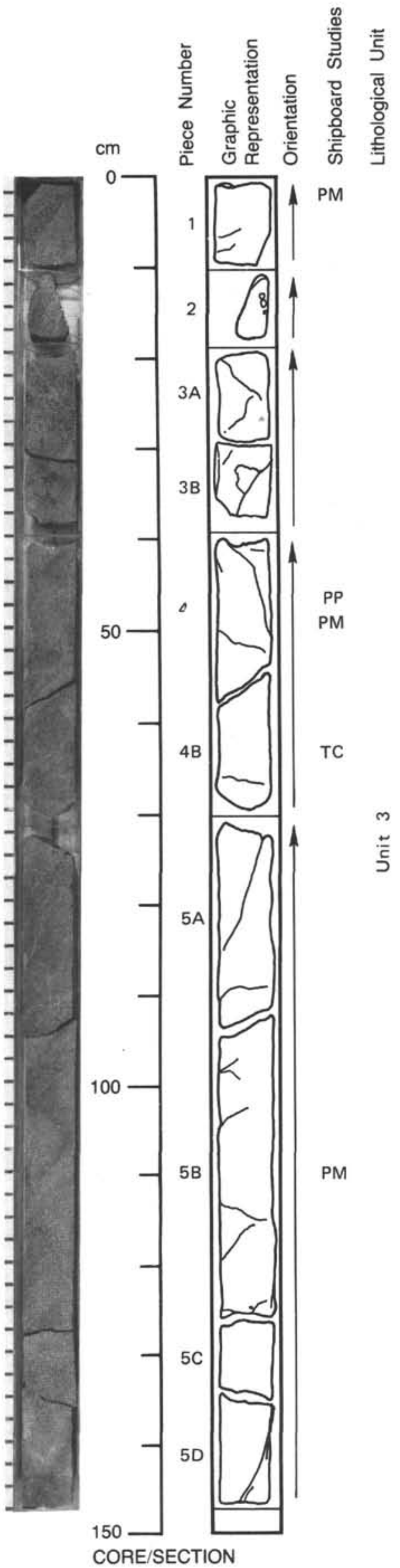

115-713A-14R-1

UNIT 3: FINE-GRAINED PLAGIOCLASE BASALT

Pieces 1-5D

PHENOCRYSTS: Plagioclase - 1-3 mm, laths and rounded.
Olivine - 0.5-1.0 mm.
Pyroxene - 0.5-1.0 mm.
GROUNDMASS: Microcrystalline to fine grained.
VESICLES: Rare, round.
ALTERATION: Varies from slight to moderate. Alteration is more pervasive near veins and fractures. Altered olivine near top of unit. Celadonite sometimes fills voids.
VEINS/FRACTURES: <1%, filled with calcite and clay, most <1 mm thick. Clay is found in fractures and voids.
Piece 3A: Calcite-filled vein.
Piece 3B: Clay-filled veins.
Pieces 4A and 5A: Veins, filled with calcite and clay minerals.
VOIDS: Rare, sometimes filled with sulfide, irregular, coated with spheres of green clay(?).

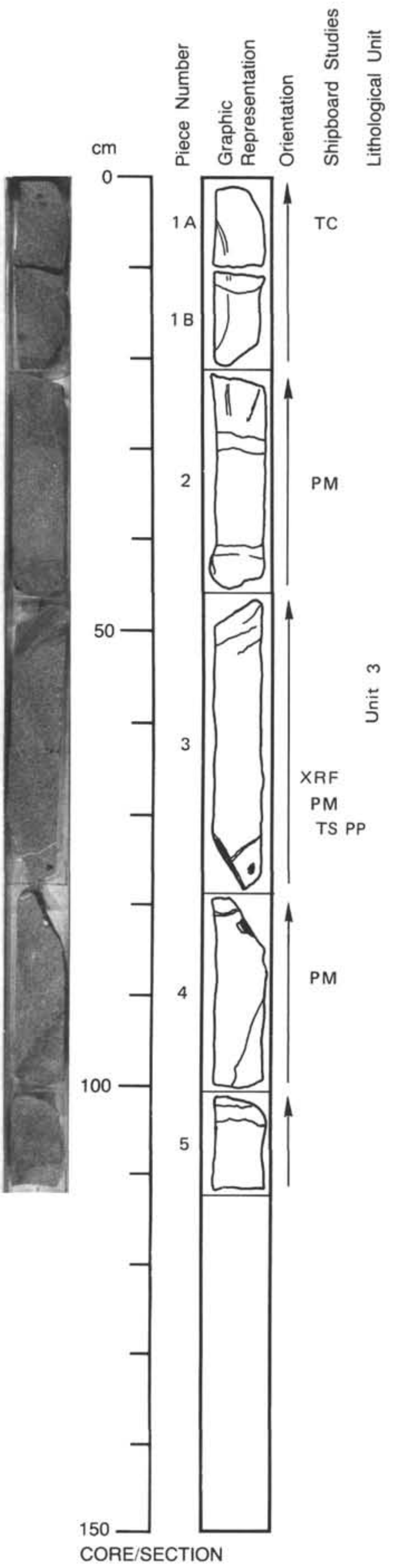

115-713A-14R-2

UNIT 3 (CONTINUED): FINE-GRAINED PLAGIOCLASE BASALT

Pieces 1A–5

Continuous with 115-713A-14R-1, Unit 3

VESICLES: Piece 4: 3 mm wide, filled with calcite.

ALTERATION: Pieces 2 and 3: Central parts, between fractures, appear relatively unaltered; in Piece 2 unaltered part is fresh.

VEINS/FRACTURES: Fractures in Pieces 1B–5.

Piece 1B: Tiny horizontal fracture filled with dark green clay.
Piece 2: Tiny (0.5 mm wide) fractures, filled with calcite.
Piece 3: Upper part: 0.2 mm wide fractures, filled with calcite and dark green clay.
Lower part: 2-3 mm wide fractures, filled with calcite.
Piece 4: Top: 2 mm wide fracture, filled with calcite.
Lower half: Fine fracture, <0.5 mm wide, filled with dark green mineral and calcite.
Piece 5: Fine <0.2 mm wide calcite-filled fracture occurs at top.

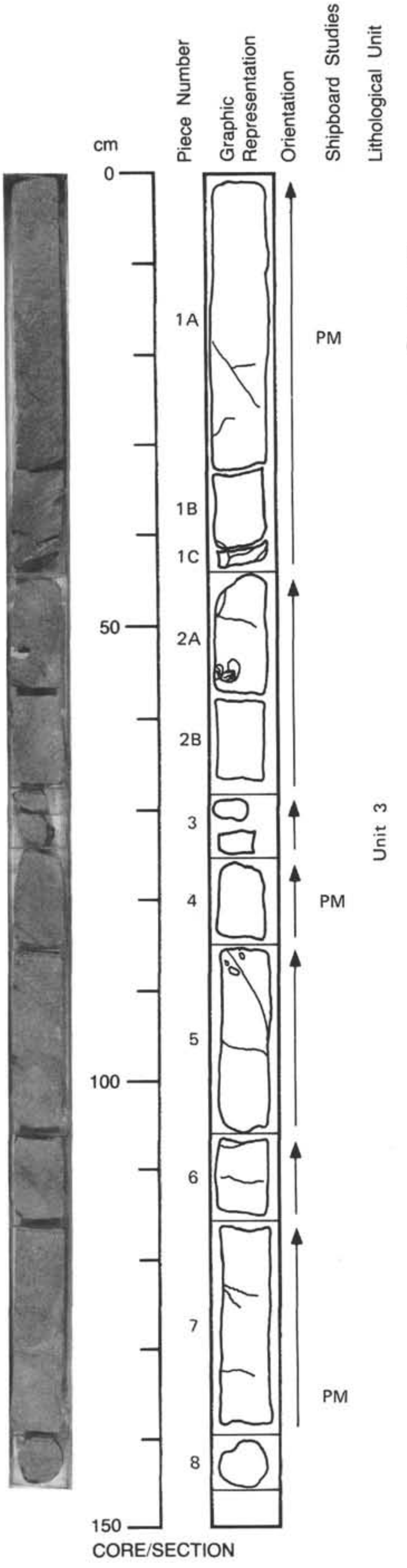

115-713A-14R-3

UNIT 3 (CONTINUED): FINE-GRAINED PLAGIOCLASE BASALT

Pieces 1A–8

Continuous with 115-713A-14R-2, Unit 3

VEINS/FRACTURES: Piece 1C: Vein, 5 mm wide, filled with soft, blue-green dessicated clay, calcite, and black needles.
Piece 7: Small veins.

VOIDS: Piece 2A: Void filled with calcite and rhodochrosite.

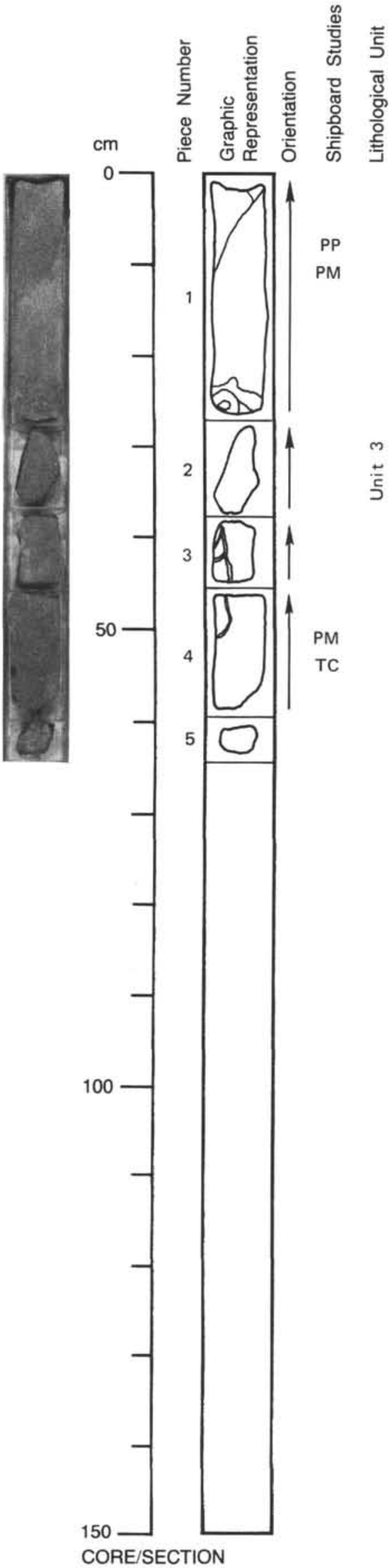

115-713A-14R-4

UNIT 3 (CONTINUED): FINE-GRAINED PLAGIOCLASE BASALT

Pieces 1–5

Continuous with 115-713A-14R-3, Unit 3

VESICLES: Piece 3: Vug or vesicle filled with olive brown (2.5Y 4/4) clay mineral.
ALTERATION: Piece 1, lower part: Wide 0.5 cm band of highly altered basalt (dark in color) surrounds veins.
VEINS/FRACTURES: Piece 1, bottom: Sinuous, 1 mm wide calcite-filled veins, surrounded with highly altered basalt.

SITE 713 HOLE A CORE 15R CORED INTERVAL 3036.5-3046.0 mbsl; 126.7-136.2 mbsf

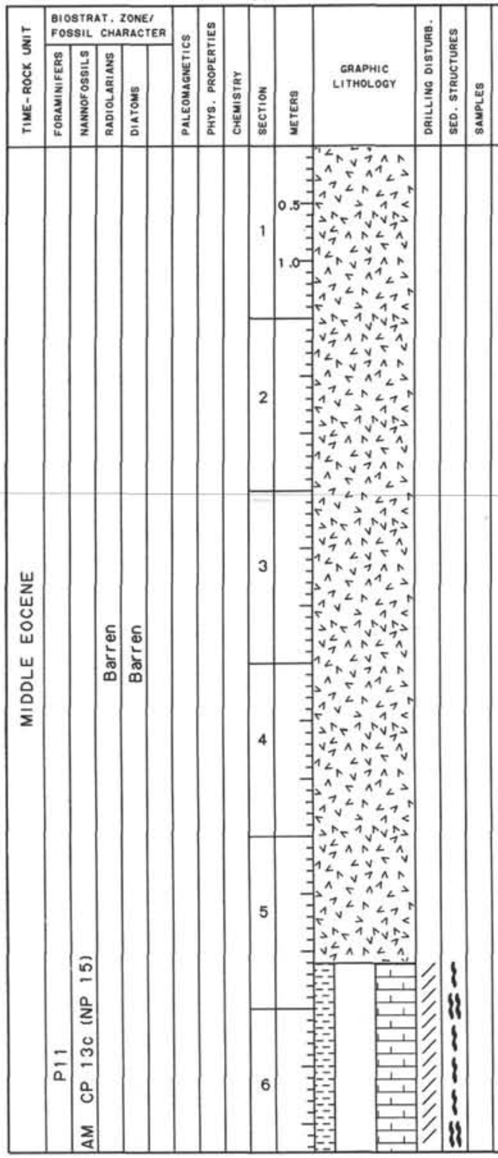

LITHOLOGIC DESCRIPTION

Interbedded FORAMINIFER-BEARING NANNOFOSSIL CHALK, VOLCANIC ASH-BEARING CLAY, and VOLCANIC ASH

Section 1 to Section 5, 112 cm, contain basalt (see visual core descriptions).

Major lithology: Foraminifer-bearing nannofossil chalk, volcanic ash-bearing clay, and volcanic ash, complexly interbedded with separate lithologies, moderately to highly mixed through bioturbation. Chalk layers are light gray (5Y 7/1) to light greenish gray (5GY 7/1), while concentrated ash layers are black (N2) to dark gray (N4). Ash-bearing clay layers and clay-bearing ash layers range from gray (5Y 5/1) and greenish gray (5GY 5/1) to grayish olive green (5GY 3/2).

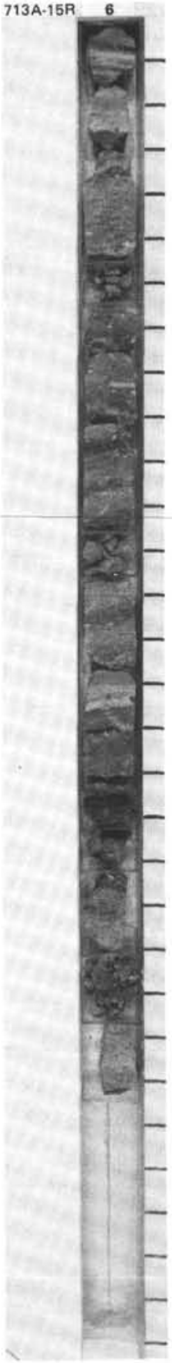

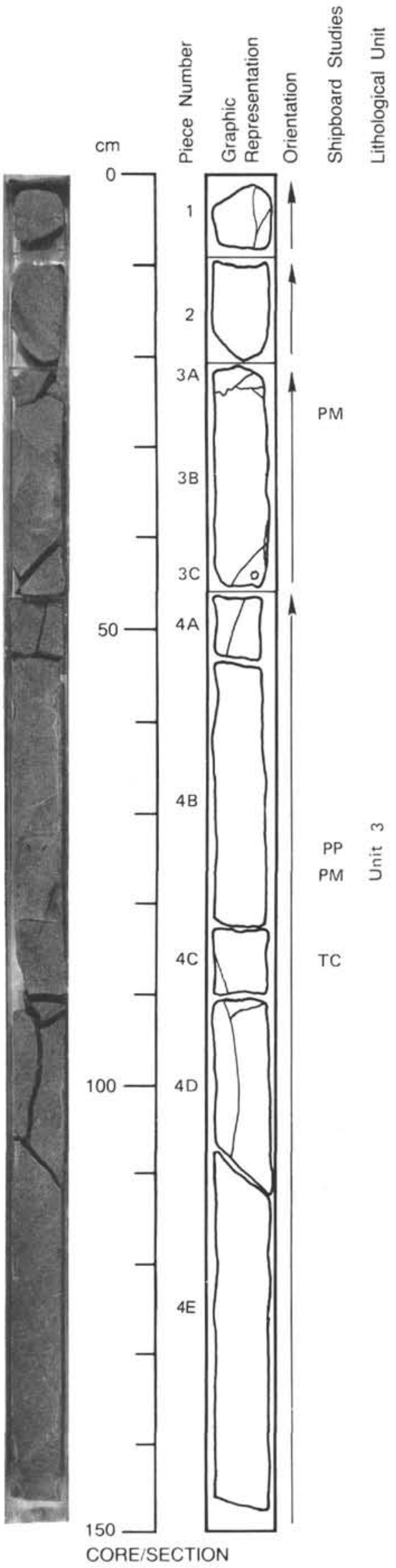

115-713A-15R-1

UNIT 3 (CONTINUED): FINE-GRAINED PLAGIOCLASE BASALT

Pieces 1-4E

Continuous with 115-713A-14R-4, Unit 3

VEINS/FRACTURES: Piece 3A: Fracture filled with clay.
Piece 4A: Fracture filled with clay, sulfide, and pyrite.
Pieces 4D and 4E: Vein between pieces.

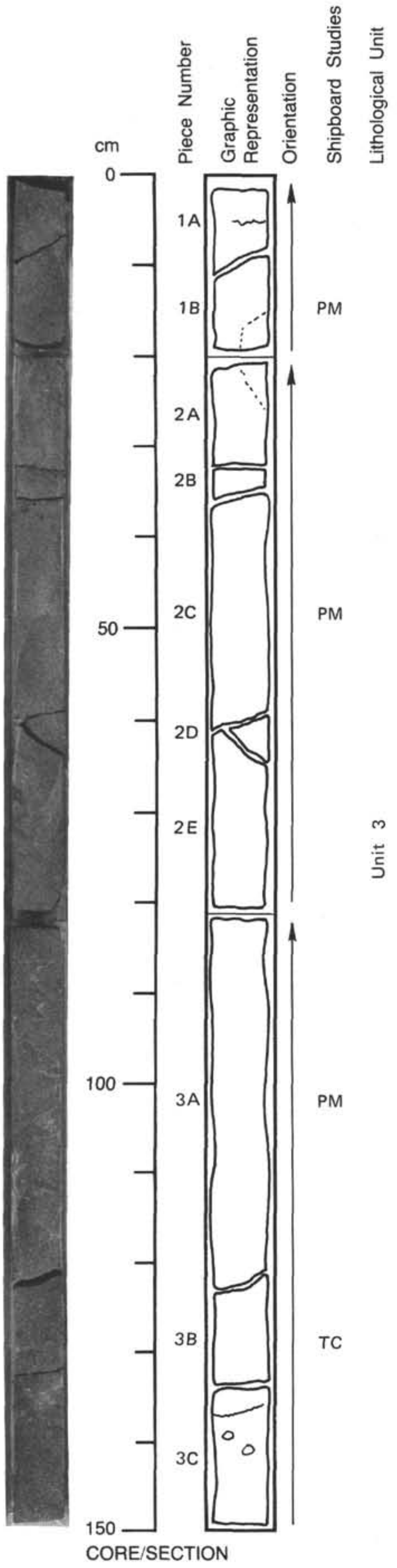

115-713A-15R-2

UNIT 3 (CONTINUED): FINE-GRAINED PLAGIOCLASE BASALT

Pieces 1A–3C

Continuous with 115-713A-15R-1, Unit 3

GROUNDMASS: Base of Piece 1B and top of Piece 2A: Textural change.
Piece 3C: Coarse xenoliths.

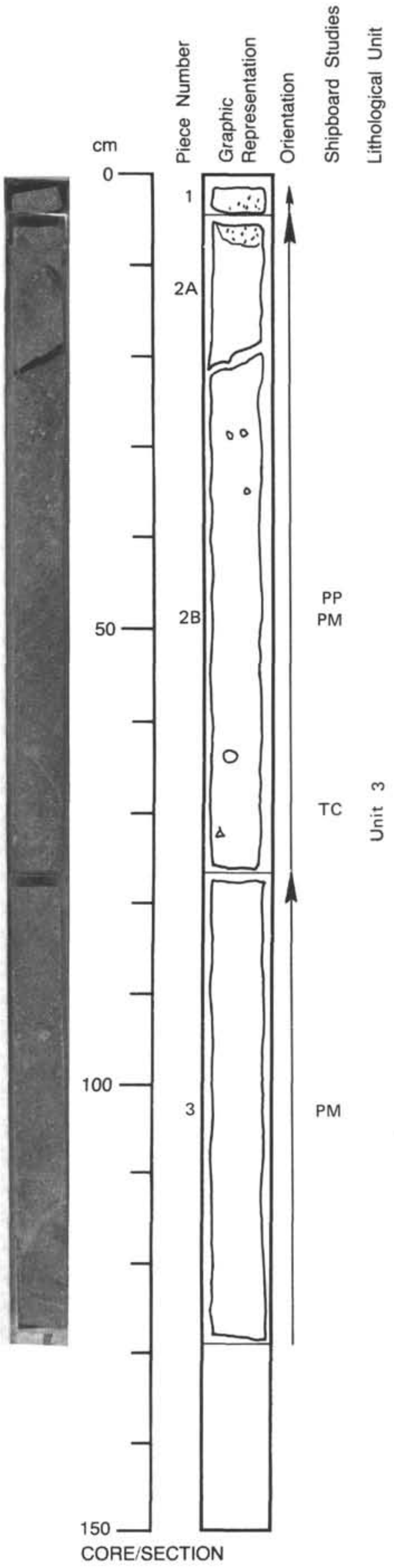

115-713A-15R-3

UNIT 3 (CONTINUED): FINE-GRAINED PLAGIOCLASE BASALT

Pieces 1–3

Continuous with 115-713A-15R-2, Unit 3

PHENOCRYSTS: Piece 2B, at 64 cm: Crystal clot.

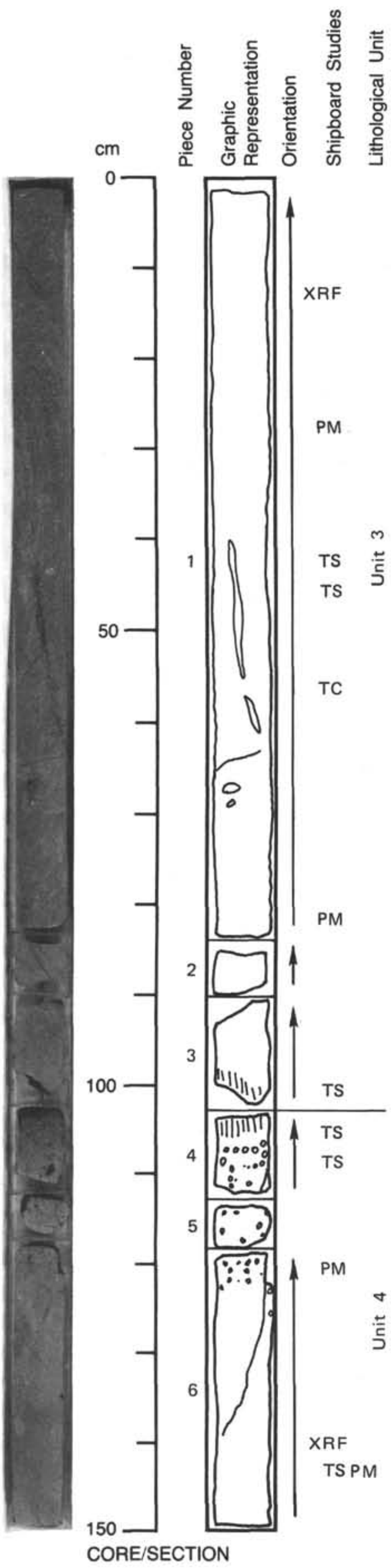

115-713A-15R-4

UNIT 3 (CONTINUED): FINE-GRAINED PLAGIOCLASE BASALT

Pieces 1-3

Continuous with 115-713A-15R-3, Unit 3

CONTACTS: Glassy flow contact at base of Piece 3.

UNIT 4: FINE-GRAINED PLAGIOCLASE-OLIVINE BASALT

Pieces 4-6

CONTACTS: Glassy flow contact at top of Piece 4.
PHENOCRYSTS: Plagioclase - Laths up to 8 mm, 2%.
Olivine - Round, altered to iddingsite, 2%.
GROUNDMASS: Fine grained; plagioclase is 0.5 mm.
COLOR: Black.
VESICLES: 0.5-2 mm near contact, grading up to 8 mm at 20 cm below contact, then no vesicles below that down to contact with 115-713A-15R-5, Unit 5. Vesicles are empty or partially filled with celadonite.
ALTERATION: Slightly altered. Olivine altered to iddingsite.
VEINS/FRACTURES: Veins inclined 70°, celadonite filled, 2-3 mm thick.

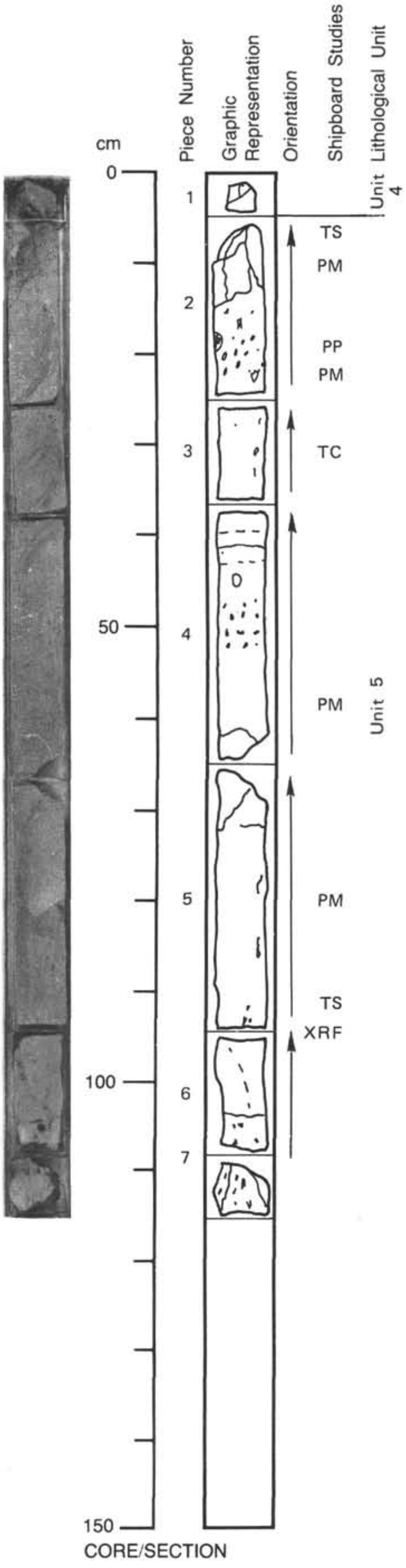

115-713A-15R-5

UNIT 4: FINE-GRAINED PLAGIOCLASE-OLIVINE BASALT

Piece 1

Continuous with 115-713A-15R-4, Unit 4

VESICLES: Filled with grayish green (5G 5/2) celadonite.
ALTERATION: One clot, 3 mm wide, of dark yellowish brown (10YR 4/6) iddingsite. Same mineral forms 0.2 mm sized grains in matrix.
VEINS/FRACTURES: Fracture filled with grayish green (5G 5/2) celadonite.

UNIT 5: FINE-GRAINED PLAGIOCLASE-PYROXENE BASALT

Pieces 2–7

CONTACTS: Sediments at Pieces 2 and 3, and below Piece 7. Glass apparent at chilled upper margin (Piece 2).
PHENOCRYSTS: Plagioclase, as large as 1 mm.
GROUNDMASS: Plagioclase and pyroxene, 0.2 mm; olivine(?), 0.3 mm.
VESICLES: Piece 2 (at upper contact): As large as 3 mm across, irregular in shape.
Piece 4: More oval in shape, many filled with calcite and/or pale green celadonite.
Piece 7 (at lower contact): Most filled with celadonite.
ALTERATION: Slightly to moderately altered. Center of Piece 5 is freshest in section.
VEINS/FRACTURES: Piece 2: A highly irregular fracture is filled with dark green alteration mineral.
Piece 5: ≈1 mm wide, filled with calcite.

NOTE: Sediments below 116 cm and in 115-713A-16R and 115-713A-17R are described on a separate description sheet.

SITE 713 HOLE A CORE 16R CORED INTERVAL 3046.0-3055.5 mbsl; 136.2-145.7 mbsf

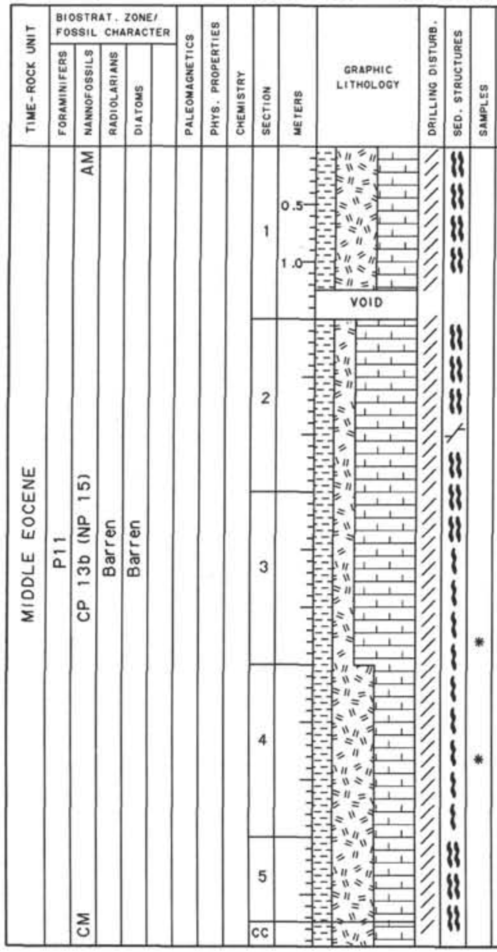

LITHOLOGIC DESCRIPTION

Interbedded FORAMINIFER-BEARING NANNOFOSSIL CHALK, VOLCANIC ASH-BEARING CLAY, and VOLCANIC ASH

Major lithology: Foraminifer-bearing nannofossil chalk, volcanic ash-bearing clay, and volcanic ash, complexly interbedded with separate lithologies moderately to highly mixed through bioturbation. Chalk layers are light gray (5Y 7/1) to light greenish gray (5GY 7/1), while concentrated ash layers are black (N2, N3) to dark gray (N4). Ash-bearing clay layers range from gray (5Y 5/1) and greenish gray (5GY 5/1) to grayish olive green (5GY 3/2). Fine carbonate is usually of nannofossil origin, but a small proportion is unidentifiable (micrite).

Microtectonic features such as microfaulting, shearing, and soft sediment deformation were observed in Sections 2, 3, and 4.

SMEAR SLIDE SUMMARY (%):

	3, 134 M	4, 86 D
TEXTURE:		
Sand	40	25
Silt	20	30
Clay	40	45
COMPOSITION:		
Clay	35	5
Volcanic glass	50	—
Accessory minerals:		
Micrite	8	—
Foraminifers	—	30
Nannofossils	5	64
Radiolarians	2	—
Sponge spicules	Tr	Tr
Calcispheres	—	1

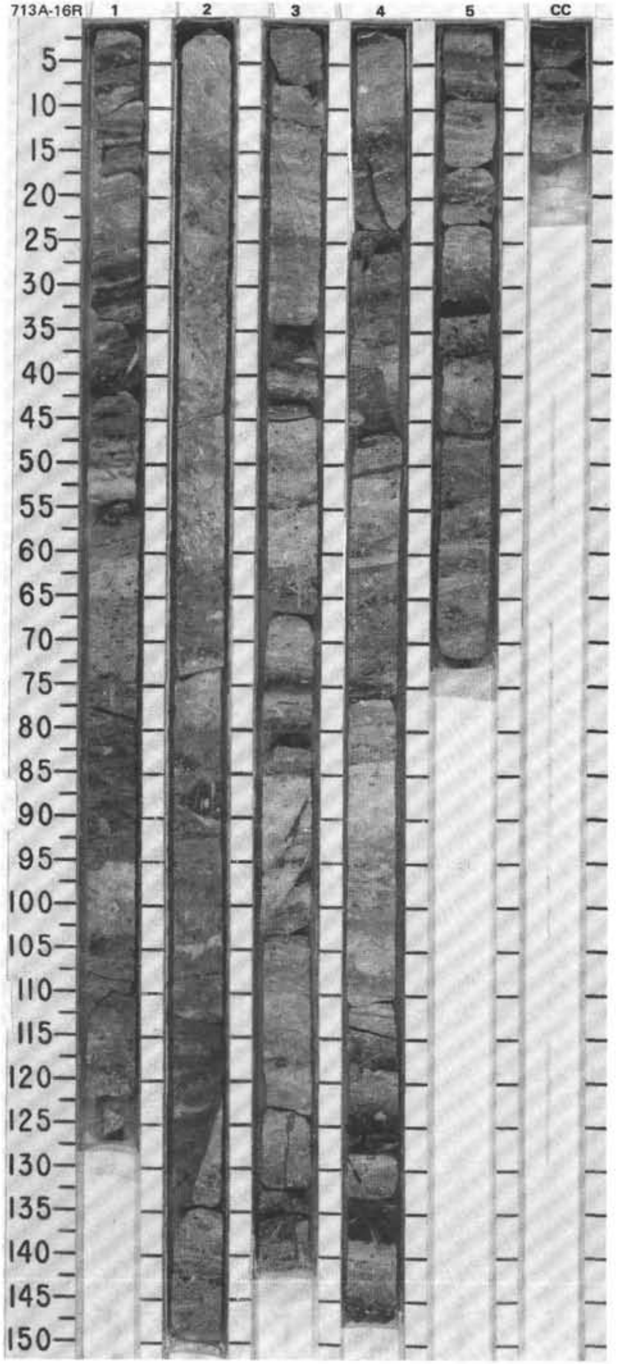

SITE 713 HOLE A CORE 17R CORED INTERVAL 3055.5-3065.0 mbsl; 145.7-155.2 mbsf

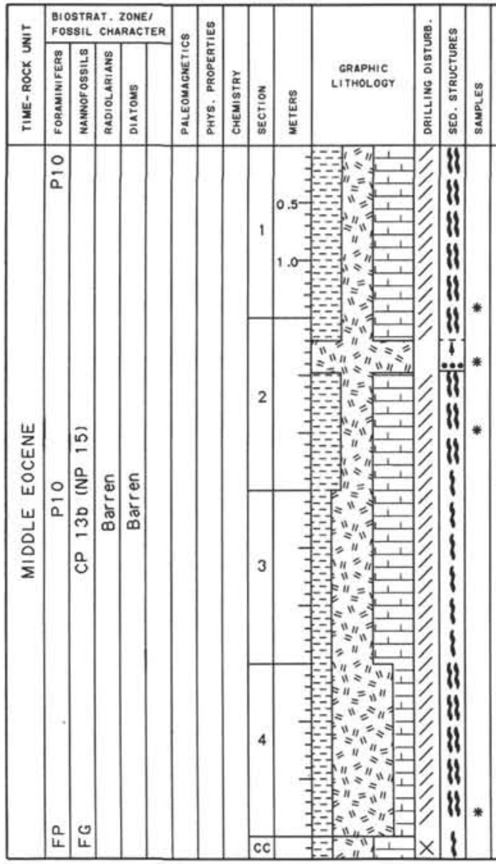

LITHOLOGIC DESCRIPTION

Interbedded FORAMINIFER-BEARING NANNOFOSSIL CHALK, VOLCANIC ASH-BEARING CLAY, and VOLCANIC ASH

Major lithology: Foraminifer-bearing nannofossil chalk, volcanic ash-bearing clay, and volcanic ash, all complexly interbedded with separate lithologies moderately to highly mixed through bioturbation. Chalk layers are light gray (5Y 7/1) to light greenish gray (5GY 7/1), while ash layers are typically black (N2, N3) to dark gray (N4). Ash-bearing clay layers range from gray (5Y 5/1) and greenish gray (5GY 5/1) to grayish olive green (5GY 3/2).

A volcanic ash turbidite occurs in Section 2, 25-45 cm. Ash in the turbidite is very coarse sand at base and graded upward, with a sharp basal contact and fine parallel laminations in the middle of the interval.

Microfaulting, shearing, soft sediment deformation, and fracture-filling are common features, particularly in Sections 3 and 4.

SMEAR SLIDE SUMMARY (%):

	1, 139 M	2, 43 M	2, 99 D	4, 126 D
TEXTURE:				
Sand	20	60	20	40
Silt	30	20	30	20
Clay	50	20	50	40
COMPOSITION:				
Quartz	2	—	2	Tr
Clay	63	5	8	20
Volcanic glass	25	82	8	65
Accessory minerals:				
Pyrite	2	10	Tr	—
Foraminifers	—	2	17	3
Nannofossils	8	1	54	12
Calcispheres	—	—	1	—

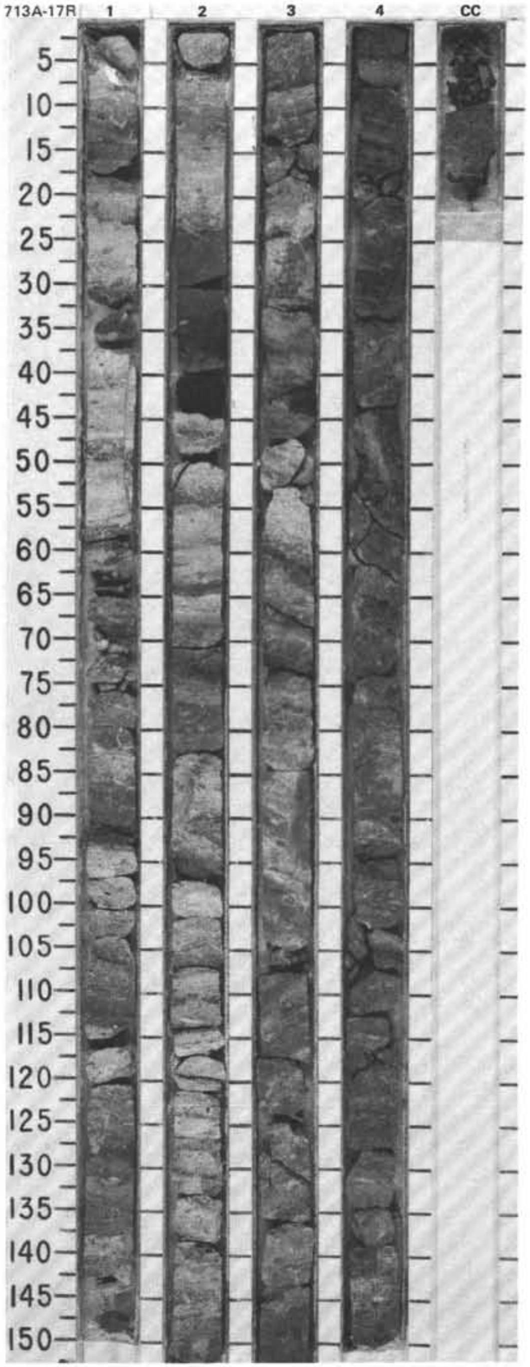

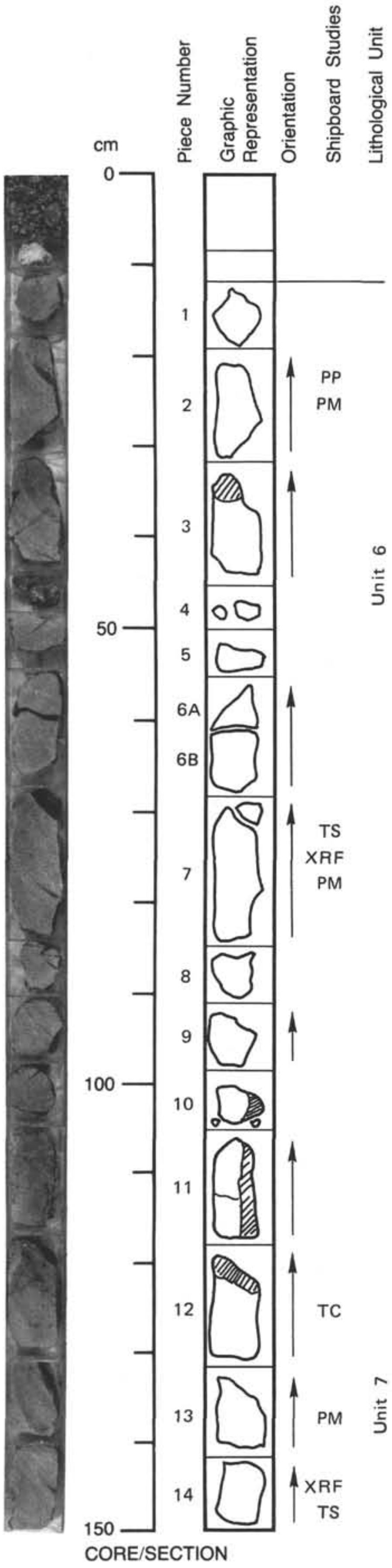

115-713A-18R-1

0–12 cm: TUFFACEOUS SEDIMENTS

UNIT 6: FINE-GRAINED, OLIVINE-PYROXENE-PLAGIOCLASE-PHYRIC MUGEARITE

Pieces 1–11

CONTACTS: Glassy parts in Pieces 3 and 10–12 may be chilled rim, showing boundary of flow unit. (Glassy areas indicated by shading.)

PHENOCRYSTS: Olivine - Euhedral to subhedral, <0.5 mm, altered to brownish phase.
Pyroxene - Euhedral to subhedral, <0.7 mm, characterized by elongate shape (≈ aegirine augite?).
Plagioclase - Subhedral, <0.5 mm.

GROUNDMASS: Fine grained, feldspar-rich, with glass.
Crystal clots, <3 mm in diameter, feldspar + pyroxene ± olivine.

COLOR: Dark gray (N4).

ALTERATION: Fresh to slightly altered.

UNIT 7: FINE-GRAINED PLAGIOCLASE-PYROXENE BASALT

Pieces 12–14

Similar to 115-713A-18R-1, Unit 6

GROUNDMASS: Slightly olivine-poor(?).

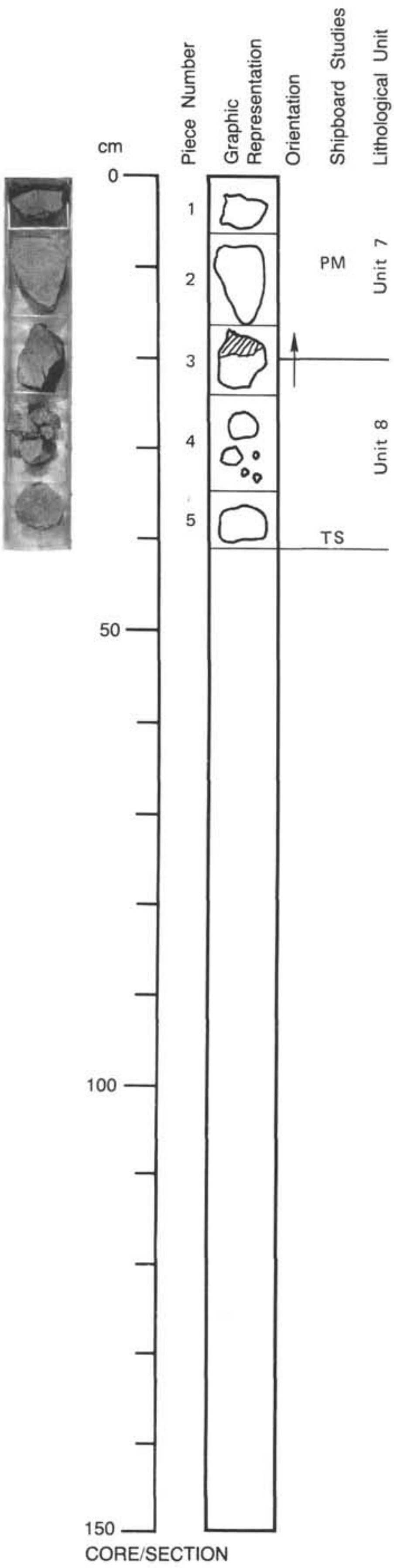

115-713A-18R-2

UNIT 7 (CONTINUED): FINE-GRAINED PLAGIOCLASE-PYROXENE BASALT

Pieces 1-2

Continuous with 115-713A-18R-1, Unit 7

CONTACTS: Piece 3 has glassy chilled rim, suggesting flow boundary.

UNIT 8: PLAGIOCLASE-PHYRIC HAWAIITE/MUGEARITE

Pieces 3–5

Similar to 115-713A-18R-1, Unit 7

GROUNDMASS: More glassy than Unit 7 rocks.

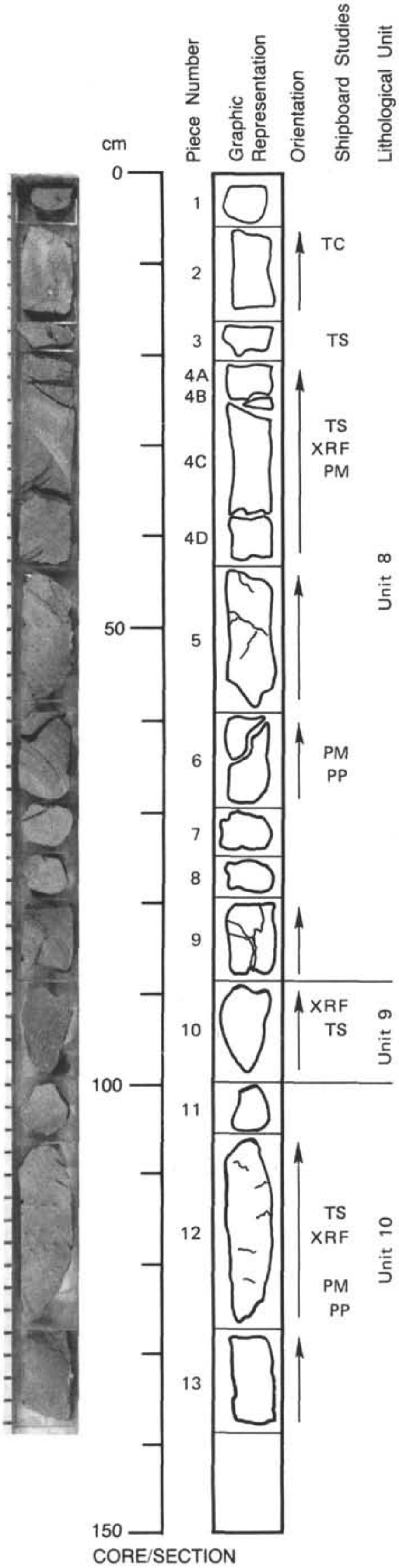

115-713A-19R-1

UNIT 8 (CONTINUED): PLAGIOCLASE-PHYRIC HAWAIITE/MUGEARITE

Pieces 1-9

Continuous with 115-713A-18R-2, Unit 8

PHENOCRYSTS: Plagioclase, subhedral, fresh, 3 mm, <10%.
GROUNDMASS: Fine grained. Plagioclase-rich, with elongate prismatic clinopyroxene and slightly altered olivine. Interstitial green clay, after glass(?).
VESICLES: Rare (<1%), infilled with calcite(?).
ALTERATION: Slight. Green clay in matrix interstices; calcite as vein filling.
VEINS/FRACTURES: Sporadic. High angle, as thick as 2 mm.

UNIT 9: PLAGIOCLASE-PHYRIC HAWAIITE/MUGEARITE WITHOUT VEINS

Piece 10

Similar to 115-713A-19R-1, Unit 8

GROUNDMASS: Fine to medium grained.
VEINS/FRACTURES: None.

UNIT 10: PLAGIOCLASE-PHYRIC HAWAIITE

Pieces 11-13

PHENOCRYSTS: Plagioclase, subhedral, fresh, as large as 3 mm, <5%.
Plagioclase, subhedral, partly altered, as large as 1 mm, <2%.
GROUNDMASS: Fine grained to quenched. Some evidence of coarsening from Piece 12 to Piece 13 downward.
VESICLES: Rare, as in 115-713A-19R-1, Unit 8.
ALTERATION: Slight, as in 115-713A-19R-1, Unit 8.

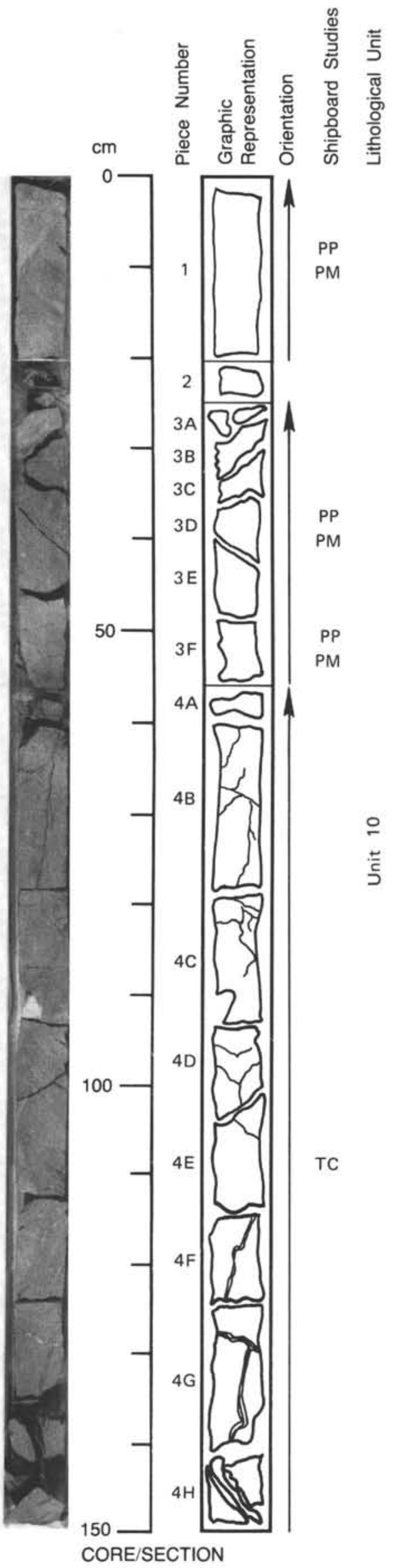

115-713A-19R-2

UNIT 10 (CONTINUED): PLAGIOCLASE-PHYRIC HAWAIITE

Pieces 1-4H

Continuous with 115-713A-19R-1, Unit 10

GROUNDMASS: Progressive coarsening away from junction seen at 115-713A-19R-1, Piece 11, is evident when Piece 1 of this section is compared with 115-713A-19R-1 pieces.

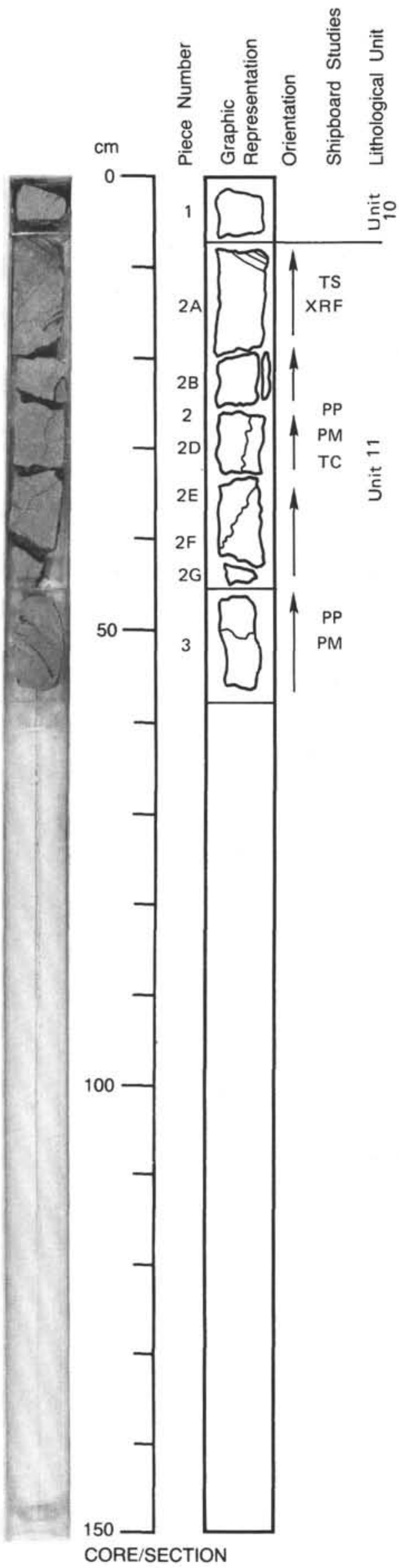

115-713A-19R-3

UNIT 10 (CONTINUED): PLAGIOCLASE-PHYRIC HAWAIITE

Piece 1

Continuous with 115-713A-19R-2, Unit 10

UNIT 11: PLAGIOCLASE-PHYRIC HAWAIITE(?)

Pieces 2A–3

CONTACTS: Chilled, top of Piece 2A.
PHENOCRYSTS: Plagioclase, subhedral, fresh, as large as 1 mm, <5%.
GROUNDMASS: Fine-grained plagioclase + clinopyroxene + olivine(?); some pyrite.
VESICLES: Rare, <1%, filled with green clay.
ALTERATION: Slight. Altered to green clay and to green clay (celadonite?) + calcite along chilled contact with Unit 10, top of Piece 2A.

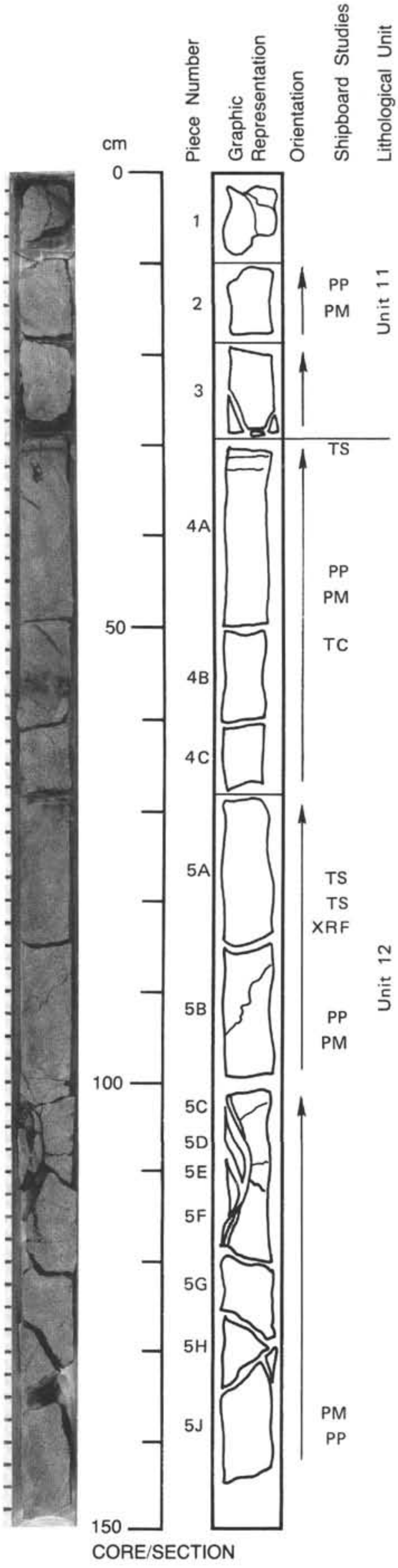

115-713A-20R-1

UNIT 11 (CONTINUED): PLAGIOCLASE-PHYRIC HAWAIITE(?)

Pieces 1–3

Continuous with 115-713A-19R-3, Unit 11

ALTERATION: Moderate.

UNIT 12: FELDSPAR-PHYRIC BASALT/HAWAIITE

Pieces 4A–5J

CONTACTS: Chill against 115-713A-20R-1, Unit 11, evident at top of Piece 4A.
PHENOCRYSTS: Plagioclase, subhedral, fresh, as large as 4 mm, 10%.
GROUNDMASS: Moderately carbonated plagioclase, clinopyroxene, and possibly olivine.
TEXTURE: Porphyritic, with phaneritic intersertal matrix.
VESICLES: Rare, ≈1%.
ALTERATION: Moderate, ≈20%; prominent alteration in 4 mm wide vein in Pieces 5C–5F.
VEINS/FRACTURES: Pieces 5C–5F: 4 mm wide vein.

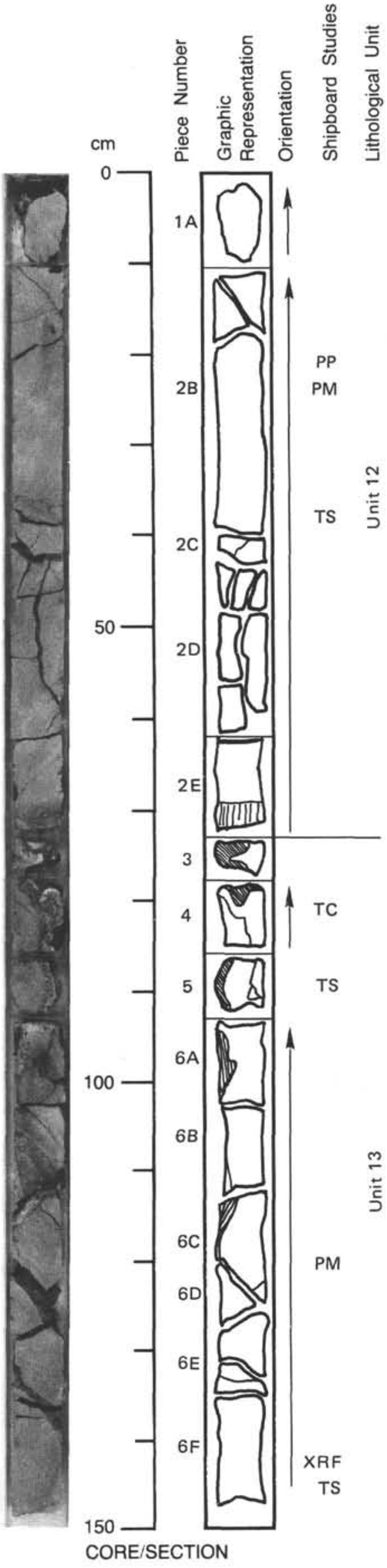

115-713A-20R-2

UNIT 12 (CONTINUED): FELDSPAR-PHYRIC BASALT/HAWAIITE

Pieces 1A–2E

Continuous with 115-713A-20R-1, Unit 12

CONTACTS: Strongly chilled contact against 115-713A-20R-2, Unit 12, seen at base of Piece 2E.

UNIT 13: PLAGIOCLASE-PHYRIC BASALT/HAWAIITE

Pieces 3–6F

CONTACTS: Strongly chilled (glassy) contact against 115-713A-20R-2, Unit 12, top of Piece 3. Intra-flow pillow junction(?) in Pieces 6A–6C, marked by celadonite + calcite zone as wide as 3 cm.

PHENOCRYSTS: Plagioclase - Subhedral, fresh, as large as 3 mm, 15%.
Olivine - Rare (≈ 1%), with fresh parts.

GROUNDMASS: Plagioclase, olivine, clinopyroxene, and magnetite(?).

TEXTURE: Porphyritic, with intersertal matrix texture.

VESICLES: Rare, spherical, infilled with celadonite(?).

ALTERATION: Moderate (≈ 20%) alteration to celadonite(?) + calcite.

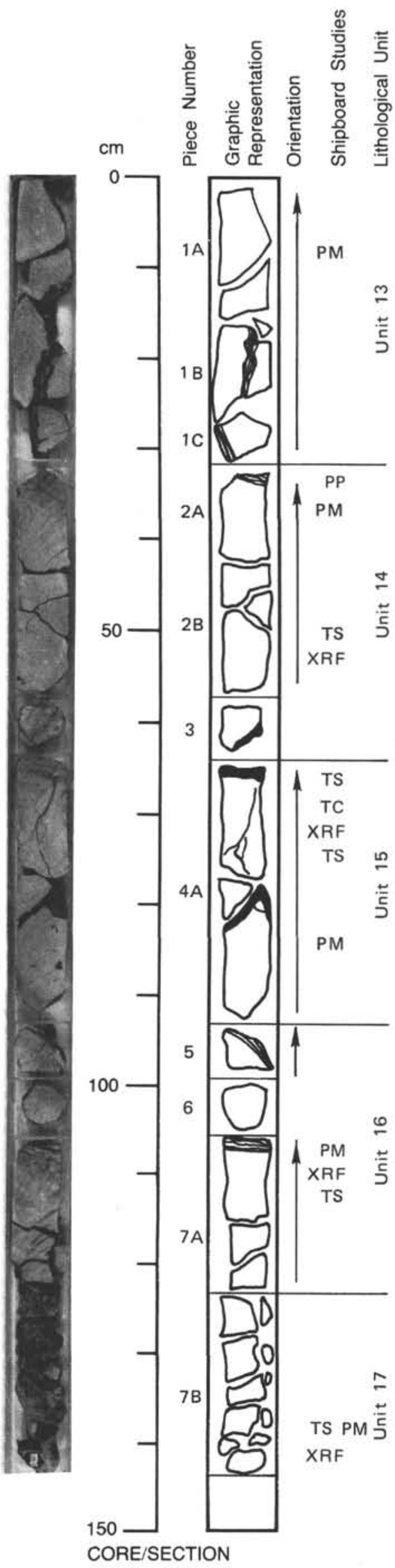

115-713A-20R-3

UNIT 13 (CONTINUED): PLAGIOCLASE-PHYRIC BASALT/HAWAIITE

Pieces 1A–1C

Continuous with 115-713A-20R-2, Unit 13

UNIT 14: OLIVINE-PLAGIOCLASE-PHYRIC BASALT

Pieces 2A–3

CONTACTS: Prominent glassy celadonitic chill at top of Piece 2A.
PHENOCRYSTS: Plagioclase - Subhedral, fresh, as large as 4 mm, 15%.
Olivine - Sparse, fresh, as large as 1 mm, ≈1%.
GROUNDMASS: Plagioclase-rich, with clinopyroxene + olivine(?).
TEXTURE: Porphyritic, with intersertal matrix.
VESICLES: Sparse (≈1%), spherical, as large as 1 mm, partly filled with calcite.
ALTERATION: Moderate alteration to carbonate and celadonite(?).

UNIT 15: OLIVINE-PLAGIOCLASE-PHYRIC BASALT

Pieces 4A–4B

CONTACTS: Prominent glassy chill at top of Piece 4A; progressive chilling toward base of Piece 4B.
PHENOCRYSTS: Plagioclase - Subhedral, fresh, as large as 5 mm, 15%.
Olivine - Subhedral, fresh, as large as 1 mm, 2%.
GROUNDMASS: Plagioclase-rich, with clinopyroxene + olivine(?).
VESICLES: Sparse (≈2%), spherical, filled with calcite.
ALTERATION: Slight alteration of matrix to calcite.

UNIT 16: OLIVINE-PLAGIOCLASE-PHYRIC BASALT

Pieces 5–7A

Similar to 115-713A-20R-3, Unit 15.

CONTACTS: Chilled at top of Piece 5.

UNIT 17: PLAGIOCLASE-PHYRIC BASALT

Pieces 7A–7B

CONTACTS: Abrupt change to heavily fractured dark basalt, different from 115-713A-20R-3, Unit 16, as seen down to Piece 7A.
PHENOCRYSTS: Plagioclase, subhedral, ≈5%.
GROUNDMASS: Slightly porphyritic; intersertal matrix of clinopyroxene + plagioclase.
COLOR: Dark.
VESICLES: Sparse (≈1%), filled with calcite.
ALTERATION: Moderate, to calcite.
VEINS/FRACTURES: Heavily fractured.

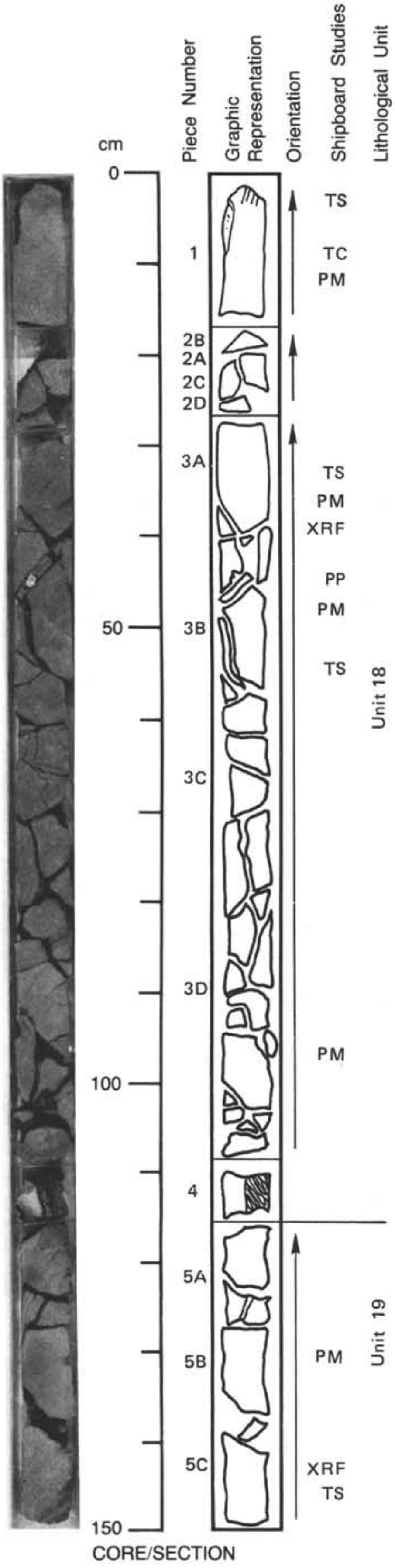

115-713A-20R-4

UNIT 18: PLAGIOCLASE-PHYRIC HAWAIITE(?)

Pieces 1-4

CONTACTS: Piece 4 contains silt layer.
PHENOCRYSTS: Plagioclase, subhedral, fresh, as large as 1 mm.
GROUNDMASS: Feldspar rich, slightly carbonated; little clinopyroxene.
TEXTURE: Porphyritic, with intersertal matrix.
VESICLES: Slightly vesicular (≈2%), spherical, as wide as 1 mm, infilled with calcite, often rimmed with green clay.
ALTERATION: Moderate to high, carbonate + minor green clay.

UNIT 19: PLAGIOCLASE-PHYRIC BASALT/HAWAIITE

Pieces 5A1-5C2

PHENOCRYSTS: Plagioclase - Subhedral, as large as 1 mm, 15%.
Olivine - Subhedral, as large as 1 mm, ≈1%.
GROUNDMASS: Plagioclase + clinopyroxene + olivine(?).
TEXTURE: Porphyritic, with intersertal matrix.
VESICLES: Sparse (≈1%).
ALTERATION: Moderate, to calcite.

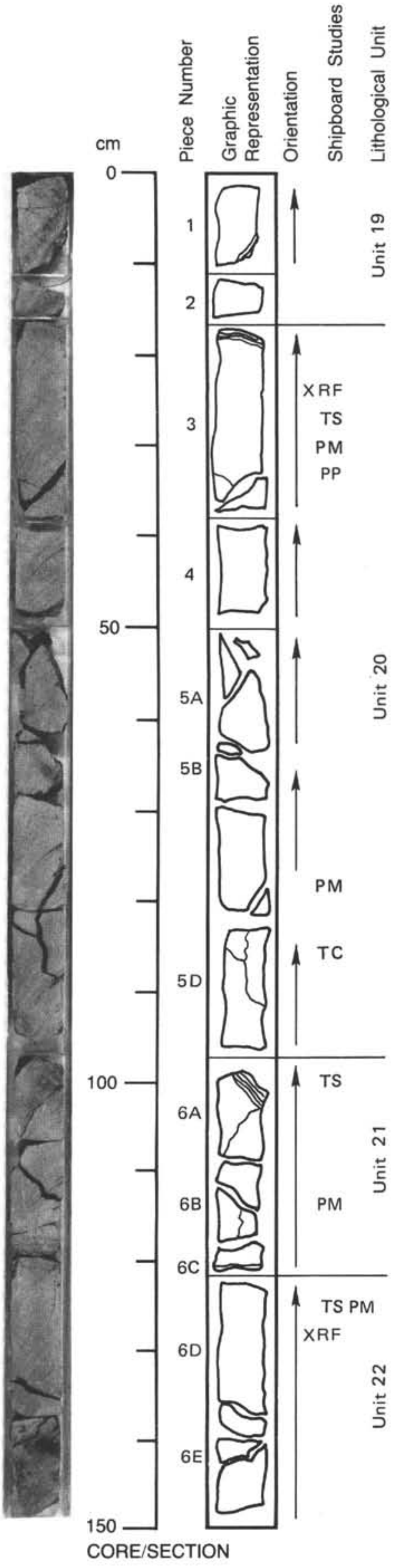

115-713A-20R-5

UNIT 19 (CONTINUED): PLAGIOCLASE-PHYRIC BASALT/HAWAIITE

Pieces 1-2

Continuous with 115-713A-20R-4, Unit 19

CONTACTS: Downward-facing chill at base of Piece 2.

UNIT 20: PLAGIOCLASE-PHYRIC BASALT/HAWAIITE

Pieces 3A-5D

Similar to 115-713A-20R-5, Unit 19

CONTACTS: Upward-facing chill at top of Piece 3A; weakly developed chill at base of Piece 5D.

PHENOCRYSTS: Plagioclase, as long as 3 mm.

UNIT 21: PLAGIOCLASE-PHYRIC BASALT/HAWAIITE

Pieces 6A-6C

Similar to 115-713A-20R-5, Unit 20

CONTACTS: Well-developed chill at top of Piece 6A; chill at base of Piece 6C; possible intra-flow pillow contact.

UNIT 22: PLAGIOCLASE-PHYRIC BASALT/HAWAIITE

Pieces 6D-6E

Similar to 115-713A-20R-5, Unit 21

VESICLES: Traces of pyrite in some vesicle infills, associated with calcite.

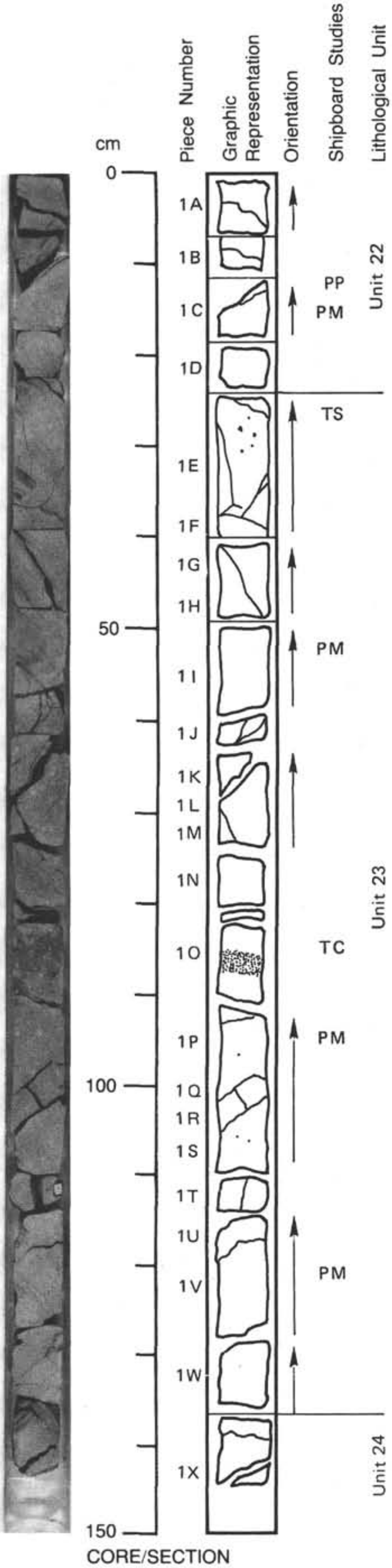

115-713A-20R-6

UNIT 22 (CONTINUED): PLAGIOCLASE-PHYRIC BASALT/HAWAIITE

Pieces 1A–1D

Continuous with 115-713A-20R-5, Unit 22

VEINS/FRACTURES: Fractures contain very dark green mineral.

UNIT 23: PLAGIOCLASE-PHYRIC BASALT (PILLOW LAVA?)

Pieces 1E–1W

CONTACTS: Upper contact has glassy upper surface; lower contact not defined.
PHENOCRYSTS: Plagioclase, ≤3 mm across, white.
GROUNDMASS: Plagioclase - 0.2 mm.
Pyroxene - 0.1 mm.
VESICLES: Round, ≤1 mm wide, <1% by volume, filled with calcite.
Piece 1E: ≤1 mm.
Piece 1I: Layering of vesicles <1 mm, filled with dark green mineral.
ALTERATION: Unit shows many fractures filled with dark green clay mineral and minor calcite.
Shaded area in Piece 10 is intensely altered(?).
VEINS/FRACTURES: Many fractures, particularly in Pieces 1E and 1F.

UNIT 24: PLAGIOCLASE-PHYRIC BASALT

Piece 1X

Similar to 115-713A-20R-5, Unit 23

CONTACTS: Glassy contact in Piece 1X contains clay-filled crack.

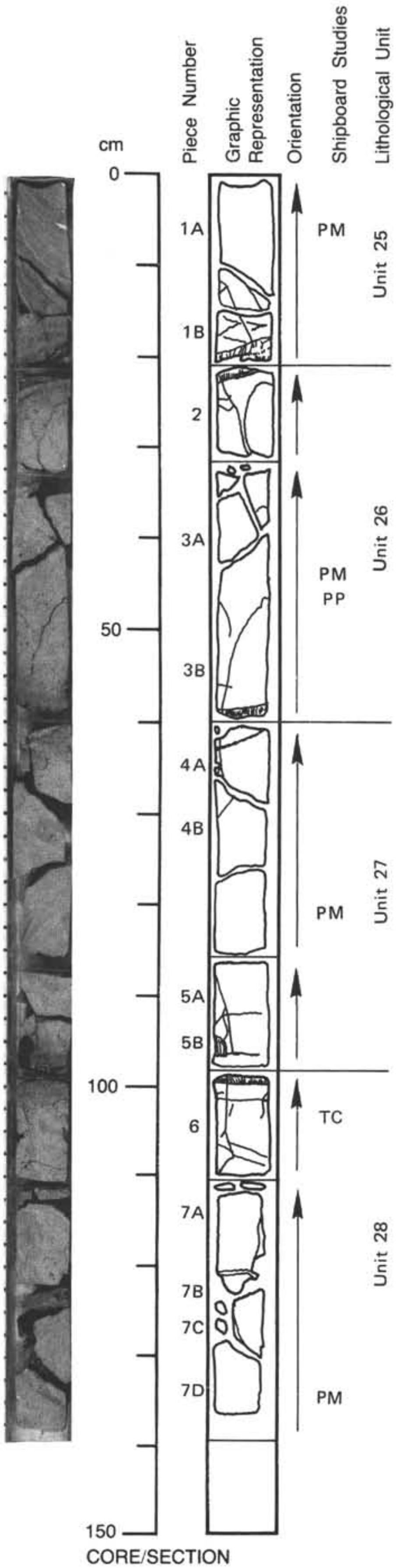

115-713A-21R-1

UNIT 25: OLIVINE-CLINOPYROXENE-PLAGIOCLASE BASALT

Pieces 1A -1B

CONTACTS: Glassy contact inclined 30° at base of Piece 1B.
GLASS: Altered to clay in bands 2-3 mm thick; some glass is preserved (fresh).
PHENOCRYSTS: Olivine - Rare, altered to clay, <1 mm in size.
Plagioclase - As large as 2 mm, euhedral and in glomerocrysts (2 - 5%).
Clinopyroxene - 1 mm, found with plagioclase, ≈ 1%.
GROUNDMASS: Fine grained.
VESICLES: Circular, <1%, 1-2 mm in size, completely filled with clay.
ALTERATION: Slight.
VEINS/FRACTURES: Veins as wide as 2 mm, filled with clay, form 1-2% of unit.
VOIDS: Irregular, <1%, 1 mm in size, filled with clay.

UNIT 26: OLIVINE-CLINOPYROXENE-PLAGIOCLASE BASALT

Pieces 2-3B

Similar to 115-713A-21R-1, Unit 25

CONTACTS: Glassy contact, as thick as 1 cm, inclined 30° at top of Piece 2; glass contact, 5 mm thick, straight, at base of Piece 5B.

UNIT 27: OLIVINE-CLINOPYROXENE-PLAGIOCLASE BASALT

Pieces 4A -5B

Similar to 115-713A-21R-1, Units 25 and 26

CONTACTS: Carbonate present at upper contact.
ALTERATION: Clay altered to green soft prismatic crystals in veins.
VEINS/FRACTURES: Veins are slightly thicker than 115-713A-21R-1, Units 25 and 26, 3 mm thick, and more fragile.
VOIDS: Piece 5B: Void 2 cm wide, filled with dark green clay.

UNIT 28: OLIVINE-CLINOPYROXENE-PLAGIOCLASE BASALT

Pieces 6-7D

Similar to 115-713A-21R-1, Units 25-27

CONTACTS: Glass contact at top.
PHENOCRYSTS: Clinopyroxene, plagioclase, and (rare) olivine.
VEINS/FRACTURES: Fractures run through unit, fragile, filled with dark green clay.

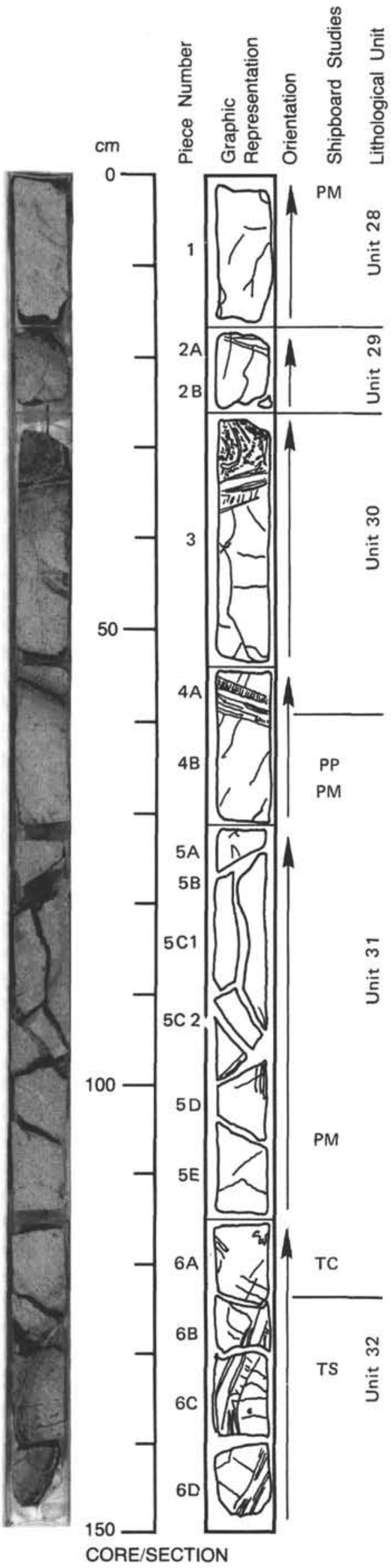

115-713A-21R-2

UNIT 28 (CONTINUED): OLIVINE-CLINOPYROXENE-PLAGIOCLASE BASALT

Piece 1

Continuous with 115-713A-21R-1, Unit 28

UNIT 29: OLIVINE-CLINOPYROXENE-PLAGIOCLASE BASALT

Pieces 2A-2B

Similar to 115-713A-21R-1, Units 25-28

CONTACTS: Glass contacts at top and base.
VEINS/FRACTURES: This piece has veins, but rock is not as fragile as in 115-713A-21R-1, Unit 28.

UNIT 30: OLIVINE-CLINOPYROXENE-PLAGIOCLASE BASALT

Pieces 3-4A

Similar to 115-713A-21R-1 and -2, Units 25-29

CONTACTS: Glass contacts at top and base.
PHENOCRYSTS: Olivine - <0.5 mm, about 1%, altered to reddish clay.
Plagioclase - ≈1 mm, 2%, intergrown with clinopyroxene.
Clinopyroxene - As large as 8 mm, ≈3%. The large size of clinopyroxene and its greater abundance distinguishes Unit 30 from Units 25-29.
GROUNDMASS: As in 115-713A-21R-1 and -2, Units 25-29.
VESICLES: As in 115-713A-21R-1 and -2, Units 25-29.
ALTERATION: As in 115-713A-21R-1 and -2, Units 25-29.
VEINS/FRACTURES: As in 115-713A-21R-1 and -2, Units 25-29.

UNIT 31: OLIVINE-CLINOPYROXENE-PLAGIOCLASE BASALT

Pieces 4B-6A

Similar to 115-713A-21R-1 and -2, Units 25-30

CONTACTS: Glass contacts at top and base.
PHENOCRYSTS: More abundant plagioclase and less abundant clinopyroxene distinguish 115-713A-21R-2, Unit 31, from Unit 30.
Olivine - Rare, <0.5 mm in size, altered to clay.
Plagioclase - 0.5-2.0 mm, 5%.
Clinopyroxene - Rarely as large as 3 mm, 1-2%.
VESICLES: As in 115-713A-21R-1 and 2, Units 25-30 and 32.
VEINS/FRACTURES: As in 115-713A-21R-1 and -2, Units 25-30 and 32.
VOIDS: As in 115-713A-21R-1 and -2, Units 25-30 and 32.

UNIT 32: OLIVINE-CLINOPYROXENE-PLAGIOCLASE BASALT PILLOW

Pieces 6B-6D

Similar to 115-713A-21R-1 and -2, Units 25-31

CONTACTS: Glass contact at top, carbonate baked at margin at base of Piece 6D.
PHENOCRYSTS: Olivine - Rare.
Plagioclase - 2-5%.
Clinopyroxene - 1-3%.

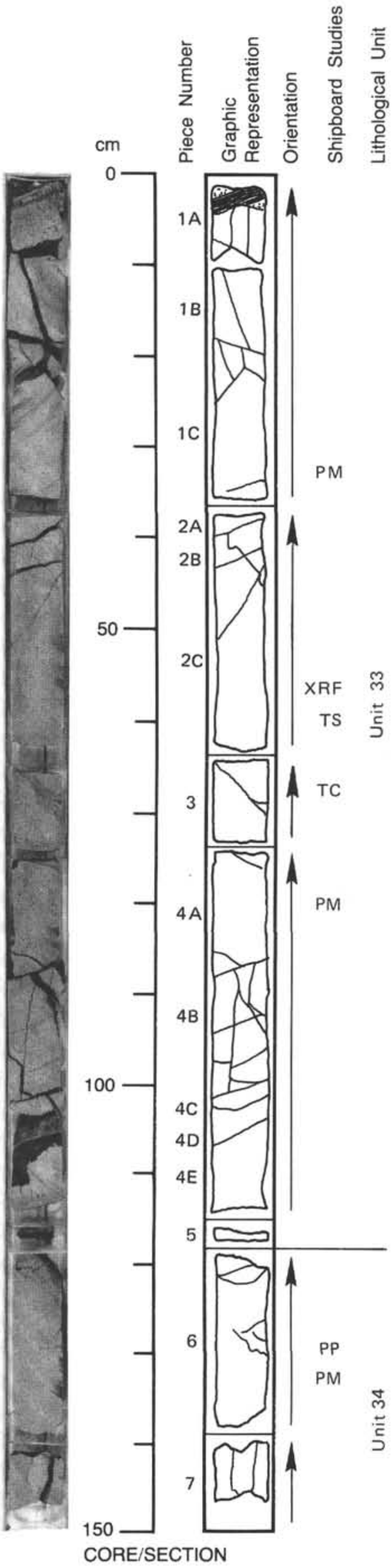

115-713A-21R-3

UNIT 33: PLAGIOCLASE-PYROXENE BASALT

Pieces 1A–5

CONTACTS: Glass in upper selvage (Piece 1A) and on lower contact.
PHENOCRYSTS: Plagioclase, ≤4 mm long, 5%.
GROUNDMASS: Plagioclase, typically 0.05 mm wide; and pyroxene, typically 0.04 mm wide. Minor pyrite scattered throughout matrix.
VESICLES: 0.8 mm wide, 5%, filled with green celadonite.
ALTERATION: Rock appears relatively fresh/unaltered.
VEINS/FRACTURES: Fractures filled with dark green clay mineral.
Pieces 4B–4D: Fractures filled with dark green mineral + minor calcite.

UNIT 34: PLAGIOCLASE-PYROXENE BASALT

Pieces 6–7

Similar to 115-713A-21R-3, Unit 33

CONTACTS: Piece 6, top, clay; outer selvage of pillow altered to black clay.
PHENOCRYSTS: Plagioclase, ≤6 mm in size, 5–10%.

115-713A-21R-4

UNIT 34 (CONTINUED): PLAGIOCLASE-PYROXENE BASALT

Pieces 1A–15

Continuous with 115-713A-21R-3, Unit 34

ALTERATION: Pieces 4A, 4B, and 4C have 10 cm area that is more altered than the rest of Unit 34.

VEINS/FRACTURES: Pieces 14 and 15: Sulfides in some cracks.

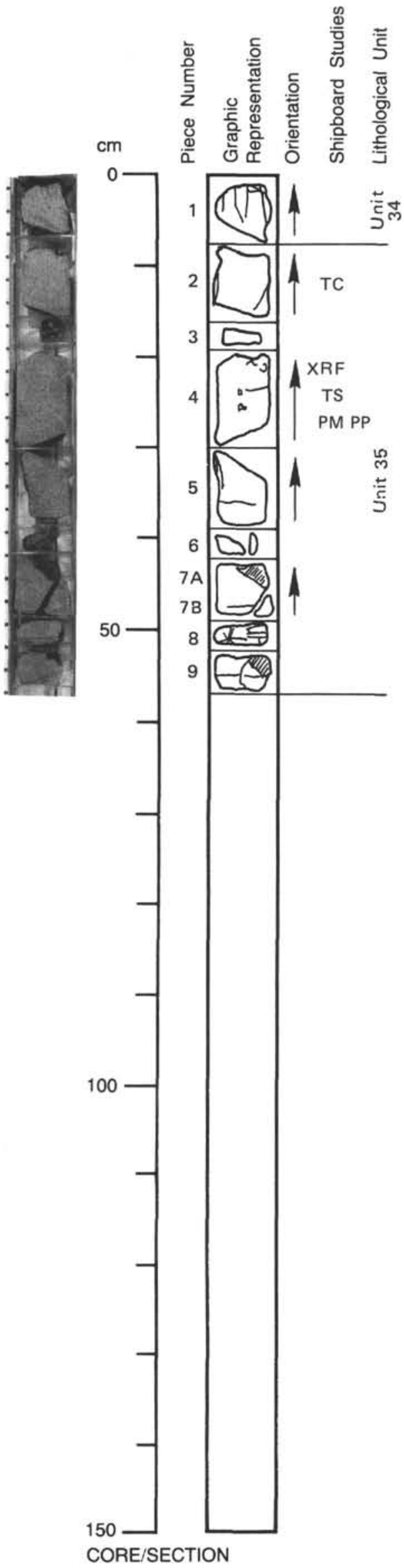

115-713A-22R-1

UNIT 34 (CONTINUED): PLAGIOCLASE-PYROXENE BASALT

Piece 1

Continuous with 115-713A-21R-4, Unit 34

UNIT 35: PLAGIOCLASE-CLINOPYROXENE BASALT

Pieces 2–9

PHENOCRYSTS: Plagioclase - 1–5 mm in size, 5%.
Clinopyroxene - <1%.
GROUNDMASS: Fine grained.
VESICLES: Round, 1 mm or less in size, <1%, filled with clay.
ALTERATION: Slight to moderate.
VEINS/FRACTURES: 1 mm or less in size, <1%.

NOTE: This unit is distinguished from those above it by larger percent of plagioclase, small amount of clinopyroxene, no olivine, and fewer fractures.

THIN SECTION DESCRIPTION

115-713A-13R-1 (Piece 9A, 67-69 cm)

ROCK NAME: Highly olivine-bearing plagioclase clinopyroxene phyric basalt

WHERE SAMPLED: Middle of Unit 1

TEXTURE: Subophitic, highly porphyritic

GRAIN SIZE: Fine

OBSERVER: MRF

PRIMARY MINERALOGY	PERCENT PRESENT	PERCENT ORIGINAL	SIZE RANGE (mm)	APPROX. COMPO-SITION	MORPHOLOGY	COMMENTS
PHENOCRYSTS						
Olivine	—	<1				
Plagioclase	5	5	0.5–2.0	An 62	Subhedral	Glomerocrysts up to 4 mm.
Clinopyroxene	10	11	0.2–1.0	Augite	Subhedral–euhedral	Subophitic
GROUNDMASS						
Plagioclase	15	17	0.1–0.5		Subhedral	1:5 to 1:10 width:length ratios.
Clinopyroxene	39	41	0.1–0.2	Augite	Subhedral	
Oxides	1	1	<0.1		Subhedral	
Glass/ fine groundmass	—	25				

SECONDARY MINERALOGY	PERCENT	REPLACING/ FILLING	COMMENTS
Clays	10	Groundmass??	
Carbonate	5	Vesicles	Calcite.
Chlorite	15	Glass or groundmass	

VESICLES/ CAVITIES	PERCENT	LOCATION	SIZE RANGE (mm)	FILLING	SHAPE	COMMENTS
Vesicles	5		4	Calcite, clay		Vesicles also filled with a mixture of oxide laths and microcrystalline mass.

THIN SECTION DESCRIPTION

115-713A-13R-3 (Piece 3, 16-18 cm)

ROCK NAME: Sparsely clinopyroxene plagioclase phyric basalt

WHERE SAMPLED: Only piece of Unit 2. Bottom-most piece in core.

TEXTURE: Sparsely porphyritic

GRAIN SIZE: Fine

OBSERVER: MRF

PRIMARY MINERALOGY	PERCENT PRESENT	PERCENT ORIGINAL	SIZE RANGE (mm)	APPROX. COMPO-SITION	MORPHOLOGY	COMMENTS
PHENOCRYSTS						
Plagioclase	2	2	1-2	An 64	Subhedral, equant to slightly elongated	
Clinopyroxene	1	1	0.1-0.5	Augite	Subhedral	Often in clusters with plag.
Spinel	1	1	0.1	Magnetite	Subhedral-euhedral	
GROUNDMASS						
Plagioclase	25	25	0.1-0.5		Subhedral, laths	
Clinopyroxene	35	40	0.1-0.2		Subhedral-anhedral	
Oxides	1	1	0.05-0.10	Magnetite	Subhedral-euhedral	
Fine-grained groundmass	—	30				

SECONDARY MINERALOGY	PERCENT	REPLACING/ FILLING	COMMENTS
Chlorite	30	Cpx, fine groundmass	
Clays	5	Cpx	Celadonite. Possibly replaces primary ol. One quarter of the slide has slightly more celadonite in the groundmass. This area is rimmed by sulfides.
Sulfides	tr	Groundmass	Possibly sphalerite, dark brown in thin section.

VESICLES/ CAVITIES	PERCENT	LOCATION	SIZE RANGE (mm)	FILLING	SHAPE	COMMENTS
Vesicles	1	Even	1	Clay	Round	Clays are zoned, red iddingsite, celadonite, chlorite from the edge of the vesicle inwards.

THIN SECTION DESCRIPTION

115-713A-14R-2 (Piece 3, 70-71 cm)

ROCK NAME: Highly plagioclase clinopyroxene phyric basalt

WHERE SAMPLED: Unit 3, middle of flow

TEXTURE: Subophitic, highly porphyritic

GRAIN SIZE: Fine to medium

OBSERVER: MRF

PRIMARY MINERALOGY	PERCENT PRESENT	PERCENT ORIGINAL	SIZE RANGE (mm)	APPROX. COMPO-SITION	MORPHOLOGY	COMMENTS
PHENOCRYSTS						
Plagioclase	21	21	0.5–2.0	An 55	Laths	2-mm phenocrysts are equant, strongly zoned at rims.
Clinopyroxene	41	41	0.5–1	Augite	Subhedral	Subophitic intergrowths.
Spinel	2	2	0.4–0.4	Magnetite	Euhedral	Skeletal. Could be alteration product, replacing groundmass.
GROUNDMASS						
Glass	—	29				Replaced by chlorite.
Plagioclase	—	5				Replaced by chlorite.
Clinopyroxene	—	2				Replaced by chlorite.

SECONDARY MINERALOGY	PERCENT	REPLACING/ FILLING	COMMENTS
Chlorite	33	Plag, glass, augite	
Carbonate	1	Cavities	Calcite?
Sulfides	2	Voids	Dark brown, anhedral. Sphalerite(?).

VESICLES/ CAVITIES	PERCENT	LOCATION	SIZE RANGE (mm)	FILLING	SHAPE
Cavities	2	Even	1–2	Magnetite, sulfide, calcite, clay	Irregular

THIN SECTION DESCRIPTION

115-713A-15R-4 (Piece 1, 43-47 cm)

ROCK NAME: Highly plagioclase clinopyroxene phyric basalt

WHERE SAMPLED: Unit 2, 50 cm above Unit 3

TEXTURE: Intersertal, highly porphyritic

GRAIN SIZE: Fine

OBSERVER: MRF

PRIMARY MINERALOGY	PERCENT PRESENT	PERCENT ORIGINAL	SIZE RANGE (mm)	APPROX. COMPO-SITION	MORPHOLOGY	COMMENTS
PHENOCRYSTS						
Plagioclase	10	10	0.1/ 0/1.5	An 65	Subhedral	Equant grains tend to be larger.
Clinopyroxene	40	40	0.1–0.5	Augite	Subhedral	Glomerocrysts with plagioclase.
Spinel	5	5	0.05–0.50	Magnetite	Euhedral, skeletal	Intergrown with plag and cpx.

SECONDARY MINERALOGY	PERCENT	REPLACING/ FILLING
Chlorite	45	Groundmass
Sulfides	tr	Voids

VESICLES/ CAVITIES	PERCENT	LOCATION	SIZE RANGE (mm)	FILLING	SHAPE
Voids	1		1–3	Clay	Irregular

THIN SECTION DESCRIPTION

115-713A-15R-4 (Piece 1, 44-46 cm)

ROCK NAME: Highly plagioclase clinopyroxene phyric basalt

WHERE SAMPLED: Unit 3

TEXTURE: Highly porphyritic, subophitic

GRAIN SIZE: Medium

OBSERVER: RBH

PRIMARY MINERALOGY	PERCENT PRESENT	PERCENT ORIGINAL	SIZE RANGE (mm)	APPROX. COMPO-SITION	MORPHOLOGY	COMMENTS
PHENOCRYSTS						
Plagioclase	35	35	51	An 50-60	Subhedral, laths	Conspicuous zoning.
Clinopyroxene	40	40	0.5 (ave)		Equant, subhedral–anhedral	Subophitic. Megacrysts; one up to 1 cm, poikilitically enclosing plag.
Titanomagnetite	<5	<5	50.5		Equant, subskeletal	Occurs interstitial, and in association with glassy/clay material.
GROUNDMASS						
Glass	—	20				

SECONDARY MINERALOGY	PERCENT	REPLACING/ FILLING	COMMENTS
Clays	20	Glass	Replaces original interstitial glass. Often encloses titanomagnetite.

THIN SECTION DESCRIPTION

115-713A-15R-4 (Piece 3, 98-100 cm)

ROCK NAME: Highly plagioclase clinopyroxene phyric basalt

WHERE SAMPLED: Unit 3

TEXTURE: Highly porphyritic

GRAIN SIZE: Fine

OBSERVER: YT

PRIMARY MINERALOGY	PERCENT PRESENT	PERCENT ORIGINAL	SIZE RANGE (mm)	APPROX. COMPOSITION	MORPHOLOGY	COMMENTS
PHENOCRYSTS						
Olivine	—	3	0.1–0.5		Euhedral	Completely altered to brown clay.
Plagioclase	7	7	0.2–0.5	An 60(?)	Euhedral	Sometimes forms crystal clots with cpx.
Clinopyroxene	7	7	0.2–0.7	Augite	Euhedral–subhedral	Zoned
GROUNDMASS						
Plagioclase	21	44	<0.2		Subhedral	
Cliopyroxene	21	21	<0.2		Subhedral	
Opaques	7	7	<0.2	Magnetite(?)	Euhedral	
Glass	—	11				Completely altered to green clay.

SECONDARY MINERALOGY	percent	REPLACING/ FILLING	COMMENTS
Clays	3	Ol	Iddingsite(?). Brown.
Clays	11	Vesicles, Glass	Green. Alteration products from groundmass, interstitial glass.
Clays	23	Plag	Unidentified fine clay.

VESICLES/ CAVITIES	PERCENT	LOCATION	SIZE RANGE (mm)	FILLING	SHAPE
Vesicles	5	Even	<0.5	Green clay	Round

THIN SECTION DESCRIPTION

115-713A-15R-4 (Piece 4, 103-105 cm)

ROCK NAME: Moderately olivine clinopyroxene plagioclase phyric basalt

WHERE SAMPLED: Unit 3

TEXTURE: Porphyritic, hyaline

GRAIN SIZE: Fine

OBSERVER: ANB

PRIMARY MINERALOGY	PERCENT PRESENT	PERCENT ORIGINAL	SIZE RANGE (mm)	APPROX. COMPOSITION	MORPHOLOGY	COMMENTS
PHENOCRYSTS						
Olivine	—	1	<0.5		Subhedral	Completely altered to red/brown iddingsite.
Plagioclase	7	7	<1	≈An 50	Euhedral	Quench forms common. Glass inclusions parallel to c-axis.
Clinopyroxene	3	3		Augite	Anhedral	Fresh. Often in glomerocrysts with plag.
GROUNDMASS						
Glass	89	89				Black. Partially oxidized.

SECONDARY MINERALOGY	PERCENT	REPLACING/ FILLING	COMMENTS
Clays	1	Ol	Red/brown iddingsite.

VESICLES/ CAVITIES	PERCENT	LOCATION	SIZE RANGE (mm)	FILLING	SHAPE	COMMENTS
Vesicles	12	Even	<3	Calcite	Irregular	Generally rimmed with calcite. Sometimes filled with calcite.

THIN SECTION DESCRIPTION

115-713A-15R-4 (Piece 4, 104-106 cm)

ROCK NAME: Highly olivine plagioclase clinopyroxene phyric basalt

WHERE SAMPLED: Unit 4, near contact

TEXTURE: Glassy, highly porphyritic

GRAIN SIZE: Microcrystalline

OBSERVER: MRF

PRIMARY MINERALOGY	PERCENT PRESENT	PERCENT ORIGINAL	SIZE RANGE (mm)	APPROX. COMPO-SITION	MORPHOLOGY	COMMENTS
PHENOCRYSTS						
Olivine	(?)	1	0.1–0.3			
Plagioclase	5	5	0.2–1.0	An 65		
Clinopyroxene	10	10	0.1–0.3	Augite		
GROUNDMASS						
Glass	73	73				Microcrystalline.
Spinel	1	1	0.005–0.020	Magnetite		
Sulfides	Tr					

SECONDARY MINERALOGY	PERCENT	REPLACING/ FILLING	COMMENTS
Chlorite	10	Voids	
Clays	1	ol	Iddingsite.

VESICLES CAVITIES	PERCENT	LOCATION	SIZE RANGE (mm)	FILLING	SHAPE
Cavities	5		0.1–2.0	Clay	Irregular

THIN SECTION DESCRIPTION

115-713A-15R-4 (Piece 6A, 143-145 cm)

ROCK NAME: Highly olivine-bearing clinopyroxene plagioclase phyric basalt

WHERE SAMPLED: Unit 4

TEXTURE: Highly porphyritic, hyalocrystalline

GRAIN SIZE: Fine

OBSERVER: ANB

PRIMARY MINERALOGY	PERCENT PRESENT	PERCENT ORIGINAL	SIZE RANGE (mm)	APPROX. COMPO-SITION	MORPHOLOGY	COMMENTS
PHENOCRYSTS						
Olivine	—	tr			Subhedral	Completely altered to carbonate.
Plagioclase	15	15	<1	An 45(?)	Subhedral	Slightly altered to sericite. Tendency to show flow alignment.
Clinopyroxene	5	5	<0.8	Augite	Subhedral	Colorless. Often in glomerocrysts with plagioclase.
GROUNDMASS						
Plagioclase	10	10	<0.2		Subhedral	
Titanomagnetite	5	5	<0.2		Subhedral	More abundant than in typical basalt.
Glass	—	65				Interstitial. Altered to microcrystalline and cryptocrystalline pale brown and green clays (celadonite?).

SECONDARY MINERALOGY	PERCENT	REPLACING/ FILLING	COMMENTS
Clays	65	Glass	Predominately pale gray/brown smectite(?). Less abundant green celadonite(?).

COMMENTS: One large (1 cm diameter) "xenolith" of cpx + plag; large cpx poikilocrysts enclose large euhedral plag (An 45). Rock in general looks somewhat evolved, almost mugearitic.

THIN SECTION DESCRIPTION

115-713A-15R-5 (Piece 2, 3-7 cm)

ROCK NAME: Moderately olivine plagioclase clinopyroxene phyric basalt

WHERE SAMPLED: Unit 5

TEXTURE: Moderately porphyritic, hyaline

GRAIN SIZE: Fine

OBSERVER: ANB

PRIMARY MINERALOGY	PERCENT PRESENT	PERCENT ORIGINAL	SIZE RANGE (mm)	APPROX. COMPO-SITION	MORPHOLOGY	COMMENTS
PHENOCRYSTS						
Olivine	—	3	<1.5		Subhedral	Totally altered to brown iddingsite.
Plagioclase	3	3	<0.6	Augite	Anhedral	Colorless. Fresh.
Clinopyroxene	7	7	<2		Euhedral	Fresh. Quench overgrowths.
GROUNDMASS						
Glass	80	80				Brown glass. Partially altered to oxides.

SECONDARY MINERALOGY	PERCENT	REPLACING/ FILLING	COMMENTS
Clays	7	Fractures	Microcrystalline pale green clay + calcite in fractures throughout the glass.
Clays	3	Ol	Brown iddingsite.

VESICLES/ CAVITIES	PERCENT	LOCATION	SIZE RANGE (mm)	FILLING	SHAPE	COMMENTS
Vesicles	5	Even	<3	Smectite, calcite	Irregular, spherical	Generally not completely filled.

COMMENTS: Glomerocrysts of plag + cpx relatively common; contain grains in the same size range as phenocrysts.

THIN SECTION DESCRIPTION

115-713A-15R-5 (Piece 5, 89-91 cm)

ROCK NAME: Highly olivine-bearing clinopyroxene plagioclase phyric basalt

WHERE SAMPLED: Unit 5

TEXTURE: Highly porphyritic, hyalocrystalline

GRAIN SIZE: Fine

OBSERVER: ANB

PRIMARY MINERALOGY	PERCENT PRESENT	PERCENT ORIGINAL	SIZE RANGE (mm)	APPROX. COMPO-SITION	MORPHOLOGY	COMMENTS
PHENOCRYSTS						
Olivine	—	tr	<1		Subhedral	Completely altered to carbonate.
Plagioclase	25	25	0.2–1.0		Subhedral–euhedral	
Clinopyroxene	5	5	<0.8	Augite	Subhedral	Zoned. Colorless augite.
GROUNDMASS						
Olivine	—	2	<0.5		Subhedral	Completely altered to carbonate.
Clinopyroxene	10	10	<0.2	Augite	Anhedral	Colorless.
Plagioclase	10	10	<0.2		Subhedral	
Magnetite	2	2	<0.1	Titano–magnetite	Subhedral	
Glass	—	46				Interstitial. Completely altered.

SECONDARY MINERALOGY	PERCENT	REPLACING/ FILLING	COMMENTS
Clays	40	Glass	Brown smectites after glass in groundmass.
Carbonate	8	Glass, ol	Alteration phase in groundmass.

VESICLES/ CAVITIES	PERCENT	LOCATION	SIZE RANGE (mm)	FILLING	SHAPE	COMMENTS
Vesicles	1	Even	<0.2		Spherical	Lined with brown smectites. Occasionally filled with calcite.

THIN SECTION DESCRIPTION

115–713A–18R–1 (Piece 7, 73–75 cm)

ROCK NAME: Highly olivine clinopyroxene plagioclase phyric basalt

WHERE SAMPLED: Unit 6

TEXTURE: Highly porphyritic, hyalocrystalline

GRAIN SIZE: Fine

OBSERVER: ANB

PRIMARY MINERALOGY	PERCENT PRESENT	PERCENT ORIGINAL	SIZE RANGE (mm)	APPROX. COMPO-SITION	MORPHOLOGY	COMMENTS
PHENOCRYSTS						
Olivine	—	2	<1		Subhedral	Completely altered to green serpentine + calcite.
Plagioclase	15	15	<2		Euhedral–subhedral	Fresh glass inclusions in larger crystals. Strong normal and oscillatory zoning common.
Clinopyroxene	3	3	<0.8	Augite	Subhedral	Colored.
GROUNDMASS						
Clinopyroxene	1	1	<0.1	Augite	Subhedral	Colorless.
Plagioclase	2	2	<0.1		Subhedral	Quench forms dominate.
Spinel	1	1	<0.02	Magnetite	Anhedral	Quench or alteration product of glass.
Glass	—	76				Totally altered to brown smectites(?).

SECONDARY MINERALOGY	PERCENT	REPLACING/ FILLING	COMMENTS
Clays	76	Glass	
Carbonate	Tr	Ol	
Serpentine	2	Ol	Associated with calcite in altered ol.

VESICLES/ CAVITIES	PERCENT	LOCATION	SIZE RANGE (mm)	FILLING	SHAPE	COMMENTS
Vesicles	1	Even	<0.5		Spherical	Filled by radially disposed siderite(?).

THIN SECTION DESCRIPTION

115–713A–18R–1 (Piece 14, 145–148 cm)

ROCK NAME: Highly olivine clinopyroxene plagioclase phyric basalt

WHERE SAMPLED: Unit 7

TEXTURE: Highly porphyritic, hyaline

GRAIN SIZE: Fine

OBSERVER: ANB

PRIMARY MINERALOGY	PERCENT PRESENT	PERCENT ORIGINAL	SIZE RANGE (mm)	APPROX. COMPO-SITION	MORPHOLOGY	COMMENTS
PHENOCRYSTS						
Olivine	—	1	<1		Subhedral	Totally altered to carbonate.
Plagioclase	15	15	<3		Euhedral–subhedral	Fresh. Quench forms present.
Clinopyroxene	7	7	<1	Augite	Subhedral	Colorless.
GROUNDMASS						
Glass	—	76				
Titanomagnetite	1	1	<0.1		Subhedral	Possibly quench product in glass.

SECONDARY MINERALOGY	PERCENT	REPLACING/ FILLING	COMMENTS
Clays	76	Glass	Calcite? Cryptocrystalline gray clays(?).
Carbonate	1	Ol	Calcite?

COMMENTS: Whole aspect of rock suggests differentiated character.

THIN SECTION DESCRIPTION

115-713A-18R-2 (Piece 5, 35-39 cm)

ROCK NAME: Highly olivine clinopyroxene plagioclase phyric basalt

WHERE SAMPLED: Unit 8

TEXTURE: Highly porphyritic, hyalocrystalline

GRAIN SIZE: Fine

OBSERVER: ANB

PRIMARY MINERALOGY	PERCENT PRESENT	PERCENT ORIGINAL	SIZE RANGE (mm)	APPROX. COMPOSITION	MORPHOLOGY	COMMENTS
PHENOCRYSTS						
Olivine	—	1	<0.8		Subhedral	Totally altered to carbonate.
Plagioclase	10	10	<1.5		Subhedral	Strongly normally zoned.
Clinopyroxene	5	5	<1	Augite	Anhedral	Colorless.
GROUNDMASS						
Glass	—	65				
Clinopyroxene	5	5	<0.2	Augite	Anhedral	
Plagioclase	10	10	<0.2		Subhedral	Fresh.
Oxides	2	2	<0.2	Titano-magnetite	Subhedral	

SECONDARY MINERALOGY	PERCENT	REPLACING/ FILLING	COMMENTS
Clays	65	Glass	Pale olive green-brown smectite.

VESICLES/ CAVITIES	PERCENT	LOCATION	SIZE RANGE (mm)	FILLING	SHAPE
Vesicles	<<1	Even	< 0.5	Smectite	Spherical

THIN SECTION DESCRIPTION

115-713A-19R-1 (Piece 3, 15-20 cm)

ROCK NAME: Highly olivine clinopyroxene plagioclase phyric basalt

WHERE SAMPLED: Unit 8

TEXTURE: Highly porphyritic, glassy

GRAIN SIZE: Fine to medium

OBSERVER: YT

PRIMARY MINERALOGY	PERCENT PRESENT	PERCENT ORIGINAL	SIZE RANGE (mm)	APPROX. COMPO-SITION	MORPHOLOGY	COMMENTS
PHENOCRYSTS						
Olivine	<1	1	0.2		Euhedral	In fresh glass, fresh ol is present.
Plagioclase	15	15	0.2–4.0	An 50	Euhedral	Larger crystal shows oscillatory zoning.
Clinopyroxene	5	5	0.2–0.7	Augite	Subhedral	Larger crystal shows hourglass structure.
GROUNDMASS						
Glass	5	71				Devitrified into unidentifiable fine-grained minerals.

SECONDARY MINERALOGY	PERCENT	REPLACING/ FILLING	COMMENTS
Clays	3	Vesicles	Green clay.
Clays	1	Ol	Brown clay (iddingsite?).
Carbonate	5	Vesicles, veins	
Devitrified glass	66	Glass	Fine minerals (devitrification products and quench products).

VESICLES/ CAVITIES	PERCENT	LOCATION	SIZE RANGE (mm)	FILLING	SHAPE	COMMENTS
Vesicles	7	Even	<2	Carbonate, green clay	Round, irregular	Larger one is round.

COMMENTS: Fresh ol.

THIN SECTION DESCRIPTION

115-713A-19R-1 (Piece 4, 27-29 cm)

ROCK NAME: Highly clinopyroxene plagioclase phyric basalt

WHERE SAMPLED: Unit 8

TEXTURE: Seriate, highly porphyritic

GRAIN SIZE: Medium to fine

OBSERVER: RBH

PRIMARY MINERALOGY	PERCENT PRESENT	PERCENT ORIGINAL	SIZE RANGE (mm)	APPROX. COMPO-SITION	MORPHOLOGY	COMMENTS
PHENOCRYSTS						
Plagioclase	20	20	0.1–1.0		Subhedral, laths	Glomerocrysts. Feathery laths present.
Clinopyroxene	13	13	<0.05		Subhedral, granules	Equant grains, and granules in matrix.
GROUNDMASS						
Glass	—	33				Partially quenched with feathery crystals of plag, cpx,and opaque granules.
Plagioclase	17	17	0.05		Feathery, laths	
Clinopyroxene	11	11	0.01		Granules	
Titanomagnetite	5	5	0.01			Mostly subequant, skeletal; dendritic form rare.

SECONDARY MINERALOGY	PERCENT	REPLACING/ FILLING	COMMENTS
Clays	33	Glass	Alteration of glassy material, residual from quench.
Carbonate	<1	Vesicles	
Zeolites	<1	Vesicles	

VESICLES/ CAVITIES	PERCENT	LOCATION	SIZE RANGE (mm)	FILLING	SHAPE	COMMENTS
Vesicles	1					Vesicles are filled with calcite or with radiating zeolites.

THIN SECTION DESCRIPTION

115-713A-19R-1 (Piece 10, 91-93 cm)

ROCK NAME: Highly olivine clinopyroxene plagioclase phyric basalt

WHERE SAMPLED: Unit 9

TEXTURE: Highly porphyritic

GRAIN SIZE: Medium to fine

OBSERVER: RBH

PRIMARY MINERALOGY	PERCENT PRESENT	PERCENT ORIGINAL	SIZE RANGE (mm)	APPROX. COMPO-SITION	MORPHOLOGY	COMMENTS
PHENOCRYSTS						
Olivine	—	>2	<0.6			Completely altered to clay and/or calcite.
Plagioclase	10	10	<1.0		Subhedral, laths	Often in glomerocrysts, sometimes with cpx.
Clinopyroxene	10	10	<1.0		Equant, subhedral	
GROUNDMASS						
Glass	—	25				Now aligned, devitrified, especially around rare vesicles.
Clinopyroxene	25	25	<0.05		Granules	Devitrification product?
Plagioclase	25	25	<0.1		Laths	Fine laths, somewhat feathery.
Opaques	3	3	0.05		Subequant, subhedral	

SECONDARY MINERALOGY	PERCENT	REPLACING/ FILLING	COMMENTS
Clays	27	Glass, ol	
Carbonate	<1	Ol	Calcite partially replacing ol.

COMMENTS: Section unpolished.

THIN SECTION DESCRIPTION

115-713A-19R-1 (Piece 12, 116-118 cm)

ROCK NAME: Highly olivine clinopyroxene plagioclase phyric basalt

WHERE SAMPLED: Unit 10

TEXTURE: Highly porphyritic

GRAIN SIZE: Fine to medium

OBSERVER: YT

PRIMARY MINERALOGY	PERCENT PRESENT	PERCENT ORIGINAL	SIZE RANGE (mm)	APPROX. COMPO-SITION	MORPHOLOGY	COMMENTS
PHENOCRYSTS						
Olivine	—	1	0.3		Euhedral	Completely altered to carbonate.
Plagioclase	10	10	0.2-2.0	An 50	Euhedral–subhedral	Zoned. Large crystals are reverse zoned.
Clinopyroxene	7	7	0.2–0.7	Augite	Subhedral	Larger crystal shows honeycomb structure.
GROUNDMASS						
Plagioclase	7	7	<0.2		Subhedral	
Clinopyroxene	3	3	<0.2	Augite	Subhedral	
Opaques	3	3	<0.1	Magnetite (?)	Euhedral	
Glass	—	66				Completely devitrified.

SECONDARY MINERALOGY	PERCENT	REPLACING/ FILLING	COMMENTS
Clays	66	Glass	Unidentifiable fine-grained clay or devitrified glass.
Carbonate	4	Ol, vesicles	

VESICLES/ CAVITIES	PERCENT	LOCATION	SIZE RANGE (mm)	FILLING	SHAPE
Vesicles	3	Even	<1	Carbonate	Round

COMMENTS: Larger plag crystals (>1.5 mm) always show reverse zoning.

THIN SECTION DESCRIPTION

115–713A–19R–3 (Piece 2A, 12–15 cm)

ROCK NAME: Highly clinopyroxene plagioclase phyric basalt

WHERE SAMPLED: Unit 11

TEXTURE: Highly porphyritic, hyaline

GRAIN SIZE: Fine

OBSERVER: ANB

PRIMARY MINERALOGY	PERCENT PRESENT	PERCENT ORIGINAL	SIZE RANGE (mm)	APPROX. COMPO-SITION	MORPHOLOGY	COMMENTS
PHENOCRYSTS						
Plagioclase	15	15	<2		Euhedral–subhedral	Normal and oscillatory zoning prominent.
Clinopyroxene	7	7	<1	Augite	Subhedral	Colorless. Zoned.
GROUNDMASS						
Titanomagnetite	2	2	<0.05		Anhedral	Alteration product or quench from glass.
Glass	—	76				Totally altered to clay.

SECONDARY MINERALOGY	PERCENT	REPLACING/ FILLING	COMMENTS
Clays	76	Glass	Cryptocrystalline gray clay (± calcite?) after glass.

VESICLES/ CAVITIES	PERCENT	LOCATION	SIZE RANGE (mm)	FILLING	SHAPE	COMMENTS
Vesicles	1	Even	<0.8	Clay	Spherical	Filled with yellow-green clay, celadonite(?).

THIN SECTION DESCRIPTION

115-713A-20R-1 (Piece 4A, 29-31 cm)

ROCK NAME: Highly olivine-bearing clinopyroxene plagioclase phyric basalt

WHERE SAMPLED: Top of Unit 12

TEXTURE: Highly porphyritic

GRAIN SIZE: Medium to cryptocrystalline

OBSERVER: ANB

PRIMARY MINERALOGY	PERCENT PRESENT	PERCENT ORIGINAL	SIZE RANGE (mm)	APPROX. COMPOSITION	MORPHOLOGY	COMMENTS
PHENOCRYSTS						
Olivine	—	Tr	<0.3		Subhedral	Completely altered to calcite + brown iddingsite.
Plagioclase	15	15	<1.5		Subhedral	Glass inclusions in larger crystals. Glomerocrysts with cpx are common.
Clinopyroxene	3	3	<1	Augite	Subhedral	Colorless.
GROUNDMASS						
Plagioclase	1	1	<0.1		Subhedral	Quench terminations.
Spinel	1	1	<0.01	Magnetite(?)	Anhedral	Probably quench or formed during devitrification.
Glass	—	80				Strong quench/devitrification texture. Variolitic. spinifex(???).

SECONDARY MINERALOGY	PERCENT	REPLACING/ FILLING	COMMENTS
Clays	80	Glass	Cryptocrystalline brown smectites.
Iddingsite	Tr	Ol	
Carbonate	Tr	Ol	Calcite.

VESICLES/ CAVITIES	PERCENT	LOCATION	SIZE RANGE (mm)	FILLING	SHAPE	COMMENTS
Vesicles	5	Even	<1	Various	Irregular	Vesicles filled with calcite, celadonite, or microcrystalline radial zeolites.

THIN SECTION DESCRIPTION

115-713A-20R-1 (Piece 5A, 77-79 cm)

ROCK NAME: Highly olivine clinopyroxene plagioclase phyric basalt

WHERE SAMPLED: Unit 12

TEXTURE: Highly porphyritic, hyalocrystalline

GRAIN SIZE: Fine

OBSERVER: ANB

PRIMARY MINERALOGY	PERCENT PRESENT	PERCENT ORIGINAL	SIZE RANGE (mm)	APPROX. COMPOSITION	MORPHOLOGY	COMMENTS
PHENOCRYSTS						
Olivine	—	1	<2		Subhedral	Totally altered to brown smectite(?) + calcite.
Plagioclase	10	10	<1.5	An 52	Subhedral	Grade into groundmass size range. Glass inclusions in larger crystals.
Clinopyroxene	5	5	<1	Augite	Subhedral	Colorless.
GROUNDMASS						
Olivine	—	Tr	<0.05		Subhedral	Totally altered to brown smectite(?) + calcite.
Clinopyroxene	5	5	<0.1	Augite	Anhedral	Interstitial grains between plag crystals.
Plagioclase	20	20	<0.2		Subhedral	
Spinel	2	2	<0.1	Titano-magnetite(?)	Subhedral	
Glass	—	57				Interstitial. Altered completely to brown smectites(?).

SECONDARY MINERALOGY	PERCENT	REPLACING/ FILLING	COMMENTS
Clays	1	Ol	Brown smectite(?).
Clays	57	Glass	Pale brown smectite(?).
Carbonate	Tr	Ol	Associated with smectite(?) clays.

VESICLES/ CAVITIES	PERCENT	LOCATION	SIZE RANGE (mm)	FILLING	SHAPE	COMMENTS
Vesicles	<1	Even	<1	Calcite	Spherical	Rimmed by brown smectite(?) and generally filled by calcite.

THIN SECTION DESCRIPTION

115-713A-20R-1 (Piece 5A, 77-80 cm)

ROCK NAME: Highly olivine clinopyroxene plagioclase phyric basalt

WHERE SAMPLED: Unit 12, 50 cm below top of the unit

TEXTURE: Intersertal, highly porphyritic

GRAIN SIZE: Fine

OBSERVER: MRF

PRIMARY MINERALOGY	PERCENT PRESENT	PERCENT ORIGINAL	SIZE RANGE (mm)	APPROX. COMPO-SITION	MORPHOLOGY	COMMENTS
PHENOCRYSTS						
Olivine	—	4	0.1–0.3		Euhedral	Replaced by clay, carbonate, and sulfide.
Plagioclase	13	13	0.2–2.0	An 65	Subhedral	Cumulate? Intergrowths of plag and augite at 120° intersections.
Clinopyroxene	13	13	0.2–1.0	Augite	Subhedral	
GROUNDMASS						
Plagioclase	33	33	0.05–0.20	An 60	Subhedral–anhedral	
Clinopyroxene	33	33	0.05–0.20	Augite	Subhedral–anhedral	
Spinel	4	4	0.005–0.050	Magnetite	Skeletal	Quench texture.

SECONDARY MINERALOGY	PERCENT	REPLACING/ FILLING
Chlorite	3	Ol
Carbonate	<1	Ol
Sulfide	<1	Ol

VESICLES/ CAVITIES	PERCENT	LOCATION	SIZE RANGE (mm)	FILLING	SHAPE
Vesicles	<1		3	Clay	Round

THIN SECTION DESCRIPTION

115-713A-20R-2 (Piece 2B, 37-39 cm)

ROCK NAME: Highly olivine clinopyroxene plagioclase phyric basalt

WHERE SAMPLED: Unit 12

TEXTURE: Microporphyritic

GRAIN SIZE: Fine to glassy

OBSERVER: RBH

PRIMARY MINERALOGY	PERCENT PRESENT	PERCENT ORIGINAL	SIZE RANGE (mm)	APPROX. COMPO-SITION	MORPHOLOGY	COMMENTS
PHENOCRYSTS						
Olivine	1	1	0.6		Euhedral	
Plagioclase	10	10	<4		Euhedral	Some glomerocrysts.
Clinopyroxene	5	5	<1		Euhedral–subhedral	
GROUNDMASS						
Glass	31	84				Glassy margins are fresh. Devitrified glass and quenched areas are altered to clay.

SECONDARY MINERALOGY	PERCENT	REPLACING/ FILLING	COMMENTS
Clays	53	Glass	Brownish clay replacing quenched groundmass.

COMMENTS: Conspicuous textural gradient from glass which is clear and unaltered to feathery quench texture. Titanomagnetite is absent in glass, ubiquitous (fine-grained crystals) in quenched areas. Alteration to brown clay.

THIN SECTION DESCRIPTION

115-713A-20R-2 (Piece 5, 89-91 cm)

ROCK NAME: Highly olivine clinopyroxene plagioclase phyric basalt

WHERE SAMPLED: Unit 13

TEXTURE: Highly porphyritic, glassy

GRAIN SIZE: Fine

OBSERVER: YT

PRIMARY MINERALOGY	PERCENT PRESENT	PERCENT ORIGINAL	SIZE RANGE (mm)	APPROX. COMPO-SITION	MORPHOLOGY	COMMENTS
PHENOCRYSTS						
Olivine	—	3	0.1–0.3	Fo 70(?)	Euhedral	Fresh in fresh glass.
Plagioclase	10	10	0.2–1.0	An 55	Euhedral–subhedral	Zoned normally.
Clinopyroxene	6	6	0.2–0.6	Augite	Subhedral	Hourglass structure.
GROUNDMASS						
Glass	—	81				Fresh glass + quenched cpx + devitrified, altered glass.

SECONDARY MINERALOGY	PERCENT	REPLACING/ FILLING	COMMENTS
Clays	3	Ol	Iddingsite(?).
Clays	81	Glass	Cpx + alteration and devitrification minerals.

COMMENTS: Fresh ol and glass.

THIN SECTION DESCRIPTION

115-713A-20R-2 (Piece 6F, 145-147 cm)

ROCK NAME: Highly olivine clinopyroxene plagioclase phyric basalt

WHERE SAMPLED: Unit 13

TEXTURE: Highly porphyritic

GRAIN SIZE: Fine to medium

OBSERVER: YT

PRIMARY MINERALOGY	PERCENT PRESENT	PERCENT ORIGINAL	SIZE RANGE (mm)	APPROX. COMPO-SITION	MORPHOLOGY	COMMENTS
PHENOCRYSTS						
Olivine	—	5	0.2–0.5		Euhedral–subhedral	Completely altered to pale brown clay.
Plagioclase	15	15	0.2–2.0	An 60	Euhedral–subhedral	No oscillatory zoning.
Clinopyroxene	7	7	0.2–0.8	Augite	Euhedral–subhedral	
GROUNDMASS						
Plagioclase	20	20	<0.2		Subhedral	
Clinopyroxene	7	7	<0.2	Augite	Subhedral	
Opaque	3	3	<0.1	Magnetite(?)	Euhedral–subhedral	
Glass	—	41				

SECONDARY MINERALOGY	PERCENT	REPLACING/ FILLING	COMMENTS
Clays	7	Ol, vesicles	Alteration products.
Clays	41	Glass	Fine-grained crystals. Alteration and devitrification products.

VESICLES/ CAVITIES	PERCENT	LOCATION	SIZE RANGE (mm)	FILLING	SHAPE	COMMENTS
Vesicles	2	Even	<1	Clay	Round	Filled by pale brown clay.

THIN SECTION DESCRIPTION

115-713A-20R-3 (Piece 2B, 50-51 cm)

ROCK NAME: Highly olivine clinopyroxene plagioclase phyric basalt

WHERE SAMPLED: Unit 14

TEXTURE: Highly porphyritic

GRAIN SIZE: Fine

OBSERVER: RBH

PRIMARY MINERALOGY	PERCENT PRESENT	PERCENT ORIGINAL	SIZE RANGE (mm)	APPROX. COMPOSITION	MORPHOLOGY	COMMENTS
PHENOCRYSTS						
Olivine	—	3				
Plagioclase	10	10	<1		Subhedral, subequant	Glomerocrysts up to several mm across.
Clinopyroxene	5	5	0.5		Subequant granules	Mostly as isolated granular crystals.
GROUNDMASS						
Plagioclase	21	20	0.1		Needles	
Clinopyroxene	16	20	0.05		Granules	
Opaques	<1	<1				Almost devoid of Fe-Ti oxide.

SECONDARY MINERALOGY	PERCENT	REPLACING/ FILLING	COMMENTS
Clays	47	Glass, cpx	As alteration of glass and cpx in groundmass.
Sulfides	1	Vesicles	

COMMENTS: This section contains almost no titanomagnetite.

THIN SECTION DESCRIPTION

115-713A-20R-3 (Piece 4A, 64-66 cm)

ROCK NAME: Highly olivine-bearing clinopyroxene plagioclase phyric basalt

WHERE SAMPLED: Unit 15

TEXTURE: Highly porphyritic, glassy

GRAIN SIZE: Fine

OBSERVER: YT

PRIMARY MINERALOGY	PERCENT PRESENT	PERCENT ORIGINAL	SIZE RANGE (mm)	APPROX. COMPOSITION	MORPHOLOGY	COMMENTS
PHENOCRYSTS						
Olivine	—	<1	<0.1		Euhedral	Tiny fresh ol can be found in fresh glass.
Plagioclase	10	10	0.2–3.0	≈An 55	Euhedral–subhedral	Bimodal crystal sizes.
Clinopyroxene	5	5	0.2–0.5	Augite	Euhedral–subhedral	Hourglass extinction.
GROUNDMASS						
Glass	—	85				In chilled margin, fresh glass can be observed. Most of the groundmass consists of devitrified and altered glass with some quenched cpx.

SECONDARY MINERALOGY	PERCENT	REPLACING/ FILLING	COMMENTS
Clays	85	Glass	Aggregates of quench cpx + alteration products and devitrification products.

VESICLES/ CAVITIES	PERCENT	LOCATION	SIZE RANGE (mm)	FILLING	SHAPE
Vesicles	<1	Even	3	Carbonate	Round

COMMENTS: Fresh ol.

THIN SECTION DESCRIPTION

115-713A-20R-3 (Piece 4A, 73-74 cm)

ROCK NAME: Highly olivine clinopyroxene plagioclase phyric basalt

WHERE SAMPLED:

TEXTURE: Highly porphyritic

GRAIN SIZE: Fine to medium

OBSERVER: YT

PRIMARY MINERALOGY	PERCENT PRESENT	PERCENT ORIGINAL	SIZE RANGE (mm)	APPROX. COMPOSITION	MORPHOLOGY	COMMENTS
PHENOCRYSTS						
Olivine	—	5	0.2–0.5		Euhedral–subhedral	Completely altered to carbonate.
Plagioclase	15	15	0.2–2.0	An 50	Euhedral–subhedral	Normally zoned.
Clinopyroxene	7	7	0.2–0.7	Augite	Subhedral–euhedral	
GROUNDMASS						
Plagioclase	20	20	<0.2		Euhedral–subhedral	
Clinopyroxene	10	10	<0.2	Augite	Subhedral	
Opaque	3	3	<0.1	Magnetite(?)	Euhedral	
Glass	—	45				Completely altered to clays + carbonate.

SECONDARY MINERALOGY	PERCENT	REPLACING/ FILLING	COMMENTS
Clays Carbonate	45	Glass	Alteration products formed from glass.

VESICLES/ CAVITIES	PERCENT	LOCATION	SIZE RANGE (mm)	FILLING	SHAPE
Vesicles	2	Even	<1	Carbonate	Round

THIN SECTION DESCRIPTION

115-713A-20R-3 (Piece 7A, 112-113 cm)

ROCK NAME: Moderately olivine-bearing plagioclase clinopyroxene phyric basalt

WHERE SAMPLED: Unit 16

TEXTURE: Moderately porphyritic (microporphyritic)

GRAIN SIZE: Fine

OBSERVER: RBH

PRIMARY MINERALOGY	PERCENT PRESENT	PERCENT ORIGINAL	SIZE RANGE (mm)	APPROX. COMPOSITION	MORPHOLOGY	COMMENTS
PHENOCRYSTS						
Olivine	—	<1				
Plagioclase	4	4	1		Thin laths	
Clinopyroxene	5	5	0.6		Equant, subhedral	Serrated crystal edges, possibly resorbed.
GROUNDMASS						
Fe-Ti Oxides	2	2	0.02		Subequant, skeletal	In matrix, very fine-grained.
Glass	—	57				
Plagioclase	15	15			Needles	Thin, needle-like crystals.
Clinopyroxene	15	15			Granular	Fine granules.

SECONDARY MINERALOGY	PERCENT	REPLACING/ FILLING	COMMENTS
Clays	59	Glass, ol, vesicles	Replacing glass and ol in groundmass. Also lines vesicles.

VESICLES/ CAVITIES	PERCENT	LOCATION	SIZE RANGE (mm)	FILLING	SHAPE	COMMENTS
Vesicles	2		≤1.4	Zeolite		Lined with green celadonite and filled with fibrous zeolite.

THIN SECTION DESCRIPTION

115-713A-20R-3 (Piece 7B, 137-138 cm)

ROCK NAME: Moderately olivine clinopyroxene plagioclase phyric basalt

WHERE SAMPLED: Unit 17

TEXTURE: Moderately porphyritic to microporphyritic

GRAIN SIZE: Fine

OBSERVER: RBH

PRIMARY MINERALOGY	PERCENT PRESENT	PERCENT ORIGINAL	SIZE RANGE (mm)	APPROX. COMPOSITION	MORPHOLOGY	COMMENTS
PHENOCRYSTS						
Olivine	—	1			Euhedral	Well-formed crystals, completely altered to iddingsite.
Plagioclase	5	5	<1		Tabular, laths, euhedral	Fresh.
Clinopyroxene	3	3	<0.5		Equant, euhedral	Fresh.
GROUNDMASS						
Glass	—	5				
Plagioclase	40	40				
Clinopyroxene	40	40				
Fe-Ti oxides	3	3	<0.05		Skeletal	

SECONDARY MINERALOGY	PERCENT	REPLACING/ FILLING	COMMENTS
Clays	8	Ol, glass	Replacing highly altered glass adjacent to rim at one end of the thin section. Also as scattered glassy patches in the groundmass.
Celadonite	1		In alteration band at one end of the thin section. Bright green.

THIN SECTION DESCRIPTION

115-713A-20R-4 (Piece 1, 1-3 cm)

ROCK NAME: Highly olivine clinopyroxene plagioclase phyric basalt

WHERE SAMPLED: Unit 18

TEXTURE: Highly porphyritic, glassy

GRAIN SIZE: Fine

OBSERVER: YT

PRIMARY MINERALOGY	PERCENT PRESENT	PERCENT ORIGINAL	SIZE RANGE (mm)	APPROX. COMPOSITION	MORPHOLOGY	COMMENTS
PHENOCRYSTS						
Olivine	—	1	0.3		Euhedral	Altered to clay.
Plagioclase	10	10	0.2–5.0	An 50	Euhedral–subhedral	Bimodal crystal sizes.
Clinopyroxene	5	5	0.2–0.5	Augite	Subhedral–euhedral	
GROUNDMASS						
Glass	—	74				Replaced by devitrification + alteration products. In a narrow zone, fresh glass can be observed.

SECONDARY MINERALOGY	PERCENT	REPLACING/ FILLING	COMMENTS
Clays	1	Ol	Iddingsite.
Clays	10	Vesicles	
Clays	74	Glass	Alteration + devitrification products.

VESICLES/ CAVITIES	PERCENT	LOCATION	SIZE RANGE (mm)	FILLING	SHAPE	COMMENTS
Vesicles	10	Even	<1	Clays	Irregular	Both green and brown clays present.

THIN SECTION DESCRIPTION

115-713A-20R-4 (Piece 3A, 35-37 cm)

ROCK NAME: Highly olivine clinopyroxene plagioclase phyric basalt

WHERE SAMPLED: Unit 18

TEXTURE: Highly porphyritic

GRAIN SIZE: Fine

OBSERVER: YT

PRIMARY MINERALOGY	PERCENT PRESENT	PERCENT ORIGINAL	SIZE RANGE (mm)	APPROX. COMPOSITION	MORPHOLOGY	COMMENTS
PHENOCRYSTS						
Olivine	—	5	0.2–0.5		Euhedral–subhedral	Completely altered to pale brown clay.
Plagioclase	15	15	0.3–2.0	An 60	Euhedral–subhedral	Bimodal crystal sizes: 1 mm and <7 mm. Larger one has dusty inclusions.
Clinopyroxene	10	10	0.2–0.6	Augite	Subhedral	Sometimes forms glomerocrysts with plag.
GROUNDMASS						
Plagioclase	10	10	<0.2		Subhedral	
Clinopyroxene	5	5	<0.2	Augite(?)	Subhedral	
Opaque	1	1	<0.1	Magnetite(?)	Euhedral	
Glass	—	54				Completely altered to clay.

SECONDARY MINERALOGY	PERCENT	REPLACING/ FILLING	COMMENTS
Clays	5	Ol	Iddingsite(?).
Clays	54	Glass	Alteration products from glass.

VESICLES/ CAVITIES	PERCENT	LOCATION	SIZE RANGE (mm)	FILLING	SHAPE	COMMENTS
Vesicles	1	Even	0.3		Round	A few vesicles are partially filled with carbonate.

THIN SECTION DESCRIPTION

115–713A–20R–4 (Piece 5C, 140–142 cm)

ROCK NAME: Highly olivine-bearing clinopyroxene plagioclase phyric basalt

WHERE SAMPLED: Unit 19

TEXTURE: Highly porphyritic

GRAIN SIZE: Fine

OBSERVER: YT

PRIMARY MINERALOGY	PERCENT PRESENT	PERCENT ORIGINAL	SIZE RANGE (mm)	APPROX. COMPO-SITION	MORPHOLOGY	COMMENTS
PHENOCRYSTS						
Olivine	—	<1	0.2		Euhedral	Altered to iddingsite.
Plagioclase	10	10	0.2–5.0	≈An 50	Euhedral–subhedral	Bimodal crystal sizes. Larger ones sometimes contain dusty inclusions.
Clinopyroxene	5	5	0.2–0.5	Augite	Subhedral	
GROUNDMASS						
Plagioclase	1	1	<0.2		Subhedral–euhedral	
Clinopyroxene	<1	<1	<0.2		Subhedral	
Opaque	2	2	<0.1	Magnetite(?)	Euhedral	
Glass	—	82				Altered and devitrified.

SECONDARY MINERALOGY	PERCENT	REPLACING/ FILLING	COMMENTS
Clays	82	Glass	Unidentifiable alteration ± devitrification products.

VESICLES/ CAVITIES	PERCENT	LOCATION	SIZE RANGE (mm)	FILLING	SHAPE	COMMENTS
Vesicles	<1		0.4	Carbonate	Round	Only a few.

THIN SECTION DESCRIPTION

115-713A-20R-5 (Piece 3, 25-28 cm)

ROCK NAME: Highly olivine clinopyroxene plagioclase phyric basalt

WHERE SAMPLED: Unit 20

TEXTURE: Highly porphyritic, hyalocrystalline

GRAIN SIZE: Fine

OBSERVER: ANB

PRIMARY MINERALOGY	PERCENT PRESENT	PERCENT ORIGINAL	SIZE RANGE (mm)	APPROX. COMPOSITION	MORPHOLOGY	COMMENTS
PHENOCRYSTS						
Olivine	—	1	<1.5		Subhedral	Completely altered to brown smectite + calcite.
Plagioclase	10	10	<3		Euhedral–subhedral	Strong normal and oscillatory zoning.
Clinopyroxene	3	3	<1	Augite	Subhedral	Colorless. Large crystals show strong marginal zoning.
GROUNDMASS						
Olivine	—	Tr	<0.1		Subhedral	Altered to brown smectite + calcite.
Clinopyroxene	2	2	<0.1	Augite	Anhedral	Colorless.
Plagioclase	10	10	<0.2		Subhedral	
Spinel	2	2	<0.1	Titano-magnetite	Anhedral	Alteration or quench product of glass.
Glass	—	72				Totally altered to cryptocrystalline clay + calcite.

SECONDARY MINERALOGY	PERCENT	REPLACING/ FILLING	COMMENTS
Clays Calcite	72	Glass	Intimate association between clays and calcite. Relative proportions not determinable.
Clays	1	Ol	Associated with trace amounts of calcite.

VESICLES/ CAVITIES	PERCENT	LOCATION	SIZE RANGE (mm)	FILLING	SHAPE
Vesicles	Tr				

COMMENTS: Trace amounts of pyrite infilling vesicles. Occasional coarse glomerocrysts of strongly zoned plag and augite.

THIN SECTION DESCRIPTION

115-713A-20R-5 (Piece 6A, 98-99 cm)

ROCK NAME: Highly olivine clinopyroxene plagioclase phyric basalt

WHERE SAMPLED: Unit 21

TEXTURE: Highly porphyritic, glassy

GRAIN SIZE: Fine

OBSERVER: YT

PRIMARY MINERALOGY	PERCENT PRESENT	PERCENT ORIGINAL	SIZE RANGE (mm)	APPROX. COMPOSITION	MORPHOLOGY	COMMENTS
PHENOCRYSTS						
Olivine	—	3	0.2–0.4		Euhedral	Fresh ol observed in fresh glass.
Plagioclase	10	10	0.2–4.0	An 50	Euhedral–subhedral	Bimodal crystal sizes.
Clinopyroxene	7	7	0.2–0.7	Augite	Subhedral–euhedral	
GROUNDMASS						
Glass	—	80				Fresh in a narrow zone.

SECONDARY MINERALOGY	PERCENT	REPLACING/ FILLING	COMMENTS
Clays	3	Ol	Iddingsite(?).
Clays	80	Glass	Alteration + devitrification + quench products (cpx).

COMMENTS: Fresh olivine.

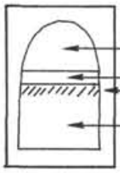
Completely altered.

Vein: serpentine + chlorite + zeolite(?).

Fresh glass, as described above.

Altered glass, as described above.

THIN SECTION DESCRIPTION

115-713A-20R-5 (Piece 6D, 127-129 cm)

ROCK NAME: Highly olivine clinopyroxene plagioclase phyric basalt

WHERE SAMPLED: Top of Unit 22

TEXTURE: Highly porphyritic, hyalocrystalline

GRAIN SIZE: Fine

OBSERVER: ANB

PRIMARY MINERALOGY	PERCENT PRESENT	PERCENT ORIGINAL	SIZE RANGE (mm)	APPROX. COMPO-SITION	MORPHOLOGY	COMMENTS
PHENOCRYSTS						
Olivine	—	1	<1		Subhedral	Completely altered to yellow-brown smectite(?).
Plagioclase	20	20	<3	An 52	Euhedral–subhedral	Strong oscillatory zoning common.
Clinopyroxene	7	7	<1	Augite	Euhedral–subhedral	Colorless. Strongly zoned.
GROUNDMASS						
Olivine	—	1	<0.1		Subhedral	Completely altered to yellow-brown smectite(?).
Clinopyroxene	4	4	<0.1	Augite	Anhedral	Colorless.
Plagioclase	13	13	<0.1		Subhedral	Quench forms common.
Spinel	3	3	<0.05		Subhedral	Possibly titanomagnetite.
Glass	—	51				Completely altered and partially devitrified.

SECONDARY MINERALOGY	PERCENT	REPLACING/ FILLING	COMMENTS
Clays	52	Glass, vesicles	Gray cryptocrystalline clay.
Clays	1	Ol	Yellow-brown smectite(?).

VESICLES/ CAVITIES	PERCENT	LOCATION	SIZE RANGE (mm)	FILLING	SHAPE	COMMENTS
Vesicles	1	Even	<1	Clay, opaques	Spherical	Lined with brown smectite. Rarely filled with devitrified residual glass containing elongate titanomagnetite crystals + smectite. Haloes of elongate titanomagnetite around vesicles common.

COMMENTS: General aspect of rock is feldspar-rich, with sub-fluidal alignment of crystals. May be a hawaiite.

THIN SECTION DESCRIPTION

115-713A-20R-6 (Piece 1E, 22-24 cm)

ROCK NAME: Highly olivine clinopyroxene plagioclase phyric basalt

WHERE SAMPLED: Unit 23

TEXTURE: Highly porphyritic, glassy

GRAIN SIZE: Fine

OBSERVER: YT

PRIMARY MINERALOGY	PERCENT PRESENT	PERCENT ORIGINAL	SIZE RANGE (mm)	APPROX. COMPO-SITION	MORPHOLOGY	COMMENTS
PHENOCRYSTS						
Olivine	—	3	0.2–0.3		Euhedral	Fresh crystals occur in fresh glass. Other crystals are altered.
Plagioclase	10	10	0.2–5	An 55(?)	Euhedral–subhedral	Bimodal crystal sizes.
Clinopyroxene	7	7	0.2–0.5	Augite	Subhedral–euhedral	
GROUNDMASS						
Glass	—	73				Composed of quench cpx + alteration and devitrification products + opaques. In the top of this section, fresh glass occurs.

SECONDARY MINERALOGY	PERCENT	REPLACING/ FILLING	COMMENTS
Clays	10	Ol, vesicles	
Clays	73	Glass	Percentage includes clay and quenched cpx. Cpx predominates in some areas.

VESICLES/ CAVITIES	PERCENT	LOCATION	SIZE RANGE (mm)	FILLING	SHAPE	COMMENTS
Vesicles	7	Even	<2	Clay	Irregular	Filled by clay which appears to be the same clay replacing ol.

COMMENTS: Fresh ol.

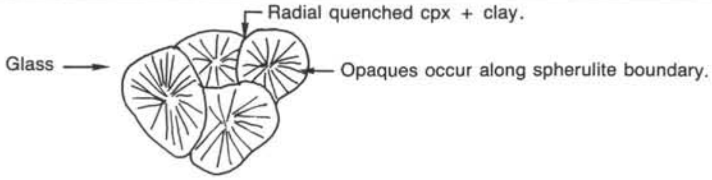

THIN SECTION DESCRIPTION

115-713A-21R-2 (Piece 6C, 130-132 cm)

ROCK NAME: Highly olivine-bearing clinopyroxene plagioclase phyric basalt

WHERE SAMPLED: Unit 32, pillow basalt rim

TEXTURE: Holohyaline, highly porphyritic

GRAIN SIZE: Microcrystalline

OBSERVER: MRF

PRIMARY MINERALOGY	PERCENT PRESENT	PERCENT ORIGINAL	SIZE RANGE (mm)	APPROX. COMPO-SITION	MORPHOLOGY	COMMENTS
PHENOCRYSTS						
Olivine	Tr	<1	0.1–1.0		Euhedral	Altered and replaced by clay.
Plagioclase	5	5	<2.5	An 62	Subhedral–anhedral	Large crystals subhedral. Small crystals anhedral.
Clinopyroxene	5	5	0.1–1.0	Augite	Subhedral	Intergrown with plag.
GROUNDMASS						
Glass	70	90				Mostly microcrystalline quench phases.

SECONDARY MINERALOGY	PERCENT	REPLACING/ FILLING	COMMENTS
Clays	20	Glass, ol	
Sulfide	Tr		In alteration rim of pillow.

THIN SECTION DESCRIPTION

115-713A-21R-3 (Piece 2C, 60-62 cm)

ROCK NAME: Highly olivine clinopyroxene plagioclase phyric basalt

WHERE SAMPLED: Unit 33, center of unit

TEXTURE: Intersertal, highly porphyritic

GRAIN SIZE: Fine

OBSERVER: MRF

PRIMARY MINERALOGY	PERCENT PRESENT	PERCENT ORIGINAL	SIZE RANGE (mm)	APPROX. COMPO-SITION	MORPHOLOGY	COMMENTS
PHENOCRYSTS						
Olivine	—	1	0.1–0.3		Euhedral	Altered to iddingsite.
Plagioclase	30	30	0.1–2.0	An 62		
Clinopyroxene	20	20	0.1–0.3	Augite		
GROUNDMASS						
Plagioclase	10	10	0.01–0.10			
Clinopyroxene	15	15	0.01–0.10			
Spinel	3	3	0.01–0.05	Magnetite		
Groundmass	—	21				Replaced by clays.

SECONDARY MINERALOGY	PERCENT	REPLACING/ FILLING	COMMENTS
Chlorite	21	Groundmass	
Clays	1	Ol	Iddingsite.

VESICLES/ CAVITIES	PERCENT	LOCATION	SIZE RANGE (mm)	FILLING	SHAPE
Vesicles	1		0.1–0.2	Clay	Round

THIN SECTION DESCRIPTION

115-713A-22R-1 (Piece 4, 23-24 cm)

ROCK NAME: Highly clinopyroxene plagioclase phyric basalt

WHERE SAMPLED: Unit 35, bottommost unit in core

TEXTURE: Interstitial

GRAIN SIZE: Fine

OBSERVER: MRF

PRIMARY MINERALOGY	PERCENT PRESENT	PERCENT ORIGINAL	SIZE RANGE (mm)	APPROX. COMPO-SITION	MORPHOLOGY	COMMENTS
PHENOCRYSTS						
Plagioclase	5	5	0.3–3.0	An 62	Subhedral	Equant crystals in glomerocrysts, L = 3 mm. Small grains are lath-like.
Clinopyroxene	5	5	0.1–0.5	Augite	Subhedral	
GROUNDMASS						
Plagioclase	26	26	0.1–1.0		Laths	L:W = 5:1
Clinopyroxene	51	51				
Spinel	3	3	0.05	Magnetite	Skeletal	Quench texture. Crosses.

SECONDARY MINERALOGY	PERCENT	REPLACING/ FILLING
Clays	10	Voids, vesicles, groundmass

VESICLES/ CAVITIES	PERCENT	LOCATION	SIZE RANGE (mm)	FILLING	SHAPE	COMMENTS
Vesicles, voids	1	Band	0.1–0.2	Clay, ± pyrite	Round	Form a band through the center of the thin section.